ABSTRACT

Title of Dissertation:	SEA TURTLE MOVEMENT ECOLOGY: CAUSES AND PATTERNS OF VARIABILITY FOR DIFFERENT SPECIES AND LIFE STAGES
	Nicole Ann Barbour, Doctor of Philosophy, 2022
Dissertation directed by:	Research Professor, Helen Bailey, University of Maryland Center for Environmental Science

Sea turtles are long lived marine reptiles, with most species having long distance, ontogenetic migrations. Movement studies have been biased towards surface and nearshore movements of females. I apply a variety of quantitative approaches to biotelemetry data for multiple species and life stages to address knowledge gaps in the movement ecology of sea turtles.

In chapter 1, neonate Caribbean leatherback turtles (*Dermochelys coriacea*) were acoustically tracked during early dispersal. Movement and statistical models showed that the main external drivers of behavioral differences were abiotic, namely the strength and direction of the currents. Variable behavior may have implications in the form of carry over effects if it results in differential long-term survival.

In chapter 2, the dive behavior of adult leatherback turtles in the Eastern Pacific (EP) was investigated using a clustering analysis, convolutional neural network, and statistical model.

Results found multiple ecologically distinct vertical behaviors, supporting the use of niche switching in the vertical dimension for EP leatherbacks during their migration.

In chapter 3, the vertical behaviors from chapter 2 and horizontal EP leatherback locations were used to create both a novel movement model and a dynamic management tool. Results produced monthly maps and quantitative indices informing bycatch risk, supporting existing conservation efforts for this population.

In chapter 4, miniature satellite tags were deployed on post-captive juvenile green turtles (*Chelonia mydas*) in multiple age classes. Comparisons with current-corrected and passive drift trajectories, a clustering analysis, and a statistical model all revealed significant differences in movement behaviors with current velocities and floating algae presence. Results support the importance of external (abiotic) factors and release effects for differences in juvenile movement.

This dissertation addresses key questions on the movement ecology of sea turtles for multiple species and life stages. Throughout, the physical environment is demonstrated to be an external driver of individual variation in movement. Movement behavior is additionally found to vary in multiple dimensions (e.g., horizontal and vertical). Despite individual variations, mean patterns of movement and behavior are identified for each population. The results found have broader implications for both conservation science and movement ecology studies of other long-distance migrants.

SEA TURTLE MOVEMENT ECOLOGY: CAUSES AND PATTERNS OF VARIABILITY FOR DIFFERENT SPECIES AND LIFE STAGES

by

Nicole Ann Barbour

Dissertation submitted to the Faculty of the Graduate School of the
University of Maryland, College Park, in partial fulfillment
of the requirements for the degree of
Doctor of Philosophy,
2022

Advisory Committee:
Dr. Helen Bailey, Chair
Dr. Bill Fagan, Co-Chair
Dr. George Shillinger
Dr. David Secor
Dr. Victoria Coles
Dr. Dong Liang
Dean's Representative: Dr. Alexandra Bely

Preface

This dissertation contains four chapters, written in manuscript form, and appendices to all chapters. With the approval of the dissertation committee chair, Dr. Helen Baily, and other members of the dissertation committee, Chapter 1 of this dissertation is included as previously published research. The citation for the publication is provided at the beginning of the chapter and also mentioned here:

Chapter 1: Barbour, N., Shillinger, G.L., Hoover, A.L., Williamson, S.A., Coles, V.J., Liang, D., Fagan, W.F. and Bailey, H., 2020. Environmental and Biological Factors Influencing Dispersal of Neonate Leatherback Turtles (Dermochelys coriacea) From an Endangered Costa Rican Nesting Population. Frontiers in Marine Science, 7: 582933.

Dedication

This dissertation is dedicated to the pursuit of knowledge for the benefit of the curious mind and the conservation of life, with its many amazing forms, species, and processes (including movement).

Personally, I dedicate this work to:

- *My fellow community college students*: Your grades and the tortuosity of your paths do not define you. Your endurance, your passion, your focus, and your determination does. Dream big and achieve bigger by tackling your fears and never being afraid to ask for help or for what you want.
- *My fellow women in science*: Your voice is your own, whether it be soft, loud, bubbly, or serious. Your body is your own, it does not define your work or your professionalism. We must support each other, in science and in life.
- *My fellow members of the LGBTQ+ community*: You are never alone. Find your people and lean on them. Never let anyone limit your joy and your creativity.

Acknowledgements

This work would not have been possible without the financial, professional, and personal support I have received from numerous people. Nothing I write is short but here, the length is more than justified (and even constrained), as there are too many amazing people that have aided me professionally and personally up to this point.

Almost all of the fieldwork and data in my chapters were provided by and supported financially by Upwell (https://www.upwell.org/); I hope the work in my dissertation furthers their mission of research-based conservation for sea turtles at sea. Additional funding for fieldwork was provided generously by Dr. Bill Fagan and by an anonymous donor passionate about sea turtle research (distributed by University of Maryland Center for Environmental Science, UMCES, and Chesapeake Biological Lab, CBL)- thank you.

Personally, I have been financially supported in many ways over the years, including numerous University of Maryland (UMD) Teaching Assistant (TA) positions, Research Assistantship positions in both the Fagan and Bailey labs, the UMD COVID Relief Grant, the UMD Dean's Fellowship, and externally through a student contractor position with the Department of Defense. I have also had the pleasure of being funded and supported professionally by a SESYNC (National Socio-Environmental Synthesis Center, https://www.sesync.org/) Graduate Pursuits Fellowship, from which I have had the opportunity apply my skillsets to synthesis work crossing into other disciplines.

Additional, chapter-specific acknowledgements are owed to those that have contributed their time, work, data, code, feedback, and suggestions for my dissertation chapters. For chapter 1, thanks are owed to: Ecology Project International for beach access; Aimee Hoover and Dr. Sean Williamson for both sharing their data and helping collect my data; to the numerous volunteers and workers that contributed to the project, including Max Gotts, Noah Ashley, the students of the Nueva School, our boat captains Eugenio Sinclair and Elden Sinclair, and all of the field and other staff at the Pacuare Nature Reserve, Thanks also to my paper coauthors, for their contributions and helpful revisions, Dr, George Shillinger, Aimee Hoover, Dr. Sean Williamson, Dr. Victoria Coles, Dr. Dong Liang, Dr. Bill Fagan, and Dr. Helen Bailey. For chapters 2 and 3, the work would not have been possible without the generous sharing of data by Dr. George Shillinger (with special acknowledgements to the Block lab at Hopkins Marine Station and collaborators at the Tagging of Pacific Predators project). Additional thanks for chapters 2 and 3 are owed to: Dr. Alexander Robillard for his amazing work on the neural network model and online tool interface; Aimee Hoover's hard work getting my DM layers added to the South Pacific TurtleWatch tool; Dr. Elie Gurarie's guidance and mentorship on creating an HMM in Stan from scratch; to the folks at Mercator Ocean (Dr. Philippe Gaspar, Tony Candela, and Julien Temple-Boyer) for their guidance and always timely help; Mike O' Brien for sharing code to help run the DTW analysis; to Dr. Anshuman Swain, Dr. Julie Mallon, and Benjamin Yura for their ideas and examples; and to all my coauthors on these two papers for their contributions and hard work, including Dr. George Shillinger, Dr. Elie Gurarie, Dr. Alexander Robillard, Dr. David Secor, Dr.

Vyacheslav Lyubchich, Aimee Hoover, Dr. Bill Fagan, Dr. Helen Bailey, Dr. Phillipe Gaspar, Tony Candela, and Julien Temple-Boyer. For chapter 4, a long list of people have been a part of this exciting tagging effort. Thanks is owed at least to: everyone at the Cayman Turtle Centre for their hard work, collaboration, and contributions, especially Dr. Walter Mustin, Dr. Vandanaa Baboolal, and Dr. Francesca Casella; to our collaborators at FAU and the Wyneken lab, especially Dr. Jeanette Wyneken, Dr. Sean Williamson, and Emily Turla; to our collaborators at Mercator Ocean, including Dr. Philippe Gaspar, Tony Candela, Julien Temple-Boyer, and Antoine Laforge; and to our collaborators at Lotek, including Padraic O' Flaherty and Peter Leijen. Thank you all!

I would additionally like to personally thank my advisors, Dr. Helen Bailey and Dr. Bill Fagan, and all the members of my committee, Dr. David Secor, Dr. George Shillinger, Dr. Victoria Coles, and Dr. Dong Liang. Helen, I already said way too much in my overly-long farewell video, but I can't thank you enough for your mentorship over the years and for giving me a chance 5 years ago. I have learned so much, from state space models and plastic pollution impacts to dynamic management and being a tough woman in science. To Bill, I can't thank you enough either, for all the opportunities you have given me over the years and for your personal and financial support this last year especially. By being in your lab, I have developed incredibly in my quantitative skills and my confidence in myself. I look forward to the many collaborations I am sure we will have in the future. To the rest of the members of my committee, each of you has contributed to my growth as a scientist

and have additionally been wonderful people to work with- thank you so much, I look forward to (hopefully) more future collaborations with you all,

I have been incredibly lucky to have two academic "families" during my time at UMD and UMCES-CBL. My time here would not nearly have been as meaningful, fruitful, or fun without you all. Thank you to all my past and present lab members I have had the opportunity to work with. Namely, from the Bailey Lab: Dr. Alexander Robillard, Aimee Hoover, Amber Fandel, Lauren Rodriguez, Jamie Testa, and Kirsten Silva. Namely, from the Fagan Lab: Dr. Julie Mallon, Dr. Anshuman Swain, Dr. Elie Gurarie, Dr. JL Weissman, Dr. Chris Fleming, Dr. Jeff Demers, Stephanie Chia, Marron McConnell, Qianru Liao, and Frank McBride.

I have come so far over the years and my determination to challenge myself, pursue a PhD, and do "quantitative stuff" was sparked, enflamed, and encouraged by numerous other colleagues, mentors, and friends over the last couple decades. From my time at California State University Monterey Bay, thank you to the those who mentored me and helped me get into research full swing, including everyone in the Undergraduate Research Opportunities Center (UROC) and: Dr. Susan Alexander, Dr. Corey Garza, Dr. Mike Navarro, Dr. Nathaniel Jue, Dr. Alana Unfried, Dr. Steve Moore, Pamela Neeb Wade, and past lab members at the Marine Landscape Ecology Lab, Jesirae Collins, Charnelle Wickliff, Veronica Larwood, and Maddie Heard. From my time at Orange Coast College, I would not be where I am today without all of you, your encouragement, and your passion. Much thanks especially to: Dennis Kelly, Karen Baker, Rob Ellis, Mary Blasius, Kelli Elliott, Marc Perkins, and the many others I have had the opportunity to befriend and work with in the Marine

Science department. Additionally, thank you to all the wonderful external collaborators and mentors that have supported me in my academic journey, especially: Dr. Kayla Causey, Mike Makofske and the OC American Cetacean Society, Kera Mathes, and Dr. Maddalena Bearzi.

Finally, my most personal of thanks, to the close friends and family that have supported me and stood by my side for the last 5 years. To my parents, Mark and Lori, thank you for your love, your financial support, and for your passion of nature and science (my mom) and writing (my dad), that you have passed onto me. Love and thanks to my siblings and other family members that have supported me, including Grace, Reuben, Yuri, Victoria, Cat, and my Aunt Linda. To my West coast besties, I love you all dearly and your continued friendship is treasured; thank you for your support, especially Shelby and Erika. To my East coast besties and queer community: thank you for keeping me fabulous, giving me a place to vent or cry or laugh, and for being my safe place in a crazy world, I love you all: Eva, Julie, Dani, Zeke, JL, Simone, Molly, Rylan, Matt, and Linda. To my other family, Laurie and Rachael, in the brief time I have known you, you have already provided me with much comfort, love, and acceptance, thank you and I love you both. And the best for last, my partner Ben. You have been my rock through one of the hardest and best years of my life. You love me so selflessly. I don't know what I would have done without your smile, your wit and humor, your ideas, your hugs, your constant presence, and your love (through many sleepless nights) to get me over the finish line. Thank you. I love you so much and I know that with you, what I do next will be a joy despite any challenge.

Table of Contents

List of Tables

(Main tables by chapter)

List of Figures

(Main figures by chapter)

Introduction

Movement ecology is a relatively recent discipline (Nathan et al 2008), that unifies a breadth of research on animal movement. It seeks to understand the "what, why, when, where, and how" of movement by focusing on the movements (spatial displacements) of individuals (Nathan et al 2008). This understanding of individuality or variation in movement allows for behavioral ecology to expand beyond just a mean comprehension of spatial-temporal habitat use for a given group of animals (Shaw 2020). Deriving both the mean and the variance of movement with respect to its inferred causes (e.g. abiotic factors) can provide a holistic understanding of both collective and individual behavior and habitat use (Shaw 2020). Movement ecology provides a bottoms-up approach to studying animal behavior that is increasingly important in studies with broader impacts in biodiversity and conservation science (Allen and Singh 2016, Jeltsch et al 2013). Variation in individual movement and behavior can extend its impacts to various ecological levels (population, community, ecosystem) (Shaw 2020) and affect ecological stability in ways that are increasingly critical to understand in the face of global climate change and heightened anthropogenic effects on natural systems (Jeltsch et al 2013).

Parsing an individual movement path into distinct behaviors that can be related to external or internal drivers relies on being able to distill it into a series of phases or movement segments (Nathan et al 2008). Quantitatively, these segments are derived from time-indexed spatial (e.g., latitude, longitude) positions, with the spatial and temporal scale of these positions and the behaviors they can be used to infer often

reliant on the sampling rate of the biotelemetry instruments used to track the individual (e.g., acoustic, ARGOS satellite, GPS) (Williams et al 2020). Behavioral segments can be characterized by various movement metrics (Edelhoff et al 2016), often by the distribution of step lengths (straight line distance between locations) or turning angles (relative angle of difference between locations) (Morales et al 2003) but also by speeds, persistence or turning velocities (tendency to persist in a given or opposite direction, respectively) (Gurarie et al 2009), net squared displacements (squared displacement between first and current location) (Turchin 1998, Bailey and Thompson 2006), first passage times (time to pass through circle with given radius) (Fauchald and Tverra 2003), and straightness indices (ratio of straight line distance between start to end location and total actual distance traveled) (Gaspar et al 2006). Determining behavior using metrics such as these can come from a variety of approaches (Edelhoff et al 2016), including topological (e.g., clustering analyses, Cleasby et al 2019), time-series (e.g., change-point analyses, Gurarie et al 2017) and process identification (e.g., Hidden Markov or state space models, Patterson et al 2008, 2009) methods. The recent and rapid evolution of open-source software packages with user-friendly interfaces for movement ecologists have made complex behavioral segmentation methods for large datasets more efficient and accessible (Joo et al 2020).

The ecological significance of movement-based behaviors can be determined by connecting identified behaviors with environmental, physical, and/or biological variables occurring or changing at the same spatial-temporal scale, although this can be challenged by the resolution of the data available (Scales et al 2016). The

advancement of technology, producing biologging (tag) devices with ever smaller sizes, longer durations, and a variety of extra sensors (e.g., for air pressure and temperature, heart-rate), has allowed for both internal and external drivers of movement to be measured simultaneously with locational data (Williams et al 2020). Additionally, movement data can be coupled with remote sensing data (Neumann et al 2015, Scales et al 2016), compared to individual-based simulations (Brosnan and Welch 2020), or validated with video or audio recordings (Williams et al 2020) to understand relationships of individuals with their environment. These approaches in combination with movement models have been especially beneficial for the studies of animals with cryptic and long-distance movements, such as birds (e.g., albatross, Connors et al 2021, and turkey vultures, Mallon et al 2021), bats (e.g., Mexican fish-eating bats, Hurme et al 2019), fish (e.g., salmon sharks, Coffey et al 2017,and skipjack tuna, Phillips et al 2018), ungulates (e.g., caribou, Gurarie et al 2019), and reptiles (e.g., green sea turtle, Hays et al 2020, and loggerhead sea turtle, Narazaki et al 2013).

Sea turtles are an especially interesting study system in movement ecology, being long-lived, oceanic reptiles that associate with a variety of habitats (e.g., coastal beaches, pelagic or neritic ocean zones) and have both intra- and inter-specific variability to their movement ecologies (Godley et al 2008, Southwood and Avens 2010). Most species of sea turtle have ontogenetic niche shifts in habitat use, starting with a developmental oceanic phase as neonates (previously termed the “Lost Years”, Carr 1987), followed by recruitment as juveniles to either neritic (e.g., green, Kemp’s ridley, loggerhead turtles) or pelagic habitats (e.g., leatherback and Olive ridley

turtles), and then alternations between coastal nesting beaches, pelagic foraging, and/or neritic inter-nesting or foraging habitats as adults (Southwood and Avens 2010). These series of ontogenetic movement phases can each occur over the period of years and massive spatial scales (Hays and Scott 2013), and the limited durations of even long-lasting biologging devices have often prevented movements between consecutive life stage phases from being empirically studied (Hazen et al 2012, Luschi et al 2013). For many sea turtle species, movement ecology studies have been biased to females and during the inter-nesting phase, due to challenges in tagging juveniles (larger tag-to-body size ratios, higher mortalities, Shillinger et al 2012) and limited accessibility to males. Additionally, of those studies that have measured long-distance, offshore migrations for sea turtles, there is a need to expand understandings of their movement to incorporate behavior in both horizontal and vertical space, as sea turtles occur in a fluid environment where resources occur on spatial-temporal gradients that vary in both dimensions (Steele 1989, Scales et al 2014) and produce behaviors at depth concealed by descriptions of horizontal movement alone (Wallace et al 2015).

This dissertation seeks to understand the movement ecology of sea turtles through the use of biotelemetry data, with a variety of sea turtle species and life stages represented. Specifically, this dissertation will use a variety of quantitative methods with sea turtle movement data to understand external (e.g., abiotic factors) and internal (e.g., body morphometrics) drivers of variability in movement paths, informing questions of ontogenetic differences in movement and broadly, using movement-derived behaviors to inform dynamic habitat and management tools.

Although not nearly comprehensive of the inter-specific and ontogenetic variety present in the movement ecology of sea turtles, the findings and methods presented have some novel and interesting applications to other sea turtle species, life stages, and other mobile taxa. Below, I provide a brief summary of each chapter and conclude with key takeaways for sea turtle science, movement ecology, and conservation science from this work.

In chapter 1, relationships between the physical environment and the early dispersal trajectories of neonate turtles are examined. The movements of neonate turtles during their "frenzy" stage, where they maintain high energy and directed swimming to rapidly displace themselves into deeper waters far from shore (Wyneken and Salmon 1992), have remained mostly enigmatic, due to challenges in tagging and observing turtles this small (Shillinger et al 2012). For the studies that have characterized neonate early dispersal, they have focused mainly on Chelonian (hard-shelled) species (Okuyama et al 2009, Thums et al 2013, Scott et al 2014, Thums et al 2016) and/or not incorporated environmental data (Thums et al 2013, Gearheart et al 2011) to understand the external drivers of movement. To address these knowledge gaps, I used a variety of movement metrics and models applied to a large dataset (N=94) of acoustically tracked Caribbean leatherback turtles (*Dermochelys coriacea*) and a suite of data encompassing potential external and internal drivers of their movement (surface current velocities, local wind speeds, body sizes). Overall, this chapter demonstrates a rigorous analysis of the variability possible for neonates during their early dispersal and highlights the importance of incorporating environmental and biological variables into models of their movement

during this phase. Although the scale of movement examined in this chapter is small relative to other movement phases in their migration, the results demonstrate variation in individual movement for Caribbean leatherbacks that may have scaled up effects on other life stages or population-level processes (Shaw 2020), if their differences in movement carry over into impacting their long-term survival (O'Connor et al 2014).

In chapter 2, a novel approach to identifying hierarchical dive behaviors for sea turtles is demonstrated. In lieu of having accelerometry (Fossette et al 2010), beak movement (Fossette et al 2008), video (Seminoff et al 2006), and/or high-quality positional data, the interpretation of subsurface movements for sea turtles has often relied on using time-at-depth (TAD) profiles from biologgers with pressure sensors (Hochscheid 2014). Dive profiles for sea turtles have been previously characterized to have 7 general shapes (Hochscheid 2014) that can fall into larger groups of dives characterized by their shared similarity in quantitative metrics (e.g., depth, duration). Leatherbacks are a key model organism for studying dive behavior, as they are deep and regular divers that spend almost their entire lives in pelagic waters, performing long-distance migrations into ocean gyres (Luschi 2013) and foraging on ephemeral patches of gelatinous zooplankton at a variety of depths (Wallace et al 2006, 2015). I applied both a clustering analysis and a convolutional neural network (CNN) model to a large and coarse dataset of Eastern Pacific (EP) adult leatherback dive profiles to, respectively, cluster dives into quantitatively similar groups and then label dives within each cluster by their standard shape. Ecological importance and abiotic drivers of different identified dive clusters was investigated using a statistical model with environmental variables. This chapter provided a method for determining

hierarchical, vertical behaviors from telemetry data that can be incorporated into movement and habitat models for leatherbacks in the Eastern Pacific, as previous efforts relying only on horizontal movement metrics (e.g., step lengths and turning angles) have had difficulty parsing out distinct behaviors, such as foraging and transiting (Bailey et al 2012).

In chapter 3, the findings of chapter 2 were extended to both a comprehensive movement model and a movement-based conservation tool for the EP leatherback population. Conservation for mobile and migratory species is often challenged by the wide-ranging or phenological nature of their movements (Fraser et al 2018) and even more so for marine fauna, which have a vertical dimension to their movements rarely incorporated in movement-based management tools (e.g., EcoCast, Hazen et al 2018; TurtleWatch, Howell et al 2008, 2015; WhaleWatch, Hazen et al 2017). I created a Hidden Markov model (HMM) that determines discrete behaviors based on both vertical and horizontal movement metrics, incorporating the dive clusters from chapter 2 with satellite-tag derived locational data for adult EP leatherbacks. A dynamic management (DM) tool (Lewison et al 2015) was developed by combining HMM behavioral states with monthly kernel density estimates and threat (fisheries effort) data. EP leatherbacks are critically endangered, primarily due to harmful interactions with fisheries in international waters (Spotila et al 2000, Ábrego et al 2020). This chapter provided a novel tool for quantifying dynamic, temporal overlap of turtles in distinct, multidimensional behavioral states with different types of fishing gear, with results being incorporated into ongoing conservation work for this

population (e.g., South Pacific TurtleWatch, Hoover et al 2019, Degenford et al 2021).

In chapter 4, miniature satellite tags were deployed on multiple age classes of post-captive green turtles (*Chelonia mydas*) to determine ontogenetic differences in movement. Green sea turtles on the Cayman Islands were almost completely extirpated by human exploitation (Groombridge 1982) and although current anthropogenic pressures are still impacting population growth (Bell et al 2006, 2007, Blumenthal et al 2021), previous mass releases of captive-raised neonates, juveniles, and adults seem to have restored a local nesting population (Bell et al 2005). As the only movement data available for this population have been for a handful of adults (Blumenthal et al 2006) and mark-recaptures of post-captives in neritic fishing grounds (Bell et al 2005, Moncada et al 2006), questions remain as to the movement ecology of Caribbean green sea turtles across age classes. To address this, a large sample size (N=40) of juvenile captive-raised turtles across three age classes (1-2, 2-3, and 3-4 years) was released by boat from the Cayman Islands, with release effects additionally being explored by releasing turtles from two different locations and times of year. Movement and behavioral analyses were performed using a combination of methods, including behavioral clustering, individual comparisons of current-corrected tracks with empirical and simulated passive-drift tracks, and a statistical model to determine the probability of movement-based behaviors with environmental variables and different body sizes. This chapter informs future conservation and headstarting efforts for the Cayman population of green turtles. Results also provide important

findings in sea turtle movement ecology on the external drivers of juvenile dispersal and timing of recruitment to developmental habitats.

To conclude, this dissertation work uses a variety of quantitative approaches to understand movement ecology and behavior from biotelemetry data for multiple sea turtle species (leatherback and green) and life stages (neonate, juvenile, adult). Results address some primary questions in marine megafauna movement ecology, including the role of the physical environment in driving variability in individual movement behaviors (Hays 2016) and the movement ecology of neonates and juveniles (Hazen et al 2012). Each chapter additionally provides recommendations for future work and broader impacts with regards to conservation and management, as one of the key challenges for studies of mobile and migratory animals is extending results so that they go beyond just the gain of knowledge and provide relevant and accessible movement-based products that can be integrated with conservation policy and management efforts on similar scales (Allen and Singh 2016, Fraser et al 2018, Maxwell et al 2015). Although much remains to be done, it is my hope that this dissertation is both useful for "real-world" conservation of sea turtles and inspires future work that integrates movement ecology with quantitative approaches and a variety of (abiotic, biotic, physiological, behavioral) data to address the "what, why, when, where, and how" of movement for multiple species and life stages.

References

Ábrego, M.E. et al. (2020) 'Enhanced, coordinated conservation efforts required to avoid extinction of critically endangered Eastern Pacific leatherback turtles', Scientific Reports, 10(1), p. 4772. Available at: https://doi.org/10.1038/s41598-020-60581-7.

Allen, A.M. and Singh, N.J. (2016) 'Linking Movement Ecology with Wildlife Management and Conservation', Frontiers in Ecology and Evolution, 3. Available at: https://www.frontiersin.org/articles/10.3389/fevo.2015.00155 (Accessed: 23 September 2022).

Bailey, H. et al. (2012) 'Identification of distinct movement patterns in Pacific leatherback turtle populations influenced by ocean conditions', Ecological Applications, 22(3), pp. 735–747. Available at: https://doi.org/10.1890/11-0633.

Bailey, H. and Thompson, P. (2006) 'Quantitative analysis of bottlenose dolphin movement patterns and their relationship with foraging', Journal of Animal Ecology, 75(2), pp. 456–465. Available at: https://doi.org/10.1111/j.1365-2656.2006.01066.x.

Bell, C.D. et al. (2006) 'Traditional Caymanian fishery may impede local marine turtle population recovery', Endangered Species Research, 2, pp. 63–69. Available at: https://doi.org/10.3354/esr002063.

Bell, C.D. et al. (2007) 'Monitoring and conservation of critically reduced marine turtle nesting populations: lessons from the Cayman Islands', Animal Conservation, 10(1), pp. 39–47. Available at: https://doi.org/10.1111/j.1469-1795.2006.00068.x.

Bell, C.D.L. et al. (2005) 'Some of them came home: the Cayman Turtle Farm headstarting project for the green turtle Chelonia mydas', Oryx, 39(2), pp. 137–148. Available at: https://doi.org/10.1017/S0030605305000372.

Blumenthal, J.M. et al. (2021) 'Cayman Islands Sea Turtle Nesting Population Increases Over 22 Years of Monitoring', Frontiers in Marine Science, 8. Available at:

https://www.frontiersin.org/articles/10.3389/fmars.2021.663856 (Accessed: 23 September 2022).

Brosnan, I.G. and Welch, D.W. (2020) 'A model to illustrate the potential pairing of animal biotelemetry with individual-based modeling', Animal Biotelemetry, 8(1), p. 36. Available at: https://doi.org/10.1186/s40317-020-00221-z.

Carr, A. (1987) 'New Perspectives on the Pelagic Stage of Sea Turtle Development', Conservation Biology, 1(2), pp. 103–121. Available at: https://doi.org/10.1111/j.1523-1739.1987.tb00020.x.

Cleasby, I.R. et al. (2019) 'Using time-series similarity measures to compare animal movement trajectories in ecology', Behavioral Ecology and Sociobiology, 73(11), p. 151. Available at: https://doi.org/10.1007/s00265-019-2761-1.

Coffey, D.M. et al. (2017) 'Oceanographic drivers of the vertical distribution of a highly migratory, endothermic shark', Scientific Reports, 7(1), p. 10434. Available at: https://doi.org/10.1038/s41598-017-11059-6.

Conners, M.G. et al. (2021) 'Hidden Markov models identify major movement modes in accelerometer and magnetometer data from four albatross species', Movement Ecology, 9(1), p. 7. Available at: https://doi.org/10.1186/s40462-021-00243-z.

Degenford, J.H. et al. (2021) 'Using fisheries observation data to develop a predictive species distribution model for endangered sea turtles', Conservation Science and Practice, 3(2), p. e349. Available at: https://doi.org/10.1111/csp2.349.

Edelhoff, H., Signer, J. and Balkenhol, N. (2016) 'Path segmentation for beginners: an overview of current methods for detecting changes in animal movement patterns', Movement Ecology, 4(1), p. 21. Available at: https://doi.org/10.1186/s40462-016-0086-5.

Fauchald, P. and Tveraa, T. (2003) 'Using First-Passage Time in the Analysis of Area-Restricted Search and Habitat Selection', Ecology, 84(2), pp. 282–288. Available at: https://doi.org/10.1890/0012-9658(2003)084[0282:UFPTIT]2.0.CO;2.

Fossette, S. et al. (2008) 'Dive and beak movement patterns in leatherback turtles Dermochelys coriacea during internesting intervals in French Guiana', Journal of Animal Ecology, 77(2), pp. 236–246. Available at: https://doi.org/10.1111/j.1365-2656.2007.01344.x.

Fossette, S. et al. (2010) 'Behaviour and buoyancy regulation in the deepest-diving reptile: the leatherback turtle', Journal of Experimental Biology, 213(23), pp. 4074–4083. Available at: https://doi.org/10.1242/jeb.048207.

Fraser, K.C. et al. (2018) 'Tracking the Conservation Promise of Movement Ecology', Frontiers in Ecology and Evolution, 6. Available at: https://www.frontiersin.org/articles/10.3389/fevo.2018.00150 (Accessed: 23 September 2022).

Gaspar, P. et al. (2006) 'Marine animal behaviour: neglecting ocean currents can lead us up the wrong track', Proceedings of the Royal Society B: Biological Sciences, 273(1602), pp. 2697–2702. Available at: https://doi.org/10.1098/rspb.2006.3623.

Gearheart, G. et al. (2011) 'Tracking leatherback (Dermochelys coriacea) hatchlings at sea using radio and acoustic tags', Mar. Turt. Newsl, 130, pp. 2–6.

Godley, B.J. et al. (2008) 'Satellite tracking of sea turtles: Where have we been and where do we go next?', Endangered Species Research, 4(1–2), pp. 3–22. Available at: https://doi.org/10.3354/esr00060.

Groombridge, B. and Wright, L. (1982) 'The IUCN amphibia-reptilia red data book, Part 1', IUCN, Gland, Switzerland [Preprint].

Gurarie, E. et al. (2017) ‘Correlated velocity models as a fundamental unit of animal movement: synthesis and applications’, Movement Ecology, 5(1), p. 13. Available at: https://doi.org/10.1186/s40462-017-0103-3.

Gurarie, E. et al. (2019) ‘Tactical departures and strategic arrivals: Divergent effects of climate and weather on caribou spring migrations’, Ecosphere, 10(12), p. e02971. Available at: https://doi.org/10.1002/ecs2.2971.

Gurarie, E., Andrews, R.D. and Laidre, K.L. (2009) ‘A novel method for identifying behavioural changes in animal movement data’, Ecology Letters, 12(5), pp. 395–408. Available at: https://doi.org/10.1111/j.1461-0248.2009.01293.x.

Hays, G.C. et al. (2016) ‘Key Questions in Marine Megafauna Movement Ecology’, Trends in Ecology & Evolution, 31(6), pp. 463–475. Available at: https://doi.org/10.1016/j.tree.2016.02.015.

Hays, G.C. et al. (2020) ‘Open Ocean Reorientation and Challenges of Island Finding by Sea Turtles during Long-Distance Migration’, Current Biology, 30(16), pp. 3236-3242.e3. Available at: https://doi.org/10.1016/j.cub.2020.05.086.

Hays, G.C. and Scott, R. (2013) ‘Global patterns for upper ceilings on migration distance in sea turtles and comparisons with fish, birds and mammals’, Functional Ecology, 27(3), pp. 748–756. Available at: https://doi.org/10.1111/1365-2435.12073.

Hazen, E.L. et al. (2012) ‘Ontogeny in marine tagging and tracking science: technologies and data gaps’, Marine Ecology Progress Series, 457, pp. 221–240. Available at: https://doi.org/10.3354/meps09857.

Hazen, E.L. et al. (2017) ‘WhaleWatch: a dynamic management tool for predicting blue whale density in the California Current’, Journal of Applied Ecology, 54(5), pp. 1415–1428. Available at: https://doi.org/10.1111/1365-2664.12820.

Hazen, E.L. et al. (2018) ‘A dynamic ocean management tool to reduce bycatch and support sustainable fisheries’, Science Advances, 4(5), p. eaar3001. Available at: https://doi.org/10.1126/sciadv.aar3001.

Hochscheid, S. (2014) ‘Why we mind sea turtles’ underwater business: A review on the study of diving behavior’, Journal of Experimental Marine Biology and Ecology, 450, pp. 118–136. Available at: https://doi.org/10.1016/j.jembe.2013.10.016.

Hoover, A.L. et al. (2019) ‘Predicting residence time using a continuous-time discrete-space model of leatherback turtle satellite telemetry data’, Ecosphere, 10(3), p. e02644. Available at: https://doi.org/10.1002/ecs2.2644.

Howell, E.A. et al. (2008) ‘TurtleWatch: a tool to aid in the bycatch reduction of loggerhead turtles Caretta caretta in the Hawaii-based pelagic longline fishery’, Endangered Species Research, 5(2–3), pp. 267–278. Available at: https://doi.org/10.3354/esr00096.

Howell, E.A. et al. (2015) ‘Enhancing the TurtleWatch product for leatherback sea turtles, a dynamic habitat model for ecosystem-based management’, Fisheries Oceanography, 24(1), pp. 57–68. Available at: https://doi.org/10.1111/fog.12092.

Hurme, E. et al. (2019) ‘Acoustic evaluation of behavioral states predicted from GPS tracking: a case study of a marine fishing bat’, Movement Ecology, 7(1), p. 21. Available at: https://doi.org/10.1186/s40462-019-0163-7.

Jeltsch, F. et al. (2013) ‘Integrating movement ecology with biodiversity research - exploring new avenues to address spatiotemporal biodiversity dynamics’, Movement Ecology, 1(1), p. 6. Available at: https://doi.org/10.1186/2051-3933-1-6.

Joo, R. et al. (2020) ‘Navigating through the r packages for movement’, Journal of Animal Ecology, 89(1), pp. 248–267. Available at: https://doi.org/10.1111/1365-2656.13116.

Lewison, R. et al. (2015) ‘Dynamic Ocean Management: Identifying the Critical Ingredients of Dynamic Approaches to Ocean Resource Management’, BioScience, 65(5), pp. 486–498. Available at: https://doi.org/10.1093/biosci/biv018.

Luschi, P. (2013) ‘Long-distance animal migrations in the oceanic environment: orientation and navigation correlates’, International Scholarly Research Notices, 2013.

Mallon, J.M., Bildstein, K.L. and Fagan, W.F. (2021) ‘Inclement weather forces stopovers and prevents migratory progress for obligate soaring migrants’, Movement Ecology, 9(1), p. 39. Available at: https://doi.org/10.1186/s40462-021-00274-6.

Maxwell, S.M. et al. (2015) ‘Dynamic ocean management: Defining and conceptualizing real-time management of the ocean’, Marine Policy, 58, pp. 42–50. Available at: https://doi.org/10.1016/j.marpol.2015.03.014.

Morales, J.M. et al. (2004) ‘Extracting More Out of Relocation Data: Building Movement Models as Mixtures of Random Walks’, Ecology, 85(9), pp. 2436–2445. Available at: https://doi.org/10.1890/03-0269.

Narazaki, T. et al. (2013) ‘Loggerhead Turtles (Caretta caretta) Use Vision to Forage on Gelatinous Prey in Mid-Water’, PLOS ONE, 8(6), p. e66043. Available at: https://doi.org/10.1371/journal.pone.0066043.

Nathan, R. et al. (2008) ‘A movement ecology paradigm for unifying organismal movement research’, Proceedings of the National Academy of Sciences, 105(49), pp. 19052–19059. Available at: https://doi.org/10.1073/pnas.0800375105.

Neumann, W. et al. (2015) ‘Opportunities for the application of advanced remotely-sensed data in ecological studies of terrestrial animal movement’, Movement Ecology, 3(1), p. 8. Available at: https://doi.org/10.1186/s40462-015-0036-7.

O'Connor, C.M. et al. (2014) 'Biological carryover effects: linking common concepts and mechanisms in ecology and evolution', Ecosphere, 5(3), p. art28. Available at: https://doi.org/10.1890/ES13-00388.1.

Okuyama, J. et al. (2009) 'Ontogeny of the dispersal migration of green turtle (Chelonia mydas) hatchlings', Journal of Experimental Marine Biology and Ecology, 379(1), pp. 43–50. Available at: https://doi.org/10.1016/j.jembe.2009.08.008.

Patterson, T. et al. (2008) 'State–space models of individual animal movement', Trends in Ecology & Evolution, 23(2), pp. 87–94. Available at: https://doi.org/10.1016/j.tree.2007.10.009.

Patterson, T.A. et al. (2009) 'Classifying movement behaviour in relation to environmental conditions using hidden Markov models', Journal of Animal Ecology, 78(6), pp. 1113–1123. Available at: https://doi.org/10.1111/j.1365-2656.2009.01583.x.

Scales, K.L. et al. (2014) 'REVIEW: On the Front Line: frontal zones as priority at-sea conservation areas for mobile marine vertebrates', Journal of Applied Ecology, 51(6), pp. 1575–1583. Available at: https://doi.org/10.1111/1365-2664.12330.

Scales, K. L., Hazen, E. L., Jacox, M. G., Edwards, C. A., Boustany, A. M., Oliver, M. J., & Bograd, S. J. (2017). Scale of inference: on the sensitivity of habitat models for wide-ranging marine predators to the resolution of environmental data. Ecography, 40(1), 210-220. Available at: https://doi.org/10.1111/ecog.02272

Scott, R. et al. (2014) 'Nano-tags for neonates and ocean-mediated swimming behaviours linked to rapid dispersal of hatchling sea turtles', Proceedings of the Royal Society B: Biological Sciences, 281(1796), p. 20141209. Available at: https://doi.org/10.1098/rspb.2014.1209.

Scutt Phillips, J. et al. (2018) 'An individual-based model of skipjack tuna (Katsuwonus pelamis) movement in the tropical Pacific ocean', Progress in Oceanography, 164, pp. 63–74. Available at: https://doi.org/10.1016/j.pocean.2018.04.007.

Seminoff, J.A., Jones, T.T. and Marshall, G.J. (2006) 'Underwater behaviour of green turtles monitored with video-time-depth recorders: what's missing from dive profiles?', Marine Ecology Progress Series, 322, pp. 269–280. Available at: https://doi.org/10.3354/meps322269.

Shaw, A.K. (2020) 'Causes and consequences of individual variation in animal movement', Movement Ecology, 8(1), p. 12. Available at: https://doi.org/10.1186/s40462-020-0197-x.

Shillinger, G.L. et al. (2012) 'Tagging through the stages: technical and ecological challenges in observing life histories through biologging', Marine Ecology Progress Series, 457, pp. 165–170. Available at: https://doi.org/10.3354/meps09816.

Southwood, A. and Avens, L. (2010) 'Physiological, behavioral, and ecological aspects of migration in reptiles', Journal of Comparative Physiology B, 180(1), pp. 1–23. Available at: https://doi.org/10.1007/s00360-009-0415-8.

Spotila, J.R. et al. (2000) 'Pacific leatherback turtles face extinction', Nature, 405(6786), pp. 529–530. Available at: https://doi.org/10.1038/35014729.

Steele, J.H. (1989) 'The ocean "landscape"', Landscape Ecology, 3(3), pp. 185–192. Available at: https://doi.org/10.1007/BF00131537.

Turchin, P. (1998) Quantitative Analysis of Movement: Measuring and Modeling Population Redistribution in Animals and Plants. Sinauer Associates, Inc., Sunderland, USA.

Thums, M. et al. (2013) 'Tracking sea turtle hatchlings — A pilot study using acoustic telemetry', Journal of Experimental Marine Biology and Ecology, 440, pp. 156–163. Available at: https://doi.org/10.1016/j.jembe.2012.12.006.

Thums, M. et al. (**2016**) 'Artificial light on water attracts turtle hatchlings during their near shore transit', Royal Society Open Science, 3(5), p. 160142. Available at: https://doi.org/10.1098/rsos.160142.

Wallace, B.P. et al. (2006) 'Energy budget calculations indicate resource limitation in Eastern Pacific leatherback turtles', Marine Ecology Progress Series, 318, pp. 263–270. Available at: https://doi.org/10.3354/meps318263.

Wallace, B.P., Zolkewitz, M. and James, M.C. (2015) 'Fine-scale foraging ecology of leatherback turtles', Frontiers in Ecology and Evolution, 3. Available at: https://www.frontiersin.org/articles/10.3389/fevo.2015.00015 (Accessed: 23 September 2022).

Williamson, M.J. et al. (2021) 'Analysing detection gaps in acoustic telemetry data to infer differential movement patterns in fish', Ecology and Evolution, 11(6), pp. 2717–2730. Available at: https://doi.org/10.1002/ece3.7226.

Wyneken, J. and Salmon, M. (1992) 'Frenzy and Postfrenzy Swimming Activity in Loggerhead, Green, and Leatherback Hatchling Sea Turtles', Copeia, 1992(2), pp. 478–484. Available at: https://doi.org/10.2307/1446208.

Chapter 1: Environmental and biological factors influencing dispersal of neonate leatherback turtles (*Dermochelys coriacea*) from an endangered Costa Rican nesting population

The contents of this chapter have been published as:

Barbour, N., Shillinger, G.L., Hoover, A.L., Williamson, S.A., Coles, V.J., Liang, D., Fagan, W.F. and Bailey, H., 2020. Environmental and Biological Factors Influencing Dispersal of Neonate Leatherback Turtles (Dermochelys coriacea) From an Endangered Costa Rican Nesting Population. Frontiers in Marine Science, 7: 582933.

Abstract

Quantifying early life movements is essential to understanding migratory pathways and habitat use that can impact individuals' success later in life. To gauge how neonatal movements set the stage for later habitat use, we tracked neonate leatherback turtles (n=94) with acoustic tags from Pacuare, Costa Rica, in 2016 and 2018. We analyzed movements using a first passage time analysis and random walk models, the results of which indicated neonates followed a fixed compass direction as they traveled away from shore and that strong currents in these areas resulted in advection. We combined the tracking data with concurrent environmental variables in a generalized additive mixed model framework. Our results showed the south-east current flow in this area has spatial and temporal structure consistent with large-scale geostrophic currents and not tidal current or local wind speed influences. After accounting for advection by currents, true neonate swimming speed was significantly related to current speed, first passage time, and the year. Neonates had three main response strategies to currents above 0.5 m s^{-1}, with most increasing their swimming speed and the rest maintaining either a constant or decreased swimming speed.

Neonates were significantly larger in 2018 than in 2016 but their average swimming speed was not significantly related to body size, indicating that environmental factors were more important contributors to their dispersal. We conclude that abiotic factors, including the strength and direction of the currents, significantly affect the swimming and dispersal strategy of neonate leatherback turtles and these results can help to inform strategies for releases of neonate turtles from hatcheries, future tracking studies, and conservation efforts.

Introduction

Advancements in biotelemetry have helped bridge the gap between animals' fine and broad-scale movement patterns, opening up new opportunities for the movement ecology of different life stages to be quantified and understood (Nathan et al. 2008). Biotelemetric monitoring is especially important for understanding individuals' movements in settings where direct observations are complicated or obscured, such as the marine environment. However, the need to attach biotelemetric instruments either directly to, or in, an organism has created limitations for studying the movements of young life stages, which may experience larger tag-to-body size ratios and higher natural mortality rates (Shillinger et al. 2012a, Hazen et al. 2012a). Although satellite tags have become progressively smaller in size and capable of attachment to the larger juvenile life stages for animals such as birds, sharks, sea turtles, and marine mammals (Kjellén et al. 2001, Vincent et al. 2002, Hsu et al. 2007, Weng et al. 2007, Mansfield et al. 2014), their application on the much smaller, dispersing neonate phase is limited. Tagging of this vulnerable life stage has most often been applied to the fledgling stage in birds (Hake et al. 2001, Hake et al. 2003,

Kooyman and Ponganis 2008, Cadahía et al. 2010, Péron and Grémillet 2013, Vega et al. 2016). This leaves a knowledge gap for many other migratory species, wherein the links between neonate fine-scale distribution and adult long-term movement paths remain unknown (Hays et al. 2010). Characterizing this early life stage is important, as the movement and behavioral responses of neonates to different environmental conditions could potentially have carryover effects on the distribution, energetics, or survival of later life stages (O'Connor et al. 2014).

The habitat uses of adult marine animals has been characterized using biotelemetry in combination with advanced statistical models (Block et al. 2011, Hazen et al. 2012a) but there is a need for the application of these methods to other life stages. Statistical tools such as first passage time analyses can allow for the detection of changes in speed in response to environmental conditions at different spatial scales (Fauchald and Tveraa 2003) and mechanistic movement models such as random walk models (Turchin 1998), can provide further insight into behavioral processes and states. The application of such approaches to the movement trajectories of marine species has allowed for migratory and foraging behavior (Bailey et al. 2006, Hurme et al. 2019) and navigational abilities (Girard et al. 2006) to be inferred for adult life stages.

Sea turtles are highly migratory species and research on their dispersal has been biased towards adult breeding females, since they can be satellite tagged on the beach and tracked globally for relatively long periods of time (Hays et al. 2006, Shillinger et al. 2008, Shillinger et al. 2011, Fossette et al. 2014). The behavior and habitat associations of neonate turtles during their early dispersal has been

characterized for some species using tracking technology (Okuyama et al 2009, Gearheart et al. 2011, Thums et al. 2013, Scott et al. 2014, Thums et al. 2016), field observations (Frick 1976, Lohmann and Lohmann 1992), and laboratory studies (Lohmann et al. 1990, Wyneken et al. 1990, Goff et al. 1998, Smith and Salmon 2009). Sea turtles have been shown to disperse from the nesting beach in a non-random fashion (Pilcher et al. 2000), using a mixture of geomagnetic information (Lohmann and Lohmann 1993, Light et al. 1993, Lohmann and Lohmann 1994), and environmental cues, such as the direction of surface waves, to set a fixed compass direction into deeper waters (Frick 1976, Lohmann et al. 1990, Wyneken et al. 1990, Lohmann and Lohmann 1996, Pilcher et al. 2000). Neonate sea turtles undergo a "frenzy" period of continuous and highly energetic swimming lasting around 24 hours during their dispersal from the nesting beach that serves to quickly transpose them into deeper waters (Wyneken and Salmon 1992). In the small number of studies conducted on neonate leatherbacks, they have been shown to be efficient dispersers during their frenzy stage, with a smaller aerobic scope than other species (Jones et al. 2007), steady swimming speeds, and moderate metabolic rates (Wyneken & Salmon 1992, Jones et al. 2007, Hoover et al. 2020).

Consequently, variability in ocean currents that result in displacement of neonates from their intended path may require different behavioral strategies in response, potentially having long-term carry over effects on their movement and distribution in older life stages (Mansfield et al. 2009, Benson et al. 2011, Shillinger et al. 2012b, O'Connor et al. 2014). Two main hypotheses on long-term carry over effects with respect to neonate and juvenile turtle dispersal have been considered

previously: 1) successful dispersal of neonates/juveniles by ocean currents determines where they will forage as adults (Hays et al. 2010, Gaspar et al. 2012, Scott et al. 2014, Lalire and Gaspar 2019), and 2) successful dispersal of neonates/juveniles into ocean currents determines population abundance at the natal beaches, as seen with regional variation in nesting densities on beaches close to favorable ocean currents (Putman et al. 2010a, Putman et al. 2010b, Okuyama et al. 2010, Shillinger et al. 2012b, Putman 2018, DuBois et al. 2020). The impact of local temporally and/or spatially heterogeneous current structures on the behavioral swimming response of dispersing neonates has not been empirically researched for leatherback sea turtles.

In this study, we collected and analyzed empirical data on Caribbean leatherback neonate dispersal during two years in relation to environmental conditions to address the following hypotheses: 1) there are inter-annual differences in current speeds and thus, neonate swimming speeds, 2) there is spatiotemporal variability in environmental drivers of current speeds and neonate swimming speeds and 3) that neonate body sizes impact their current-corrected or "true" swimming speeds. Specifically, we acoustically tracked and quantitatively analyzed Caribbean leatherback neonate movement tracks using first passage time and random walk models. We then modelled the effect of the tidal and lunar cycle and changes in current speeds over different time and years in relation to neonate true speeds and tested for significant relationships between neonate true swimming speeds and their body size. These results provide important information for designing future neonate tracking studies, distribution modeling, and informing coastal conservation efforts.

Methods

Neonate Collection and Study Site

Fieldwork was conducted in waters directly off the shore from Pacuare Nature Reserve in the Limón Province, Costa Rica (Fig 1.1.a).

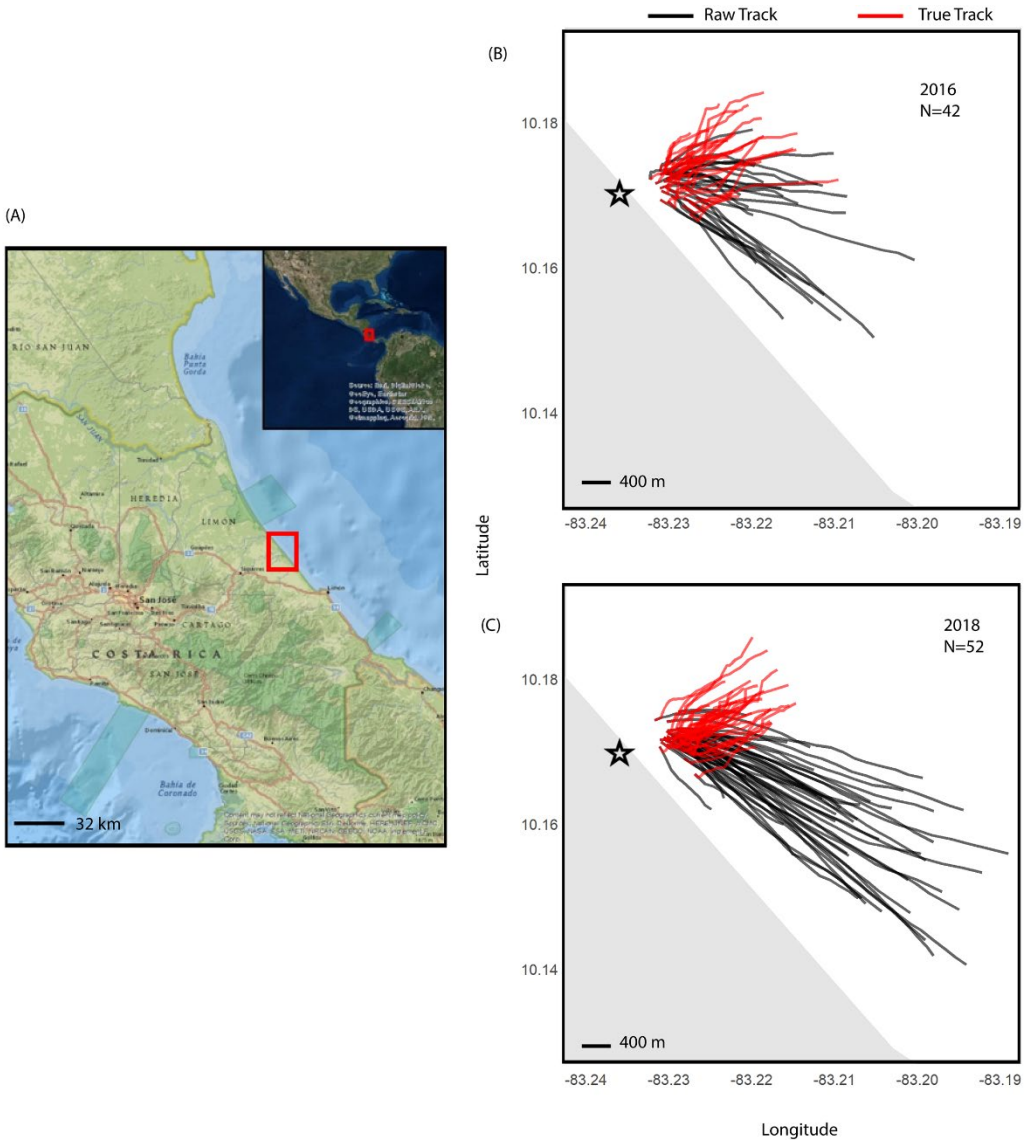

Figure 1.1. *Maps of neonate tracks off the shore of Pacuare Nature Reserve, Costa Rica a) for 2016 b) and 2018 c), with the reserve location indicated with a red box. Maps of true neonate tracks (red), were plotted using their heading and true*

swimming speeds, and raw neonate tracks (black). The black star shows the hatchery where turtles would emerge naturally from.

Data from Hoover et al. (2020) collected in 2016 was combined with new data collected in 2018. Atlantic leatherback neonates (n=94) were obtained from eggs that had been collected from multiple in situ nests in 2016 (n=42) and 2018 (n=52). These eggs were then either reburied in a hatchery (n=60) in Pacuare Nature Reserve or hatched in incubators near the hatchery (n=34), following the protocol outlined in Williamson et al. (2017). Before trials began, neonates were weighed and standard morphometric measurements (standard carapace length and width, flipper length, and head width) were taken. Neonates were chosen based upon availability and body condition, with only individuals showing healthy body conditions and activity used. Neonates were then tagged an hour prior to release, using Vemco V5-180kHz transmitter tags that were attached to a 2 m line-float tether set-up and temporarily fixed to the neonates' carapaces with Vetbond adhesive, following the methods outlined in Hoover et al. (2017) (Figure A1.1).

Acoustic Tracking

Acoustic tracking was conducted from a small (6 m) powerboat from August to September in 2016 and from July to August in 2018, time periods which reflected peak emergence for neonates and were chosen based on accessibility to the field site. Tracking began around 400 m from the shore to be outside of the surf zone, where neonates could not be tracked with the boat and where high predation occurs (Gyuris et al. 1994, Pilcher et al.2000, Wyneken et al. 2000, Wilson et al. 2019). Tracking

took place in front of the hatchery to mimic as realistically as possible the path the neonates would have taken if dispersing naturally from the hatchery. Tracking was conducted during daylight hours (0600-1600 hours), beginning at different times and tidal states. Although neonates often emerge at night, they are also known to depart during the daytime and previous neonate tracking and observational studies have been performed successfully during the day (Frick 1976, Lohmann and Lohmann 1992, Okuyama et al. 2009, Scott et al. 2014). Additionally, due to neonates being in their continuous swimming "frenzy" stage during the entire period of our study, we did not anticipate any difference in swimming behavior during the day versus at night. After tagging, each neonate was brought onto the boat and released from the same location (~400 m offshore, outside of the surf zone, and directly in front of the hatchery, with some variation depending on where the hatchlings were placed in the water relative to the boat) and tracked individually with a Vemco VR100 acoustic receiver and a VH180-D-10M directional hydrophone for as long as weather conditions and neonate availability permitted, generally 30-120 minutes. Releasing the neonates past the surf zone ensured that the swimming trajectories of the neonates were not directly influenced by nearshore waves and the bottom topography, but instead by surface currents. The boat remained behind neonate turtles at a distance of approximately 20 m, and all positions were recorded with the receiver. At 15-minute intervals along each track, a Holdpeak 866B hand-held digital anemometer was used to collect wind speed. A Barska 7x42 WP range-finder monocular and Plastimo Iris 50 hand-held compass were used to determine the distance and bearing of the neonates from the boat to ensure accuracy of recorded neonate positions. At the end of the tracking

period for each neonate, the turtle was recovered, the acoustic transmitter and tether removed, and the turtle was released. All procedures were approved by the University of Maryland Center for Environmental Science's Institutional Animal Care and Use Committee (IACUC) (Research Protocol No. S-CBL-16-11 for 2016, Research Protocol No. S-CBL-18-02 for 2018) and the Costa Rican Ministerio Del Ambiente y Energia, Sistema Nacional de Áreas de Conservación (SINAC), and Área de Conservación La Amistad Caribe (ACLAC) (R-SINAC-ACLAC-PIME-VS-R-022-2016, R-SINAC-ACLAC-PIME-VS-R-025-2016, R-SINAC-PNI-ACLAC-045-2018).

Surface Drifters

Surface drifters were constructed following a similar method to Hoover et al. (2020). These drifters had over two meters of line connected to a metal drogue and a bright orange flag on the top that increased visibility but was also heavy enough to lay horizontally on the surface; the drifters were tracked using a GPS-enabled phone (Figure A1.2). To minimize the wind-induced movement of the drifters (slippage), the drifters had a large submerged to unsubmerged ratio (Niiler and Paduan 1995, Lumpkin and Pazos 2007). These surface drifters were deployed every 20-30 minutes along the tracks, when the weather permitted, to determine surface current speeds.

Processing of Acoustic Tracking Data

All data processing and analysis was conducted using R statistical software (R Core Team 2018). Each neonate turtle and drifter track were divided into regular 5-minute position intervals. Neonate and drifter data were then merged on their

matching time stamps for each position. Neonate positions were corrected using bearing and distance of the neonates from the boat for each 5-minute time point of the tracks. Raw track speed of both the neonates and drifters was found by taking the distance traveled between each point divided by the time duration between points. The "geosphere" R package (Hijmans et al. 2019) was used to find the bearing of each neonate and drifter point.

True neonate swimming speed (termed "in-water swimming speed" by Hoover et al. 2020), which accounts for the effect of the currents on the neonate swimming speed, was found by using the raw track speed of the neonates (S_N) and the heading in radians (Θ) to determine the neonate east-west (u_N) and north-south (v_N) speed components (1-2) (Bailey and Thompson 2010, Hoover et al. 2020). The drifter east-west (u_D) and north-south (v_D) speed components were found using similar equations, but using the raw track speed and direction of the drifters instead of the raw track speed and direction of the neonates. The final true speed (V_N) for each neonate position point was found using equation (3). Neonate true headings (Θ_I) were derived from taking the arc tangent of the absolute difference in neonate east-west and north-south speed components with drifter north-south and east-west components (4).

$$u_N = S_N \sin \Theta \quad (1)$$

$$v_N = S_N \cos \Theta \quad (2)$$

$$V_N = \sqrt{(u_N - u_D)^2 + (v_N - v_D)^2} \quad (3)$$

$$\Theta_I = \operatorname{atan} \frac{|u_N - u_D|}{|v_N - v_D|} \quad (4)$$

Time of day for each data point was classified as either morning (0600-0900 hours), late morning (0900-1200 hours), afternoon (1200-1400 hours), or late afternoon (1400-1600 hours).

It is worth noting that in computing the true headings of the neonates, wave, wind, and inertial influences could differentially impact the neonates and the drifters and we did not have measurements of the wave height, direction, or water depth along the hatchling trajectories. However, inertial influences are unlikely to be important, as the mean size of the neonates gives them an effective radius that minimizes inertial effects to less than 5 degrees of the deflection angle (Beron-Vera et al. 2015, Brooks et al. 2019) and at the modest wind speeds measured (1-5 m s^{-1}), assuming a 0.27% windage effect calculated from a similar drifter (Meyerjurgens et al. 2019), the error associated with the windage would be (0.0027-0.0135 m s^{-1}), which is orders of magnitude smaller than the neonate swimming speeds. Wave influences, or Stokes drift, would be aligned onshore in these nearshore waters and perpendicular to the isobaths and would potentially hinder the neonate's offshore trajectory and slow their swimming speed. However, recent work in the Gulf of Mexico suggests that the summertime Stokes drift has a sharp maximum in probability distribution in inshore waters of depths less than 100 m at 0.01 m s^{-1} (Clark et al. 2015), and even in hurricane conditions the median drift was only 0.03 m s^{-1}. Thus, over the short time scales of these experiments, the drifter and neonate motions are only very weakly influenced by these effects and this influence is within measurement error.

First Passage Time Analysis

To determine where neonates were spending more time along their track within a given spatial radius, a first passage time (FPT) analysis was conducted. The R package "adehabitat" (Calenge 2018) was used to calculate the FPT in hours for each neonate position. After accounting for a 5-minute acclimation period at the beginning of each track, the minimum and maximum step length for each of the tracks was used to develop a range of radii. For each neonate track, the log-transformed variance in FPT was then calculated and used to identify the peak in variance and associated radius of interest. The mean radius was calculated by averaging the radii of interest across tracks, and this overall spatial radius was then used to determine the FPT for every position within each individual track.

Random Walk Models

Random walk models can be used as a null hypothesis of movement, as they assume an individual is moving through its environment randomly with independent distributions of move lengths and angles and no correlation between current and previous positions. The net squared displacement (NSD), or the squared distance between each position along a track and the first position of the same track, can be used to determine whether an individual is following a correlated random walk (each position is correlated with the previous position), or biased random walk (each position has a directional bias). To test whether each of our individual neonates were moving randomly in their dispersal phase or following a fixed compass direction (biased random walk) as they left the shore, the net squared displacement (NSD) was calculated for each current-corrected position for each neonate (see Methods, Section

2.4). The NSD's were found for each of these true neonate tracks by taking the distance between each position along a track and the first location and squaring it. NSD for true tracks was then compared to the NSD expected for a correlated random walk (CRW) and a biased random walk (BRW). The expected CRW and BRW NSD's were calculated using the following equations (Turchin 1998):

$$\mathrm{NSD_{CRW}} = nm_2 + 2m_1^2\left(\frac{c}{1-c}\right)\left(\frac{n-(1-cn)}{1-c}\right) \quad (4)$$

$$\mathrm{NSD_{BRW}} = nm_2 + n(n\text{-}1)m_1^2\theta^2 \quad (5)$$

Where n is the number of moves from the first location, m_1 is the mean step length, m_2 is the mean squared step length, θ is the mean cosine of absolute move direction, and c is the mean cosine of the turning angles (the angle between sequential moves).

Environmental Drivers of Current Speed Variability

To determine environmental drivers of current speed, and therefore any inter-annual or spatial differences that could impact neonate dispersal, a generalized additive mixed model (GAMM) was fit to the 2016 and 2018 data. This model predicted the speed of the local currents (derived from the raw track speed of the drifters) as a function of local wind speed and the categorical variables of lunar cycle phase (classified as spring tide conditions or full and new moon phases; neap tide conditions or quarter moon phases; and mid-tidal conditions or three days before/after full, new, and quarter moon phases), time of day, year, and tidal current direction

(classified as ebb, flood, or slack, with slack being within 15 minutes of high/low water). Tidal data were obtained for the surrounding region of Limón, Costa Rica (10.00°N, 83.03°W), which experiences a mixed semi-diurnal tidal cycle, from Mobile Geographics LLC©. A smoothed interaction function of latitude and longitude was included to account for spatial autocorrelation present in current speed. Exploratory analysis using backward model selection and F-tests to remove non-significant terms and compare terms with and without the non-linear smooth of latitude and longitude indicated the presence of non-linear relationships, indicating a GAMM approach was appropriate. Individual drifter tracks were included as random effects to account for correlation in current speed within each track.

All GAMMs were fit in R using the "mgcv" package (Wood 2011). The error distribution for the current speed model was Gaussian with an identity link function, and the smoother terms for the interaction of latitude and longitude were fit using penalized regression splines. Backwards stepwise model selection was used to select the final model, using Akaike information criterion values (AIC) and only retaining variables with significant p-values ($p < 0.05$). Model assumptions were checked using a plot of the standardized residuals versus fitted values and auto-correlation function (ACF) and partial auto-correlation function (PACF) plots of the standardized residuals.

To determine the environmental drivers of nearshore current flows measured by the drifters and if they were impacted by large-scale geostrophic current flows, geostrophic current velocity was calculated using extracted mean values for 2016 and 2018 to explore variations in external forcing in each year. For geostrophic current

velocity, the delayed time, global altimetry dataset from the AVISO+ Live Access Server (LAS, https://tides.mobilegeographics.com/locations/4273.html) was used to create plots for the weeks of the 8th August 2016 and the 6th August 2018 for absolute geostrophic vector velocity for the grid area 88° to 75° W and 7° to 19° N. These dates were chosen based on availability from the LAS dataset and that the second week of August was a shared week of neonate tracking for both 2016 and 2018; as these plots reflect large-scale geostrophic currents, the week chosen for the dataset did not change the velocity patterns observed.

Generalized Additive Mixed Model for Neonate True Speed

We fit a GAMM to examine how neonate true speed was influenced by FPT (derived from the neonate raw tracks), local current speed and direction (derived from the drifters raw track speed and direction), tidal current direction, lunar phase, wind speed, year, latitude and longitude, and time along the track. The GAMM was fit after using a backward model selection exploratory analysis to compare term significance with and without non-linear smooths to determine that non-linear relationships were present. Current speed, FPT, and the interaction of latitude and longitude each had non-linear smoother terms. Individual neonates were included as random effects to account for correlation in true neonate speed within each track. The error distribution was Gaussian with an identity link function, and the smoother terms for the interaction of latitude and longitude were fit using penalized regression splines. The smoother terms for current speed were estimated by building departures for each individual neonate from a common smooth, using a factor smooth interaction and five basis functions (k=5) to avoid over-fitting. This allowed for random curves to be built

for each neonate, using splines that share the same smoothing parameters and an un-penalized null space. Model selection was performed in the same manner as for the current speed GAMM.

To rule out whether neonates were responding to changes in the environmental conditions they encountered or simply to natural variation in behavior from the time spent swimming, we ran an additional linear mixed effects model predicting the variance in swimming speed for the neonates as a function of time along their track, with individual neonates included as random effects and controlling for the speed of the currents. The variance in swimming speed was extracted as residuals from the final chosen GAMM model fit for the neonates and the time along their track was represented by move number, as each track was broken into regularized 5-minute time steps.

Body Morphometrics and Neonate True Speed Analysis

A principal component analysis (PCA) was used to derive an index of neonate body size, using the body morphometric variables which demonstrated covariance (carapace length, body mass, carapace width). The first principle component was extracted and used as a neonate size index (Burgess et al. 2006, Fig A1.8). This index was used to compare variability in body size between years and nest treatments (incubator versus hatchery nests), using independent t-tests.

A linear mixed effects model was fit in R using the "nlme" package (Pinheiro et al. 2020) to determine if there was a relationship between neonate body size, represented by the PCA-derived size index, and their average true swimming speed. The year and treatment of origin (incubator versus hatchery nest) were used as

random effects in the model after a stepwise model comparison. Neonate swimming speed was standardized for the body length of the neonates by dividing their average true swimming speed by their carapace length. Model assumptions of normality and independence were checked using residual plots.

Results

Acoustic Tracking

A total of 27 neonates tracked from hatchery nests and 15 from incubator-hatched eggs in 2016, and 33 neonates tracked from hatchery nests and 19 from incubator-hatched eggs in 2018. Drifters were deployed for the majority of neonate tracks (n=76) to determine current speed and direction. Average values for track distance and duration, current speed, raw track and true neonate speed, current direction, and raw track and true heading of all neonates in each year are reported in Table 1.1, demonstrating any inter-annual differences in current speeds or neonate trajectories.

Table 1.1. *Summary statistics for 2016 (see Hoover et al. 2020) and 2018 neonate tracking trials. Columns show mean values and standard deviation of values in parentheses, for each year.*

	2016	***2018***
Average Track Distance	2.0 km (± 0.7)	3.4 km (± 1.7)
Average Track Duration	83 min (± 9.12)	98 min (± 14.1)
Average Current Speed	0.30 m s^{-1} (± 0.29)	0.52 m s^{-1} (± 0.23)
Average Raw Track Speed of Neonates	0.40 m s^{-1} (± 0.18)	0.55 m s^{-1} (± 0.17)
Average True Speed of Neonates	0.27 m s^{-1} (± 0.25)	0.25 m s^{-1} (± 0.20)
Average Current Direction	147° (± 55.0)	135° (± 28.7)
Average Raw Track Heading of Neonates	110° (± 25.2)	121° (± 13.0)
Average True Heading of Neonates	67.0° (± 31.2)	55.1° (± 22.9)

Current speeds in 2018 were higher on average than in 2016, but neonate true speed was similar during the two years. The mean current directions and raw track headings of the neonates had a strong south-east direction both years, but neonate true headings were in a more north-east direction and similar between years (Table 1.1, Fig 1.1.b, 1.c).

First Passage Time

A radius of 59 m (± 57 SD, range 5-228 m) was the mean spatial scale of interest for the neonate tracks (n=94). Plots of the FPT over time for each track at this scale indicated that the majority of tracks had a higher FPT in the first third of the track (Fig 1.2.a, Figure A1.3), even when a 5-minute acclimation period was accounted for.

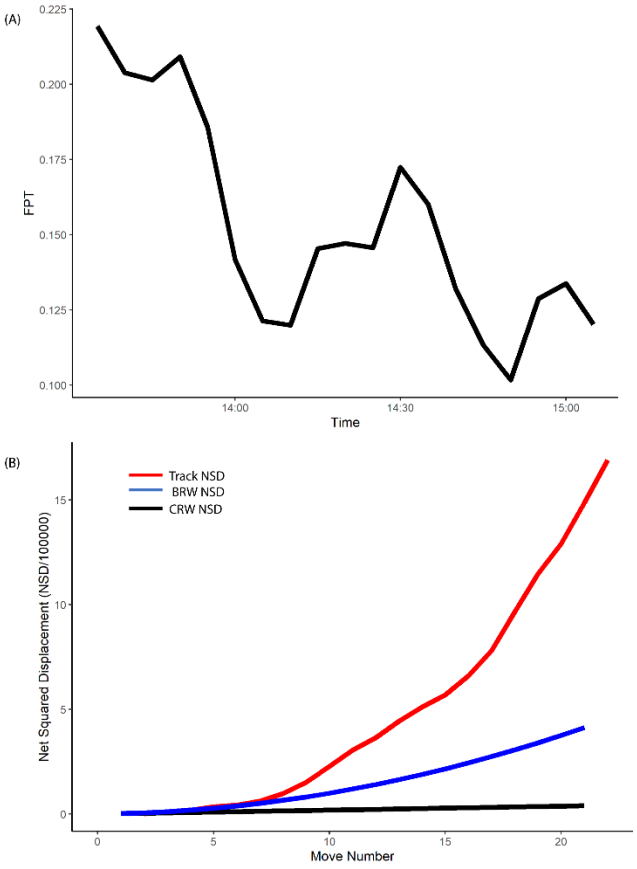

Figure 1.2. *For example neonate track (ID no. E5): a) First passage time (FPT, hours) versus time, and b) Net squared displacement (NSD, m^2) versus move number for example neonate track. The red line represents the NSD for the true neonate track, the blue line the expected NSD for a biased random walk (BRW), and the black line the expected NSD for a correlated random walk (CRW).*

Lower FPT values coincided with higher values for true speed of the neonates (Figure A1.4). The higher values for FPT observed in the first third of each track reflected some spatial variability in FPT, with areas nearshore having higher FPT values and areas farther from shore having lower FPT values (Figure A1.3).

Random Walk Models

All neonate true tracks during 2016 and 2018 followed a BRW during the first 5 move numbers, with an NSD following that expected with a BRW (example track shown in Fig 1.2.b), indicating that the neonate current-corrected positions had a directional bias consistent with the movements of an animal with a fixed compass direction. However, plots of NSD for true tracks showed they had a greater NSD than predicted for a BRW with move numbers higher than 5 (Fig 1.2.b), indicating that they were moving quicker than expected away from their release point with directed movement .

Inter-Annual Variability and Environmental Drivers of Current Speeds

Drifter-derived current speed (41 drifter tracks in 2016 and 93 drifter tracks in 2018) had a south-east orientation and significant inter-annual and spatial variability (Table 1.2).

Table 1.2. *Results of a generalized additive mixed model (GAMM) for current speeds (m s^{-1}, Gaussian error, identity link function) in relation to year (2016 as the reference level to 2018) and the interaction of latitude and longitude, with each track included as a random effect. Overall deviance explained was 51%. edf: estimated degrees of freedom.*

Fixed Effect	**Estimate**	**Estimate Error**	**p-value**
Intercept	0.332	0.022	< 2e-16
Year (2018)	0.118	0.030	9.18e-05
Smoother Term	**edf**	**F**	**p-value**
Latitude, Longitude	10.15	10.88	< 2e-16

Current speeds in the 2018 study period were significantly higher than 2016 (p-value<0.0001, Figure A1.5). The significant interaction smoother for latitude and longitude in the GAMM showed currents had significant spatial variation in both years (p-value<0.0001, Table 1.2), with lower current speeds nearshore (~300-1,000 m from shore) and higher current speeds farther from shore (~1,800-3,800 m from shore) (Fig 1.3.b).

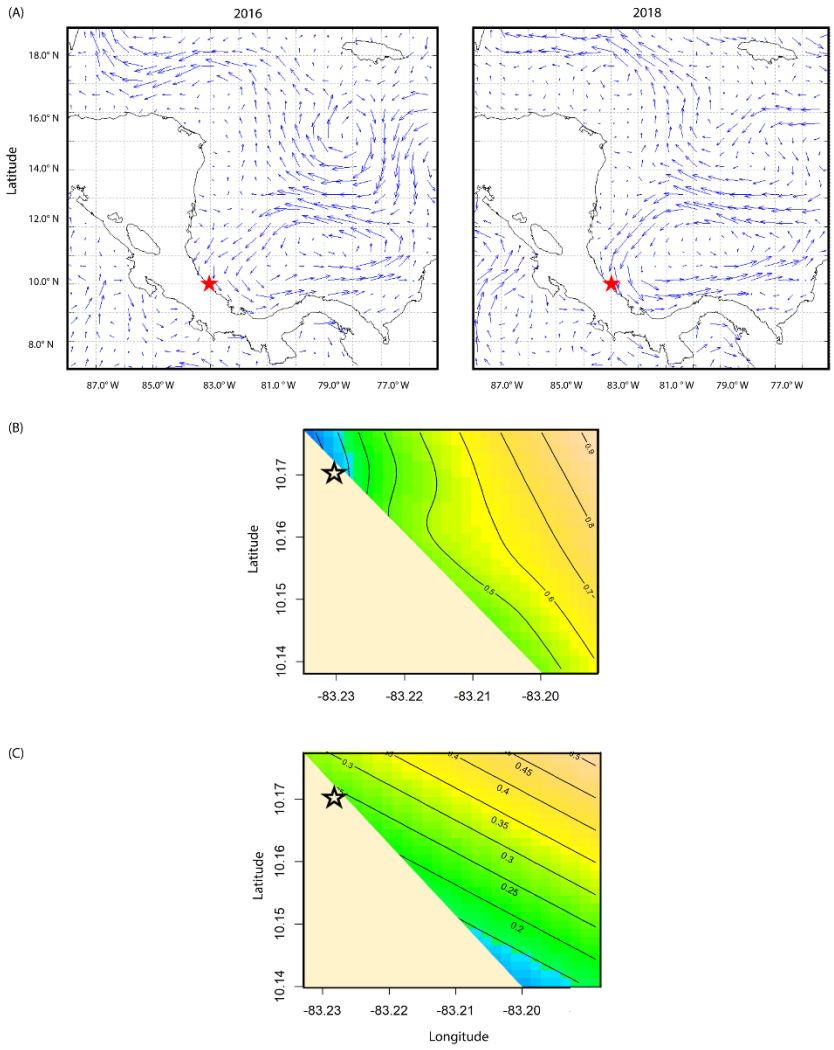

Figure 1.3. a) *Plot of delayed mode absolute geostrophic current velocity vectors with the study site in Pacuare, Costa Rica (red star). Plot on the left is for the week of August 8th, 2016, and plot on the right is for the week of August 6th, 2018. Mean velocity was 0.665 m* s^{-1} *for this time period in 2018 and 0.552 m* s^{-1} *for this time period in 2016. Plots were created using the AVISO+ satellite altimetry data Live Access Server (LAS). b) Spatial contour plot of the raw track speed of the current, with higher values shown in yellow and lower values shown in blue. Black lines show contours of current speed as output from a generalized additive mixed*

model predicting current speed as a function of year and smoothed interaction of latitude and longitude. c) Spatial contour plot of neonate true speed (m s^{-1}), with higher values shown in yellow and lower values shown in blue Black lines show contours of true neonate swimming speed as output from a generalized additive mixed model predicting neonate true swimming speed as a function of year, current speed (m s^{-1}), first passage time, and the smoothed interaction of latitude and longitude.

Nearshore drifter-derived current speed and direction was broadly consistent with large-scale geostrophic current flow, suggesting that the inter-annual variations in large-scale current flow are relevant to nearshore current processes in our tracking area. For the geostrophic current velocity, there were stronger currents in 2018 than in 2016 within the spatial area of the obtained data within the south Colombia Basin (Fig 1.3.a), with a higher mean absolute vector velocity of 0.646 m s^{-1} in 2018 compared to 0.578 m s^{-1} in 2016.

Environmental Variables and Neonate True Speed

Significant spatial autocorrelation for neonate true speed was seen in plots of the residuals, indicating the need for an autoregressive correlation structure. A model selection process using AIC values revealed that the best model was neonate true speed as a function of year and non-linear, smoothed variables of current speed and FPT (Table 1.3), with an autoregressive-moving-average (ARMA) lag 1 correlation structure.

Table 1.3. *Results of a generalized additive mixed model (GAMM) for neonate true speeds (m s^{-1}, Gaussian error, identity link function) in relation to year (2016 as the reference level to 2018), first passage time (FPT), and the current speed (m s^{-1}), with each individual track included as a random effect ("Identifier"). Current speed was fit with a basis dimension of k=5 and factor smooth interactions, with separate smoother terms for current speed for each individual track. A correlation autoregressive-moving-average (ARMA) structure was added with p=1 and q=1. Overall deviance explained was 35% edf: estimated degrees of freedom.*

Fixed Effect	**Estimate**	**Estimate Error**	**p-value**
Intercept	0.26	0.014	< 2e-16
Year (2018)	-0.047	0.020	0.020
Smoother Term	**edf**	**F**	**p-value**
Current Speed | Identifier	47.25	*NA*	*NA*
FPT	2.42	13.67	3.82e-07
Latitude, Longitude	2.00	13.15	2.47e-06

Neonates swam at a steady speed until current speeds reached 0.5 m s^{-1}. A plot of the smoother for neonate true speed versus the current speeds showed three different response strategies to high current speed conditions (>0.5 m s^{-1}). Most individuals had speeds that increased rapidly in positive association with the currents (n=41), while others maintained either a constant swimming speed (n=14) or had a negative association (n=21) between their swimming speed and the currents (Fig 1.4.a).

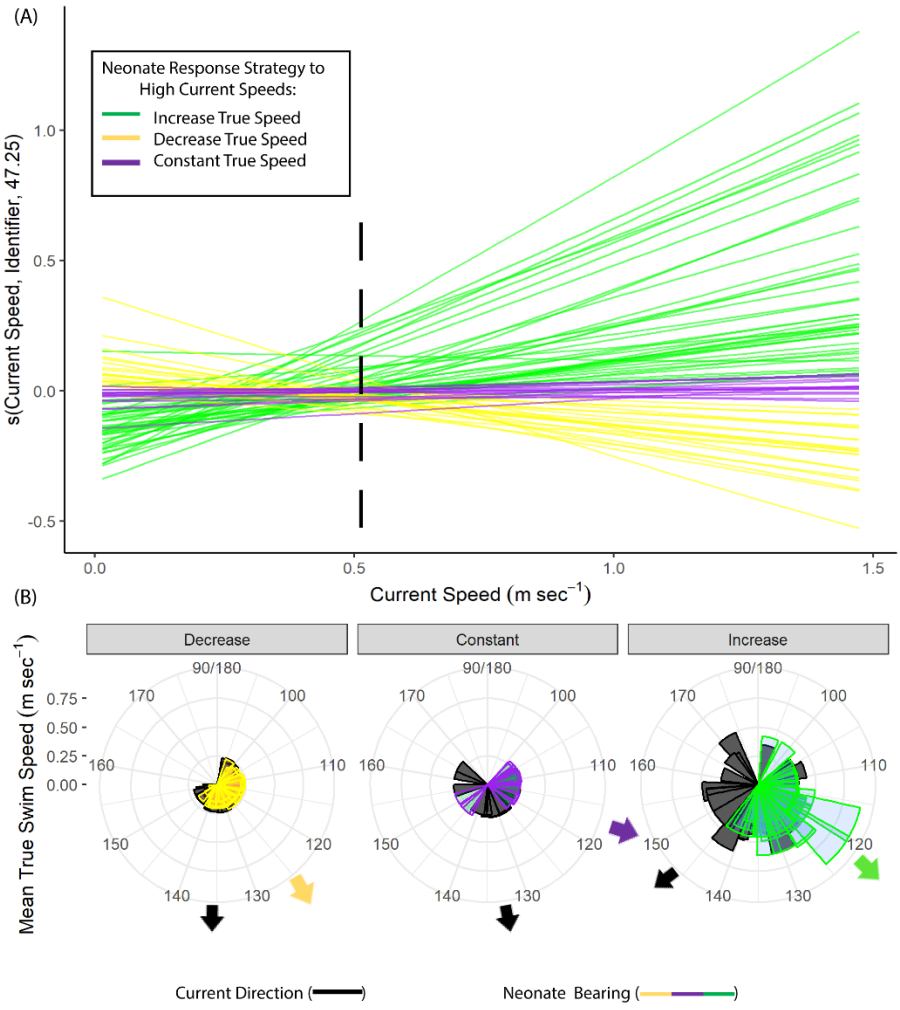

Figure 1.4. *a) Generalized additive mixed model (GAMM) smoothing curve for current speed (m s^{-1}) as a function of neonate true swimming speeds for 2016 and 2018, with an estimated random departure from the mean true speed trajectory for each neonate represented by colored lines and k=5 basis functions. Each color represents the response strategy of each neonate to high current speed conditions (>0.5 m s^{-1}): mean increase in true speed (green), mean decrease in true speed (yellow), or no change in mean true speed (purple). The threshold for high current speed conditions is shown with a black dashed line. b) Roseplots for the frequency of*

mean neonate true swimming speed plotted by neonate raw track bearing or current direction. Colors represent neonate raw track bearing for each swimming speed response strategy in currents greater than 0.5 m s^{-1} (decrease/yellow, constant/purple, increase/green), and black represents current direction for current speeds greater than 0.5 m s^{-1}.

Neonates that increased their swimming speed in response to high current speed conditions had tracks with directions that deviated in a northerly direction from the currents, while those with a decrease or constant response strategy had tracks that were more closely matched with the direction of the currents (Fig 1.4.b). This was further evidenced with an increase in current speed resulting in a greater difference in neonate north-south and east-west vector components compared to current vectors ("Mean Difference in East-West/North-South Vectors", Table 1.4).

Table 1.4. *Mean and standard deviation values (in parentheses) for true neonate swim speed, current speed, current direction, neonate raw track and true heading, mean difference in north-south and east-west vector components for neonates and the current, and mean north-south and east-west vector components for neonates for different current speed categories (low < 0.3 m s^{-1}, medium 0.3-0.5 m s^{-1}, high > 0.5 m s^{-1}). More positive values for mean neonate east-west vectors indicate a more easterly direction, whereas more positive values for mean neonate north-south vectors indicate a more northerly direction.*

	Low Current	*Medium Current*	*High Current*
Percentage of Data	0.31	0.45	0.24
Mean Neonate True Speed	0.25 m s^{-1} (±0.13)	0.25 m s^{-1} (±0.13)	0.30 m s^{-1} (±0.34)
Mean Current Direction	147° (± 62)	142° (± 53)	139° (± 27)
Mean Neonate Raw Track Heading	106° (± 30)	111° (± 28)	125° (± 12)
Mean Neonate True Heading	61° (± 23)	59° (± 24)	51° (± 25)
Mean Difference in East-West Vectors	0.17 (± 0.11)	0.16 (± 0.13)	0.35 (± 0.47)
Mean Difference in North-South Vectors	0.19 (± 0.12)	0.23 (± 0.14)	0.56 (± 0.55)
Mean East-West Vector for Neonates	0.21 (± 0.14)	0.20 (± 0.14)	0.13 (± 0.28)
Mean North-South Vector for Neonates	0.02 (± 0.13)	0.01(± 0.14)	0.08 (± 0.32)

The neonates' north-south vector components were stronger when currents were faster, indicating that they were swimming in a more northerly compass direction in faster current speeds (Table 1.4). Individual variation in neonate swimming response to the currents for both years resulted in the standard deviation of the neonates' true compass headings (24°) being greater than the standard deviation of their raw track compass headings (20°), despite a consistent mean north-east trajectory (mean true heading of 56°).

Further supporting these results in individual responses to high current speed conditions, the linear mixed effects model for the variance in swimming speed as a function of time spent swimming for the neonates showed no significant positive linear relationship (Table A2.2, Figure A1.7).

Even though individual variability was present in responses to high current speed conditions, neonates at the population level maintained a consistent mean swimming speed between years, with a mean speed of 0.27 m s-1 in 2016 and 0.25 m s-1 in 2018 (Table 1.1).The significant interaction smoother for latitude and longitude in the GAMM indicates neonates had spatial structure to their swimming speed (Table 1.3). This reflected the spatial structure seen in the current speeds, with neonates swimming faster in areas farther from shore (Fig 1.3.c). This was further confirmed with the smoothed relationship of their true speed as a function of FPT (Figure A1.6), with neonates having higher swimming speeds with lower FPT values, which correlated with areas farther from shore with faster current speeds (Figure A1.5, Fig A2.3.b).

Body Size and Neonate Swimming Speeds

The PCA results showed that mass and carapace length had the largest correlations and loadings with the first principal component, which explained 56% of total variance and was loaded with carapace length, width, and body mass. (Figure A1.8). Scores from the first principal component were extracted for each turtle and used as a size index (Burgess et al. 2006). Body size measurements for neonates appear in Table A2.1. An independent t-test showed a significant difference in the size index for neonates between years, with 2018 having a larger mean size index

than 2016 (2018: 0.501; 2016: -0.453, p-value=7.95e-04) (Fig 1.5.a). Independent t-test results showed that neonates from hatcheries had significantly larger body size indices on average than incubator neonates in 2018 (hatchery: 0.815, incubator: 0.068, p-value=0.036) but not in 2016 (hatchery: -0.412, incubator: -0.527 p-value=0.802) (Fig 1.5.b).

The linear mixed effects model did not show a significant relationship between average neonate swimming speed and neonate body size (Table 1.5, Fig 1.5.c).

Table 1.5. *Results of a linear mixed effects model predicting neonate average true swimming speed (body lengths in m s^{-1}) as a function of average current speed (m s^{-1}) and a PCA-derived body size index. Year and origin (incubator or hatchery) were included as random effects.*

Fixed Effect	Estimate	Estimate Error	p-value
Intercept	3.70	0.456	0.000
Size Index	-0.026	0.156	0.871
Average Current Speed	1.092	1.066	0.310

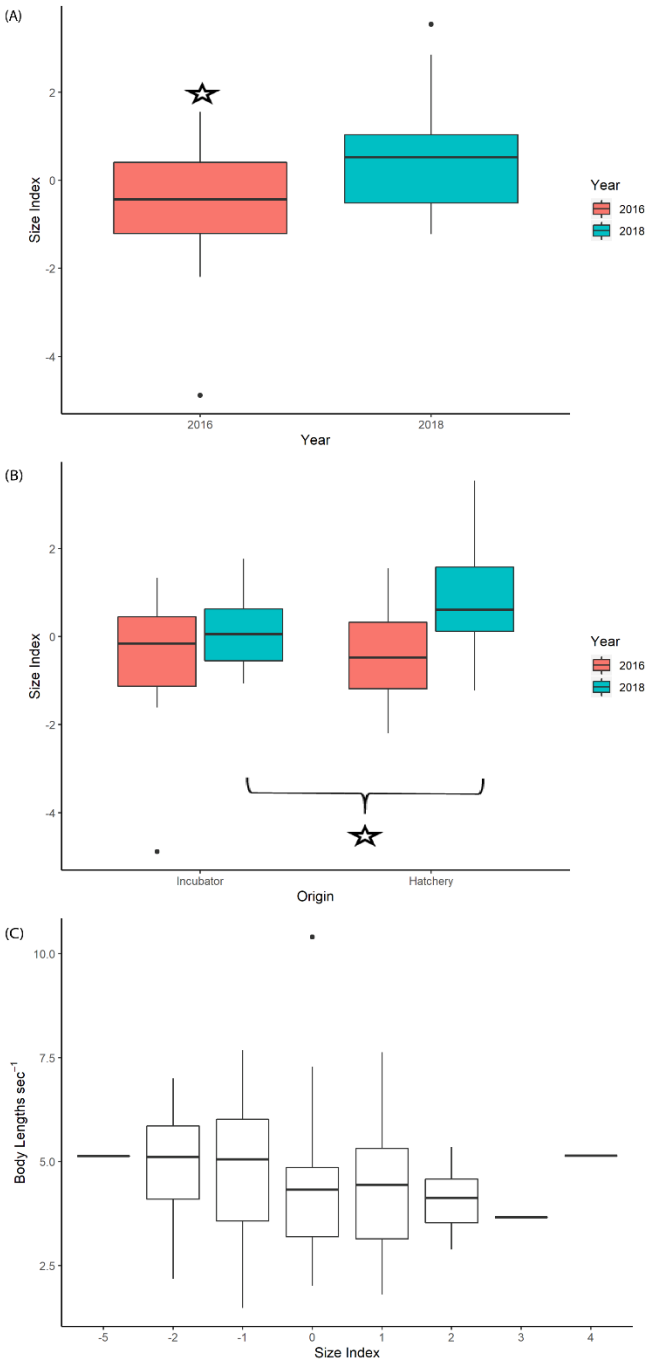

Figure 1.5. *a) Boxplots of the size index for neonates in 2016 versus 2018, with a star indicating a significant difference between years using an independent t-test (p-value < 0.05). b) Boxplots of the size index for 2016 and 2018, with the star showing significant differences between incubator and hatchery individuals using an*

independent t-test (p-value < 0.05). c) Boxplots comparing body size index values versus average true swimming speed for neonates, standardized by body lengths per time (m s^{-1}). Results from a linear mixed effects model did not indicate significance for this relationship, even when controlling for variability in body size index with treatment (hatchery or incubator) and year.

Discussion

Dispersal of leatherback neonates from Pacuare, Costa Rica is significantly affected by current speed, with spatial and temporal variability in the currents resulting in three different behavioral response strategies in neonate swimming speed and orientation. This could have implications for individual neonate fitness and survival, as changes in strength and direction of the currents could impact the energy use of neonates (Jones et al. 2007, Shillinger et al. 2012b), the amount of time spent in predator-rich waters (Gyuris 1994, Pilcher et al. 2000, Bolten 2003, Stewart & Wyneken 2004, Santidrián et al. 2007), and potentially have carry-over effects into their long-term migratory pathway and ability to find resource patches offshore in older life stages (Gaspar et al. 2012, Shilinger et al. 2012b, Putman & Mansfield 2015, Briscoe et al. 2016, Cardona & Hays 2018). Although we identified significant inter-annual differences in current speed and neonate body size, the larger sizes of neonates in 2018 did not significantly impact their swimming speed, showing that variability in average neonate swimming speed was due to environmental, not biological, conditions. These findings are especially important for the future conservation and management of this endangered and declining subpopulation of Caribbean leatherback turtles (Troëng et al. 2007, Stewart et al. 2016, The Northwest

Atlantic Leatherback Working Group 2019), as the faster currents experienced during anomalous years may either enhance neonate dispersal or require them to have higher energy expenditures to maintain their heading away from shore.

Our findings substantiate that leatherback neonates swim at a mean constant speed in their frenzy stage to efficiently move offshore and out of high-risk, nearshore zones (Wyneken & Salmon 1992, Wyneken et al. 1998, Jones et al. 2007, Okuyama et al. 2009), areas where we observed higher FPT's and slower current speeds. Neonates had similar mean true speeds between years and in different current speed conditions (low, medium, high speeds) (Table 1.4), despite significantly faster current speeds in 2018 versus 2016. On average, as current speeds increased, neonates increased the difference in their directional components with the currents, indicating they were swimming increasingly in the opposite direction of the currents. An increase in current speed also resulted in most of the neonates swimming more strongly, on average, into a given compass heading opposite of, and in a more northerly direction to, the currents. This reinforces the theory that neonate sea turtles are following a fixed compass direction as they disperse from shore (Lohmann 1991, Lohmann and Lohmann 1996, Goff et al. 1998).

Despite relatively constant mean true swimming speeds between years (Table 1.1) and in different current conditions at the population level (Table 1.4), there was individual variability in neonate swimming speed in response to faster current conditions, with three main response strategies observed and no indication that these behaviors were simply due to time spent swimming (Figure A1.7, Table A2.2)When currents surpassed speeds of 0.5 m s^{-1}, more than half of the individuals (54 percent)

increased their true speed in positive association with the current velocity and in an oriented, more northerly direction from the currents (Fig 1.4). Increased velocity in high current speed conditions (> 0.5 m s^{-1}, see Fig 1.4.a) may have negative implications for the neonates' energy storage, as leatherback neonates have a metabolic scope and morphometrics optimized for continuous, slow swimming and a limited yolk storage that is needed to sustain them in their long journey offshore to find foraging areas (Davenport 1987, Wyneken et al. 1998, Jones et al. 2007). The other two response strategies observed were: 1) neonates maintaining a constant mean, oriented true swimming speed around 0.25 m s^{-1}, or 2) decreasing their true speed in high current speed conditions (>0.5 m s^{-1}) but having raw track bearings more closely matching the direction of currents (Fig 1.4.b). Neonates that utilize either a constant or decreased swimming speed strategy in faster currents father from shore could conserve yolk storage and have higher chances of survival as currents transport them to larger current systems offshore in a shorter amount of time (Shillinger et al. 2012b) and decrease the amount of time spent in predator-rich areas (Wyneken & Salmon 1992, Wyneken et al. 1998, Okuyama et al. 2010, Santidrian Tomillo et al. 2010). This was further suggested by the lower first passage times and raw track speeds for neonates in areas farther from shore (>1,800 m from shore), where the currents were faster (Figure A1.5, Fig 3.b) and their ability to more efficiently displace themselves than predicted by a biased random walk further into their track (Fig 2.b).

Overall, the variability in individual swimming behavior in high current speeds seen in our results may either boost dispersal and/or incur metabolic costs for

this decreasing subpopulation of Caribbean leatherbacks (The Northwest Atlantic Leatherback Working Group 2019). The optimization of leatherback neonates for continuous, slow swimming (Jones et al. 2007) raises concerns that 53 percent of our neonates appeared to increase their swimming speed under high current speed conditions (Fig 1.4a), despite a population-level response of relatively constant swimming effort in different current speed categories (Table 1.4). These individual-level responses to extreme current speed conditions could possibly prematurely exhaust valuable yolk reserves that would otherwise be used to reach offshore foraging habitats. However, in the absence of these potential metabolic costs, the diversity in neonate swimming responses to high current speeds may increase their survival and aid their dispersal offshore. These fast currents could transport neonates away from dangerous nearshore waters where predation is high (Gyuris et al 1994, Pilcher et al. 2000, Wyneken et al 2000, Wilson et al. 2019) and potentially result in neonates having a wider distribution as they encounter variable current systems offshore, increasing their population resiliency to environmental change (Mansfield et al. 2017).

The combination of statistical models and inter-annual data collected on current speeds with environmental predictors show currents impacting neonate movements in this area are not driven by tidal current direction, time of day, lunar cycle phase, or local wind speed. Nearshore current flow spatial and temporal structure in this region is instead likely driven by changes in large-scale geostrophic currents within a cyclonic gyre in the southern Colombia Basin (Centurioni & Niiler 2003). The inter-annual differences in nearshore local currents measured by our

drifters reflected inter-annual differences in geostrophic currents in this region, with faster mean geostrophic current speeds during our 2018 tracking period than in 2016 (Fig 1.3.a). The impact of large-scale geostrophic current flow in the Colombia Basin on local nearshore current flow and thus neonate dispersal supports that future variability in juvenile and adult dispersal behavior in oceanic gyres may depend on their swimming behavior responses as neonates to these environmental conditions (Shillinger et al. 2012b, O'Connor et al. 2014).

Higher precipitation in 2018 may have affected the incubation duration and body morphometrics of neonates in this study (11.96 mm day^{-1} for 2016 and 15.57 mm day^{-1} for 2018, Figure A1.6). Higher precipitation may result in decreased nest temperatures and longer incubation durations (Lolavar & Wyneken 2015), which subsequently produce larger body sizes but decreased locomotor abilities and overall fitness (Booth et al. 2004, Fisher et al. 2014, Booth et al. 2017). This is likely due to a decreased fatigue resistance and inability to power stroke for long periods (Burgess et al. 2006). Although we were unable to retrieve precise data on the incubation duration for individual neonates from hatchery nests, the reported average for all neonates from the hatchery nests in 2018 was 70 days (Sean A. Williamson, personal communication), which is longer than the known average of 60 days for leatherbacks (Bilinski et al. 2001). Additionally, neonates in 2018 were significantly larger than in 2016 (Fig 1.5.a), and of these, eggs hatched in the hatchery, where nest temperature was not controlled and vulnerable to precipitation effects, were significantly larger than those hatched in incubators (Fig 1.5.b). Body mass for neonate leatherback neonates is usually 30-47 g (Mickelson & Downie 2010), a range which was greatly

exceeded by more than 75% of the neonates in 2018 (range: 42-56 g). However, we did not find a significant relationship between neonate body size and average true swimming speed (Fig 1.5.c). These results show that environmental variables, such as current speed and direction, may have a greater impact on neonate swimming behavior for this Costa Rican rookery than biological factors, such as neonate size, incubation duration, or incubation treatment. However, to fully test the impact of each of these biological variables on their true or current-correct swimming speed, fitness tests would need to be performed on individuals. Future research efforts that can inform conservation for this population should incorporate longer tracking durations through the deployment of fixed acoustic telemetry arrays in nearshore neonate dispersal corridors highlighted in this study. Use of miniature satellite tags on larger juveniles or other age classes would extend our understanding of the potential carryover effects of environmental conditions on Caribbean leatherback turtle distribution, their ability to successfully find foraging areas, and the risk of interaction with fisheries (Shillinger et al. 2012a, Putman & Mansfield 2015, Christiansen et al. 2016, Mansfield et al. 2017). The long-term probability of neonate survival and dispersal success leaving the nesting beach during different climatic and oceanographic conditions could be assessed using model simulations with particle tracking techniques, ocean current models, and empirically-informed parameters on neonate movement, growth, and metabolism (Putman et al. 2012, Scott et al. 2012, Shillinger et al. 2012b;, Briscoe et al. 2016, Christiansen et al. 2016, Gaspar & Lalire 2017, Lalire & Gaspar 2019, DuBois et al. 2020).

The methodological approach used in this study allowed us to successfully track a large number of sea turtles during a vulnerable life stage that has previously had its movement ecology characterized mainly by observational or laboratory studies (Frick 1976, Lohmann et al. 1990, Wyneken et al. 1990, Lohmann and Lohmann 1992, Goff et al. 1998, Smith and Salmon 2009). The methods used allowed us to identify three different neonate behavioral response strategies in high current speed conditions and these results may have long-term implications for neonate energetics, survival, distribution, and overall population success in the face of varied environmental conditions at sea. This methodological approach could be applied to the neonate stage in other marine species, which is understudied in movement ecology due to the difficulty of tag attachments (small body size relative to equipment) and often high mortality rates (Shillinger et al. 2012a). Juvenile movements are generally better understood, such as for sturgeon, where studies have used biotelemetry with acoustic tags to look at home-ranges, seasonal and ontogenetic habitat associations, first passage times, and movements predicted by environmental covariates (Smith and King 2005, Geist and Brown 2011, Thomas and Peterson 2019). These and other highly migratory marine taxa, such as sharks, billfish, and swordfish, may take advantage of either the affordable miniature acoustic tag and drifter design used in this study and/or the combined analytical approach utilizing statistical models to provide an integrated interpretation of the relationship between an individual's movement and its environment during dispersal. The characterization of these movements of younger life stages can then be used to inform management,

conservation efforts, and responses to climate change scenarios, as has been performed for older life stages (e.g., Hazen et al. 2012b).

References

Bailey, H. and Thompson, P. (2006). Quantitative analysis of bottlenose dolphin movement patterns and their relationship with foraging. Journal of Animal Ecology, 75(2), 456-465.

Bailey, H., and Thompson, P. (2010). Effect of oceanographic features on fine-scale foraging movements of bottlenose dolphins. Marine Ecology Progress Series, 418, 223-233.

Bailey, H., and Thompson, P. (2010). Effect of oceanographic features on fine-scale foraging movements of bottlenose dolphins. Marine Ecology Progress Series, 418, 223-233.

Bailey, H., Benson, S.R., Shillinger, G.L., Bograd, S.J., Dutton, P.H., Eckert, S.A., Morreale, S.J., Paladino, F.V., Eguchi, T., Foley, D.G. and Block, B.A. (2012). Identification of distinct movement patterns in Pacific leatherback turtle populations influenced by ocean conditions. Ecological Applications, 22(3), pp.735-747.

Benson, S.R., Eguchi, T., Foley, D.G., Forney, K.A., Bailey, H., Hitipeuw, C., Samber, B.P., Tapilatu, R.F., Rei, V., Ramohia, P. and Pita, J. (2011). Large-scale movements and high-use areas of western Pacific leatherback turtles, Dermochelys coriacea. *Ecosphere*, *2*(7), pp.1-27.

Beron-Vera, F.J., Olascoaga, M.J., Haller, G., Farazmand, M., Triñanes, J. and Wang, Y. (2015). Dissipative inertial transport patterns near coherent Lagrangian eddies in the ocean. Chaos: An Interdisciplinary Journal of Nonlinear Science, 25(8), p.087412.

Brooks, M.T., Coles, V.J. and Coles, W.C. (2019). Inertia influences pelagic sargassum advection and distribution. Geophysical Research Letters, 46(5), pp.2610-2618.

Bilinski, J. J., Reina, R. D., Spotila, J. R., and Paladino, F. V. (2001). The effects of nest environment on calcium mobilization by leatherback turtle embryos (*Dermochelys coriacea*) during development. Comparative Biochemistry and Physiology Part A: Molecular & Integrative Physiology, 130(1), 151-162.

Block, B.A., Jonsen, I.D., Jorgensen, S.J., Winship, A.J., Shaffer, S.A., Bograd, S.J., Hazen, E.L., Foley, D.G., Breed, G.A., Harrison, A.L. and Ganong, J.E. (2011). Tracking apex marine predator movements in a dynamic ocean. Nature, 475(7354), 86-90.

Bolten, A. B. (2003). Variation in sea turtle life history patterns: neritic vs. oceanic developmental stages. The Biology of Sea Turtles, 2, 243-257.

Booth, D. T., Burgess, E., McCosker, J., and Lanyon, J. M. (2004). The influence of incubation temperature on post-hatching fitness characteristics of turtles. In International Congress Series Elsevier.1275, 226-233.

Booth, D. T. (2017). Influence of incubation temperature on sea turtle neonate quality. Integrative Zoology, 12(5), 352-360.

Briscoe, D.K., Parker, D.M., Balazs, G.H., Kurita, M., Saito, T., Okamoto, H., Rice, M., Polovina, J.J. and Crowder, L.B. (2016). Active dispersal in loggerhead sea turtles (*Caretta caretta*) during the 'lost years'. Proceedings of the Royal Society B: Biological Sciences, 283(1832), 20160690.

Burgess, E. A., Booth, D. T., and Lanyon, J. M. (2006). Swimming performance of neonate green turtles is affected by incubation temperature. Coral reefs, 25(3), 341-349.

Cadahía, L., López-López, P., Urios, V., and Negro, J. J. (2010). Satellite telemetry reveals individual variation in juvenile Bonelli's eagle dispersal areas. European Journal of Wildlife Research, 56(6), 923-930.

Calenge, C. (2006). The package adehabitat for the R software: tool for the analysis of space and habitat use by animals. Ecological Modelling, 197, 1035.

Cardona, L. and Hays, G.C. (2018). Ocean currents, individual movements and genetic structuring of populations. Marine Biology, 165(1), 10.

Centurioni, L. R. and Niiler, P. P. (2003). On the surface currents of the Caribbean Sea. Geophysical Research Letters, 30(6).

Christiansen, F., Putman, N.F., Farman, R., Parker, D.M., Rice, M.R., Polovina, J.J., Balazs, G.H. and Hays, G.C. (2016). Spatial variation in directional swimming enables juvenile sea turtles to reach and remain in productive waters. Marine Ecology Progress Series, 557, 247-259.

Clark, M. (2015). Quantification of Stokes Drift as a Mechanism for Surface Oil Advection in the Gulf of Mexico during the Deepwater Horizon Oil Spill.

Crouse, D.T., Crowder, L.B. and Caswell, H. (1987). A stage-based population model for loggerhead sea turtles and implications for conservation. Ecology, 68(5), 1412-1423.

Crowder, L. B., Crouse, D. T., Heppell, S. S. and Martin, T. H. (1994). Predicting the impact of turtle excluder devices on loggerhead sea turtle populations. Ecological Applications, 4(3), 437-445

Davenport, J. (1987). Locomotion in neonate leatherback turtles *Dermochelys coriacea*. Journal of Zoology, 212(1), 85-101.

DuBois, M.J., Putman, N.F. and Piacenza, S.E. (2020). Hurricane frequency and intensity may decrease dispersal of Kemp's ridley sea turtle hatchlings in the Gulf of Mexico. Frontiers in Marine Science, 7, p.301.

Fauchald, P. and Tveraa, T. (2003). Using first-passage time in the analysis of area-restricted search and habitat selection. Ecology, 84(2), 282-288.

Fisher, L. R., Godfrey, M. H. and Owens, D. W. (2014). Incubation temperature effects on neonate performance in the loggerhead sea turtle (Caretta caretta). PLoS ONE, 9(12), 1-22.

Fossette, S., Witt, M.J., Miller, P., Nalovic, M.A., Albareda, D., Almeida, A.P., Broderick, A.C., Chacón-Chaverri, D., Coyne, M.S., Domingo, A. and Eckert, S. (2014). Pan-Atlantic analysis of the overlap of a highly migratory species, the

leatherback turtle, with pelagic longline fisheries. Proceedings of the Royal Society B: Biological Sciences, 281(1780), 20133065.

Frick, J. (1976). Orientation and behaviour of hatchling green turtles (Chelonia mydas) in the sea. Animal Behaviour, 24(4), pp.849-857.

Gaspar, P., Benson, S.R., Dutton, P.H., Réveillère, A., Jacob, G., Meetoo, C., Dehecq, A. and Fossette, S. (2012). Oceanic dispersal of juvenile leatherback turtles: going beyond passive drift modeling. Marine Ecology Progress Series, 457, 265-284.

Gaspar, P. and Lalire, M. (2017). A model for simulating the active dispersal of juvenile sea turtles with a case study on western Pacific leatherback turtles. PloS one, 12(7).

Gearheart, G., Maturbongs, A., Dutton, P.H., Sprintall, J., Kooyman, G.L., Tapilatu, R.F. and Johnstone, E. (2011). Tracking leatherback (*Dermochelys coriacea*) neonates at sea using radio and acoustic tags. Mar. Turtle Newsl, 130, 2-6.

Geist, D.R., Brown, R.S., Cullinan, V., Brink, S.R., Lepla, K., Bates, P. and Chandler, J.A. (2005). Movement, swimming speed, and oxygen consumption of juvenile white sturgeon in response to changing flow, water temperature, and light level in the Snake River, Idaho. Transactions of the American Fisheries Society, 134(4), 803-816.

Girard, C., Sudre, J., Benhamou, S., Roos, D. and Luschi, P. (2006). Homing in green turtles *Chelonia mydas*: oceanic currents act as a constraint rather than as an information source. Marine Ecology Progress Series, 322, 281-289.

Goff, M., Salmon, M. and Lohmann, K.J. (1998). Hatchling sea turtles use surface waves to establish a magnetic compass direction. Animal Behaviour, 55(1), pp.69-77.

Gurarie, E., Bracis, C., Delgado, M., Meckley, T.D., Kojola, I. and Wagner, C.M. (2016). What is the animal doing? Tools for exploring behavioral structure in animal movements. Journal of Animal Ecology, 85(1), 69-84.

Gyuris, E. (1994). The rate of predation by fishes on neonates of the green turtle (*Chelonia mydas*). Coral Reefs, 13(3), 137-144.

Hake, M., Kjelle´n, N. and Alerstam, T. (2001). Satellite tracking of Swedish ospreys *Pandion haliaetus*: autumn migration routes and orientation. J. Avian Biol. 32: 47–56.

Hake, M., Kjellén, N. and Alerstam, T. (2003). Age-dependent migration strategy in honey buzzards *Pernis apivorus* tracked by satellite. Oikos, 103(2), 385-396.

Hays, G.C., Hobson, V.J., Metcalfe, J.D., Righton, D. and Sims, D.W. (2006). Flexible foraging movements of leatherback turtles across the North Atlantic Ocean. Ecology, 87(10), 2647-2656.

Hays, G.C., Fossette, S., Katselidis, K.A., Schofield, G. and Gravenor, M.B. (2010). Breeding periodicity for male sea turtles, operational sex ratios, and implications in the face of climate change. Conservation Biology, 24(6), 1636-1643.

Hazen, E.L., Maxwell, S.M., Bailey, H., Bograd, S.J., Hamann, M., Gaspar, P., Godley, B.J. and Shillinger, G.L. (2012). Ontogeny in marine tagging and tracking science: technologies and data gaps. Marine Ecology Progress Series, 457, 221-240.

Hazen, E. L., Jorgensen, S., Rykaczewski, R. R., Bograd, S. J., Foley, D. G., Jonsen, I. D., . . . Block, B. A. (2012). Predicted habitat shifts of Pacific top predators in a changing climate. *Nature Climate Change, 3*, 234-238.

Hijmans, R. J., Williams, E., and Vennes, C. (2019). Geosphere: spherical trigonometry. R Package (R Foundation for Statistical Computing, Vienna), Version X.

Hoover, A.L., Shillinger, G.L., Swiggs, J. and Bailey, H. (2017). Comparing acoustic tag attachments designed for mobile tracking of neonate sea turtles. Frontiers in Marine Science, 4, 225.

Hoover, A. L., Shillinger, G. L., Williamson, S. A., Reina, R. D., & Bailey, H. (2020). Nearshore neonate dispersal of Atlantic leatherback turtles (Dermochelys coriacea) from a non-recovering subpopulation. Scientific reports, 10(1), 1-10.

Hurme, E., Gurarie, E., Greif, S., Flores-Martínez, J.J., Wilkinson, G.S. and Yovel, Y. (2019). Acoustic evaluation of behavioral states predicted from GPS tracking: a case study of a marine fishing bat. Movement ecology, 7(1), 21.

Hsu, H.H., Joung, S.J., Liao, Y.Y. and Liu, K.M. (2007). Satellite tracking of juvenile whale sharks, *Rhincodon typus*, in the Northwestern Pacific. Fisheries Research, 84(1), 25-31.

Jones, T. T., Reina, R. D., Darveau, C. A. and Lutz, P. L. (2007). Ontogeny of energetics in leatherback (*Dermochelys coriacea*) and olive ridley (*Lepidochelys olivacea*) sea turtle neonates. Comparative Biochemistry and Physiology - A Molecular and Integrative Physiology, 147(2 SPEC. ISS.), 313-322.

Kjellén, N., Hake, M. and Alerstam, T. (2001). Timing and speed of migration in male, female and juvenile Ospreys *Pandion haliaetus* between Sweden and Africa as revealed by field observations, radar and satellite tracking. Journal of Avian Biology, 32(1), 57-67.

Kooyman, G.L. and Ponganis, P.J. (2007). The initial journey of juvenile emperor penguins. Aquatic conservation: marine and freshwater ecosystems, 17(S1), S37-S43.

Lalire, M. and Gaspar, P. (2019). Modeling the active dispersal of juvenile leatherback turtles in the North Atlantic Ocean. Movement ecology, *7*(1), pp.1-17.

Lohmann, K.J., Salmon, M. and Wyneken, J. (1990). Functional autonomy of land and sea orientation systems in sea turtle hatchlings. The Biological Bulletin, 179(2), pp.214-218.

Lohmann, K.J. (1991). Magnetic orientation by hatchling loggerhead sea turtles (Caretta caretta). Journal of Experimental Biology, 155(1), pp.37-49.

Lohmann, K.J. and Lohmann, C.M.F. (1992). Orientation to oceanic waves by green turtle hatchlings. Journal of Experimental Biology, 171(1), pp.1-13.

Lohmann, K.J. and Lohmann, C.M.F., (1993). A light-independent magnetic compass in the leatherback sea turtle. The Biological Bulletin, 185(1), pp.149-151.

Lohmann, K.J. and Lohmann, C.M.F., (1994). Acquisition of magnetic directional preference in hatchling loggerhead sea turtles. Journal of Experimental Biology, 190(1), pp.1-8.

Lohmann, K. and Lohmann, C. (1996). Orientation and open-sea navigation in sea turtles. Journal of Experimental Biology, 199(1), pp.73-81.Lohmann, K.J., Putman, N.F. and Lohmann, C.M. (2012). The magnetic map of hatchling loggerhead sea turtles. Current opinion in neurobiology, 22(2), pp.336-342.

Lolavar, A. and Wyneken, J. (2015). Effect of rainfall on loggerhead turtle nest temperatures, sand temperatures and neonate sex. Endangered Species Research, 28(3), 235-247.

Light, P., Salmon, M., and Lohmann, K.J., (1993). Geomagnetic orientation of loggerhead sea turtles: evidence for an inclination compass. Journal of Experimental Biology, 182(1), pp.1-10.

Lumpkin, R. and Pazos, M. (2007). Measuring surface currents with Surface Velocity Program drifters: the instrument, its data, and some recent results. Lagrangian analysis and prediction of coastal and ocean dynamics, 2, 39.Mansfield, K. L., Saba, V. S., Keinath, J. A. and Musick, J. A. (2009). Satellite tracking reveals a dichotomy in migration strategies among juvenile loggerhead turtles in the Northwest Atlantic. Marine Biology, 156(12), 2555-2570.

Mansfield, K. L., Wyneken, J., Porter, W. P. and Luo, J. (2014). First satellite tracks of neonate sea turtles redefine the 'lost years' oceanic niche. Proceedings of the Royal Society B: Biological Sciences, 281(1781).

Mansfield, K.L., Mendilaharsu, M.L., Putman, N.F., dei Marcovaldi, M.A., Sacco, A.E., Lopez, G., Pires, T. and Swimmer, Y., (2017). First satellite tracks of South Atlantic sea turtle ‘lost years’: seasonal variation in trans-equatorial

movement. Proceedings of the Royal Society B: Biological Sciences, 284(1868), p.20171730.

Meyerjürgens, J., Badewien, T.H., Garaba, S.P., Wolff, J.O. and Zielinski, O. (2019). A state-of-the-art compact surface drifter reveals pathways of floating marine litter in the German bight. Frontiers in Marine Science, 6, p.58.

Mickelson, L. E. and Downie, J. R. (2010). Influence of incubation temperature on morphology and locomotion performance of leatherback (*Dermochelys coriacea*) neonates. Canadian Journal of Zoology, 88(4), 359-368.

Nagelkerken, I., Pors, L. P. and Hoetjes, P. (2003). Swimming behaviour and dispersal patterns of headstarted loggerhead turtles *Caretta caretta*. Aquatic Ecology, 37(2),183-190.

Nathan, R., Getz, W.M., Revilla, E., Holyoak, M., Kadmon, R., Saltz, D. and Smouse, P.E. (2008). A movement ecology paradigm for unifying organismal movement research. Proceedings of the National Academy of Sciences, 105(49), pp.19052-19059.

Niiler, P.P. and Paduan, J.D. (1995). Wind-driven motions in the northeast Pacific as measured by Lagrangian drifters. Journal of Physical Oceanography, 25(11), 2819-2830.

O'Connor, C.M., Norris, D.R., Crossin, G.T. and Cooke, S.J. (2014). Biological carryover effects: linking common concepts and mechanisms in ecology and evolution. Ecosphere, 5(3), pp.1-11.

Okuyama, J., Abe, O., Nishizawa, H., Kobayashi, M., Yoseda, K. and Arai, N. (2009). Ontogeny of the dispersal migration of green turtle (*Chelonia mydas*) neonates. Journal of Experimental Marine Biology and Ecology, 379(1-2), 43-50.

Okuyama, J., Shimizu, T., Abe, O., Yoseda, K. and Arai, N. (2010). Wild versus head-started hawksbill turtles *Eretmochelys imbricata*: post-release behavior and feeding adaptions. Endangered Species Research, 10, 181-190.

Péron, C. and Grémillet, D. (2013). Tracking through life stages: adult, immature and juvenile autumn migration in a long-lived seabird. PloS one, 8(8).

Pilcher, N.J., Enderby, S., Stringell, T. and Bateman, L. (2000). Nearshore turtle neonate distribution and predation. Sea turtles of the Indo-Pacific. ASEAN Academic Press, London, 151-166.

Pinheiro J, Bates D, DebRoy S, Sarkar D, R Core Team (2020). nlme: Linear and Nonlinear Mixed Effects Models. R package version 3, 1-147.

Putman, N.F., Shay, T.J. and Lohmann, K.J. (2010). Is the geographic distribution of nesting in the Kemp's ridley turtle shaped by the migratory needs of offspring? Integrative and Comparative Biology, 50(3), 305-314.

Putman, N.F., Bane, J.M. and Lohmann, K.J. (2010). Sea turtle nesting distributions and oceanographic constraints on hatchling migration. Proceedings of the Royal Society B: Biological Sciences, 277(1700), pp.3631-3637.

Putman, N.F., Endres, C.S., Lohmann, C.M. and Lohmann, K.J. (2011). Longitude perception and bicoordinate magnetic maps in sea turtles. Current Biology, 21(6),

pp.463-466.Putman, N.F., Scott, R., Verley, P., Marsh, R. and Hays, G.C. (2012). Natal site and offshore swimming influence fitness and long-distance ocean transport in young sea turtles. Marine Biology, 159(10), 2117-2126.

Putman, N. F. and Mansfield, K. L. (2015). Direct evidence of swimming demonstrates active dispersal in the sea turtle "lost years". Current Biology, 25(9), 1221-1227.

Putman, N. (2018). Marine migrations. Current Biology, 28(17), pp.R972-R976.

R Core Team. (2018). R: A language and environment for statistical computing.

Saba, V.S., Stock, C.A., Spotila, J.R., Paladino, F.V. and Tomillo, P.S. (2012). Projected response of an endangered marine turtle population to climate change. Nature Climate Change, 2(11), 814-820.

Salmon, M., Todd Jones, T. and Horch, K. W. (2004). Ontogeny of Diving and Feeding Behavior in Juvenile Seaturtles: Leatherback Seaturtles (*Dermochelys coriacea*) and Green Seaturtles (*Chelonia mydas)* in the Florida Current. Journal of Herpetology, 38(1), 36-43.

Santidrián Tomillo, P., Vélez, E., Reina, R.D., Piedra, R., Paladino, F.V. and Spotila, J.R. (2007). Reassessment of the leatherback turtle (*Dermochelys coriacea*) nesting population at Parque Nacional Marino Las Baulas, Costa Rica: effects of conservation efforts. Chelonian Conservation and Biology, 6(1), 54-62.

Scott, R., Hodgson, D.J., Witt, M.J., Coyne, M.S., Adnyana, W., Blumenthal, J.M., Broderick, A.C., Canbolat, A.F., Catry, P., Ciccione, S. and Delcroix, E. (2012).

Global analysis of satellite tracking data shows that adult green turtles are significantly aggregated in Marine Protected Areas. Global Ecology and Biogeography, 21(11), 1053-1061.

Scott, R., Biastoch, A., Roder, C., Stiebens, V.A. and Eizaguirre, C. (2014). Nano-tags for neonates and ocean-mediated swimming behaviors linked to rapid dispersal of neonate sea turtles. Proceedings of the Royal Society B: Biological Sciences, 281(1796), 20141209.

Shillinger, G. L. et al. (2008). Persistent leatherback turtle migrations present opportunities for conservation. PLoS Biology, 6(7),1408-1416.

Shillinger, G.L., Swithenbank, A.M., Bailey, H., Bograd, S.J., Castelton, M.R., Wallace, B.P., Spotila, J.R., Paladino, F.V., Piedra, R. and Block, B.A. (2011). Vertical and horizontal habitat preferences of post-nesting leatherback turtles in the South Pacific Ocean. Marine Ecology Progress Series, 422, 275-289.

Shillinger, G.L., Bailey, H., Bograd, S.J., Hazen, E.L., Hamann, M., Gaspar, P., Godley, B.J., Wilson, R.P. and Spotila, J.R. (2012). Tagging through the stages: technical and ecological challenges in observing life histories through biologging. Marine Ecology Progress Series, 457, 165-170.

Shillinger, G.L., Di Lorenzo, E., Luo, H., Bograd, S.J., Hazen, E.L., Bailey, H. and Spotila, J.R. (2012). On the dispersal of leatherback turtle neonates from Mesoamerican nesting beaches. Proceedings of the Royal Society B: Biological Sciences, 279(1737), 2391-2395.

Smith, K.M. and King, D.K. (2005). Movement and habitat use of yearling and juvenile lake sturgeon in Black Lake, Michigan. Transactions of the American Fisheries Society, 134(5), 1159-1172.

Smith, M.M. and Salmon, M. (2009). A comparison between the habitat choices made by hatchling and juvenile green turtles (Chelonia mydas) and loggerheads (Caretta caretta). Marine Turtle Newsletter, 126, pp.9-13.

Stewart, K. R. and Wyneken, J. (2004). Predation risk to loggerhead neonates at a high-density nesting beach in southeast Florida. Bulletin of Marine Science, 74(2), 325-335.

Stewart, K.R., LaCasella, E.L., Roden, S.E., Jensen, M.P., Stokes, L.W., Epperly, S.P. and Dutton, P.H. (2016). Nesting population origins of leatherback turtles caught as bycatch in the US pelagic longline fishery. Ecosphere, 7(3), e01272.

Tapilatu, R.F., Dutton, P.H., Tiwari, M., Wibbels, T., Ferdinandus, H.V., Iwanggin, W.G. and Nugroho, B.H. (2013). Long-term decline of the western Pacific leatherback, *Dermochelys coriacea*: a globally important sea turtle population. Ecosphere, 4(2), 1-15.

The Northwest Atlantic Leatherback Working Group. (2019). *Dermochelys coriacea* (Northwest Atlantic Ocean subpopulation). The IUCN Red List of Threatened Species 2019: e.T46967827A83327767.

Thomas, M.J., Peterson, M.L., Chapman, E.D., Fangue, N.A. and Klimley, A.P. (2019). Individual habitat use and behavior of acoustically-tagged juvenile green

sturgeon in the Sacramento-San Joaquin Delta. Environmental Biology of Fishes, 102(8), 1025-1037.

Thums, M., Whiting, S.D., Reisser, J.W., Pendoley, K.L., Pattiaratchi, C.B., Harcourt, R.G., McMahon, C.R. and Meekan, M.G. (2013). Tracking sea turtle neonates—a pilot study using acoustic telemetry. Journal of Experimental Marine Biology and Ecology, 440, 156-163.

Thums, M., Whiting, S.D., Reisser, J., Pendoley, K.L., Pattiaratchi, C.B., Proietti, M., Hetzel, Y., Fisher, R. and Meekan, M.G. (2016). Artificial light on water attracts turtle neonates during their near shore transit. Royal Society open science, 3(5), 160142.

Tomillo, P.S., Paladino, F.V., Suss, J.S. and Spotila, J.R. (2010). Predation of leatherback turtle neonates during the crawl to the water. Chelonian Conservation and Biology, 9(1), 18-25.

Troëng, S., Harrison, E., Evans, D., Haro, A.D. and Vargas, E. (2007). Leatherback turtle nesting trends and threats at Tortuguero, Costa Rica. Chelonian Conservation and Biology, 6(1), 117-122

Turchin, P. (1998). Quantitative analysis of movement: measuring and modeling population redistribution in animals and plants. Sunderland, MA, USA: Sinauer Associates, Inc. 396.

Vega, M.L., Willemoes, M., Thomson, R.L., Tolvanen, J., Rutila, J., Samaš, P., Strandberg, R., Grim, T., Fossøy, F., Stokke, B.G. and Thorup, K. (2016). First-time

migration in juvenile common cuckoos documented by satellite tracking. PloS one, 11(12).

Vincent, C., Ridoux, V., Fedak, M.A. and Hassani, S. (2002). Mark-recapture and satellite tracking in rehabilitated juvenile grey scals (*Halichoerus grypus*): dispersal and potential effects on wild populations. Aquatic Mammals, 28(2), 121-130.

Wallace, B.P., Tiwari, M. and Girondot, M. (2013). *Dermochelys coriacea*. The IUCN Red List of Threatened Species 2013: e.T6494A43526147. https://dx.doi.org/10.2305/IUCN.UK.2013-2.RLTS.T6494A43526147.en. Downloaded on 12 May 2020.

Williamson, S. A. (2018). Control and ecological significance of embryonic development in turtles and crocodiles. Monash University.

Wilson, P., Thums, M., Pattiaratchi, C., Whiting, S., Pendoley, K., Ferreira, L.C., and Meekan, M. (2019) High predation of marine turtle hatchlings near a coastal jetty. Biological Conservation 236, 571-579.

Weng, K.C., O'Sullivan, J.B., Lowe, C.G., Winkler, C.E., Dewar, H. and Block, B.A. (2007). Movements, behavior and habitat preferences of juvenile white sharks *Carcharodon carcharias* in the eastern Pacific. Marine Ecology Progress Series, 338, 211-224.

Whyte, F.S., Taylor, M.A., Stephenson, T.S. and Campbell, J.D. (2008). Features of the Caribbean low-level jet. International Journal of Climatology: A Journal of the Royal Meteorological Society, 28(1), 119-128.

Wood, S.N. (2011). Fast stable restricted maximum likelihood and marginal likelihood estimation of semiparametric generalized linear models. Journal of the Royal Statistical Society b), 73(1), 3-36.

Wyneken, J., Salmon, M. and Lohmann, K.J. (1990). Orientation by hatchling loggerhead sea turtles Caretta caretta L. in a wave tank. Journal of Experimental Marine Biology and Ecology, 139(1-2), pp.43-50.

Wyneken, J. and Salmon, M. (1992). Frenzy and postfrenzy swimming activity in loggerhead, green, and leatherback neonate sea turtles. Copeia, 478-484.

Wyneken, J., De Carlo, L., Glenn, L., Salmon, M., Davidson, D., Weege, S. and Fisher, L. (1998). On the consequences of timing, location and fish for neonates leaving open beach hatcheries. In Proceedings of the sixteenth annual symposium on sea turtle biology and conservation. National Oceanic and Atmospheric Administration Tech Memo NMFS, Vol. 412, 155-156.

Wyneken, J., Salmon, M., Fisher, L. and Weege, S. (2000). Managing relocated sea turtle nests in open-beach hatcheries. Lessons in hatchery design and implementation in Hillsboro Beach, Broward County, Florida. In Proceedings of 19th Annual Sea Turtle Symposium. H. Kalb and T. Wibbels (compilers). US Department of Commerce, NOAA Technical Memorandum NMFS-SEFSC-443.

Chapter 2: Clustering and classification of vertical movement profiles for ecological inference of behavior

Abstract

Vertical movements can expose individuals to rapid changes in physical and trophic environments- for aquatic fauna, dive profiles from biotelemetry data can be used to quantify and categorize vertical movements. Inferences on classes of vertical movement profiles typically rely on subjective summaries of parameters or statistical clustering techniques that utilize Euclidean matching of vertical movement profiles with vertical observation points. These approaches are prone to subjectivity, error, and bias. We used machine learning approaches on a large dataset of vertical time series (N=28,217 dives) for 31 post-nesting leatherback turtles (Dermochelys coriacea). We applied dynamic time warp (DTW) clustering to group vertical movement (dive) time series by their metrics (depth and duration) into an optimal number of clusters. We then identified environmental covariates associated with each cluster using a generalized additive mixed effects model (GAMM). A convolutional neural network (CNN) model, trained on standard dive shape types from the literature, was used to classify dives within each DTW cluster by their shape. Two clusters were identified with the DTW approach- these varied in their spatial and temporal distributions, with dependence on environmental covariates, sea surface temperature, bathymetry, sea surface height anomaly, and time-lagged surface chlorophyll-a concentrations. CNN classification accuracy of the five standard dive profiles was 95%. Subsequent analyses revealed that the two clusters differed in their

composition of standard dive shapes, with each cluster dominated by shapes indicative of distinct behaviors (pelagic foraging and exploration, respectively). The use of these two machine learning approaches allowed for discrete behaviors to be identified from vertical time series data, first by clustering vertical movements by their movement metrics (DTW) and second, by classifying dive profiles within each cluster by their shapes (CNN). Statistical inference for the identified clusters found distinct relationships with environmental covariates, supporting hypotheses of vertical niche switching and vertically structured foraging behavior. This approach could be similarly applied to the time series of other animals utilizing the vertical dimension in their movements, including aerial, arboreal, and other aquatic species, to efficiently identify different movement behaviors and inform habitat models.

Introduction

Advances in movement ecology owing to large-scale applications of biotelemetry have resulted in an era of discovery on the previously poorly understood behaviors of migratory species. A current challenge is to generalize these movements into mechanistic and conservation frameworks (Nathan et al. 2008, Patterson et al. 2008, Lowerre-Barbieri et al. 2019). Many of these studies have focused on horizontal movement patterns, using movement models in combination with telemetry data to classify behavioral segments (Bailey et al. 2008, Jonsen et al. 2013, Hurme et al. 2019). Movement in the vertical dimension, which more rapidly exposes animals to changes in trophic and physical conditions (particularly in marine ecosystems Steele 1989, Shepard et al. 2013), has received less attention. The causes and consequences of various classes of vertical movements are often less understood

than horizontal movement categories, especially for remote portions of the migratory path (Hochscheid 2014, Roncon et al. 2018). For air-breathing marine animals that utilize both vertical and horizontal dimensions for signature behaviors such as foraging and transiting, ecological trade-offs have important implications, where dive duration and depth balance respiratory demands against energy gains (Thomson et al 2011, Hochscheid 2014).

For migratory marine species (such as marine mammals, seabirds, turtles, sharks, and tuna) that traverse large distances, classifying dive profiles has often relied on subjective manual classification of individual dive profiles or Euclidean distance clustering methods (Schreer and Testa 1996, Wilson and Block 2009, Howell et al. 2010, Thomson et al. 2011). These time-consuming methods are prone to either human error and bias (in the case of manual classification) or potential loss of information and misclassification (in the case of Euclidean distance clustering) (Melnykov and Maitra 2010, Lee et al. 2020). Machine learning methods offer an alternative approach to matching phenomena in time and magnitude, as the classifications made by machine learning models are guided by the data and not the observer (Lucas 2020).

Machine learning algorithms have proven useful for a variety of ecological studies due to their flexibility, computational performance, and ability to recognize patterns in noisy observational data, and they have become increasingly applicable for movement ecology studies. DTW clustering is a method of unsupervised machine learning that identifies groups of similar time series by allowing the time series to be offset in time and length, thereby avoiding high dissimilarities between entities that

are similar in shape but differ only in spatiotemporal offset (Lee et al. 2020). Despite being an older technique most popular for speech classification, DTW clustering methods have only recently been applied to animal movement data (Cleasby et al. 2019, Frankish et al. 2020; Secor et al. 2021). Convolutional neural network (CNN) image classification models are a form of supervised machine learning that have often been applied to video or image data for species classification (Siddiqui et al 2017, Tabak et al 2018, Willi et al 2019) or animal detection (Salman et al 2020). In ecology, neural networks have broadly been used to model movement in response to the landscape (Tracey et al. 2011) and determine behavioral states from migratory paths (Wijeyakulasuriya et al. 2020). However, the application of a CNN to movement data is rare, although novel work has used them to classify fly behaviors from video still frames of movement trajectories (Stern et al. 2015). The application of a DTW analysis and CNN model to vertical movement data for clustering and classification, respectively, of behavior would be novel.

Sea turtles are migratory marine reptiles that spend the majority of their lives in the ocean, where vertical structure of resources results in a variety of behaviors at depth. These behaviors can be basically described by their dive time series or profiles (often derived from time-at-depth or TAD data), including the general shape of the dive and the parameters or metrics of the dive (e.g., depth and duration). There are 7 standard and previously described dive profile shapes for sea turtles (Shapes A, B, C, D, E, F, G, H, see Fig 3 in Hochscheid 2014), 6 of which relate to turtles diving at depth (Shapes A, B, D, D, E, F, although Shape B can only be detected with fine-scale movement data). Shapes have general behaviors associated with them (e.g.,

Shape A being bottom feeding and Shape C exploration) but the shape of a dive is not necessarily indicative of any one behavior (Seminoff et al 2006) and can occur at a variety of depths or durations. Determining the most likely behavior associated with any one dive profile, then, is challenging without also describing its metrics, shape, and if possible, its time of day and spatial location (Hochscheid 2014). Determining dive shapes from vertical movement profiles has previously been reliant on time-consuming methods, such as manual or visual classification of dive profiles (Salmon et al 2004, Seminoff et al. 2006, Okuyama et al 2016), and methods to group these dives into quantitatively distinct clusters have included Euclidean distance-based methods (Howell et al 2010) or principal components analyses (PCA; Houghton et al 2002, Fossette et al 2007), both of which do not account for time mismatches and variances in input dive time series data. The use of machine learning for both of these tasks (classification and clustering of dive profiles) represents a modern solution to determining discrete behavior from large numbers of dives.

To determine vertical behavior from a large sample size of vertical time series data, we explored the use of a DTW clustering analysis and CNN image classification model, utilizing leatherback turtles (*Dermochelys coriacea*) as a model organism. Leatherbacks dive actively during their migration and foraging periods at sea, where they target ephemeral, pelagic patches of gelatinous zooplankton that aggregate along ocean fronts and density gradients at a variety of depths (Graham et al. 2001, Wallace et al. 2006). Dive behavior for leatherbacks has mostly been described for female Atlantic leatherbacks during the inter-nesting period (Fossette et al. 2007, 2008, 2010; Hamelin et al 2014). Dive behavior for leatherbacks during

their post-nesting migratory and pelagic foraging phases is mostly undescribed, especially for the critically endangered Eastern Pacific (EP) leatherback population. EP leatherbacks have the longest remigration interval of any leatherback population, spending years foraging in the nutrient-poor South Pacific Gyre (SPG) between nesting periods (Reina et al 2002, 2009). Previous models of only their horizontal (surface) movements have had difficulty parsing out foraging behavior (Bailey et al. 2012b). To identify discrete vertical behaviors, including foraging, for EP leatherbacks, we 1) applied a DTW clustering analysis to group dives by their metrics (depth and duration) 2) used a CNN to classify images of dive profiles within each DTW cluster by their shape and 3) determined ecological significance and distinction of the DTW clusters using a generalized additive mixed model (GAMM) with environmental covariates. This work represents a unique approach to determining behavior from vertical time series data and provides a fast and novel alternative method for dive profile classification and clustering for sea turtles. The methods are generalizable to other species with multidimensional movements and behaviors, including other aquatic taxa and aerial and arboreal species.

Methods

Dataset and Processing

We used dive data from a set of published tracking data for 31 post-nesting female adult Eastern Pacific leatherback turtles in this study (see Shillinger et al. 2008), each of which had been tagged with Sea Mammal Research Unit (SMRU) Satellite Relay Data Logger (SRDL) tags from 2004 to 2007. The tags reported both

ARGOS-derived surface locations and dive depths from pressure sensors. Transmitted data included latitude and longitude, time, and dive metrics (total dive duration, maximum dive depth, four intermediate depth and duration points for each dive). The dive time series used in both the DTW analysis and the CNN model were extracted from the four intermediate depth and duration points and the beginning and end surface points for each dive. After removing very shallow (< 10 m) and duplicate dives, the final dataset had 28,217 dive time series, with 118 to 3,534 dive profiles per individual (Shillinger et al. 2011). A "dive" was considered to be vertical movements between greater than 10 m and less than 1500 m depth, to exclude surface movements and errors. Dives had an interannual mean depth of 49.2 m (± 10.1 m SD) and mean dive duration of 24.9 min (± 4.3 min SD) (Shillinger et al. 2011).

Dynamic Time Warp Clustering

DTW clustering was used to group dives by their metrics (depth and duration) - this method uses unsupervised machine learning to match time series in a direction that minimizes both the distance between the time series and the variance of the data within each final cluster (Lee et al. 2020). It can be implemented in the R statistical language and computing environment (R Core Team 2021), using the "dtwclust" R package (Sarda-Espinosa 2019a). The function used to carry out the DTW clustering requires data imputation so that each dive time series has the same interval time steps. This was accomplished using the "imputeTS" R package and its "na_interpolation" function (Moritz and Bartz-Beielstein 2017), which linearly imputed each dive time series' points at regular 20 sec intervals. This interval was chosen based on the range of dive durations (80 - 5,190 sec) and the minimum resolved time step (2 sec). The

20 sec interval was judged sufficient to capture the shape of both short and long duration dives (Fig A2.1).

DTW clustering also requires choosing both a clustering and centroid method to, respectively, determine how to assign data to clusters and specify what will be the central object of each cluster. We applied the partitioning around medoids (PAM) method, which uses actual time series from the input data as the cluster centroids, to iteratively assign time series to one of k clusters based upon within-cluster similarity, where k or the number of clusters is determined by the user (Lee et al. 2020). Here, a range of values for k were tested (2–7), with the final value for k chosen based on the majority vote from six internal cluster validity indices (Sarda-Espinosa 2019b). The DTW clustering allowed for each input time series to be of different lengths and the central object or final centroid for each cluster to be one of the time series from the input data (Lee et al. 2020). The DTW analysis with the specified chosen clustering and centroid methods was conducted using the "ts_clust" function from the "dtwclust" R package (Sarda-Espinosa 2019a).

Convolutional Neural Network Image Classification Model

Using images of the shape of each dive profile (generated in R as 72 ppi resolution and 480 pixel black and white JPGs) as input data, we trained a CNN to label images according to five standardized, previously published shapes (Shapes A, C, D, E, and F) , irrespective of their dive depth and duration (Seminoff et al. 2006, Hochscheid 2014, Seminoff et al. 2021). The supervised nature of the CNN allowed us to train our model using these, assigning the most similar standardized shape to each dive time series within the DTW clusters.

To create the dataset to be used in the training and validation of the CNN (N=189 dive profiles), we combined 139 randomly selected and manually labeled dive profiles with 50 images (10 of each type) representing the most generalizable shape for the five standard dive types (Fig. 3 from Hochscheid 2014 and Fig 2.1.a).

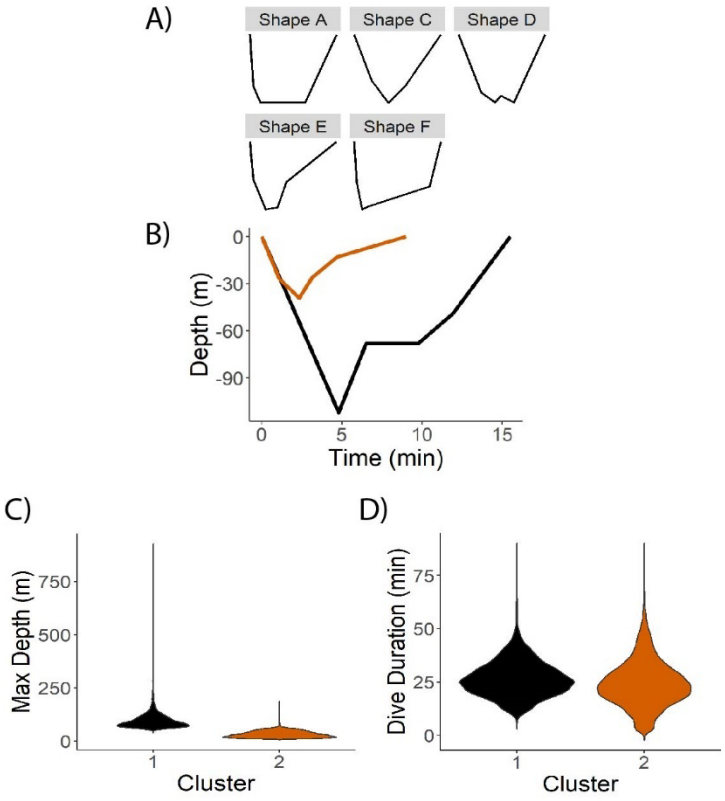

Fig 2.1. *a) Example plots for the different standard dive shapes (N=5) used in the image classifier convolutional neural network model (CNN). b) Centroids for each dive cluster (black - cluster 1, orange - cluster 2) from the dynamic time warp (DTW) clustering analysis. c) Violin plots for the maximum depth (m) and d) dive duration (min) for the two different dive clusters from the DTW clustering analysis.*

Manually labeled dive profiles from the dataset (N=139) were chosen to best represent the variety present in the different shapes possible (Fig A2.3). Synthetic dive profiles (N=50) represented the "gold standard" for each shape (see Hochscheid

2014, Fig 3) and early tests of the CNN with these showed that they improved model accuracy.

The CNN for image classification was created on a highly efficient computing system (Smithsonian computing cluster 'Hydra' and Nvidia GeForce GPU) and implemented using the "fast.ai" deep learning wrapper library from PyTorch (Howard and Gugger 2020). Due to the basic shape of our target images (Fig 2.1.a), we were able to use transfer learning to develop our model, whereby a pre-trained and generalizable CNN image classification model (ResNet-34 architecture) was applied to our personal dataset to sort images into 5 classes with distinct and simple line shapes (He et al. 2016).

The CNN was then fine-tuned by using the dive profile images from the dataset described above and randomly assigning them into a training (N=152) and validation set (N=37, 20% of the training set). The model was run iteratively with the training dataset over 480 epochs (8 min and 2 sec). A more detailed description of deep machine learning methods and image classification can be obtained from Weinstein (2018) and Norouzzadeh et al. (2018). Model validity and accuracy was assessed using a confusion matrix (Fig A2.4). Training loss and validation loss functions were monitored for balance to assess and prevent model overfitting. After the model had reached a high accuracy with the training data (> 90%), it was applied to the whole dataset (N=28,217 dive time series) to predict the standard dive shape for each dive time series within the DTW clusters.

Environmental Relationships for Clusters

A GAMM (Wood 2006) was used to examine environmental relationships for the DTW dive clusters. To match the temporal resolution of environmental covariates, daily positions for the turtles were estimated using the "foieGras" R package, which fits a continuous time state space model to predict locations in regular time intervals (Jonsen et al. 2019, Jonsen and Patterson 2020). The daily proportion of each DTW dive cluster was used as a response variable.

A total of five environmental covariates (sea surface height anomaly, sea surface temperature, bathymetry, surface chlorophyll-a concentration, and Ekman upwelling) were considered, with variables being chosen based on previous association with leatherback horizontal (surface) movements (Bailey et al. 2012a). Environmental variables were obtained from the National Oceanic and Atmospheric Administration CoastWatch ERDDAP server (Table A2.1). Three variables typically used as proxies for leatherback gelatinous zooplankton prey include surface chlorophyll-a concentration, Ekman upwelling, and sea surface height anomaly, of which there may be a time lag (about 30 days) between peak surface chlorophyll-a concentrations, the bloom of gelatinous plankton, and the arrival of foraging tertiary consumers (Feigenbaum and Kelly 1984, Schedler-Meyer et al. 2018), such as leatherbacks. We tested time lags of 30 days in candidate models for surface chlorophyll-a (Abrahms et al. 2019) and included sea surface height anomaly and Ekman upwelling as additional candidate variables. Year of tracking (2004, 2005, or 2007) was also considered as a covariate, as individuals tagged in 2005 experienced

an El Niño Southern Oscillation event that affected sea surface temperatures and primary productivity (Saba et al. 2008).

The GAMM was fit using the "mgcv" R package (Wood 2017). Individual tracks were included as a random effect to account for within track correlation. A quasibinomial distribution with a logit link function was used to account for non-normality. Backward stepwise model selection was performed to select the final model using the lowest Akaike information criterion (AIC) score. The final model was checked for concurvity (collinearity of non-linear model terms), normality, and uncorrelatedness of the residuals, and for the optimal number of knots (k) for each smoothed covariate (using the "gam.check" function from the "mgcv" R package).

Spatial, Latitudinal, and Temporal Patterns for Dive Clusters and Shapes

As dive depth and behavior have previously been shown to be affected by spatial and temporal variables, such as phase of migration, latitude, and time of day (Shillinger et al. 2011), relationships were investigated for these for the different dive clusters and shapes.

For dive clusters found with the DTW analysis, dive time series were categorized as being in either the migratory corridor ("migratory" phase) or the foraging region ("foraging" phase), delimited at 8.27˚S (latitude) (Bailey et al. 2008). Latitudinal patterns were visualized using density plots of dive clusters by latitude. Diel patterns were investigated by deriving the sun altitude for each dive time series (using the "suncalc" R package and the "getSunlightPosition" function, Thieurmel and Elmarhraoui 2019) and by extracting night (sunset until before dawn) and day (dawn until before sunset) categories (using the "StreamMetabolism" R package,

Sefick 2016). A Fisher's exact test was applied to counts of dives belonging to clusters found with the DTW analysis to test for differences between categories for 1) the migratory vs. foraging phase and 2) day vs. night.

Further spatial and temporal trends in behavior were investigated for identified dive shapes within each cluster, with density histograms being used to visualize distributions of shapes within each cluster by latitude and hour of the day.

Results

Dynamic Time Warp Clustering

Analyses revealed two clusters of dive profiles (see Fig A2.4 for further description of the selection of *k*). The centroid for each cluster depicted seminal behavioral differences in dive metrics (depth and duration) (Fig. 1.b). Centroids for both clusters were Shape E (Fig 2.1.a.; Hochscheid 2014). Violin plots and descriptive statistics showed that the two clusters differed primarily in their mean maximum depth, with smaller differences in mean duration (Fig 2.1.c-d, Table 2.1).

Table 2.1. *Descriptive statistics and counts for dive clusters (1, 2) found with a dynamic time warp (DTW) clustering analysis. Columns include the mean, standard deviation, and range (min, max) of maximum dive depth (m) and duration (min); total number of dives; and number of deep dives (> 300 m).*

Cluster	Mean Max Depth (± SD)	Max Depth (Min, Max)	Mean Duration (± SD)	Duration (Min, Max)	Total Dives	Total Deep Dives
1	104 (±70)	51-914	27 (±9)	7-87	6,824	122
2	32 (±14)	11-182	24 (±11)	1-87	21,395	0

Dives from cluster 1 were deeper on average (mean 104 m, ± 70 SD) than those from cluster 2 (mean 32 m, ± 14 SD). Cluster 2 dives were similar in mean duration to cluster 1, with cluster 2 dives being slightly shorter (24 min, ± 11 SD) on average than cluster 1 dives (27 min, ± 9 SD).

Convolutional Neural Network Image Classification Model

The image classifier CNN trained on a dataset of randomly sampled, labeled dive profiles and the five standardized dive types from the literature achieved an accuracy of 95% on the validation data set. During the training period, the model correctly labeled the majority of images, with only two out of the N=37 used in the testing set being labeled incorrectly (Fig A2.5).

The fully trained CNN predicted the majority of the dataset to be Shape C, followed by similar proportions of Shapes E and F (Fig 2.2.b).

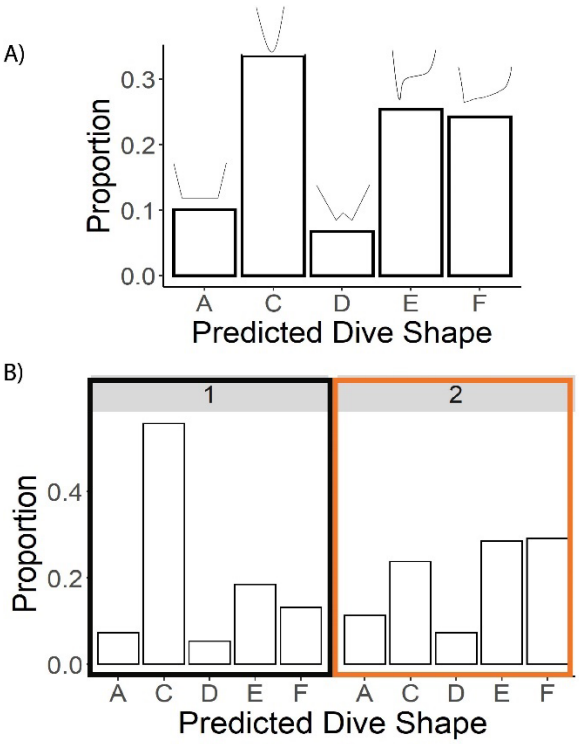

Fig 2.2. *a) Proportion of each dive shape predicted by the image classifier, convolutional neural network model (CNN) for the entire dataset of dive time series (N=28,217). b) Proportion of each predicted dive shape type with respect to the two dive clusters found with the dynamic time warp (DTW) clustering analysis.*

When the dive profiles were separated by their assigned cluster, cluster 1 (deeper) had Shape C dives as its highest proportion, followed by Shapes E and F. Cluster 2 (shallower) had Shape F as its highest proportion, followed by similar proportions of Shapes E and C (Fig. 2.b).

Descriptive statistics for predicted shapes (A, C, D, E, F) for all dives (N=28,217) and by DTW cluster membership (1, 2) showed differences between shapes and clusters (Table 2).

Table 2.2. *Descriptive statistics and counts for dive shapes (A, C, D, E, F), found with a Convolutional Neural Network (CNN) image classification model, and dive*

clusters (1,2) found with a dynamic time warp (DTW) clustering analysis, with values shown for the mean, standard deviation, and range (min, max) of maximum dive depth (m) and dive duration (min); total count of dives; and count of deep (> 300 m) dives for each grouping.

Cluster 1						
Dive Shape	Mean Max Depth (± SD)	Max Depth (Min, Max)	Duration (± SD)	Duration (Min, Max)	Proportion of Dives in Cluster	Total Deep Dives
A	88 (±33)	51-362	26 (±8)	7-50	0.07	2
C	115 (±82)	57-914	26 (±9)	8-81	0.56	104
D	89 (±24)	59-330	27 (±9)	11-79	0.05	1
E	96 (±54)	55-818	28 (±10)	9-87	0.19	11
F	88 (±47)	51-722	28 (±8)	8-59	0.13	4
Cluster 2						
Dive Shape	Mean Max Depth (± SD)	Max Depth (Min, Max)	Duration (± SD)	Duration (Min, Max)	Proportion of Dives in Cluster	Total Deep Dives
A	27 (±13)	11-182	23 (±9)	2-70	0.12	0
C	39 (±17)	11-84	22 (±9)	1-65	0.24	0
D	32 (±14)	12-80	24 (±10)	3-65	0.07	0
E	30 (±16)	11-134	25 (±13)	1-87	0.28	0
F	30 (±12)	11-76	26 (±11)	1-81	0.29	0

Dives with Shape C were the deepest in both clusters (cluster 1 mean 115 m ±82 SD, cluster 2 mean 39 m ±17 SD) and in cluster 1, were overall the deepest dives and comprised the majority of extremely deep (> 300 m) dives (N=104). Shape E dives were second in having a high mean depth (cluster 1 mean 96±54 m SD, cluster 2 mean 39±17 m SD) and had the second highest count of extremely deep dives (N=11). Despite having the deepest mean depths, Shape C dives had the lowest mean dive duration in cluster 1 and a lower mean dive duration overall (cluster 1 mean 26±9 min SD, cluster 2 mean 22±9 min SD) than Shapes E (cluster 1 mean 28±10 min SD, cluster 2 mean 25±13 min SD) and F (cluster 1 mean 28±8 min SD, cluster 2 mean 26±11 min SD). A scatterplot of the maximum depth for dives and their predicted shapes versus their dive duration (Fig A2.2.b) showed that for dives in cluster 1, a linear smoother for all combined dive shapes and for individual dive shapes C, D, E, and F had a strong positive relationship; for cluster 2 dives, there did not appear to be any relationship between maximum dive depth and duration.

Environmental Relationships for Clusters

The GAMM was implemented to model proportion of cluster 1 dives (since there were only two clusters, the relationships for cluster 2 are inverse cluster 1). The model selection process resulted in non-linear, smoothing terms for sea surface height anomaly, sea surface temperature, chlorophyll-a concentration (log transformed due to non-normality), and bathymetry (Table A2.2). A 30-day lag term was selected for surface chlorophyll-a concentration (Table A2.2). Cluster 1 (deeper) dives were

frequent with more positive sea surface height anomalies (Fig 2.3.a-b) and lower lagged, log chlorophyll-a concentrations, deeper depths, and higher sea surface temperatures (Fig 2.3.c-e)- opposite relationships were then observed for cluster 2 (shallower) dives.

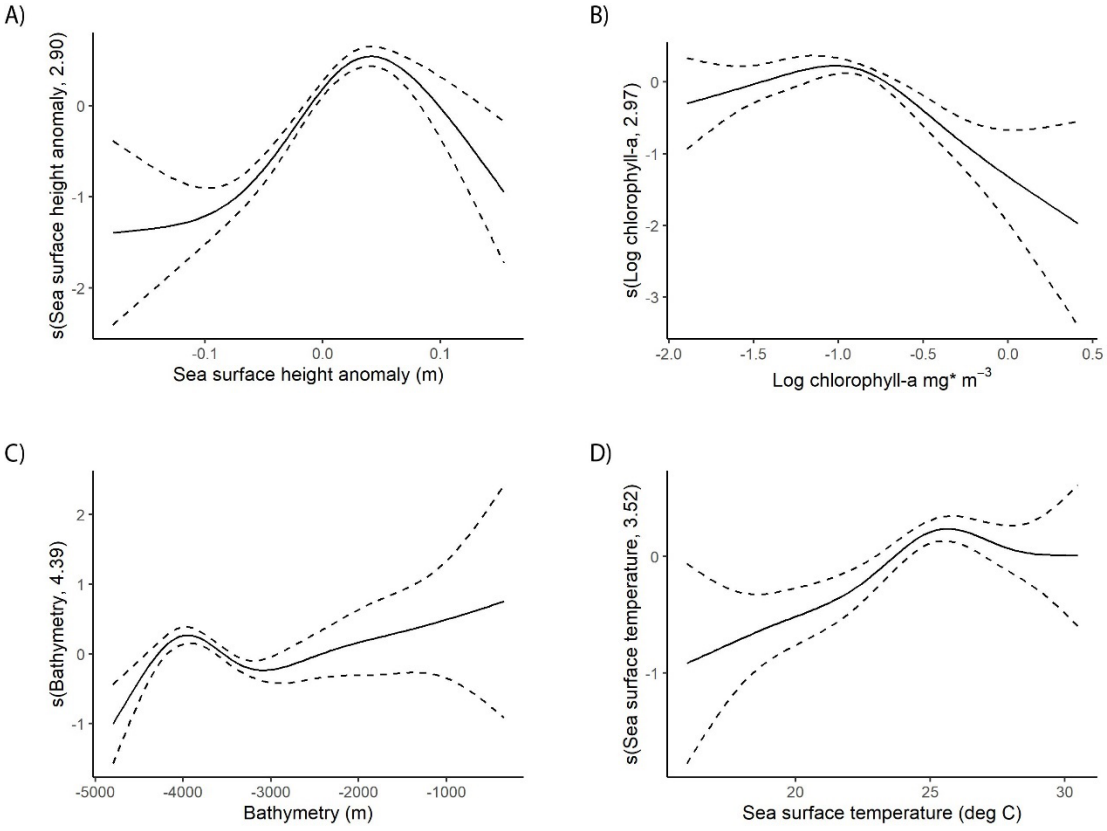

Figure 2.3. *Final generalized additive mixed model (GAMM) linear and non-linear (smoothing) terms for daily proportion of cluster 1 dives as a function of a) sea surface height anomaly c) log transformed surface chlorophyll-a (30-day lag) d) bathymetry and e) sea surface temperature. Since the response is a binary proportion (e.g. proportion of cluster 2 dives = 1 – proportion of cluster 1 dives), the results for cluster 2 dives show an opposite pattern.*

Spatial, Latitudinal, and Temporal Patterns for Dive Clusters and Shapes

Both spatial and temporal trends in dive clusters were apparent. A significantly higher proportion of cluster 1 (deeper) dives occurred during the foraging region (Fig 2.4.a, Fishers exact test p-value < 0.0001).

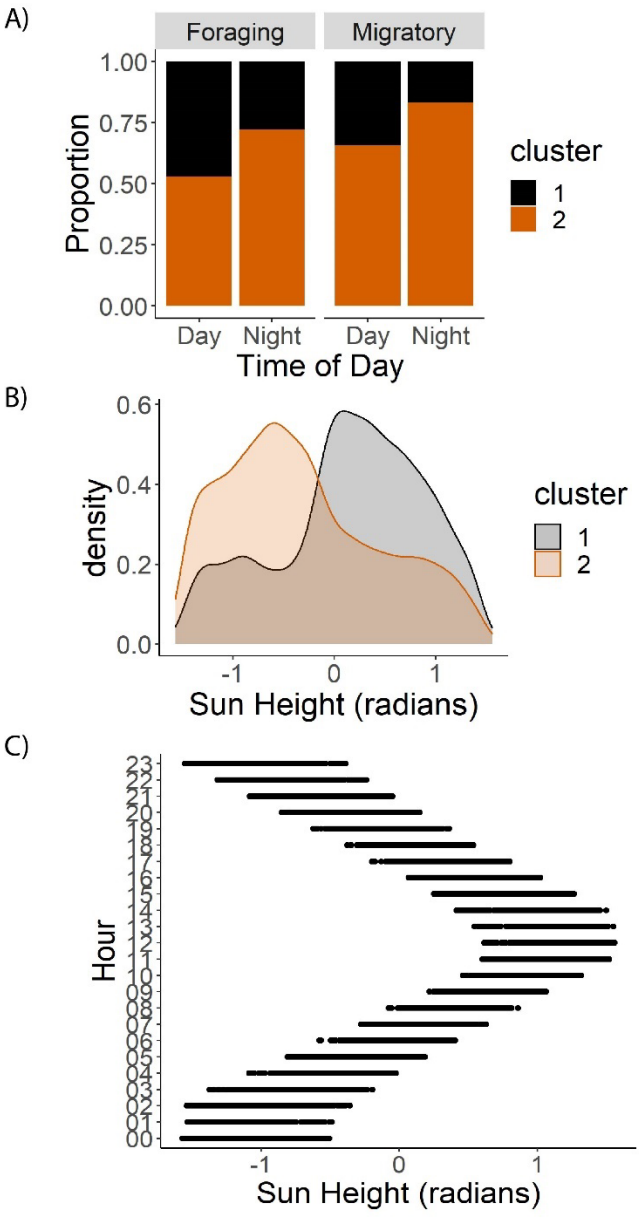

Figure 2.4. *a) Proportion of each dive cluster category for night vs. day and migratory vs. foraging categories. b) Density plot for sun height (radians), colored by*

dive cluster group identified with the dynamic time warp (DTW) analysis and c) scatterplot of time of day (hrs) as a function of sun height, with zero representing the sun being at the horizon.

Cluster 1 (deeper) dives had peak densities in both mid (5-20˚south) and low latitude (north of 0˚) areas, whereas cluster 2 (shallower) dives had peak densities in mainly low latitudes (Fig 2.5.a-b).

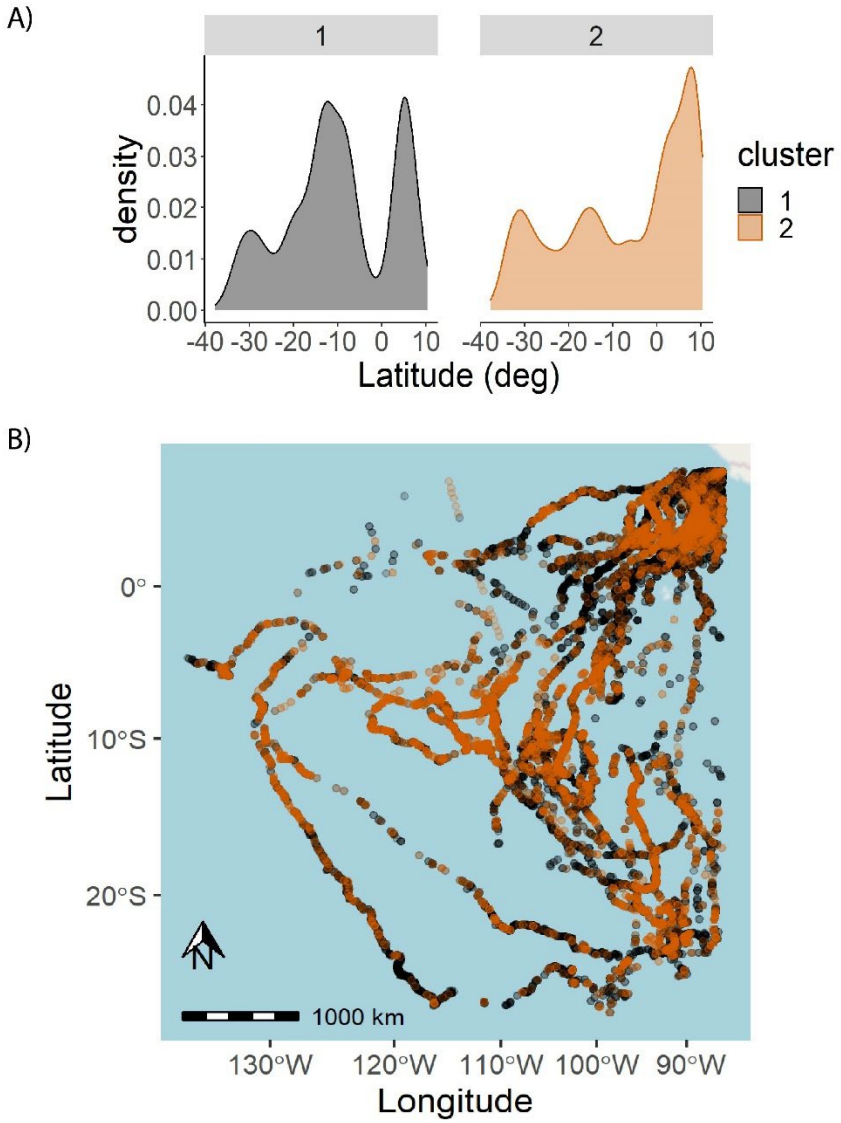

Fig 2.5. *a) Density plots for the dive clusters (cluster 1- black, cluster 2- orange) from the dynamic time warp (DTW) analysis by latitude (deg). b) Map of the different dive clusters, colored by cluster. The map was made using the "rosm" R package (Dunnington 2019).*

Both cluster 1 and cluster 2 type dives had another peak in density in low latitude areas south of the equator (around 30˚south, Fig 2.5.a-b). Diel patterns showed a significantly lower proportion of cluster 1 (deeper) dives and a higher proportion of cluster 2 (shallower) dives at night than during the day (Fig 2.4.a, Fishers exact test p-value < 0.0001). Further, dives occurred predominantly at lower sun heights, with an increased presence of cluster 1 (deeper) dives during post-sunrise and pre-sunset hours and cluster 2 (shallower) dives during pre-sunrise and post-sunset hours (Fig 2.4.b-c).

There were also noticeable differences between DTW clusters in the spatial and temporal distribution of predicted dive shapes (Fig 2.6.a-d).

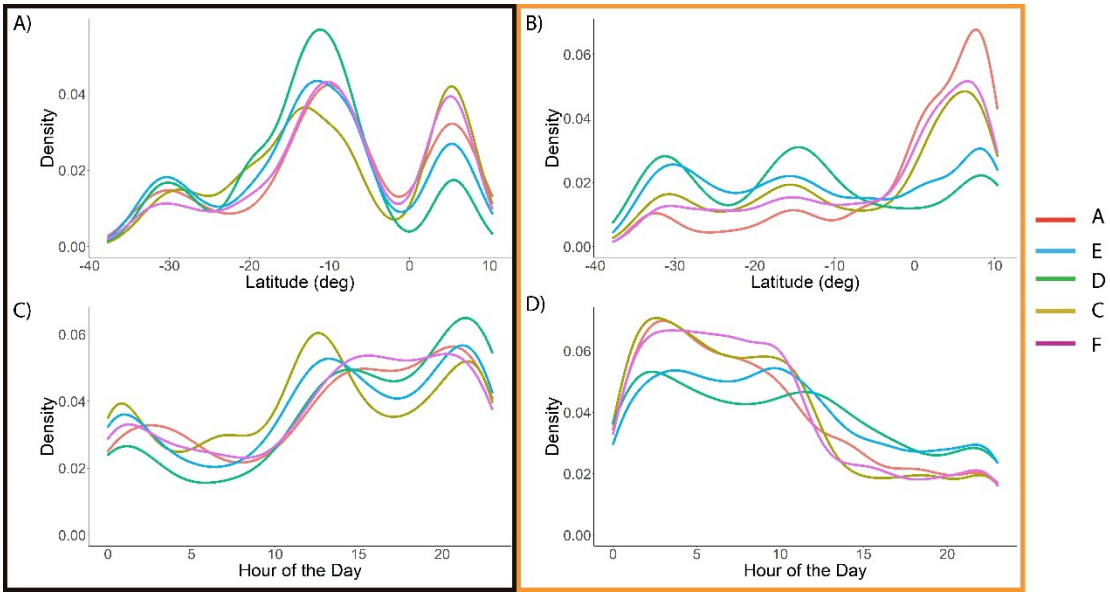

Fig 2.6. *Density histograms (kernel density estimates of probability distribution functions) for dive profile shapes identified with an image classifier, convolutional neural network (CNN) model, with separate plots shown for density of dive shapes as a function of latitude (deg) for a) cluster 1 (black) and b) cluster 2 (orange); and for density of dive shapes as a function hour of the day for c) cluster 1 (black) and d) cluster 2 (orange).*

For cluster 1, Shape C dives had the highest peak density out of the shapes within low latitude (north of 0˚) areas, with Shape D having the lowest (Fig 2.6. a). In mid latitude (5-20˚south) areas, this pattern was reversed, with Shape D having the highest density and Shape C the lowest (although somewhat similar densities here between Shapes C, A, E, and F) (Fig 2.6.a). In low latitudes of the foraging region south of the equator (around 30˚south), dive shapes for cluster 1 had similar densities (Fig 2.6.a). For cluster 2, low latitude (north of 0˚) areas were dominated by Shape A, followed by Shapes F and C (Fig 2.6.b).

Similar to cluster 1, mid latitude (5-20˚south) areas for cluster 2 had peak densities in Shape D dives, followed by Shape E and with some separation between other shapes (Fig 2.6.b). South of the equator in low latitudes (around 30˚south), peak densities for cluster 2 dives were seen for both Shapes D and E, followed by Shape C (Fig 2.6.b).

Density histograms (kernel density estimates of probability distribution functions) of predicted dive shapes versus time of day showed that during the day at hours of peak sun height (~ 11-14 hrs, Fig 2.4.c), dive shapes for cluster 1 were predominantly Shape C, followed by Shape D (Fig 2.6.c). At night when sun height is

low, there was a peak for cluster 1 in Shape D dives (around hour 20) and Shape C and E dives (around hour 0 or midnight) (Fig 2.6.c). For cluster 2, there were broad peaks for dive shapes A, C, and F during early to late morning (hours 3-10) when the sun height is low (Fig 2.6.d).

In contrast, during daytime all the way through nighttime hours, dives for cluster 2 were dominated by Shapes D and E (Fig 2.6.d).

Discussion

This study presented an integrative machine learning approach to identifying discrete vertical behaviors. Dynamic Time Warp (DTW) analysis allowed us to first place vertical profiles of movement (dives) for leatherback turtles into distinct groups or clusters based on metrics (dive depth and duration). An image classifier Convolutional Neural Network (CNN) was then used to classify vertical movement profiles in each DTW cluster according to standardized dive shapes for this species (Hochscheid 2014). A Generalized Additive Mixed Model (GAMM) of DTW clusters and their temporal and spatial trends allowed us to further infer ecological significance for identified vertical behaviors. With advances in tagging technology, it is increasingly common for movement datasets to have multiple dimensions (e.g., vertical and horizontal) and large sample sizes, the latter of which makes manual classification of tracks difficult. Machine learning methods offer efficient alternatives to both clustering and classification of vertical time series data. Our approach, which combined unsupervised time series clustering and supervised image classification together to identify vertical behaviors, will be useful for other movement studies where 1) input time series may have offset times or variable

lengths 2) shapes of vertical movement can occur at a variety of metric values 3) vertical movements need to be placed into discrete classes 4) previously known standard shapes exist against which to compare movement profiles and 5) have large numbers of profiles that make manual classification or parameter-heavy clustering methods inefficient. For the turtles in this study, the ecologically distinct classes of vertical movement we identified will inform future modeling and conservation efforts.

The supervised nature of the CNN allowed for specific dive shapes to be found within each DTW cluster according to their similarity to published ("standardized") dive shapes for sea turtles, providing a fast new method for dive shape classification with known vertical profiles of movement. Although deep learning models have been previously used for species photo-identification (Siddiqui et al. 2017, Tabak et al. 2018, Willi et al. 2018, Salmon et al. 2020), the profile analyses introduced here can be adapted for other species where classification of behaviors can be related to pre-defined categories and images of movement shape. The use of a CNN to classify sea turtle dives is a significant improvement over time costly and error prone manual and visual methods. It additionally provides an alternative classification method to other supervised machine learning methods (e.g., random forests for leatherback dive profiles, Okuyama et al 2021), as it classifies profiles solely based on the image or shape. This allows for the clustering of shapes into groups (in our case, two clusters; Fig 2.2.b). Our methods produce a highly accurate model that is trained simply on the shapes (not species-specific quantitative values) of dive profiles known for sea turtles and thus, can be extended to other

species and populations. Once fully trained, a CNN such as ours is extremely fast and efficient when applied to other datasets. To aid other studies of sea turtle dive behavior, we have developed a graphical user interface of our trained CNN (see "Code and Tool Availability" section). Users can upload either a single image or multiple images of sea turtle dive shapes and receive the predicted dive shape and certainty estimates in an output text file. This generalizes our CNN for application to other sea turtle studies and also demonstrates how supervised machine learning might be more broadly useful within movement ecology.

The two clusters of vertical movements for this population of leatherback turtles differed in their quantitative metrics. The dives from the first cluster were found to be deeper and slightly longer than the dives from the second cluster, which were shallower and shorter (see Tables 1-2 and Fig 2.1.c-d). The similarity in mean dive durations between the clusters was not unexpected, as a previous study on migratory post-nesting leatherbacks in the Pacific also showed similarities in dive durations across dive types (Okuyama et al 2021). However, the longer mean dive duration for deeper dives within cluster 1 (Tables 1, 2) and the positive trend between maximum depth of dives in cluster 1 with dive duration (Fig A2.2.b) support previous work suggesting a linkage between dive depth and duration (Okuyama et al 2021), with leatherbacks likely approaching their aerobic dive threshold around 30-40 min (Hays et al 2004, Sale et al 2006, Okuyama et al 2016).

Our two dive clusters also differed in their spatial and temporal distributions. Cluster 1 (deeper) dives occurred more frequently during the day and during the foraging phase (south of 8.27˚S latitude), whereas cluster 2 (shallower) dives were

more often at night and during the migratory phase (north of 8.27˚S latitude) (see Fig 2.4.a-c). These results support previous findings of deeper mean dive depth during daytime hours in the foraging phase (Shillinger et al. 2011). Turtles likely perform mostly shallower traveling dives during their migratory phase and have a mixture of deep and shallow dives during their foraging phase, where they dive shallower at night to match the diurnal vertical migration of their prey and deeper during the day to search for prey patches and/or shed heat (Eckert 2006, Bailey et al. 2008, Shillinger et al. 2011, Okuyama et al. 2021). Nevertheless, daytime dives for foraging and feeding may also occur where turtles can use higher light levels to visually detect prey at a distance (Brudenall et al 2008, Narazaki et al 2013).

Further distinction between DTW clusters was clear with regards to the identified dive shapes within each cluster. Both clusters had dominant dive shapes corresponding to shapes ("C", "E", and "F", see Fig 2.1.a and Fig 2.2.b) that have been previously associated with a variety of behaviors, including transiting, exploration, prey searching, thermoregulation, resting, or pelagic foraging behavior (Fossette et al 2007, Thomsen et al. 2011, Narazaki et al. 2013, Hochscheid 2014, Okuyama et al 2016). These dive shape types have been observed for other leatherback populations and life phases, such as those occurring during the inter-nesting period as well as during post-nesting migration (Hays et al. 2004, Sale et al. 2006, Fossette et al. 2007, Okuyama et al. 2021). Overall, the majority of our dives were classified as Shape C (Fig 2.2.a), especially for cluster 1 (deeper) (Fig 2.2.b, Table 2). Previous work classifying dives for migratory West Pacific leatherbacks similarly found that Shape C (i.e., dives shaped like 'V') were most common, with

functions likely corresponding to thermoregulation, prey searching, extraordinarily deep dives (> 300 m), or gliding during travel to reduce energy costs and metabolic heat production (Fossette et al 2007, Okuyama et al 2021). Indeed, with our study we found that Shape C dives were deepest on average across both clusters, and that the majority of very deep dives (> 300 m) observed were for Shape C, cluster 1 dives (Table 2).

Spatial variability of resources may explain observed latitudinal differences in the distribution of the two dive clusters. Overall, cluster 1 (deeper) dives had a higher density around mid-latitudes (10-20˚south) and cluster 2 (shallower) dives had a higher density around equatorial (5˚north- 5˚south) and low latitude areas (see Fig 2.6.a-b). The turtles in this population are thought to migrate in a corridor through warmer, energetic, and productive low latitude and equatorial areas (Shillinger et al. 2008) into the more nutrient-poor South Pacific Gyre, where prey is patchily distributed in lower densities at depth (Saba et al. 2008, Bailey et al. 2012b). Although the edges of the gyre foster frontal zones that boost productivity and prey encounters (Saba et al. 2008), deeper dives may be required closer to the gyre centre to locate ephemeral patches of prey. The higher density of cluster 1 (deeper) dives around upper mid-latitudes corresponds with areas of the gyre featuring potentially higher zooplankton biomass due to a shallower thermocline and nutricline (Fernandez-Alamo and Farber-Lorda 2006, Bailey et al. 2012b). Previous modelling of turtle horizontal movements in this region found area-restricted search behavior (ARS) (Bailey et al. 2012a), which is often associated with foraging (Narazaki et al. 2013), and our results support these findings.

The shape of dives within cluster 1 and in mid-latitudes (5-20˚south) additionally highlight this as a foraging region at depth for leatherbacks. Shape D and ,arguably, Shape E, ("W" dives) have been characterized as feeding dives in previous studies, with bottom "wiggles" of the dive corresponding to turtles searching for, chasing, and handling prey (Fossette et al 2008, Okuyama et al 2021). Shape D and E dives also likely correspond to feeding, searching, and foraging behavior, with deeper (cluster 1) Shape D and E dives occurring in peak densities in mid latitudes at night (especially Shape D) or during midday (Shape E) (Fig 2.6.a, c). The oligotrophic SPG habitats used by these turtles in their foraging phase have dispersed aggregations of gelatinous zooplankton prey and a deeper thermocline (Saba et al. 2008, Stromberg et al. 2009, Shillinger et al. 2011). Such environmental conditions may promote a higher proportion of searching and foraging (Shape D and E) dives at depth to find higher quality food patches throughout the water column. Leatherbacks may also be changing the depth (e.g., cluster 1 versus cluster 2 dives) of their foraging behaviors (Shapes D and E) with the time of day to match diurnal changes in their prey distribution (Fossette et al 2007, Okuyama et al 2021). Similar to Shapes D and E, Shape A ('U' shaped dives) have also been previously characterized as feeding dives when occurring at depth, although their lack of bottom wiggles may be indicative of lower foraging success (Fossette et al 2008). Accordingly, we found a peak in deeper (cluster 1) Shape A dives in mid latitudes (5-20˚south) (Fig 2.6.a), where resources are thought to be more dispersed and difficult to find, and at night (Fig 2.6.c) when other foraging-type (D, E) dives are occurring.

Spatial and temporal differences in distribution of different identified dive shapes for our DTW clusters further support use of the migratory corridor (Shillinger et al 2008) by EP leatherbacks for traveling and thermoregulation. Shape C dives were found primarily in lower latitudes north of the equator, followed by mid latitudes (5-20˚south) and during daylight hours with peak sun height values (Fig 2.6.b, c). The high occurrence of deep Shape C and extremely deep dives in the migratory corridor for these leatherbacks (Fig A2.2.a) supports previous hypotheses that turtles are likely using these behaviors to shed excess heat and thermoregulate as they migrate through warmer equatorial waters (Wallace and Jones 2008, Shillinger et al. 2011, Okuyama et al. 2021). When shallow, Shape A dives may be indicative of traveling behavior close to the surface (Fossette et al 2007, Okuyama et al 2021), aligning with our own findings of shallower (cluster 2) Shape A dives occurring in the migratory corridor north of the equator (Fig 2.6.b, Shillinger et al 2008). Shape F dives, with a rapid descent and slower ascent, although they can also represent foraging dives (Fossette et al 2007, Hochscheid 2014) can serve as resting or thermoregulation dives where turtles slowly ascend to the surface to minimize energy expenditure and heat production (Okuyama et al 2016). The latter hypothesis aligns with the peak in shallower (cluster 2) Shape F dives in lower latitudes (north of 0˚, Fig 2.6.b), where vigorous daily swimming and frequent diving occurs as turtles travel towards their foraging region in the South Pacific Gyre (SPG, Shillinger et al 2011).

Both cluster and dive shape results further support that EP leatherbacks have diurnal differences in foraging strategy, utilizing deeper (cluster 1) dives during the

daylight (Fig 2.4.b) to identify prey patches deeper in the water column (Narazaki et al. 2013, Hamelin et al. 2014). In low latitudes (< 25˚south), similar diurnal patterns can occur, with deeper (cluster 1) daytime dives to find aggregations of prey around frontal areas (Shillinger et al. 2011, Saba et al. 2008) and shallower (cluster 2) night dives to target prey patches closer to the surface, without reliance on visual cues and daylight (Shillinger et al. 2011, Bailey et al. 2012a, Narazaki et al. 2013). Our results support this, with a peak in density for foraging behaviors (Shape D and E dives) in both clusters (1, 2) in this region (Fig 2.6.a-b). The presence of deeper (cluster 1) Shape D and E dives in evening and nighttime hours and shallower (cluster 1) Shape D and E dives in early to late morning hours (Fig 2.6.c-d) might indicate that turtles are following diurnal migrations of gelatinous plankton prey closer to the surface as sun height decreases (Fig 2.4.c, hours 18-24).

Our GAMM model allowed us to determine ecological significance for the DTW clusters and improved upon previous habitat models for this population. Chlorophyll-a concentrations are thought to serve as a good proxy for availability of gelatinous zooplankton prey for leatherbacks (Bailey et al 2012a), but past habitat use models (Bailey et al 2012a, Shillinger et al 2008, 2011) found only weak relationships with chlorophyll-a values in areas where foraging is expected for EP leatherbacks. There may be a time lag or delay in blooms of gelatinous zooplankton after peak levels. This would accord with previous studies of migratory marine species that have found time-lagged chlorophyll-a concentrations critical to understanding movement (Abrahms et al. 2019). The results of our GAMM model support that both sea surface height anomalies and 30-day time-lagged surface

chlorophyll-a concentrations significantly influence vertical behavior for leatherbacks in the Eastern Pacific. Cluster 1 (deeper) dives had a higher daily proportion in areas with positive sea surface height anomalies (mesoscale ocean eddies), lower lagged chlorophyll-a concentrations, deeper depths, and warmer temperatures (Fig 2.6), with opposite relationships seen for days with higher proportions of cluster 2 (shallow) dives. These patterns align with spatial trends discussed previously, with cluster 1 dives having peaks in density in the SPG where primary productivity is low, further supporting that foraging behavior in this area is more correlated with variables of vertical movement and water column structure (Bailey et al 2012b). EP leatherbacks overall using different dive depths with varied environmental variables suggests that they may be utilizing different vertical niches throughout their foraging phase through adaptive feeding behavior or "niche switching", whereby different vertical niche space is used along the horizontal, latitudinal migration to compensate for spatiotemporal variation in resources (John and Post 2021).

Our methods have application for further integrative studies for sea turtles, such as with species distribution models and conservation work. As an example, our study species, the EP leatherback, is critically endangered and thought to be most at risk from interaction (bycatch) with fisheries in international waters (Spotila et al. 2000, Lewison et al. 2004, Kaplan 2005, Wallace et al. 2013). These results may inform future conservation efforts for EP leatherbacks, as our study produces discrete vertical movement behaviors at the same resolution as available horizontal (surface) movement data for this population (Bailey et al 2012a). Existing conservation tools for this population (e.g., "South Pacific TurtleWatch", Hoover et al 2019, Degenford

et al 2020) that currently only model surface locations of turtles could potentially benefit by integrating these vertical and surface movements within movement models (e.g., state space or Hidden Markov models) to identify important phases of behavior that can be overlapped with threat data (e.g., fishing effort) and identify priority conservation areas within the SPG.

Beyond sea turtles, we expect that our methods will aid understanding of the 3-D movements of diverse species. Examples include (1) pinnipeds that also have diverse dive types (Davis et al. 2003); (2) migratory fishes such as tuna where studies have used manual classification techniques to parse out dive classes (Wilson and Block 2009); (3) birds that have aerial classes of movement and in some species diving behaviors (Frankish et al. 2021); and (4) arboreal mammals, that have vertical movement within forest canopies (Scheffers et al. 2017, Allan et al. 2019). In summary, application of DTW and CNN approaches to movement data for species moving in three-dimensions may go a long way in helping to understand cryptic behaviors that hinge on vertical context.

Code and Tool Availability

Example code, data, and the developed GUI interface to run our trained CNN are available on my GitHub repository:

https://github.com/barb3800

References

Abrahms, Briana, Elliott L. Hazen, Ellen O. Aikens, Matthew S. Savoca, Jeremy A. Goldbogen, Steven J. Bograd, Michael G. Jacox, Ladd M. Irvine, Daniel M. Palacios, and Bruce R. Mate. 2019. “Memory and Resource Tracking Drive Blue

Whale Migrations." Proceedings of the National Academy of Sciences 116 (12): 5582–87. https://doi.org/10.1073/pnas.1819031116.

Allan, Blake M., Dale G. Nimmo, John PY Arnould, Jennifer K. Martin, and Euan G. Ritchie. 2019. "The Secret Life of Possums: Data Loggers Reveal the Movement Ecology of an Arboreal Mammal." Journal of Mammalogy 100 (1): 158–68.

Bailey, H., G. Shillinger, D. Palacios, S. Bograd, J. Spotila, F. Paladino, and B. Block. 2008. "Identifying and Comparing Phases of Movement by Leatherback Turtles Using State-Space Models." Journal of Experimental Marine Biology and Ecology, Sea turtles: physiological, molecular and behavioural ecology and conservation biology, 356 (1): 128–35. https://doi.org/10.1016/j.jembe.2007.12.020.

Bailey, Helen, Scott R. Benson, George L. Shillinger, Steven J. Bograd, Peter H. Dutton, Scott A. Eckert, Stephen J. Morreale, et al. 2012. "Identification of Distinct Movement Patterns in Pacific Leatherback Turtle Populations Influenced by Ocean Conditions." Ecological Applications 22 (3): 735–47. https://doi.org/10.1890/11-0633.

Bailey, Helen, Sabrina Fossette, Steven J. Bograd, George L. Shillinger, Alan M. Swithenbank, Jean-Yves Georges, Philippe Gaspar, et al. 2012. "Movement Patterns for a Critically Endangered Species, the Leatherback Turtle (Dermochelys Coriacea), Linked to Foraging Success and Population Status." PLOS ONE 7 (5): e36401. https://doi.org/10.1371/journal.pone.0036401.

Bestley, Sophie, Ian Jonsen, Robert G. Harcourt, Mark A. Hindell, and Nicholas J. Gales. 2016. “Putting the Behavior into Animal Movement Modeling: Improved Activity Budgets from Use of Ancillary Tag Information.” Ecology and Evolution 6 (22): 8243–55. https://doi.org/10.1002/ece3.2530.

Brudenall, Denise K., Ivan R. Schwab, and Kerstin A. Fritsches. 2008. “Ocular Morphology of the Leatherback Sea Turtle (Dermochelys Coriacea).” Veterinary Ophthalmology 11 (2): 99–110. https://doi.org/10.1111/j.1463-5224.2008.00607.x.

Chamberlain, Scott. 2021. “rerddap: General Purpose Client for 'ERDDAP' Servers”. R package version 0.7.6. https://CRAN.R-project.org/package=rerddap.

Cleasby, Ian R., Ewan D. Wakefield, Barbara J. Morrissey, Thomas W. Bodey, Steven C. Votier, Stuart Bearhop, and Keith C. Hamer. 2019. “Using Time-Series Similarity Measures to Compare Animal Movement Trajectories in Ecology.” Behavioral Ecology and Sociobiology 73 (11): 151. https://doi.org/10.1007/s00265-019-2761-1.

Bryan Wallace, Manjula Tiwari, and Marc Girondot. 2013. “IUCN Red List of Threatened Species: Dermochelys Coriacea.” IUCN Red List of Threatened Species, June. https://www.iucnredlist.org/en.

Degenford, Jennie Hannah, Dong Liang, Helen Bailey, Aimee L. Hoover, Patricia Zarate, Jorge Azócar, Daniel Devia, et al. 2021. “Using Fisheries Observation Data to Develop a Predictive Species Distribution Model for Endangered Sea

Turtles." Conservation Science and Practice 3 (2): e349. https://doi.org/10.1111/csp2.349.

Dodge, Kara L., Amy L. Kukulya, Erin Burke, and Mark F. Baumgartner. 2018. "TurtleCam: A 'Smart' Autonomous Underwater Vehicle for Investigating Behaviors and Habitats of Sea Turtles." Frontiers in Marine Science 0. https://doi.org/10.3389/fmars.2018.00090.

Dunnington, Dewey. 2019. "rosm: Plot Raster Map Tiles from Open Street Map and Other Sources". R package. version 0.2.5. https://CRAN.R-project.org/package=rosm

Eckert, Scott A. 2006. "High-Use Oceanic Areas for Atlantic Leatherback Sea Turtles (Dermochelys Coriacea) as Identified Using Satellite Telemetered Location and Dive Information." Marine Biology 149 (5): 1257–67. https://doi.org/10.1007/s00227-006-0262-z.

Feigenbaum, D, and M Kelly. 1984. "Changes in the Lower Chesapeake Bay Food Chain in Presence of the Sea Nettle Chrysaora Quinquecirrha (Scyphomedusa)." Marine Ecology Progress Series 19: 39–47. https://doi.org/10.3354/meps019039.

Fernández-Álamo, María Ana, and Jaime Färber-Lorda. 2006. "Zooplankton and the Oceanography of the Eastern Tropical Pacific: A Review." Progress in Oceanography, A Review of Eastern Tropical Pacific Oceanography, 69 (2): 318–59. https://doi.org/10.1016/j.pocean.2006.03.003.

Fossette, Sabrina, Sandra Ferraroli, Hideji Tanaka, Yan Ropert-Coudert, Nobuaki Arai, Katsufumi Sato, Yasuhiko Naito, Yvon Le Maho, and Jean-Yves Georges. 2007. “Dispersal and Dive Patterns in Gravid Leatherback Turtles during the Nesting Season in French Guiana.” Marine Ecology Progress Series 338 (May): 233–47. https://doi.org/10.3354/meps338233.

Fossette, Sabrina, Philippe Gaspar, Yves Handrich, Yvon Le Maho, and Jean-Yves Georges. 2008. “Dive and Beak Movement Patterns in Leatherback Turtles Dermochelys Coriacea during Internesting Intervals in French Guiana.” Journal of Animal Ecology 77 (2): 236–46. https://doi.org/10.1111/j.1365-2656.2007.01344.x.

Fossette, Sabrina, Victoria J. Hobson, Charlotte Girard, Beatriz Calmettes, Philippe Gaspar, Jean-Yves Georges, and Graeme C. Hays. 2010. “Spatio-Temporal Foraging Patterns of a Giant Zooplanktivore, the Leatherback Turtle.” Journal of Marine Systems 81 (3): 225–34. https://doi.org/10.1016/j.jmarsys.2009.12.002.

Frankish, Caitlin K., Andrea Manica, Joan Navarro, and Richard A. Phillips. 2021. “Movements and Diving Behaviour of White-Chinned Petrels: Diurnal Variation and Implications for Bycatch Mitigation.” Aquatic Conservation: Marine and Freshwater Ecosystems.

Frankish, Caitlin K., Richard A. Phillips, Thomas A. Clay, Marius Somveille, and Andrea Manica. 2020. “Environmental Drivers of Movement in a Threatened

Seabird: Insights from a Mechanistic Model and Implications for Conservation." Diversity and Distributions 26 (10): 1315–29. https://doi.org/10.1111/ddi.13130.

Graham, William M., and Ryan M. Kroutil. 2001. "Size-Based Prey Selectivity and Dietary Shifts in the Jellyfish, Aurelia Aurita." Journal of Plankton Research 23 (1): 67–74. https://doi.org/10.1093/plankt/23.1.67.

Graham, William M., Fransesc Pagès, and William M. Hamner. 2001. "A Physical Context for Gelatinous Zooplankton Aggregations: A Review." In Jellyfish Blooms: Ecological and Societal Importance, edited by J. E. Purcell, W. M. Graham, and H. J. Dumont, 199–212. Developments in Hydrobiology. Dordrecht: Springer Netherlands. https://doi.org/10.1007/978-94-010-0722-1_16.

Hamelin, Kayla M., Daniel E. Kelley, Christopher T. Taggart, and Michael C. James. 2014. "Water Mass Characteristics and Solar Illumination Influence Leatherback Turtle Dive Patterns at High Latitudes." Ecosphere 5 (2): art19. https://doi.org/10.1890/ES13-00158.1.

Hays, Graeme C., Jonathan D. R. Houghton, and Andrew E. Myers. 2004. "Pan-Atlantic Leatherback Turtle Movements." Nature 429 (6991): 522–522. https://doi.org/10.1038/429522a.

He, Kaiming, Xiangyu Zhang, Shaoqing Ren, and Jian Sun. 2016. "Deep Residual Learning for Image Recognition." In , 770–78. https://openaccess.thecvf.com/content_cvpr_2016/html/He_Deep_Residual_Learning_CVPR_2016_paper.html.

Heaslip, Susan G., Sara J. Iverson, W. Don Bowen, and Michael C. James. 2012. "Jellyfish Support High Energy Intake of Leatherback Sea Turtles (Dermochelys Coriacea): Video Evidence from Animal-Borne Cameras." PLOS ONE 7 (3): e33259. https://doi.org/10.1371/journal.pone.0033259.

Hochscheid, Sandra. 2014. "Why We Mind Sea Turtles' Underwater Business: A Review on the Study of Diving Behavior." Journal of Experimental Marine Biology and Ecology, Charismatic marine mega-fauna, 450 (January): 118–36. https://doi.org/10.1016/j.jembe.2013.10.016.

Hoover, Aimee L., Dong Liang, Joanna Alfaro-Shigueto, Jeffrey C. Mangel, Peter I. Miller, Stephen J. Morreale, Helen Bailey, and George L. Shillinger. 2019. "Predicting Residence Time Using a Continuous-Time Discrete-Space Model of Leatherback Turtle Satellite Telemetry Data." Ecosphere 10 (3): e02644. https://doi.org/10.1002/ecs2.2644.

Houghton, Jonathan D. R., Annette C. Broderick, Brendan J. Godley, Julian D. Metcalfe, and Graeme C. Hays. 2002. "Diving Behaviour during the Internesting Interval for Loggerhead Turtles Caretta Caretta Nesting in Cyprus." Marine Ecology Progress Series 227 (February): 63–70. https://doi.org/10.3354/meps227063.

Howard, Jeremy, and Sylvain Gugger. 2020. "Fastai: A Layered API for Deep Learning." Information 11 (2): 108. https://doi.org/10.3390/info11020108.

Howell, Evan A., Peter H. Dutton, Jeffrey J. Polovina, Helen Bailey, Denise M. Parker, and George H. Balazs. 2010. “Oceanographic Influences on the Dive Behavior of Juvenile Loggerhead Turtles (Caretta Caretta) in the North Pacific Ocean.” Marine Biology 157 (5): 1011–26. https://doi.org/10.1007/s00227-009-1381-0.

Hurme, Edward, Eliezer Gurarie, Stefan Greif, L. Gerardo Herrera M., José Juan Flores-Martínez, Gerald S. Wilkinson, and Yossi Yovel. 2019. “Acoustic Evaluation of Behavioral States Predicted from GPS Tracking: A Case Study of a Marine Fishing Bat.” Movement Ecology 7 (1): 21. https://doi.org/10.1186/s40462-019-0163-7.

John, Christian, and Eric Post. n.d. “Seasonality, Niche Management and Vertical Migration in Landscapes of Relief.” Ecography n/a (n/a). Accessed July 28, 2021. https://doi.org/10.1111/ecog.05774.

Jonsen, I. D., M. Basson, S. Bestley, M. V. Bravington, T. A. Patterson, M. W. Pedersen, R. Thomson, U. H. Thygesen, and S. J. Wotherspoon. 2013. “State-Space Models for Bio-Loggers: A Methodological Road Map.” Deep Sea Research Part II: Topical Studies in Oceanography, Fourth International Symposium on Bio-logging Science, 88–89 (April): 34–46. https://doi.org/10.1016/j.dsr2.2012.07.008.

Jonsen, I. D., C. R. McMahon, T. A. Patterson, M. Auger-Méthé, R. Harcourt, M. A. Hindell, and S. Bestley. 2019. “Movement Responses to Environment: Fast

Inference of Variation among Southern Elephant Seals with a Mixed Effects Model." Ecology 100 (1): e02566. https://doi.org/10.1002/ecy.2566.

Jonsen, Ian D., Toby A. Patterson, Daniel P. Costa, Philip D. Doherty, Brendan J. Godley, W. James Grecian, Christophe Guinet, et al. 2020. "A Continuous-Time State-Space Model for Rapid Quality Control of Argos Locations from Animal-Borne Tags." Movement Ecology 8 (1): 31. https://doi.org/10.1186/s40462-020-00217-7.

Kaplan, IC. 2005. "A Risk Assessment for Pacific Leatherback Turtles (Dermochelys Coriacea)." Canadian Journal of Fisheries and Aquatic Sciences 62 (8): 1710–19. https://doi.org/10.1139/f05-121.

Kershenbaum, Arik, Laela S. Sayigh, and Vincent M. Janik. 2013. "The Encoding of Individual Identity in Dolphin Signature Whistles: How Much Information Is Needed?" PLOS ONE 8 (10): e77671. https://doi.org/10.1371/journal.pone.0077671.

Lee, Seulbi, Jaehoon Kim, Jongyeon Hwang, EunJi Lee, Kyoung-Jin Lee, Jeongkyu Oh, Jungsu Park, and Tae-Young Heo. 2020. "Clustering of Time Series Water Quality Data Using Dynamic Time Warping: A Case Study from the Bukhan River Water Quality Monitoring Network." Water 12 (9): 2411. https://doi.org/10.3390/w12092411.

Lowerre-Barbieri, Susan K., Roland Kays, James T. Thorson, and Martin Wikelski. 2019. “The Ocean’s Movescape: Fisheries Management in the Bio-Logging Decade (2018–2028).” ICES Journal of Marine Science 76 (2): 477–88.

Lucas, Tim C. D. 2020. “A Translucent Box: Interpretable Machine Learning in Ecology.” Ecological Monographs 90 (4): e01422. https://doi.org/10.1002/ecm.1422.

Melnykov, Volodymyr, and Ranjan Maitra. 2010. “Finite Mixture Models and Model-Based Clustering.” Statistics Surveys 4 (none): 80–116. https://doi.org/10.1214/09-SS053.

Michelot, Théo, Roland Langrock, Sophie Bestley, Ian D. Jonsen, Theoni Photopoulou, and Toby A. Patterson. 2017. “Estimation and Simulation of Foraging Trips in Land-Based Marine Predators.” Ecology 98 (7): 1932–44. https://doi.org/10.1002/ecy.1880.

Moritz, Steffen. and Bartz-Beielstein, Thomas. 2017. “imputeTS: Time Series Missing Value Imputation in R”. The R Journal 9(1), 207-218. doi: 10.32614/RJ-2017-009.

Narazaki, Tomoko, Katsufumi Sato, Kyler J. Abernathy, Greg J. Marshall, and Nobuyuki Miyazaki. 2013. “Loggerhead Turtles (Caretta Caretta) Use Vision to Forage on Gelatinous Prey in Mid-Water.” PLOS ONE 8 (6): e66043. https://doi.org/10.1371/journal.pone.0066043.

Nathan, Ran, Wayne M. Getz, Eloy Revilla, Marcel Holyoak, Ronen Kadmon, David Saltz, and Peter E. Smouse. 2008. “A Movement Ecology Paradigm for Unifying Organismal Movement Research.” Proceedings of the National Academy of Sciences 105 (49): 19052–59. https://doi.org/10.1073/pnas.0800375105.

Ngô, Manh Cuong, Mads Peter Heide-Jørgensen, and Susanne Ditlevsen. 2019. “Understanding Narwhal Diving Behaviour Using Hidden Markov Models with Dependent State Distributions and Long Range Dependence.” PLOS Computational Biology 15 (3): e1006425. https://doi.org/10.1371/journal.pcbi.1006425.

Norouzzadeh, Mohammad Sadegh, Anh Nguyen, Margaret Kosmala, Alexandra Swanson, Meredith S. Palmer, Craig Packer, and Jeff Clune. 2018. “Automatically Identifying, Counting, and Describing Wild Animals in Camera-Trap Images with Deep Learning.” Proceedings of the National Academy of Sciences 115 (25): E5716–25. https://doi.org/10.1073/pnas.1719367115.

Okuyama, Junichi, Scott R. Benson, Peter H. Dutton, and Jeffrey A. Seminoff. 2021. “Changes in Dive Patterns of Leatherback Turtles with Sea Surface Temperature and Potential Foraging Habitats.” Ecosphere 12 (2): e03365. https://doi.org/10.1002/ecs2.3365.

Okuyama, Junichi, Jeffrey A. Seminoff, Peter H. Dutton, and Scott R. Benson. 2016. “Fine-Scale Monitoring of Routine Deep Dives by Gravid Leatherback Turtles during the Internesting Interval Indicate a Capital Breeding Strategy.”

Frontiers in Marine Science 3.
https://www.frontiersin.org/articles/10.3389/fmars.2016.00166.

Patterson, Toby A., Len Thomas, Chris Wilcox, Otso Ovaskainen, and Jason Matthiopoulos. 2008. "State–Space Models of Individual Animal Movement." Trends in Ecology & Evolution 23 (2): 87–94. https://doi.org/10.1016/j.tree.2007.10.009.

R Core Team. 2021. "R: A Language and environment for statistical computing. R Foundation for Statistical Computing, Vienna, Austria". URL: https://www.R-project.org/

Reina, Richard D., Philippe A. Mayor, James R. Spotila, Rotney Piedra, and Frank V. Paladino. 2002. "Nesting Ecology of the Leatherback Turtle, Dermochelys Coriacea, at Parque Nacional Marino Las Baulas, Costa Rica: 1988–1989 to 1999–2000." Edited by W. L. Montgomery. Copeia 2002 (3): 653–64. https://doi.org/10.1643/0045-8511(2002)002[0653:NEOTLT]2.0.CO;2.

Reina, Richard D., James R. Spotila, Frank V. Paladino, and Arthur E. Dunham. 2009. "Changed Reproductive Schedule of Eastern Pacific Leatherback Turtles Dermochelys Coriacea Following the 1997–98 El Niño to La Niña Transition." Endangered Species Research 7 (2): 155–61. https://doi.org/10.3354/esr00098.

Roncon, Giulia, Sophie Bestley, Clive R. McMahon, Barbara Wienecke, and Mark A. Hindell. 2018. "View from below: Inferring Behavior and Physiology of

Southern Ocean Marine Predators from Dive Telemetry." Frontiers in Marine Science 5: 464.

Saba, Vincent S., George L. Shillinger, Alan M. Swithenbank, Barbara A. Block, James R. Spotila, John A. Musick, and Frank V. Paladino. 2008. "An Oceanographic Context for the Foraging Ecology of Eastern Pacific Leatherback Turtles: Consequences of ENSO." Deep Sea Research Part I: Oceanographic Research Papers 55 (5): 646–60. https://doi.org/10.1016/j.dsr.2008.02.006.

Sale, Alessandro, Paolo Luschi, Resi Mencacci, Paolo Lambardi, George R. Hughes, Graeme C. Hays, Silvano Benvenuti, and Floriano Papi. 2006. "Long-Term Monitoring of Leatherback Turtle Diving Behaviour during Oceanic Movements." Journal of Experimental Marine Biology and Ecology 328 (2): 197–210. https://doi.org/10.1016/j.jembe.2005.07.006.

Salman, Ahmad, Shoaib Ahmad Siddiqui, Faisal Shafait, Ajmal Mian, Mark R Shortis, Khawar Khurshid, Adrian Ulges, and Ulrich Schwanecke. 2020. "Automatic Fish Detection in Underwater Videos by a Deep Neural Network-Based Hybrid Motion Learning System." ICES Journal of Marine Science 77 (4): 1295–1307. https://doi.org/10.1093/icesjms/fsz025.

Salmon, Michael, T. Todd Jones, and Kenneth W. Horch. 2004. "Ontogeny of Diving and Feeding Behavior in Juvenile Seaturtles: Leatherback Seaturtles (Dermochelys Coriacea L) and Green Seaturtles (Chelonia Mydas L) in the Florida Current." Journal of Herpetology 38 (1): 36–43. https://doi.org/10.1670/228-01A.

Sardá-Espinosa, Alexis. 2019. “Time-Series Clustering in R Using the Dtwclust Package.” The R Journal 11 (1): 22. https://doi.org/10.32614/RJ-2019-023.

Sardá-Espinosa, A. 2019. “dtwclust: Time Series Clustering Along with Optimizations for the Dynamic Time Warping Distance.”, R package version 5.5.6. https://CRAN.R-project.org/package=dtwclust .

Scheffers, Brett R., Luke Shoo, Ben Phillips, Stewart L. Macdonald, Alex Anderson, Jeremy VanDerWal, Collin Storlie, Arnaud Gourret, and Stephen E. Williams. 2017. “Vertical (Arboreality) and Horizontal (Dispersal) Movement Increase the Resilience of Vertebrates to Climatic Instability.” Global Ecology and Biogeography 26 (7): 787–98.

Schick, Robert S., Jason J. Roberts, Scott A. Eckert, Patrick N. Halpin, Helen Bailey, Fei Chai, Lei Shi, and James S. Clark. 2013. “Pelagic Movements of Pacific Leatherback Turtles (Dermochelys Coriacea) Highlight the Role of Prey and Ocean Currents.” Movement Ecology 1 (1): 1–14.

Schnedler-Meyer, Nicolas A., Thomas Kiørboe, and Patrizio Mariani. 2018. “Boom and Bust: Life History, Environmental Noise, and the (Un) Predictability of Jellyfish Blooms.” Frontiers in Marine Science 5: 257.

Schreer, Jason F., and J. Ward Testa. 1996. “Classification of Weddell Seal Diving Behavior.” Marine Mammal Science 12 (2): 227–50. https://doi.org/10.1111/j.1748-7692.1996.tb00573.x.

Schwarz, Jonas F. L., Sina Mews, Eugene J. DeRango, Roland Langrock, Paolo Piedrahita, Diego Páez-Rosas, and Oliver Krüger. 2021. “Individuality Counts: A New Comprehensive Approach to Foraging Strategies of a Tropical Marine Predator.” Oecologia 195 (2): 313–25. https://doi.org/10.1007/s00442-021-04850-w.

Secor, D. H., H. Bailey, A. Carroll, V. Lyubchich, M. H. P. O’Brien, and C. J. Wiernicki. 2021. “Diurnal Vertical Movements in Black Sea Bass (Centropristis Striata): Endogenous, Facultative, or Something Else?” Ecosphere 12 (6): e03616. https://doi.org/10.1002/ecs2.3616.

Secor, David H., Michael H. P. O’Brien, Benjamin I. Gahagan, Dewayne A. Fox, Amanda L. Higgs, and Jessica E. Best. 2020. “Multiple Spawning Run Contingents and Population Consequences in Migratory Striped Bass Morone Saxatilis.” PLOS ONE 15 (11): e0242797. https://doi.org/10.1371/journal.pone.0242797.

Sefick Jr., Steven. 2016. “Stream Metabolism-A package for calculating single station metabolism from diurnal Oxygen curves”. R package version 1.1.2. https://cran.r-project.org/package=StreamMetabolism .

Seminoff, Jeffrey A., T. Todd Jones, and Greg J. Marshall. 2006. “Underwater Behaviour of Green Turtles Monitored with Video-Time-Depth Recorders: What’s Missing from Dive Profiles?” Marine Ecology Progress Series 322 (September): 269–80. https://doi.org/10.3354/meps322269.

Seminoff, Jeffrey A., Elizabeth R. Whitman, Bryan P. Wallace, Ali Bayless, Antonio Resendiz, and T. Todd Jones. 2020. “No Rest for the Weary: Restricted Resting Behaviour of Green Turtles (Chelonia Mydas) at a Deep-Neritic Foraging Area Influences Expression of Life History Traits.” Journal of Natural History 54 (45–46): 2979–3001. https://doi.org/10.1080/00222933.2021.1887387.

Shepard, Emily L. C., Rory P. Wilson, W. Gareth Rees, Edward Grundy, Sergio A. Lambertucci, and Simon B. Vosper. 2013. “Energy Landscapes Shape Animal Movement Ecology.” The American Naturalist 182 (3): 298–312. https://doi.org/10.1086/671257.

Shillinger, George L., Daniel M. Palacios, Helen Bailey, Steven J. Bograd, Alan M. Swithenbank, Philippe Gaspar, Bryan P. Wallace, et al. 2008. “Persistent Leatherback Turtle Migrations Present Opportunities for Conservation.” PLOS Biology 6 (7): e171. https://doi.org/10.1371/journal.pbio.0060171.

Shillinger, George L., Alan M. Swithenbank, Helen Bailey, Steven J. Bograd, Michael R. Castelton, Bryan P. Wallace, James R. Spotila, Frank V. Paladino, Rotney Piedra, and Barbara A. Block. 2011. “Vertical and Horizontal Habitat Preferences of Post-Nesting Leatherback Turtles in the South Pacific Ocean.” Marine Ecology Progress Series 422 (January): 275–89. https://doi.org/10.3354/meps08884.

Siddiqui, Shoaib Ahmed, Ahmad Salman, Muhammad Imran Malik, Faisal Shafait, Ajmal Mian, Mark R Shortis, and Euan S Harvey. 2018. “Automatic Fish Species Classification in Underwater Videos: Exploiting Pre-Trained Deep Neural

Network Models to Compensate for Limited Labelled Data." ICES Journal of Marine Science 75 (1): 374–89. https://doi.org/10.1093/icesjms/fsx109.

Spotila, James R., Richard D. Reina, Anthony C. Steyermark, Pamela T. Plotkin, and Frank V. Paladino. 2000. "Pacific Leatherback Turtles Face Extinction." Nature 405 (6786): 529–30. https://doi.org/10.1038/35014729.

Steele, John H. 1989. "The Ocean 'Landscape.'" Landscape Ecology 3 (3): 185–92. https://doi.org/10.1007/BF00131537.

Stern, Ulrich, Ruo He, and Chung-Hui Yang. 2015. "Analyzing Animal Behavior via Classifying Each Video Frame Using Convolutional Neural Networks." Scientific Reports 5 (1): 1–13.

Strömberg, K. H. Patrik, Timothy J. Smyth, J. Icarus Allen, Sophie Pitois, and Todd D. O'Brien. 2009. "Estimation of Global Zooplankton Biomass from Satellite Ocean Colour." Journal of Marine Systems 78 (1): 18–27. https://doi.org/10.1016/j.jmarsys.2009.02.004.

Tabak, M. A., M. S. Norouzzadeh, D. W. Wolfson, S. J. Sweeney, K. C. VerCauteren, N. P. Snow, J. M. Halseth, P. A. Di Salvo, J. S. Lewis, and M. D. White. n.d. "Machine Learning to Classify Animal Species in Camera Trap Images: Applications in Ecology. BioRxiv. 2018."

Tan, Lee N., Abeer Alwan, George Kossan, Martin L. Cody, and Charles E. Taylor. 2015. "Dynamic Time Warping and Sparse Representation Classification for Birdsong Phrase Classification Using Limited Training Data." The Journal of

the Acoustical Society of America 137 (3): 1069–80. https://doi.org/10.1121/1.4906168.

Thieurmel, Benoit. and Elmarhraoui, Achraf. 2019. “suncalc: Compute Sun Position, Sunlight Phases, Moon Position and Lunar Phase”. R package version 0.5.0. https://CRAN.R-project.org/package=suncalc .

Thomson, Jordan A., Michael R. Heithaus, and Lawrence M. Dill. 2011. “Informing the Interpretation of Dive Profiles Using Animal-Borne Video: A Marine Turtle Case Study.” Journal of Experimental Marine Biology and Ecology 410 (December): 12–20. https://doi.org/10.1016/j.jembe.2011.10.002.

Tracey, Jeff A., Jun Zhu, and Kevin R. Crooks. 2011. “Modeling and Inference of Animal Movement Using Artificial Neural Networks.” Environmental and Ecological Statistics 18 (3): 393–410. https://doi.org/10.1007/s10651-010-0138-8.

Wallace, Bryan P., and T. Todd Jones. 2008. “What Makes Marine Turtles Go: A Review of Metabolic Rates and Their Consequences.” Journal of Experimental Marine Biology and Ecology, Sea turtles: physiological, molecular and behavioural ecology and conservation biology, 356 (1): 8–24. https://doi.org/10.1016/j.jembe.2007.12.023.

Wallace, Bryan P., Susan S. Kilham, Frank V. Paladino, and James R. Spotila. 2006. “Energy Budget Calculations Indicate Resource Limitation in Eastern Pacific Leatherback Turtles.” Marine Ecology Progress Series 318 (August): 263–70. https://doi.org/10.3354/meps318263.

Watson, William E., Scott R. Benson, and James T. Harvey. 2010. “An Application of Underwater Imaging for Marine Vertebrate Ecology.” In OCEANS 2010 MTS/IEEE SEATTLE, 1–6. https://doi.org/10.1109/OCEANS.2010.5664044.

Weinstein, Yana, Christopher R. Madan, and Megan A. Sumeracki. 2018. “Teaching the Science of Learning.” Cognitive Research: Principles and Implications 3 (1): 2. https://doi.org/10.1186/s41235-017-0087-y.

Wijeyakulasuriya, Dhanushi A., Elizabeth W. Eisenhauer, Benjamin A. Shaby, and Ephraim M. Hanks. 2020. “Machine Learning for Modeling Animal Movement.” Plos One 15 (7): e0235750.

Willi, Marco, Ross T. Pitman, Anabelle W. Cardoso, Christina Locke, Alexandra Swanson, Amy Boyer, Marten Veldthuis, and Lucy Fortson. 2019. “Identifying Animal Species in Camera Trap Images Using Deep Learning and Citizen Science.” Methods in Ecology and Evolution 10 (1): 80–91. https://doi.org/10.1111/2041-210X.13099.

Wilson, Steven G., and Barbara A. Block. 2009. “Habitat Use in Atlantic Bluefin Tuna Thunnus Thynnus Inferred from Diving Behavior.” Endangered Species Research 10: 355–67.

Wood, Simon N. 2006. “On Confidence Intervals for Generalized Additive Models Based on Penalized Regression Splines.” Australian & New Zealand

Journal of Statistics 48 (4): 445–64. https://doi.org/10.1111/j.1467-842X.2006.00450.x.

Wood, Simon N. 2017. “Generalized Additive Models: An Introduction with R (2nd edition)”. Chapman and Hall/CRC

Chapter 3: Incorporating multidimensional behavior into a dynamic management tool for a critically endangered and migratory species

Abstract

Conservation of migratory species exhibiting wide-ranging and multidimensional behaviors is challenged by existing management efforts that only utilize horizontal movements or produce static products in space and time. For the deep-diving and critically endangered Eastern Pacific (EP) leatherback turtle, tools that predict locations where turtles have high risks of being caught as bycatch are urgently needed to prevent further population decline. We incorporated horizontal-vertical movement model results with spatio-temporal kernel density estimates and threat data (gear-specific fishing) to develop dynamic maps of spatial risk. Specifically, we applied multi-state Hidden Markov Models (HMMs) to a large biotelemetry dataset (N=28 EP leatherback tracks, 2004-2007). Tracks with associated dive information were used to characterize turtle behavior as belonging to one of three behavioral states (S1-transiting, S2-residential/mixed diving, and S3-residential/deep diving). Recent fishing effort data from Global Fishing Watch were integrated with predicted behaviors and monthly space use estimates to create maps of relative risk of turtle-fisheries interactions as functions of fishing gear type, behavioral state, and month. Drifting (pelagic) longline fishing gear had the highest average monthly fishing effort

in the study region, and risk indices were highest for this gear when associated with residential and deep-diving behaviors. Monthly relative risk surfaces for all gears and behaviors have been added to South Pacific TurtleWatch (SPTW) (https://www.upwell.org/sptw), a dynamic management (DM) tool for this leatherback population. These modifications will refine SPTW's capability to provide important predictions of potential high risk bycatch areas for turtles undertaking specific behaviors. Our results demonstrate how multidimensional movement data, spatio-temporal density estimates, and threat data can be used to create a DM conservation tool. These methods serve as a framework for incorporating behavior into similar tools for other aquatic, aerial, and terrestrial taxa with 3-dimensional movement behaviors.

Introduction

For animals that traverse long distances between habitats throughout their lifetime, conservation efforts solely utilizing fixed management measures, such as static spatial area closures, are often ineffective (Bolger et al. 2008, Bull et al. 2013, Runge et al. 2014, Meisingset et al. 2017). Successfully conserving a migratory species depends not only on alleviating harm in the habitats where they face significant threat, but also on understanding their movement ecology (Fraser et al. 2018, Westley et al. 2018). The efficacy of conservation efforts involving animals with vertical dimensions to their behavior (e.g. flying, arboreal, diving) will be improved through the application of predictive models that consider threat risk in relation to vertical behaviors.

Dynamic management (DM), whereby models and tools of target species' spatial habitat use generate real (or near real) time predictions and risk assessments (Bull et al. 2013, Hobday and Hartog 2014, Lewison et al. 2015), has become increasingly useful for conservation of migratory species. DM has been applied to a variety of taxa, including blue whales (Hazen et al. 2017), sharks and tuna (White et al. 2019), sea turtles (Degenford et al. 2021), shorebirds (Johnston et al. 2020), and manatees (Udell et al. 2018). However, existing DM approaches often rely on horizontal species distribution or presence/presence-absence based models to predict species habitat use. These approaches do not include multidimensional movement models that allow for understanding where a target species is with respect to threats, and the "what, why, how, when, and where" of their movement with respect to those threats (Nathan et al. 2008, Allen & Singh 2016).

Hidden Markov Models (HMMs) encompass a suite of statistical models for time series data that can be applied to movement tracks for inference on behaviors without direct detection (as is often the case with long-distance migrants). These models describe two stochastic processes, a) an observed, state-dependent process of the telemetry data and accompanying metrics (e.g., locational positions, speeds, or turning angles between successive locations) and b) a hidden process (Markov chain) that consists of N-discrete unobservable states or behaviors an animal is undertaking, which produce the observed telemetry metrics (Patterson et al. 2009). HMMs have progressed rapidly in their application and uses for migratory fauna, with recent developments allowing for multiple states of behavior to be predicted from

multidimensional data (see as example, Connors et al. 2021, DeRuiter et al. 2016, Leos-Barajas et al. 2017, Adam et al. 2019).

These HMMs can be paired with DM approaches to create integrative conservation tools, expanding beyond static conservation methods. A recent application in Bedriñana-Romano et al. (2021) paired a species distribution model (SDM) for blue whales with a fast-fitting movement model and marine vessel traffic data to determine significant areas of overlap. This comprehensive approach can be adapted for other current DM tools lacking incorporation of multidimensional movement into risk predictions. For example, the "TurtleWatch" approach, which was first developed to mitigate interactions between Hawaiian pelagic longline fisheries and loggerhead and leatherback turtles (Howell et al. 2008, 2015), has been modified to incorporate multiple environmental predictors and has been applied in other areas to predict the residence time of critically endangered Eastern Pacific (EP) leatherback turtles (Hoover et al. 2019) across their range in the entire South East Pacific (South Pacific Turtlewatch, SPTW, https://www.upwell.org/sptw and see Hoover et al. 2019, Degenford et al. 2021). The cryptic, highly migratory, and deep diving nature of leatherback turtles (*Dermochelys coriacea*) has created challenges for both understanding their movement ecology and conserving them from the most acute threats at sea. The EP leatherbacks, more so than other leatherback populations, likely spend extensive amounts of time searching for food at depth in the oligotrophic South Pacific gyre (Shillinger et al. 2011, Bailey et al. 2012a, Bailey et al. 2012b, Schick et al. 2013). Therefore, previous movement models using only horizontal

movement metrics for EP leatherbacks have likely underrepresented the number and location of foraging and residential behaviors.

Here, we expand SPTW to determine relative risk of interaction of turtles with different fishing gears during their migration and foraging in international waters, using multidimensional movement data for EP leatherbacks and fishing vessel effort data. Our approach builds on the methods of similar studies (see Roe et al. 2014, Bedriñana-Romano et al. 2021), allowing us to estimate relative risk by combining layers on gear-specific fishing effort, spatial intensities of notable movement behaviors, and kernel density estimates of overall population space use. We provide a novel modification to this approach by incorporating both horizontal and vertical movement data to infer behavior. We developed a fast-fitting and "simple" multidimensional HMM easily adapted to future studies on other taxa. Additionally, we employed a rarely used, multidimensional approach to estimate space use of our population over time, applying the product kernel estimator algorithm to the movement tracks to estimate monthly 3D utilization distributions, where the third dimension is time (Keating & Cherry 2009). We demonstrate this technique using the most recent, large biotelemetry dataset for the critically endangered EP population of leatherbacks from Shillinger et al. (2008). Our results contribute significantly to ongoing conservation efforts for this critically endangered species by advancing the SPTW DM conservation tool. We also create a framework for integrating movement and behavior with DM models. This novel approach can be applied to a wide range of urgent conservation issues in environments of dynamic risk.

Methods

Datasets and Processing

Biotelemetry data consisted of N=28 post-nesting, migratory adult female leatherbacks from the EP population in Playa Grande, Costa Rica (Shillinger et al. 2008). Individuals were tagged while nesting in January and February of each tracking year (2004, 2005, 2007). Sea Mammal Research Unit (SMRU) Satellite Relay Data Logger (SRDL) tags transmitted surface locations via the ARGOS satellite system. Additional pressure-sensor dive information (e.g. total dive duration, maximum dive depth, summary dive data, and dive profiles, including intermediate depth, inflection and duration points) was available from SRDL tags, with dives being categorized as vertical movements greater than 10 meters and less than 1500 meters in depth. Tracks were processed in R version 4.2.0 (R Core Team 2022) to have variables for each daily location of current-corrected persistence velocities (Copernicus Marine Service, https://marine.copernicus.eu/), total dive counts, and counts of deep versus shallow dive types (D1 vs. D2) (see Chapter 2; details also available in Appendix).

Behavioral Intensity: Hidden Markov Movement Models

To predict behavioral and multidimensional states of movement, we developed an HMM that consisted of three hidden, discrete states of vertical (diving) and horizontal (surface) movement for each time series (individual movement tracks). The three movement states corresponded to a transiting behavior state (S1: shallow dives, fast and directed horizontal movement) and two different residential behavior

states (S2: mixture of dive depths, area-restricted-search horizontal movement; S3: deep dives, slower and less directed horizontal movement), as previous models for this population using only two behavior states and horizontal data have had difficulty discerning foraging and residential behavior (Bailey et al. 2012b). Each state had a unique set of values for mean daily persistence velocity (horizontal movement), mean number of dives, and the unique proportion of D1 and D2 dives per day. HMMs were fit with a Markov Chain Monte Carlo algorithm and were implemented using the Bayesian programming language Stan and its R interface, rstan (Stan Development Team 2019). See Appendix for details on the HMM specification and fitting.

Behavioral Intensity: Surface Creation

To create spatial surfaces of behavioral intensity useful in overlap analysis, each unique HMM behavioral state prediction was aggregated across individuals into a 1˚ resolution grid for the study area, summing each behavioral state within each grid cell for all tracks combined. This resolution captured enough positions, which were on average 28 km apart. The product of this was three spatial layers of behavioral intensity (B) within our study region, one for each movement state (s), with each being a matrix of size *m* x *n* (5):

$$\mathbf{B}^{(s)} = \begin{bmatrix} b_{11}^{(s)} & \cdots & b_{1n}^{(s)} \\ \vdots & \ddots & \vdots \\ b_{m1}^{(s)} & \dots & b_{mn}^{(s)} \end{bmatrix} \quad (5)$$

Monthly Kernel Density Estimates

To effectively estimate a spatially explicit estimate of the utilization distribution for EP leatherbacks, a 3D utilization distribution was used. This was performed on regularized location data using the product kernel estimator algorithm developed by Keating and Cherry (2009). The R package "adehabitatHR" and its "kernelkcbase" function (Calenge 2006) were used for these purposes.

To create a probability density distribution of turtles at the same temporal scale as the currently existing SPTW tool, monthly 3D utilization distributions (UD) were estimated for each turtle. A smoothing parameter (h) must be specified to determine these UDs. The choice of this value is somewhat subjective (Keating and Cherry 2009), and we chose an h of three degrees for the spatial dimension (X,Y) and 30 days for the third dimension, time. This was based on both an initial exploration of values for h that yielded a sufficiently heterogeneous surface and an understanding of the resolution of our data, with respect to our goal of estimating monthly surfaces.

To obtain monthly UD surfaces at the population level, monthly UD surfaces were averaged across individuals. Following a migratory corridor into lower latitudes, turtles in this dataset have high densities in the months and region near their release location from the nesting beach in Playa Grande, Costa Rica (Shillinger et al. 2008). To prevent these track sections from biasing other monthly UD surface results, and to aid in visualizations of UDs for each month independent of other months, values for each monthly UD surface were normalized between zero and one.

Each UD surface was estimated on an $m \times n$ sized grid equivalent to that of the three behavioral state intensity layers. This grid was converted to a matrix format,

resulting in a final product of 12 UD surface layers (**U**), one for each unique month (*mo*) (6).

$$\mathbf{U}^{(m)} = \begin{bmatrix} u_{11}^{(mo)} & \cdots & u_{1n}^{(mo)} \\ \vdots & \ddots & \vdots \\ u_{m1}^{(mo)} & \cdots & u_{mn}^{(mo)} \end{bmatrix} \quad (6)$$

Monthly Fishing Effort

To create layers of monthly fishing effort within our study region, we utilized open-source data from Global Fishing Watch (GFW), an online database which provides high resolution (1/100th deg) global datasets on fishing effort across different gear types (Copyright 2022, Global Fishing Watch, Inc., https://globalfishingwatch.org/).

Data for vessels included location and gears used. Fishing effort for GFW datasets is reported with Automatic Identification System (AIS) devices deployed on industrial, motorized fishing vessels (6-146 m length) and is measured in hours fishing in a grid cell (Kroodsma et al. 2018). Average fishing effort (2018-2020) was used to best capture recent, high effort fishing effort in the study region and the data was aggregated to the same spatial resolution as the behavior and UD layers.

To match the monthly temporal resolution of the SPTW map that has been produced for EP leatherbacks, fishing effort was further split by month (*mo*). To assess gear-specific interactions, fishing effort was also subset by gear type (*g*), of which there were nine unique categories (drifting longline, fishing, purse seines, pole and line, set gillnets, set longlines, squid jigger, trawlers, and tuna purse seines). Each gear-specific and monthly fishing effort raster was converted into an *m x n* matrix (**F**) (7).

$$\mathbf{F}^{(m,g)} = \begin{bmatrix} f_{11}^{(mo,g)} & \cdots & f_{1n}^{(mo,g)} \\ \vdots & \ddots & \vdots \\ f_{m1}^{(mo,g)} & \cdots & f_{mn}^{(mo,g)} \end{bmatrix} \quad (7)$$

Overlap Analysis: Relative Risk of Interaction

To determine the relative risk of bycatch in multiple dimensions for specific fishing gears, we applied an overlap analysis. This consisted of using elementwise multiplication of the individual matrices for turtle behavior (**B**), monthly fishing effort for each gears (F), and UD estimates (**U**) (Fig A3.1). Results were used to produce both monthly surface estimates and indices of overlap for each fishing gears.

All matrix layers were first scaled to have the same non-zero, positive range (values 1-5). Elementwise cell multiplication (Fig A3.1) was used to find the resulting monthly overlap matrices (**O**) between fishing effort, UD estimates, and turtle behavioral states. This resulted in N=324 initial overlap matrices (one for each unique combination of month, fishing gears, and behavioral state) (8). To create a matrix of relative risk (**RR**, 9), the value of each cell in the initial overlap matrix (**O**) was divided by the sum of all cells within the matrix (**O**), representing the proper weight of each cell within the matrix. Each final matrix (**RR**) was then visualized as part of a monthly heat map of relative risk of interaction that will be incorporated into SPTW online monthly DM maps.

$$\mathbf{O}^{(m,s,g)} = \begin{bmatrix} f_{11}^{(mo,g)} b_{11}^{(s)} u_{11}^{(mo)} & \cdots & f_{1n}^{(mo,g)} b_{1n}^{(s)} u_{1n}^{(mo)} \\ \vdots & \ddots & \vdots \\ f_{m1}^{(mo,g)} b_{m1}^{(s)} u_{m1}^{(mo)} & \cdots & f_{mn}^{(mo,g)} b_{mn}^{(s)} u_{mn}^{(mo)} \end{bmatrix} \quad (8)$$

$$\mathbf{RR}^{(mo,s,g)} = \frac{1}{\sum_{i=1}^{m}\sum_{j=1}^{n} f_{ij}^{(mo,g)} b_{ij}^{(s)} u_{ij}^{(mo)}} \mathrm{O}^{(\mathrm{mo,s,g})} \quad (9)$$

To create an index of when high relative risk of interaction may occur for each unique grouping of behavioral state, month, and fishing gears, values within the 75th to 100th quantiles for each final matrix (**RR**) were extracted and summed across each unique combination of variables (behavioral state, month, gears), providing a quantitative table of the relative risk of significant overlap for each combination.

Results

Behavioral Intensity: Hidden Markov Movement Models

HMMs converged for each individual, for a total of N=28 successful models. The three hidden states for the HMM were distinct with respect to the means and standard deviations of their state dependent parameters (Table 3.1, Fig 3.1a).

Table 3.1. *Population-level parameter means and standard deviations for behavioral states (S1, S2, S3) of individually fit Hidden Markov models (HMMs) for N=28 individuals in the Eastern Pacific leatherback population. Variables are shown for: move persistence (μ, σ - Cauchy distribution) and the proportion of deep (D1) type dives (P- Poisson distribution).*

Parameter	State 1	State 2	State 3
μ	30 (9.9 ± SD)	2.0 (1.3 ± SD)	21 (8.4 ± SD)
σ	8.9 (3.0 ± SD)	5.9 (4.6 ± SD)	4.8 (3.2 ± SD)
P	0.16 (0.048 ± SD)	0.68 (0.096 ± SD)	0.84 (0.048 ± SD)

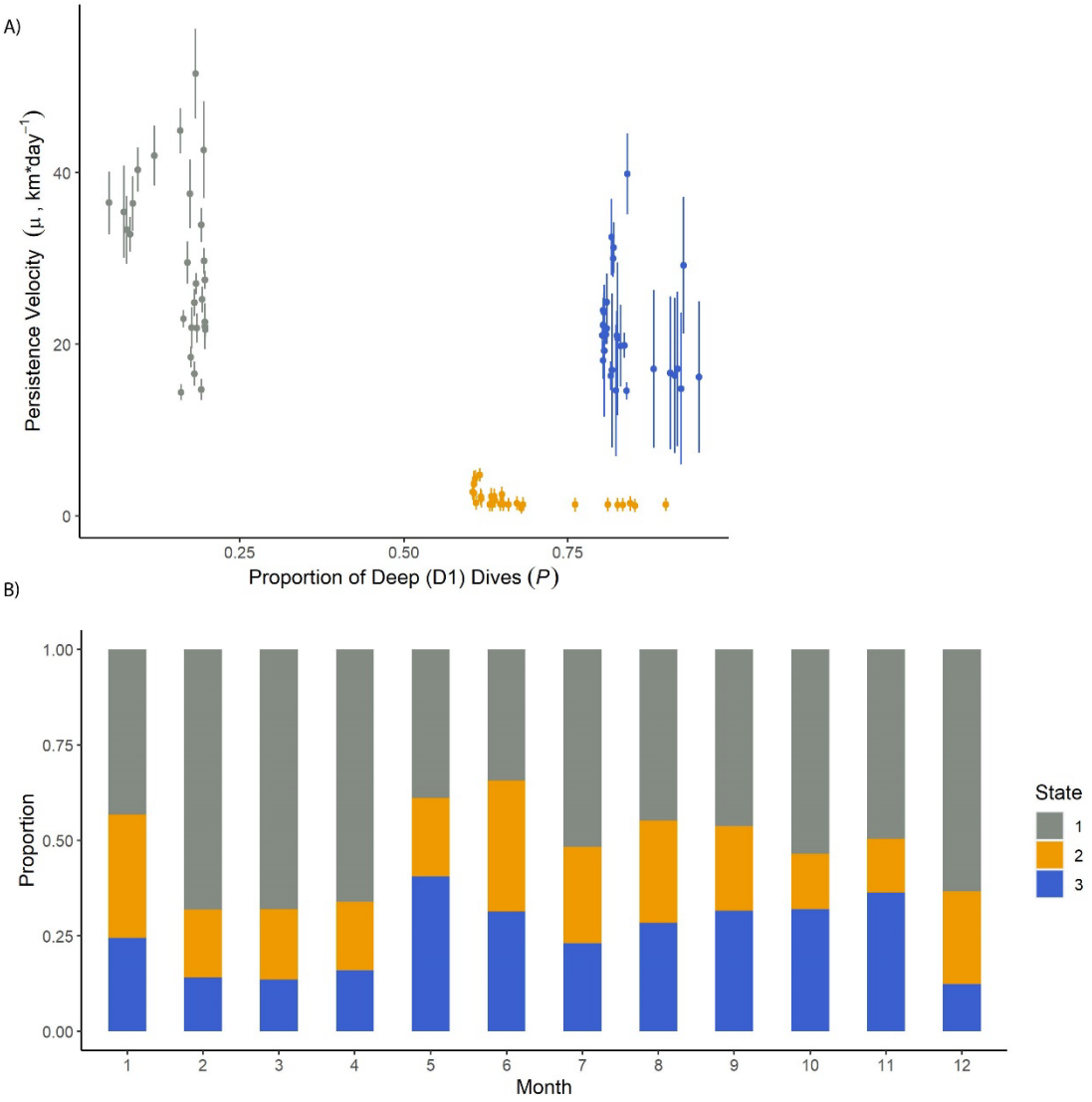

Figure 3.1. *a) Plot of individual means and standard deviations for Hidden Markov Model (HMM) parameters for move persistence (μ) as a function of the parameters for the proportion of deep (D1 type) dives (P) and b) monthly proportions of HMM-*

derived behavioral states (1-3) for N=28 leatherback turtles in the Eastern Pacific region.

Population level inferences were obtained by examining the distribution of horizontal and vertical movement variables for each predicted behavioral state. On average, turtles spent 62% (19 ± SD) of their time in S1 behaviors (shallower dives, high persistence velocity), 19% (10 ± SD) in S2 behaviors (mixture of dive depths, low persistence velocities), and 20% (14 ± SD) in S3 behaviors (deeper dives, intermediate persistence velocities) (Table 3.2).

Table 3.2. *Vertical and horizontal movement variables for Hidden Markov model (HMM) predicted behavioral states (S1, S2, S3) for daily locations of N=28 Eastern Pacific leatherback turtles. Columns include: Mean percent time and number of dives in a given state, mean and standard deviation of move persistence velocity, mean proportion of dives classified as D1 (deeper) or D2 (shallower), and median maximum dive depth and time-at-depth, both of which were right-skewed.*

Predicted State	Mean Percent Time (%)	Mean Dive Count	Mean Move Persistence Velocity (absolute, km*day^{-1})	Mean Proportion D1 Dives	Mean Proportion D2 Dives	Median Maximum Dive Depth (m)	Median Time-at-Depth (min)
S1	62 (19 ± SD)	444 (332 ± SD)	27.8 (16.3 ± SD)	0.112	0.888	57	13.5
S2	19 (10 ± SD)	128 (120 ± SD)	17.9 (15.1 ± SD)	0.411	0.589	92	12.8
S3	20 (14 ± SD)	209 (233 ± SD)	22.0 (13.2 ± SD)	0.803	0.197	112	13.7

When in an S1 state, turtles on average dived 444 times (332 ± SD), versus 128 (120 ± SD) and 209 (233 ± SD) times, respectively, in S2 and S3 states, and

moved with an average persistence velocity of 27.8 km/day (16.3 ± SD) vs. 17.9 (15.1 ± SD) and 22.0 (13.2 ± SD).

The behavioral states also showed strong latitudinal and temporal trends. S1 behaviors were dominant around the equator, through the migratory corridor in latitudes north of the equator (Shillinger et al. 2008), and throughout the middle of the South Pacific Gyre (15-35 deg S) (Fig 3.2.a).

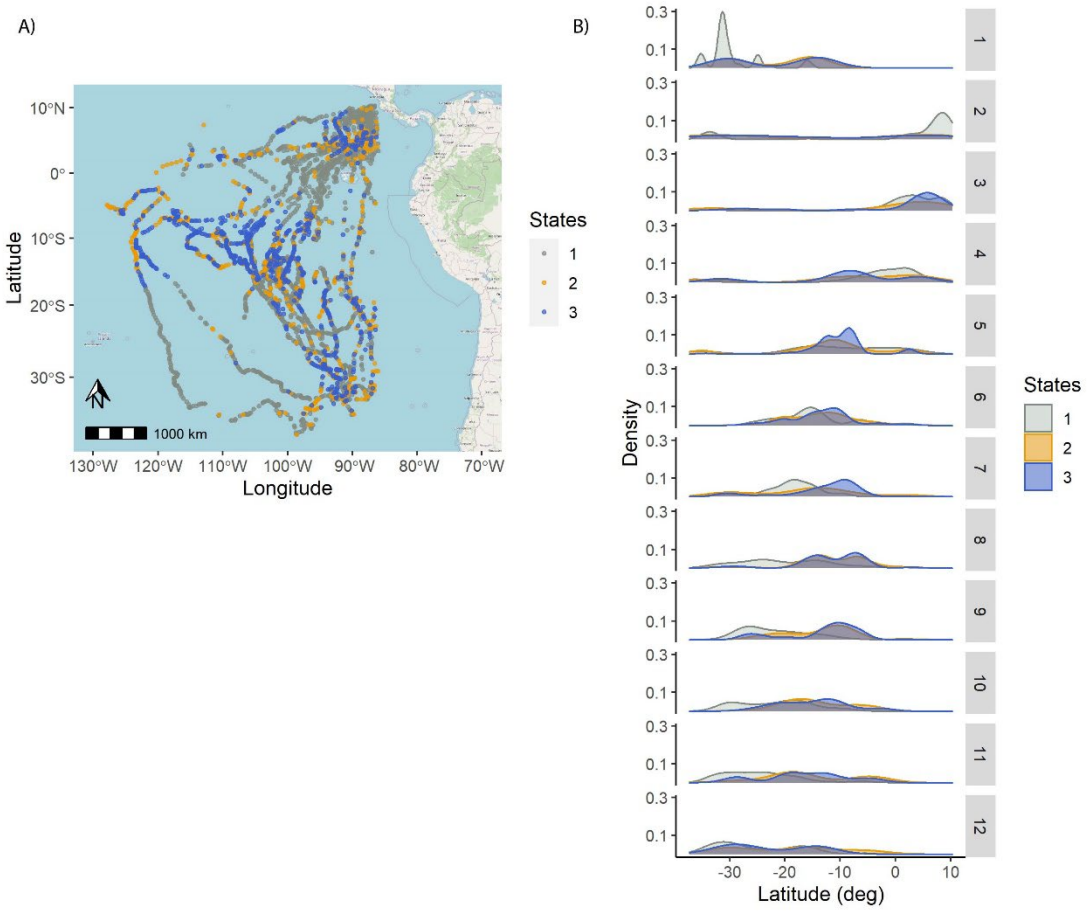

Fig 3.2. *a) Map and b) monthly densities of Hidden Markov model-derived behavioral states (1-3) as a function of latitude for daily positions of N=28 leatherback turtles in the Eastern Pacific region.*

Maps indicated peaks in S2 and S3 behaviors at low latitudes (~5 deg N), latitudes south of the equator (5-20 deg S), and along the edges of the gyre into higher latitudes (20-30 deg S) (Fig 3.2.a). Plotting the proportion of each behavioral state by month indicated the highest proportions of: S1 behaviors in December and February through April, S2 behaviors in May and January and S3 behaviors in May and November (Fig 3.1.b). Density histograms of behavioral states by month and latitude showed S2 and S3 behaviors to have the largest peaks in mid-latitudes (5-20 deg S) from April to August (Fig 3.2.b), with another March peak in areas north of the equator (0-10 deg N). S1 behaviors had the largest peaks in latitudes north of the equator in February and March and in lower latitudes below the equator (~30 deg S) in January (Fig 3.2.b). For both latitude and month, S2 and S3 behaviors were mostly co-distributed with respect to patterns in the horizontal dimension.

Monthly Kernel Density Estimates

The monthly UD estimates for leatherbacks in our region revealed variation in core use areas over time (Figure A3.2).

Turtles initially had a single peak in their probability density surface during February and March, as they departed the nesting beach and followed a migration corridor into more southerly latitudes. Around April, they passed into their foraging region (south of 8.27 deg S, Bailey et al. 2008, Shillinger et al. 2008, Shillinger et al. 2011) and began to radiate out into the South Pacific (SP) Gyre, where multiple core use areas emerged. Of note are peaks in their distribution near the Galapagos Islands (equator) in April and May; in the center of the gyre May through July; along the

eastern edge of the gyre (~ 90 deg W) in May, June, and September; and near the southern edges of the gyre (30 deg S) in November and December.

Monthly Fishing Effort

Fishing effort varied by month and gear (A3.3 and A3.4; also see https://globalfishingwatch.org/map). Of the nine fishing gears, drifting longline and squid jigger gears had very high average monthly fishing effort relative to the others (Fig A3.3). Average fishing effort for drifting longline gear peaked September through December. Average fishing effort for tuna purse seines exhibited a smaller peak in October. In contrast, squid jigger gear exhibited reduced fishing effort September through November but had bimodal peaks January through February and July to August.

Aggregated across gears, monthly fishing effort was quite variable spatially and monthly (Fig A3.4). February through March, effort had broader spatial distributions, with concentrations in latitudes south of the equator (~10-20 deg S). Effort was focused around the equator in January and May through July. Effort occurred in hotspots slightly south of the equator (~5 deg S) and towards the eastern edge of the SP Gyre in April and September through December.

Overlap Analysis: Relative Risk of Interaction

We produced dynamic monthly relative risk of interaction maps between turtles performing specific behaviors with a variety of fishing gears (https://www.upwell.org/sptw), where monthly predictions of relative risk are visualized for each gear and behavior of interest. Here, we provide the monthly maps

of relative risk for leatherbacks performing deep diving behaviors (behavior S3) with drifting longline gear as an example (Fig 3.3).

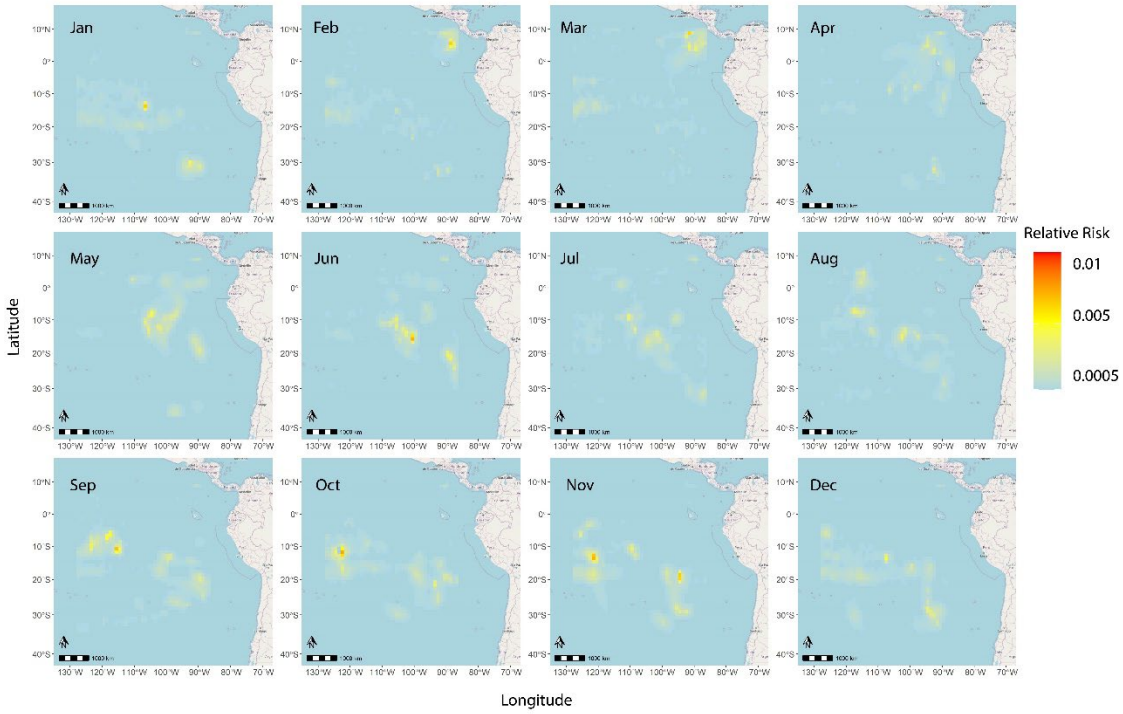

Fig 3.3. *Example monthly maps for the relative risk of Eastern Pacific leatherbacks interacting with drifting longline gear while they are in a deep diving behavioral state (S3). Relative risk is shown on a 1 ° resolution grid found through elementwise multiplication of monthly matrices of: 1) deep diving behavioral intensities 2) drifting longline fishing effort and 3) 3D utilization distributions. Maps are currently incorporated in the dynamic online tool, South Pacific TurtleWatch (https://www.upwell.org/sptw).*

Results showed temporal and spatial differences in relative risk for leatherbacks performing S3 behaviors, with peaks in latitudes north of the equator in February through March; in the center of the SP Gyre (~10-20 deg S) May through June and September through November; and along the eastern and southern edges of the gyre in June and November through December.

These results were further reflected with the developed indices of high relative risk, summarized across the unique groupings of month, behavioral state, and fishing gear (Table 3.3).

Table 3.3. *Summary table of the relative risk index of nine fishing gears by Hidden Markov Model inferred behavioral states (S1, S2, S3) and month. Note: some gears had months with no fishing data available (NA). All fishing data were sourced from Global Fishing Watch (Copyright 2022, Global Fishing Watch, Inc., https://globalfishingwatch.org/). High values for each gear column (< 0.9) and fishing gear column totals are italicized.*

Month	State	Drifting Longline	Fishing	Pole and Line	Purse Seine	Set Gillnet	Set Longline	Squid Jigger	Trawlers	Tuna Purse Seine
1	S1	0.026	0.040	0.039	0.039	0.039	0.039	0.038	0.038	0.038
1	S2	0.057	0.069	0.071	0.071	0.071	0.071	0.067	0.068	0.067
1	S3	0.029	0.043	0.042	0.042	0.042	0.042	0.041	0.041	0.040
2	S1	0.056	0.051	0.056	0.056	0.056	0.056	0.052	0.058	0.056
2	S2	0.035	0.035	0.036	0.036	0.036	0.036	0.037	0.037	0.045
2	S3	0.052	0.051	0.054	0.054	0.054	0.054	0.052	0.054	0.060
3	S1	0.089	*0.10*	*0.11*	*0.11*	*0.11*	*0.11*	*0.11*	*0.11*	*0.12*
3	S2	*0.10*	*0.11*	*0.12*	*0.11*	*0.11*	*0.12*	*0.11*	*0.11*	*0.12*
3	S3	0.046	0.049	0.052	0.052	0.052	0.053	0.051	0.052	0.064
4	S1	0.065	0.08	0.075	0.076	0.081	0.077	0.074	0.074	0.088
4	S2	0.065	0.064	0.072	0.069	0.071	0.064	0.063	0.063	0.069
4	S3	0.042	0.050	0.053	0.051	0.054	0.046	0.047	0.045	0.049
5	S1	0.094	*0.10*	0.097	0.099	0.099	*0.10*	0.096	0.10	0.098
5	S2	*0.12*	*0.12*	*0.12*	*0.12*	*0.12*	*0.12*	*0.12*	*0.13*	*0.11*
5	S3	0.085	0.087	0.081	0.083	0.084	0.085	0.081	0.090	0.077
6	S1	0.047	0.048	0.049	0.047	0.047	0.049	0.049	0.047	0.043
6	S2	0.058	0.061	0.062	0.060	0.060	0.063	0.062	0.060	0.054
6	S3	0.078	0.080	0.080	0.079	0.080	0.082	0.081	0.080	0.078
7	S1	*0.12*	*0.12*	*0.12*	*0.12*	*0.12*	*0.12*	*0.12*	*0.12*	*0.12*
7	S2	0.043	0.051	0.053	0.053	0.053	0.055	0.051	0.053	0.047
7	S3	0.041	0.047	0.047	0.047	0.049	0.047	0.047	0.049	0.045
8	S1	0.081	0.083	0.083	0.083	*NA*	0.084	0.083	0.083	0.075
8	S2	0.052	0.051	0.051	0.051	*NA*	0.055	0.051	0.051	0.051
8	S3	0.067	0.065	0.065	0.065	*NA*	0.065	0.065	0.065	0.066
9	S1	0.063	0.055	0.055	0.055	*NA*	0.055	0.055	*NA*	0.052
9	S2	0.067	0.038	0.039	0.039	*NA*	0.039	0.038	*NA*	0.035
9	S3	0.082	0.071	0.073	0.073	*NA*	0.073	0.073	*NA*	0.070
10	S1	*0.12*	0.084	0.078	0.078	*NA*	0.078	0.078	*NA*	0.073
10	S2	0.092	0.050	0.051	0.051	*NA*	0.051	0.053	*NA*	0.053
10	S3	*0.11*	0.046	0.046	0.046	*NA*	0.046	0.048	*NA*	0.045
11	S1	*0.12*	0.089	0.089	0.089	*NA*	0.090	0.089	*NA*	0.084
11	S2	*0.10*	0.059	0.059	0.059	*NA*	0.059	0.059	*NA*	0.051
11	S3	*0.12*	0.084	0.084	0.084	*NA*	0.084	0.084	*NA*	0.080
12	S1	0.072	0.069	0.074	*NA*	*NA*	0.074	0.069	*NA*	0.062
12	S2	0.048	0.054	0.059	*NA*	*NA*	0.059	0.054	*NA*	0.047
12	S3	0.048	0.052	0.053	*NA*	*NA*	0.053	0.052	*NA*	0.042
Totals		***2.6***	***2.4***	***2.4***	***2.2***	***1.5***	***2.5***	***2.4***	***1.7***	***2.4***

Drifting longline gear had the highest relative risk of interaction with deep-diving leatherbacks in October through November and the lowest risk of interaction in January. Across gears, the highest values for relative risk of interaction were seen for turtles performing a mixture of dive types (D1, deeper, and D2, shallower) with lower move persistence (S2 behaviors) in March and May. For turtles performing transiting behaviors with shallower dives (S1 behaviors), peak risk was in March and July. Other notable very high relative risks of interaction were seen for fishing, set longline, and trawler gears, with turtles displaying transiting (S1) behaviors in May. Gear totals across all months and behavioral states showed drifting longline gear to have the highest overall relative risk of interaction with leatherbacks, followed by set longline gear.

Discussion

Our study demonstrates how multidimensional movement data for a critically endangered and highly migratory species can be integrated with spatio-temporal data on overlapping threats to produce a Dynamic Management (DM) tool. This approach can be used by conservationists and managers to target areas on a chosen temporal (e.g., monthly) and spatial scale where species are performing behaviors that put them at risk for harmful interactions with threats. Additionally, we provide a method for creating a risk index that extends these predictions beyond just illustrative maps of interactions, allowing for the level of overlap of a species performing particular behaviors to be quantified with respect to time and threat type. Our results provide a novel addition to the DM tool for this species, South Pacific TurtleWatch (SPTW,

Hoover et al. 2019, https://www.upwell.org/sptw). Our approach provides a model for similar studies involving other taxa of conservation interest, especially those with cryptic and multidimensional behaviors that have challenged previous conservation initiatives.

The results of both our Hidden Markov Model (HMM) and 3D utilization distributions showed Eastern Pacific (EP) leatherbacks have multidimensional behaviors that vary in space and time. Previous work using dynamic time warp clustering techniques found that dives for turtles in this population can be classified into unique categories (D1 or D2) representing different vertical behaviors (see Chapter 2). Our HMM determined three distinct states of movement (S1, S2, S3) for EP leatherbacks that varied with respect to their horizontal parameters (persistence velocity), the proportion of dives belonging to the D1 dive class, and their temporal and spatial distributions (Figs 3.1 and 3.2, Tables 3.1 and 3.2). Although S2 and S3 behaviors were co-distributed with respect to latitude (Fig 3.2.a-b), they varied in their monthly proportions (Figs 3.1.b, 3.2.b).

Latitudinal differences in monthly space use and identified behaviors (S1, S2, S3) were consistent with previous findings for this population. For the HMM results, the S3 behavioral state likely corresponds to where and when turtles are using deep dives to shed excess heat gained from traveling through warm equatorial waters (Wallace and Jones 2008, Shillinger et al. 2010, Shillinger et al. 2011, Okuyama et al. 2021) and search for prey patches in the nutrient-poor South Pacific Gyre, where zooplankton prey is dispersed at depth (Saba et al. 2008, Stromberg et al. 2009, Shillinger et al. 2011). In contrast, the S2 behavioral state is likely more of a

traditional foraging or residential state, where turtles are using slower speeds and more tortuous movements to perform diurnal dives (deep during the day, shallow at night) and forage on targeted prey patches near the more productive areas of the gyre (Saba et al. 2008, Fernandez-Alamo and Farber-Lorda 2006, Shillinger et al. 2011, Bailey et al. 2012b, Okuyama et al. 2021). S1 behaviors were the shallowest and had the highest move persistence (fast and straight), corresponding to a transiting behavioral state. S1 behaviors had peaks north of the equator, where turtles are known to be migrating within a corridor into the South Pacific Gyre (Shillinger et al. 2008). Peaks were also seen in southern latitudes (~20-35 deg S), corresponding to a couple of individual tracks that deviated from the rest to migrate through the oligotrophic centre of the gyre (Fig 3.2.a). The 3D kernel density estimates of monthly space use for the turtles at the population level reflected patterns seen in the HMMs, with hotspots near the Galapagos Islands (~ 5 deg N latitude), along the eastern (~90-100 deg W) and southern (south of 30 deg S) edges of the gyre, and in the region around 10 deg S latitude (Fig A3.2 and Fig 3.2.a). These correspond to potential foraging areas, due (respectively) to equatorial and island upwelling, frontal and convergence zones, and a shallower thermocline and nutricline (Saba et al. 2008, Fernandez-Alamo & Farber-Lorda 2006, Bailey et al. 2012b).

Although modifying the structure of our HMM would require the user to have a reasonable understanding of HMMs, Bayesian methods, and the coding software used (R, Stan), it is designed to be tailored for user's desired taxa and dataset. Multiple R packages have recently been developed to quickly and easily fit more complex HMMs to time series movement data (e.g. "moveHMM", Michelot et al.

2016, and "momentuHMM", McClintock & Michelot 2018). However, these packages have little room for user modification of parameters and can result in issues with convergence, identifiability, and biologically meaningful inference (Auger-Methe et al. 2016). We provide example code and data for fitting our multistate HMMs in Stan programming language with an R interface (See "Code and Tool Availability" section). We highlight where users can modify model parameters and input data, perform essential checks for convergence issues, and determine optimal model structures through model selection and comparison.

The combination of the monthly 3D UD surfaces with the intensity of each behavioral state (S1, S2, S3) and monthly fishing effort for specific risks (different fishing gears) allowed for the identification of priority conservation areas. Of the nine fishing gears incorporated into our analysis, drifting longlines and squid jiggers surpassed other gears in their average monthly fishing effort within the study region (Fig A3.3). However, the overlap analysis showed that leatherback turtles in this region are most at risk of interaction with drifting longline gear, due to both spatial and temporal overlap (Table 3.3). The index of relative risk determined for each unique gear, month, and behavioral state combination showed drifting or "pelagic" longline gear to have the most high-value indices, especially where turtles are moving slower and/or diving at depth (S2 and S3 behaviors, Table 3.3). Research has shown that pelagic longlines are of a particularly high danger to leatherbacks at depth (Spotila et al. 2000, Moore et al. 2009, Wallace et al. 2010), but previous risk models have not accounted for vertical behavior in their predictions of spatio-temporal overlap between leatherbacks and longlines (Roe et al. 2014). Conservation efforts

for this population can use the dynamic monthly surface maps and quantitative indices of risk we produce with this analysis to disseminate dynamic products to both managers and fishers. These can serve as spatio-temporal predictions of when and where time-area closures or fishing avoidance may be most beneficial (Welch et al. 2018). Application can be further extended to identify which fishing gears could employ gear modifications to increase target prey catches, while reducing bycatch (Watson et al. 2005, Sales et al. 2010).

Dynamic management methods have become increasingly useful and accessible for marine migratory species. Such species often utilize international waters outside the feasible scope of static management approaches that are limited by national jurisdictions and physical boundaries. However, such management approaches (deemed "Dynamic Ocean Management" tools, Maxwell et al. 2015) typically use presence/absence data of target species in relation to environmental covariates without integrating ecologically significant models of movement and/or multidimensional behaviors. Our application of HMMs to both horizontal and vertical movement data allowed for a more comprehensive understanding of space use over time. Although DM approaches have primarily been developed for marine species, many terrestrial migratory species (e.g., altitudinal migrants such as birds, bats, and ungulates, Hsiung et al. 2018) also demonstrate multidimensionality and temporal complexity to their spatial movements. As such, these species could benefit from incorporating multidimensional, multistate movement models into conservation efforts and the identification of priority conservation areas.

For species that cross tens of degrees of latitude during their migrations, the massive spatial scale of their movements, combined with individual variability in their habitat use and behavior, can make highlighting priority conservation areas challenging. These challenges are further magnified if the species is critically endangered, as a rapidly shrinking population inherently limits how many animals can be observed or tagged over time, potentially biasing understanding of recent habitat use and behavior. As the movement data we used for our study is the only large tracking dataset that exists for the EP population of leatherbacks, we were limited to using biotelemetry data that did not overlap temporally with recent fishing effort data. We made the assumption that EP leatherbacks currently follow the same behavioral and spatio-temporal patterns as when this dataset was originally collected (2004-2007). This assumption is not implausible, as it is hypothesized based on round-trip migration data from other populations that adults and sub-adults will return to foraging sites inter-annually with fidelity (James et al. 2005, Saba et al. 2008).

The results and DM product we produce with this analysis are immediately applicable, as a recent population viability assessment (PVA, Philip Miller, IUCN SSC Conservation Planning Specialist Group), indicated a high probability (>90%) of extirpation for the Costa Rica EP leatherback subpopulation (<45 years), with the Mexico subpopulation and the combined metapopulation facing extirpation in less than 55 years (Miller et al., 2022, Copsey et al., 2022). Another PVA (Laúd OPO Network 2020) estimated that EP leatherbacks will be extirpated by the year 2059 if bycatch levels aren't significantly reduced. Our results highlight that drifting (pelagic) longlines have a high relative risk of interaction with EP leatherbacks while

they are performing S2 and S3 behaviors in productive areas of the SP Gyre (Table 3.3, Fig 3.3). It is unlikely another tagging dataset of an equivalent size to Shillinger et al. (2008) will ever be acquired for this population and we provide a method to identify where and when these high-risk interactions are occurring that will be used as part of SPTW and other ongoing conservation efforts to mitigate turtle-fisheries interactions and slow the decline of this critically endangered population.

By combining density-based time-space use predictions with movement models and spatio-temporal data on threats, we provide a holistic approach to dynamic conservation for migratory species that demonstrate multidimensional and cryptic behaviors. This approach could be further advanced in the future by 1) incorporating relationships with environmental or habitat covariates; 2) creating higher resolution predictions of risk and behavior by using more fine-scale movement data in models; 3) estimating population-level UDs while simultaneously accounting for autocorrelation and duration bias in movement tracks; and 4) hybridizing both biotelemetry and observational (presence-absence) datasets to estimate spatial and temporal patterns. We demonstrated this method on a critically endangered population of leatherback turtles, with the goal of both informing current conservation approaches for this population and providing a framework for integrative DM that can be modified to benefit other taxa, including both aquatic and terrestrial species with pronounced three-dimensional movement.

Code and Tool Availability

The DM maps produced with this work are available as part of Upwell's South Pacific TurtleWatch interactive and online tool at:

https://www.upwell.org/sptw

Example code and data to replicate this analysis are available on my GitHub repository:

https://github.com/barb3800

References

Abrahms, B., Welch, H., Brodie, S., Jacox, M. G., Becker, E. A., Bograd, S. J., Irvine, L. M., Palacios, D. M., Mate, B. R., & Hazen, E. L. (2019). Dynamic ensemble models to predict distributions and anthropogenic risk exposure for highly mobile species. *Diversity and Distributions*, *25*(8), 1182–1193.

Adam, T., Griffiths, C. A., Leos-Barajas, V., Meese, E. N., Lowe, C. G., Blackwell, P. G., Righton, D., & Langrock, R. (2019). Joint modelling of multi-scale animal movement data using hierarchical hidden Markov models. *Methods in Ecology and Evolution*, *10*(9), 1536–1550.

Allen, A. M., & Singh, N. J. (2016). Linking Movement Ecology with Wildlife Management and Conservation. *Frontiers in Ecology and Evolution*, *3*.

Auger-Méthé, M., Field, C., Albertsen, C. M., Derocher, A. E., Lewis, M. A., Jonsen, I. D., & Mills Flemming, J. (2016). State-space models' dirty little secrets: Even simple linear Gaussian models can have estimation problems. *Scientific Reports*, *6*(1), 26677.

Auger-Méthé, M., Newman, K., Cole, D., Empacher, F., Gryba, R., King, A. A., Leos-Barajas, V., Flemming, J. M., Nielsen, A., Petris, G., & Thomas, L. (2021). A guide to state-space modeling of ecological time series. *Ecological Monographs*, *91*(4). https://doi.org/10.1002/ecm.1470

Bailey, H., Benson, S. R., Shillinger, G. L., Bograd, S. J., Dutton, P. H., Eckert, S. A., Morreale, S. J., Paladino, F. V., Eguchi, T., Foley, D. G., Block, B. A., Piedra, R., Hitipeuw, C., Tapilatu, R. F., & Spotila, J. R. (2012). Identification of distinct movement patterns in Pacific leatherback turtle populations influenced by ocean conditions. *Ecological Applications*, *22*(3), 735–747.

Bailey, H., Fossette, S., Bograd, S. J., Shillinger, G. L., Swithenbank, A. M., Georges, J.-Y., Gaspar, P., Strömberg, K. H. P., Paladino, F. V., Spotila, J. R., Block, B. A., & Hays, G. C. (2012). Movement Patterns for a Critically Endangered Species, the Leatherback Turtle (Dermochelys coriacea), Linked to Foraging Success and Population Status. *PLOS ONE*, *7*(5), e36401.

Bailey, H., Shillinger, G., Palacios, D., Bograd, S., Spotila, J., Paladino, F., & Block, B. (2008). Identifying and comparing phases of movement by leatherback turtles using state-space models. *Journal of Experimental Marine Biology and Ecology*, *356*(1–2), 128–135.

Bedriñana-Romano, L., Hucke-Gaete, R., Viddi, F. A., Johnson, D., Zerbini, A. N., Morales, J., Mate, B., & Palacios, D. M. (2021). Defining priority areas for blue whale conservation and investigating overlap with vessel traffic in Chilean Patagonia, using a fast-fitting movement model. *Scientific Reports*, *11*(1), 2709.

Bolger, D. T., Newmark, W. D., Morrison, T. A., & Doak, D. F. (2008). The need for integrative approaches to understand and conserve migratory ungulates. *Ecology Letters*, *11*(1), 63–77

Bull, J. W., Suttle, K. B., Singh, N. J., & Milner-Gulland, E. (2013). Conservation when nothing stands still: Moving targets and biodiversity offsets. *Frontiers in Ecology and the Environment*, *11*(4), 203–210.

Calenge, C. (2006) The package adehabitat for the R software: a tool for the analysis of space and habitat use by animals. *Ecological Modelling*, *197*, 516-519

Conners, M. G., Michelot, T., Heywood, E. I., Orben, R. A., Phillips, R. A., Vyssotski, A. L., Shaffer, S. A., & Thorne, L. H. (2021). Hidden Markov models identify major movement modes in accelerometer and magnetometer data from four albatross species. *Movement Ecology*, *9*(1), 7.

Copsey, J., Ábrego, M., Alvarez, C., Bandimere, A., Baron, J., Barragán, A., Benson, S., Cáceres, V.,Davalos, N.,Dueñas, C., Dutton, P., Flanagan, J., Gadea, V., Gray, K., Gunn, A., Hall, M., Harfush, M., Heppell, S.,... & Shillinger, G. (2021). Eastern Pacific Leatherback Turtle: Ex situ Management Recommendation Development Workshop Report. IUCN SSC Conservation Planning Specialist Group, Apple Valley, MN, USA.

DeRuiter, S. L., Langrock, R., Skirbutas, T., Goldbogen, J. A., Chalambokidis, J., Friedlaender, A. S., & Southall, B. L. (2016). *A multivariate mixed hidden Markov model to analyze blue whale diving behaviour during controlled sound exposures* (arXiv:1602.06570). Pre-Print. arXiv. http://arxiv.org/abs/1602.06570

Dickey, T. D. (2003). Emerging ocean observations for interdisciplinary data assimilation systems. *Journal of Marine Systems*, *40–41*, 5–48.

Fernández-Álamo, M. A., & Färber-Lorda, J. (2006). Zooplankton and the oceanography of the eastern tropical Pacific: A review. *Progress in Oceanography*, *69*(2–4), 318–359.

Fossette, S., Witt, M. J., Miller, P., Nalovic, M. A., Albareda, D., Almeida, A. P., Broderick, A. C., Chacón-Chaverri, D., Coyne, M. S., Domingo, A., Eckert, S., Evans, D., Fallabrino, A., Ferraroli, S., Formia, A., Giffoni, B., Hays, G. C., Hughes, G., Kelle, L., … Godley, B. J. (2014). Pan-Atlantic analysis of the overlap of a highly migratory species, the leatherback turtle, with pelagic longline fisheries. *Proceedings of the Royal Society B: Biological Sciences*, *281*(1780), 20133065.

Fraser, K. C., Davies, K. T. A., Davy, C. M., Ford, A. T., Flockhart, D. T. T., & Martins, E. G. (2018). Tracking the Conservation Promise of Movement Ecology. *Frontiers in Ecology and Evolution*, *6*. https://www.frontiersin.org/article/10.3389/fevo.2018.00150

Gaspar, P., Georges, J.-Y., Fossette, S., Lenoble, A., Ferraroli, S., & Le Maho, Y. (2006). Marine animal behaviour: Neglecting ocean currents can lead us up the wrong track. *Proceedings of the Royal Society B: Biological Sciences*, *273*(1602), 2697–2702.

Gurarie E (2022). bcpa: Behavioral Change Point Analysis of Animal Movement. R package version 1.3.2, https://CRAN.R-project.org/package=bcpa.

Gurarie, E., Andrews, R. D., & Laidre, K. L. (2009). A novel method for identifying behavioural changes in animal movement data. *Ecology Letters*, *12*(5), 395–408.

Hijmans R (2022). raster: Geographic Data Analysis and Modeling. R package version 3.5-15, https://CRAN.R-project.org/package=raster.

Hobday, A. J., & Hartog, J. R. (2014). Derived Ocean Features for Dynamic Ocean Management. *Oceanography*, *27*(4), 134–145.

Hoover, A. L., Liang, D., Alfaro-Shigueto, J., Mangel, J. C., Miller, P. I., Morreale, S. J., Bailey, H., & Shillinger, G. L. (2019). Predicting residence time using a continuous-time discrete-space model of leatherback turtle satellite telemetry data. *Ecosphere*, *10*(3), e02644.

Howell, E. A., Hoover, A., Benson, S. R., Bailey, H., Polovina, J. J., Seminoff, J. A., & Dutton, P. H. (2015). Enhancing the TurtleWatch product for leatherback sea turtles, a dynamic habitat model for ecosystem-based management. *Fisheries Oceanography*, *24*(1), 57–68.

Howell, E., Kobayashi, D., Parker, D., Balazs, G., & Polovina, aJJ. (2008). TurtleWatch: A tool to aid in the bycatch reduction of loggerhead turtles Caretta caretta in the Hawaii-based pelagic longline fishery. *Endangered Species Research*, *5*, 267–278.

Hsiung, A. C., Boyle, W. A., Cooper, R. J., & Chandler, R. B. (2018). Altitudinal migration: Ecological drivers, knowledge gaps, and conservation implications. *Biological Reviews*, *93*(4), 2049–2070.

James, M. C., Andrea Ottensmeyer, C., & Myers, R. A. (2005). Identification of high-use habitat and threats to leatherback sea turtles in northern waters: New directions for conservation. *Ecology Letters*, *8*(2), 195–201.

Johnston, A., Auer, T., Fink, D., Strimas-Mackey, M., Iliff, M., Rosenberg, K. V., Brown, S., Lanctot, R., Rodewald, A. D., & Kelling, S. (2020). Comparing abundance distributions and range maps in spatial conservation planning for migratory species. *Ecological Applications*, *30*(3), e02058.

Jonsen, I., Myers, R., & James, M. (2007). Identifying leatherback turtle foraging behaviour from satellite telemetry using a switching state-space model. *Marine Ecology Progress Series*, *337*, 255–264.

Jonsen, I & Patterson, T (2020). foieGras: fit latent variable movement models to animal tracking data for location quality control and behavioural inference Zenodo. https://doi.org/10.5281/zenodo.3899972

Kaplan, I. C. (2005). A risk assessment for Pacific leatherback turtles (*Dermochelys coriacea*). *Canadian Journal of Fisheries and Aquatic Sciences*, *62*(8), 1710–1719.

Kavanaugh, M. T., Oliver, M. J., Chavez, F. P., Letelier, R. M., Muller-Karger, F. E., & Doney, S. C. (2016). Seascapes as a new vernacular for pelagic ocean monitoring, management and conservation. *ICES Journal of Marine Science*, *73*(7), 1839–1850.

Keating, K. A., & Cherry, S. (2009). Modeling utilization distributions in space and time. *Ecology*, *90*(7), 1971–1980.

Kroodsma, D. A., Mayorga, J., Hochberg, T., Miller, N. A., Boerder, K., Ferretti, F., Wilson, A., Bergman, B., White, T. D., Block, B. A., Woods, P., Sullivan, B., Costello, C., & Worm, B. (2018). Tracking the global footprint of fisheries. *Science*, *359*(6378), 904–908.

Lellouche, J. M., Greiner, E., Bourdallé-Badie, R., Garric, G., Melet, A., Drévillon, M., ... & Le Traon, P. Y. (2021). The Copernicus global 1/12 oceanic and sea ice GLORYS12 reanalysis. *Frontiers in Earth Science*, 9, 698876.

Leos-Barajas, V., Gangloff, E. J., Adam, T., Langrock, R., van Beest, F. M., Nabe-Nielsen, J., & Morales, J. M. (2017). Multi-scale Modeling of Animal Movement and General Behavior Data Using Hidden Markov Models with Hierarchical Structures. *Journal of Agricultural, Biological and Environmental Statistics*, *22*(3), 232–248.

Leos-Barajas, V., & Michelot, T. (2018). *An Introduction to Animal Movement Modeling with Hidden Markov Models using Stan for Bayesian Inference* (arXiv:1806.10639). PrePrint. arXiv. http://arxiv.org/abs/1806.10639

Lewison, R., Hobday, A. J., Maxwell, S., Hazen, E., Hartog, J. R., Dunn, D. C., Briscoe, D., Fossette, S., O'Keefe, C. E., Barnes, M., Abecassis, M., Bograd, S., Bethoney, N. D., Bailey, H., Wiley, D., Andrews, S., Hazen, L., & Crowder, L. B. (2015). Dynamic Ocean Management: Identifying the Critical Ingredients of Dynamic Approaches to Ocean Resource Management. *BioScience*, *65*(5), 486–498.

Lewison, R. L., Freeman, S. A., & Crowder, L. B. (2004). Quantifying the effects of fisheries on threatened species: The impact of pelagic longlines on loggerhead and leatherback sea turtles. *Ecology Letters*, *7*(3), 221–231.

Maxwell, S. M., Hazen, E. L., Lewison, R. L., Dunn, D. C., Bailey, H., Bograd, S. J., Briscoe, D. K., Fossette, S., Hobday, A. J., Bennett, M., Benson, S., Caldwell, M. R., Costa, D. P., Dewar, H., Eguchi, T., Hazen, L., Kohin, S., Sippel, T., & Crowder, L. B. (2015). Dynamic ocean management: Defining and conceptualizing real-time management of the ocean. *Marine Policy*, *58*, 42–50.

McClintock, B. T., & Michelot, T. (2018). momentuHMM: R package for generalized hidden Markov models of animal movement. *Methods in Ecology and Evolution*, *9*(6), 1518–1530.

Meisingset, E. L., Loe, L. E., Brekkum, Ø., Bischof, R., Rivrud, I. M., Lande, U. S., Zimmermann, B., Veiberg, V., & Mysterud, A. (2018). Spatial mismatch between management units and movement ecology of a partially migratory ungulate. *Journal of Applied Ecology*, *55*(2), 745–753.

Michelot, T., Langrock, R., & Patterson, T. A. (2016). moveHMM: An R package for the statistical modelling of animal movement data using hidden Markov models. *Methods in Ecology and Evolution*, *7*(11), 1308–1315.

Miller, P. (2021) Population Viability Analysis of the Eastern Pacific Leatherback Turtle An assessment of ex situ management options to inform species conservation. Report prepared for Upwell in consultation with Eastern Pacific Leatherback PVA Workshop participants; facilitated by the IUCN SSC Conservation Planning Specialist Group.

Moore, J. E., Wallace, B. P., Lewison, R. L., Žydelis, R., Cox, T. M., & Crowder, L. B. (2009). A review of marine mammal, sea turtle and seabird bycatch in USA

fisheries and the role of policy in shaping management. *Marine Policy*, *33*(3), 435–451.

Nathan, R., Getz, W. M., Revilla, E., Holyoak, M., Kadmon, R., Saltz, D., & Smouse, P. E. (2008). A movement ecology paradigm for unifying organismal movement research. *Proceedings of the National Academy of Sciences*, *105*(49), 19052–19059.

Okuyama, J., Benson, S. R., Dutton, P. H., & Seminoff, J. A. (2021). Changes in dive patterns of leatherback turtles with sea surface temperature and potential foraging habitats. *Ecosphere*, *12*(2), e03365.

Patterson, T. A., Basson, M., Bravington, M. V., & Gunn, J. S. (2009). Classifying movement behaviour in relation to environmental conditions using hidden Markov models. *Journal of Animal Ecology*, *78*(6), 1113–1123.

R Core Team (2021). 'R: A Language and environment for statistical computing. R Foundation for Statistical Computing, Vienna, Austria'. URL: https://www.R-project.org/

Roe, J. H., Morreale, S. J., Paladino, F. V., Shillinger, G. L., Benson, S. R., Eckert, S. A., Bailey, H., Tomillo, P. S., Bograd, S. J., Eguchi, T., Dutton, P. H., Seminoff, J. A., Block, B. A., & Spotila, J. R. (2014). Predicting bycatch hotspots for endangered leatherback turtles on longlines in the Pacific Ocean. *Proceedings of the Royal Society B: Biological Sciences*, *281*(1777), 20132559.

Runge, C. A., Martin, T. G., Possingham, H. P., Willis, S. G., & Fuller, R. A. (2014). Conserving mobile species. *Frontiers in Ecology and the Environment*, *12*(7), 395–402.

Saba, V. S., Shillinger, G. L., Swithenbank, A. M., Block, B. A., Spotila, J. R., Musick, J. A., & Paladino, F. V. (2008). An oceanographic context for the foraging ecology of eastern Pacific leatherback turtles: Consequences of ENSO. *Deep Sea Research Part I: Oceanographic Research Papers*, *55*(5), 646–660.

Sales, G., Giffoni, B. B., Fiedler, F. N., Azevedo, V. G., Kotas, J. E., Swimmer, Y., & Bugoni, L. (2010). Circle hook effectiveness for the mitigation of sea turtle bycatch and capture of target species in a Brazilian pelagic longline fishery. *Aquatic Conservation: Marine and Freshwater Ecosystems*, *20*(4), 428–436.

Schick, R. S., Roberts, J. J., Eckert, S. A., Halpin, P. N., Bailey, H., Chai, F., Shi, L., & Clark, J. S. (2013). Pelagic movements of pacific leatherback turtles (dermochelys coriacea) highlight the role of prey and ocean currents. *Movement Ecology*, *1*(1), 11.

Shillinger, G. L., Palacios, D. M., Bailey, H., Bograd, S. J., Swithenbank, A. M., Gaspar, P., Wallace, B. P., Spotila, J. R., Paladino, F. V., Piedra, R., Eckert, S. A., & Block, B. A. (2008). Persistent Leatherback Turtle Migrations Present Opportunities for Conservation. *PLOS Biology*, *6*(7), e171.

Shillinger, G. L., Swithenbank, A. M., Bailey, H., Bograd, S. J., Castelton, M. R., Wallace, B. P., Spotila, J. R., Paladino, F. V., Piedra, R., & Block, B. A. (2011). Vertical and horizontal habitat preferences of post-nesting leatherback turtles in the South Pacific Ocean. *Marine Ecology Progress Series*, *422*, 275–289.

Shillinger, G., Swithenbank, A., Bograd, S., Bailey, H., Castelton, M., Bp, W., Spotila, J., Paladino, F., Piedra, R., & Block, B. (2010). Identification of high-use

internesting habitats for eastern Pacific leatherback turtles: Role of the environment and implications for conservation. *Endangered Species Research*, *10*, 215–232.

Spotila, J. R., Reina, R. D., Steyermark, A. C., Plotkin, P. T., & Paladino, F. V. (2000). Pacific leatherback turtles face extinction. *Nature*, *405*(6786), 529–530.

Stan Development Team (2022). RStan: the R interface to Stan. R package version 2.21.5. https://mc-stan.org/.

Strömberg, K. H. P., Smyth, T. J., Allen, J. I., Pitois, S., & O'Brien, T. D. (2009). Estimation of global zooplankton biomass from satellite ocean colour. *Journal of Marine Systems*, *78*(1), 18–27.

The Laud OPO Network. (2020). Enhanced, coordinated conservation efforts required to avoid extinction of critically endangered Eastern Pacific leatherback turtles. *Scientific Reports*, *10*, 4772.

Udell, B. J., Martin, J., Fletcher Jr., R. J., Bonneau, M., Edwards, H. H., Gowan, T. A., Hardy, S. K., Gurarie, E., Calleson, C. S., & Deutsch, C. J. (2019). Integrating encounter theory with decision analysis to evaluate collision risk and determine optimal protection zones for wildlife. *Journal of Applied Ecology*, *56*(5), 1050–1062.

Vehtari, A., Gelman, A., & Gabry, J. (2017). Practical Bayesian model evaluation using leave-one-out cross-validation and WAIC. *Statistics and Computing*, *27*(5), 1413–1432.

Wallace, B. P., & Jones, T. T. (2008). What makes marine turtles go: A review of metabolic rates and their consequences. *Journal of Experimental Marine Biology and Ecology*, *356*(1–2), 8–24.

Wallace, B. P., Lewison, R. L., McDonald, S. L., McDonald, R. K., Kot, C. Y., Kelez, S., Bjorkland, R. K., Finkbeiner, E. M., Helmbrecht, S., & Crowder, L. B. (2010). Global patterns of marine turtle bycatch. *Conservation Letters*, *3*(3), 131–142.

Watson, J. W., Epperly, S. P., Shah, A. K., & Foster, D. G. (2005). Fishing methods to reduce sea turtle mortality associated with pelagic longlines. *Canadian Journal of Fisheries and Aquatic Sciences*, *62*(5), 965–981.

Welch, H., Hazen, E. L., Bograd, S. J., Jacox, M. G., Brodie, S., Robinson, D., Scales, K. L., Dewitt, L., & Lewison, R. (2019). Practical considerations for operationalizing dynamic management tools. *Journal of Applied Ecology*, *56*(2), 459–469.

Westley, P. A. H., Berdahl, A. M., Torney, C. J., & Biro, D. (2018). Collective movement in ecology: From emerging technologies to conservation and management. *Philosophical Transactions of the Royal Society B: Biological Sciences*, *373*(1746), 20170004.

White, T. D., Ferretti, F., Kroodsma, D. A., Hazen, E. L., Carlisle, A. B., Scales, K. L., Bograd, S. J., & Block, B. A. (2019). Predicted hotspots of overlap between highly migratory fishes and industrial fishing fleets in the northeast Pacific. *Science Advances*, *5*(3), eaau3761.

Yao Y, Vehtari A, Simpson D, & Gelman A (2017). Using stacking to average Bayesian predictive distributions. *Bayesian Analysis*. doi:10.1214/17-BA1091

Zucchini, W., & MacDonald, I. L. (2009). *Hidden Markov Models for Time Series: An Introduction Using R*. Chapman and Hall/CRC.

Chapter 4: Evidence of release effects and recruitment to developmental habitats for post captive, juvenile Caribbean green turtles (*Chelonia mydas*)

Abstract

Juvenile life stages are often understudied in movement ecology, especially for migratory species in dynamic and fluid environments (e.g. aquatic, marine, and aerial). Sea turtles have ontogenetic niche shifts between foraging habitats as juveniles that have been difficult to describe due to cryptic movements and a paucity of empirical tagging studies for this life stage, due to tag restrictions producing limited tracking durations and large tag-to-body size ratios. To address these knowledge gaps, we tagged and released N=40 juvenile green sea turtles (*Chelonia mydas*) across three age classes (1-2, 2-3, and 3-4 years) using miniature satellite tags. Turtles were released from Grand Cayman, Cayman Islands from two different release locations during different times of year (January, July) to additionally determine release effects on post captive individuals. Observed trajectories for individuals were compared to both current-corrected and simulated, passive drift trajectories. A k-means clustering analysis was used to cluster data across individuals into discrete behaviors based on movement metrics and current velocities. A statistical model was used to identify significant differences in the occurrences of these behavioral clusters with environmental and biological variables. Of the N=40 turtles released, N=22 effectively dispersed from the Islands during the tracking

period to surrounding geographic areas. Most observed tracks deviated from passive drift trajectories over time, with turtles demonstrating the use of oriented swimming to maintain directed paths to nearshore areas. Clustering and statistical analyses revealed significant differences for the proportion of identified movement behaviors with release time period, current velocities, and floating algae (*Sargassum*) presence. Overall, these results point to the importance of release timing and location for post captive (headstarted) sea turtles and support that post captive juvenile green turtles have the capacity to forage, navigate, and recruit to key developmental habitats. Our results inform ongoing conservation initiatives for the Caymanian green turtle population and we recommend modifications to our methods for future tracking studies. Movement ecology studies for other species with post-captive individuals, enigmatic juvenile life stages, and/or ontogenetic niche shifts in a fluid environment may benefit from applying similar approaches.

Introduction

An ever-present and challenging goal in movement ecology is to describe the "lifetime track" or the entirety of movement phases for an individual throughout its entire lifetime (Nathan et al 2008). Given that tag technology with the ability to report animal spatial-temporal positions is generally limited in duration to time periods less than a year, understanding the lifetime movements of any one individual has been all but impossible, although advances are being made for some taxa (e.g., white storks, Flack et al 2018, Cheng et al 2019). Instead, understanding ontogenetic movements, behavior, and habitat use has often been dependent on independently tracking individuals within different age classes and using quantitative methods combined

with biological knowledge to infer connections between lifestages. Additionally, active biotelemetry studies on more than one lifestage have often been biased towards larger and adult animals, due to challenges with tagging neonates and juveniles, such as higher mortality rates, large tag-to-body-size ratios, and for animals that disperse long distances, accessibility to intermediate age classes (Shillinger et al 2012, Hazen et al 2012). Of those studies that have successfully tracked these younger and smaller age classes (e.g. recently, neonate leatherback turtles, Barbour et al 2020; juvenile green turtles, Chambault et al 2020; juvenile bearded seals, Breed et al 2018; juvenile Scopoli shearwaters, Peron and Gremillet 2013; juvenile cuckoos, Vega et al 2016; juvenile king penguins, Orgeret et al 2019; juvenile silky sharks, Hutchinson et al 2019; neonate caribou, Bonar et al 2018), the high monetary cost of long-lasting tags combined with the challenges listed previously has often resulted in smaller sample sizes, shorter tracking durations, and/or only one age class tracked at a time.

The complexity of life cycles for many migratory marine taxa and their presence within a dynamic, vast, and fluid medium has further resulted in a paucity of understanding of juvenile movements at sea. Of particular interest is the sea turtle, a long-lived taxa where most species demonstrate ontogenetic separation in foraging habitats (Bolten 2003, Meylan et al 2011), inter-specific and even population level differences in migration strategies (Godley et al 2008), and the presence of a cryptic, developmental lifestage previously termed “The Lost Years” (Carr 1987), where neonates and young juveniles spend years in pelagic foraging habitats far from both nearshore reproductive and foraging grounds. Although most sea turtle movement studies have focused on adult post-nesting females (Godley et al 2008, Hazen et al

2012), a growing body of literature has targeted understanding the "when" and "where" of movement (Nathan et al 2008) of this pelagic developmental period and when transitions occur switching to different developmental habitats as older juveniles. Although studies on the navigational abilities and large-scale habitat use of juvenile sea turtles have mostly been limited to simulated Individual Based Models (IBMs) and/or laboratory studies (Fuxjager et al 2011, Putman et al 2015, Gaspar and Lalire 2017, Lalire and Gaspar 2019), the progression and miniaturization of long-lasting satellite tags has recently allowed for empirical measurements of juvenile sea turtle movement (Mansfield et al 2012, Kobayashi et al 2014, Putman and Mansfield 2015, Briscoe et al 2016, Mansfield et al 2017). However, simultaneous tracking of multiple age classes is rare and for many species and populations of sea turtles, the physical drivers and role of ontogeny in dispersal is mostly empirically undescribed.

Chelonian sea turtles (green, hawksbill, and loggerheads) have been shown through a combination of mark-recapture, stable isotope, and tracking studies to transition from offshore, pelagic developmental habitats (often in association with patches of drifting *Sargassum* algae) to nearshore, benthic developmental habitats as larger juveniles (Carr 1987, Reich et al 2007, Meylan et al. 2011, Witherington et al. 2012). Studies of green sea turtle (*Chelonia mydas*) movement ecology have shown that during their developmental pelagic stage, juveniles do not act as passive, drifting particles but instead, actively orient and swim against ocean currents to remain in or encounter favorable foraging habitats (Putman and Mansfield 2015, Mansfield et al 2021). Further work is needed to determine if there is ontogeny in the relationship of

juvenile's directed movements with the physical environment (e.g., ocean currents, variable sea surface temperatures, floating *Sargassum* algae communities).

The Cayman Islands in the Caribbean once hosted one of the world's largest green turtle nesting colonies (Groombridge 1982), but human over-consumption and exploitation resulted in near extirpation by the late 1800s. Recent research, however, has shown that previous mass releases of neonate and juvenile captive-bred green turtles from the Cayman Turtle Centre, a breeding and captive center for green turtles of all age classes, most likely allowed for the successful reestablishment of a green turtle nesting population in the Cayman Islands (Blumenthal et al 2021). Previous mark-recapture studies of these mass releases found that turtles dispersed throughout the Caribbean before some returned to nest (Bell et al 2005, Moncada et al 2006) and although there are currently no satellite tracking studies of neonates and juveniles from the Centre or the local wild population, limited satellite tracking of adult wild Cayman greens has shown that they utilize foraging grounds off of Central America (Blumenthal et al 2006).

To investigate ontogeny in green turtle movement ecology and dispersal, we satellite tagged and released a large number of captive-raised, green sea turtles in multiple juvenile age classes from the Cayman Islands. Having been in captivity during the period of time that they would have been in their pelagic, developmental stage, this experiment gave the unique opportunity to test the ability of post-captive juveniles to disperse effectively away from the release site and into a novel ocean environment. To determine whether there was ontogeny in their movements, differences in dispersal with release site location and timing, and relationships with

environmental variables, we used a) a behavioral clustering analysis b) a multinomial regression and c) comparisons of individual turtle tracks with both current-corrected and passive, simulated trajectories. This work adds to a growing body of knowledge on movement ecology for juvenile lifestages and has implications for conservation of this and other species of sea turtles, with results informing the design of head-starting initiatives.

Methods

Satellite Tag Deployment and Turtle Releases

Juvenile green sea turtles were obtained from the Cayman Turtle Centre on Grand Cayman, Cayman Islands. Obtaining turtles from the Centre allowed for turtles to be hatched and raised in a captive setting until they had reached the desired age class and were ready for release. N=40 turtles in three different age classes (1-2 years, 2-3 years, 3-4 years) were acquired based upon availability, with N=10 turtles in the 2-3 and 3-4 year age classes and N=20 turtles in the 1-2 year age classes (Table 4.1).

Table 4.1. *Individual-level (N=40) data for: age class, number of raw locations, body mass (kg), curved carapace length (CCL, cm) and width (CCW, cm), tag (S= Solar, NS= non-solar/satellite) and adhesive (E= epoxy, FC= Fast Cure) type, median timestep between raw locations (hrs), and tag duration (days). Individuals 214082 and 203086 are greyed out, as they only had one location each outside the boundaries of Grand Cayman Island and were removed from further analysis.*

ID	Tracking Period	Age Class	No. of Raw Locations	Mean Locations *per day*	Body Mass *kg*	CCL *cm*	CCW *cm*	Adhesive Type	Tag Type	Median Timestep *hrs*	Days Tracked *days*
202985	Jan	1-2 Yrs	15	1.6	5.3	37	32	E	NS	22.7	10.0
203084	Jan	1-2 Yrs	32	3.7	4.3	37	29	FC	NS	11.9	23.5
203407	Jan	1-2 Yrs	79	6.6	5.6	37	32	FC	S	10.5	12.5
203408	Jan	1-2 Yrs	40	5.8	4.2	35	30	E	S	11.3	18.0
203410	Jan	1-2 Yrs	126	14.2	4.3	35	31	FC	S	1.7	12.5
212846	Jan	1-2 Yrs	22	3.7	4.3	35	31	E	NS	10.8	32.5
214069	Jan	1-2 Yrs	19	3.5	6.8	40	34	FC	NS	12.0	10.5
214083	Jan	1-2 Yrs	87	4.1	4.8	38	31	FC	S	11.0	29.5
214085	Jan	1-2 Yrs	115	12.7	5.0	38	33	E	S	2.4	16.5
203436	Jan	1-2 Yrs	5	1.0	6.3	40	31	E	NS	17.7	3.0
203080	Jan	2-3 Yrs	9	2.0	12.8	51	43	E	NS	23.3	10.0
203087	Jan	2-3 Yrs	28	2.6	17.2	53	46	E	NS	11.2	12.5
203403	Jan	2-3 Yrs	50	4.2	23.3	61	51	E	S	11.2	11.5
203404	Jan	2-3 Yrs	13	2.5	12.9	51	42	E	S	13.2	5.4
203406	Jan	2-3 Yrs	16	3.6	19.5	62	51	E	S	6.1	3.5
212847	Jan	2-3 Yrs	37	3.5	14.8	51	46	E	NS	12.1	18.9
212867	Jan	2-3 Yrs	29	2.8	14.2	51	44	E	NS	11.3	23.0
214081	Jan	2-3 Yrs	60	7.4	9.6	44	38	E	S	10.7	10.5
214082	Jan	2-3 Yrs	1	-	11.6	47	41	E	S	-	0
203086	Jan	2-3 Yrs	1	-	15.2	51	45	E	NS	-	0
203089	Jan	3-4 Yrs	13	1.4	22.7	60	51	E	NS	22.3	19.0
203405	Jan	3-4 Yrs	27	9.1	22.6	59	52	E	S	1.3	3.0
203409	Jan	3-4 Yrs	41	3.0	29.4	65	55	E	S	12.5	15.0
203411	Jan	3-4 Yrs	207	7.8	20.4	58	51	E	S	1.8	28.1
203412	Jan	3-4 Yrs	6	2.6	24.9	58	53	E	S	12.0	3.0
212837	Jan	3-4 Yrs	26	2.9	29.5	62	54	E	NS	10.7	11.5
212845	Jan	3-4 Yrs	10	2.2	29.4	62	52	E	NS	23.7	5.6
212862	Jan	3-4 Yrs	25	1.9	20.4	54	48	E	NS	23.3	19.0
212866	Jan	3-4 Yrs	13	2.8	13.6	54	44	E	NS	47.8	19.0
228045	Jan	3-4 Yrs	73	8.3	31.8	62	53	E	S	10.7	18.5
229669	Jul	1-2 Yrs	55	13.3	5.1	37	32	FC	S	1.3	11.6
229670	Jul	1-2 Yrs	56	12.3	5.7	38	33	FC	S	1.1	24.6
229671	Jul	1-2 Yrs	60	16.1	6.3	40	34	FC	S	0.9	10.5
229672	Jul	1-2 Yrs	43	12.6	5.2	39	32	FC	S	1.5	9.5
229673	Jul	1-2 Yrs	54	14.8	5.3	37	33	FC	S	1.2	10.5
229674	Jul	1-2 Yrs	42	10.1	5.0	37	32	FC	S	1.3	10.5
229675	Jul	1-2 Yrs	59	17.1	6.4	38	34	FC	S	0.8	10.6
229676	Jul	1-2 Yrs	55	17.4	4.9	36	32	FC	S	1.1	10.6
229677	Jul	1-2 Yrs	54	12.7	5.3	36	33	FC	S	1.2	10.5
229678	Jul	1-2 Yrs	41	15.4	4.8	36	33	FC	S	1.0	8.0

All turtles were designated to be in good health and body condition. All handling and procedures were covered by University of Maryland Center for Environmental Science's Institutional Animal Care and Use Committee (IACUC; Research Protocol No. S-CBL-2021-03). Turtles were either tagged with miniature (~1 g) solar (N=25) or battery-powered satellite tags (N=15). The majority of tags were adhered to the carapaces of the turtles using epoxy adhesive (N=25), but N=15 (1-2 years) used 3M 5200 Fast Cure (FC) marine adhesive instead. All tags reported positions and error information through the ARGOS satellite system.

Based upon availability of the turtles, turtles in different age classes were tagged and released at two separate time periods. N=20 turtles across three age classes (1-2 years, 2-3 years, 3-4 years) were tagged and released on Jan 22, 2022 and N=10 turtles in the youngest age class (1-2 year) was tagged and released on July 20, 2022. All age classes were released by boat offshore of Grand Cayman; however, in order to compare impacts of releasing turtles in different locations, January turtles were released ~ 10 km north of Rum Point, Grand Cayman, whereas July turtles were released ~ 10 south of Spotts Beach, Grand Cayman. Surface drifters (January, N=1 Pacific Gyre REEF Drifter; July, N=1 Microstar GPS Drifter) were released simultaneously with turtles and reported regular (every 10 min) locations for use in understanding smaller scale surface current trajectories upon release and in the study region.

All data processing and analyses were performed in R version 4.2.0 (R Core Team 2022).

Environmental Data Annotation

To match the resolution of environmental data products and filter out error positions, tracks of "dispersive" individuals (those that left the vicinity of the island, N=22) had locations within a 1 km buffer of the island removed; remaining locations were filtered and regularized through the "foieGras" R package (Jonsen et al. 2019) to have daily positions (Fig A4.1). Regularized trajectories for each individual turtle were then corrected for the influence of ocean currents using the methods of Gaspar et al. (2006). All current corrections were provided by the Copernicus Marine Service (https://marine.copernicus.eu/). Mean ground velocities were derived from daily observed positions; estimated surface current velocities derived from ocean current data were subtracted from these ground velocities to produce daily mean swimming speeds and current-corrected trajectories (Gaspar et al. 2006). Ocean current data was obtained from the Operational Mercator global ocean analysis and forecast system (DOI: https://doi.org/10.48670/moi-00016), which produces daily mean estimates of sea surface temperature and surface current velocity at a 1/12th degree resolution. Global surface current estimates can be provided from two different ocean products (PSY4V3 or SMOC); the SMOC product, however, additionally accounts for tidal and wave (Stokes drift) effects in its surface current estimates. To determine which product to use, a pairwise distance analysis of current-corrected trajectories from the PSY4V3 vs SMOC products was performed. The majority (65%) of locations showed large differences between these two products (Fig A4.2), suggesting that Stokes drift effects not accounted for in the PSY4V3 product may be significant in these portions

of the tracks. SMOC was used for the rest of the analysis to produce current-corrected trajectories and swimming speeds.

In addition to daily mean surface current estimates for each dispersive turtle location, environmental data for *Sargassum* presence and sea surface temperature was obtained. Mean daily sea surface temperature (SST) data were derived from the PSY4V3 ocean product (Fig A4.3). *Sargassum* data were sourced from a processed product of *Sargassum* density for the region (University of South Florida, Wang and Hu 2016), where weekly *Sargassum* density fields have been estimated at a 0.01 degree resolution from MODIS Alternate Floating Algae Index (AFAI) data and processed for errors from clouds and cloud shadows, sun glint, and gaps in satellite coverage (Wang and Hu 2016). Underlying *Sargassum* density values were extracted for turtle track locations within a 1 km radius (Fig A4.4). Sargassum presence/absence was determined by categorizing *Sargassum* density values, where values greater than 0 indicate the presence of *Sargassum*. Results showed that *Sargassum* was present for 35% (85/246 locations) of daily observed track locations across individuals (Fig A4.4).

Comparison of Current-Corrected, Observed, and Simulated Passive Drift Trajectories

Circular histograms, straightness indices, and maps were used to compare the current-corrected trajectories with the empirical (observed) trajectories.
When there is a similar number of steps for two comparable trajectories, the straightness index (SI), or straight-line distance between the first and last points divided by the overall length of a track, can be useful for determining differences

between two trajectories in their tortuosity or directedness (Benhamou 2004). An SI was derived for each individual's observed and current-corrected track, using the "trajr" R package (McLean and Volponi 2018) and visual comparisons were made using density histograms.

Circular histograms were used to visualize differences in the distribution of bearings of observed vs current-corrected trajectories from true north and with respect to the corresponding bearings of daily mean surface currents.

Differences between observed, current-corrected, and passive drift trajectories were additionally visualized with maps for each individual and tracking period (January, July). To compare both current-corrected and observed trajectories with passive drift trajectories (or the path that the turtles would have followed if they had not performed active swimming and simply drifted with the currents), passive trajectories were simulated for each individual, starting from the start position of their trajectory and lasting the duration of their track. Simulated trajectories were created by single particles for each individual forced by surface currents from the PSY4V3 product. Daily mean surface current fields were also derived from the PSY4V3 product and averaged over the maximum duration of the tracks from each tracking period (January: 28 days, July: 10 days), to provide a visualization of mean current velocities for each map. Passive drift simulations and surface current velocity fields were provided by the Copernicus Marine Service (https://marine.copernicus.eu/).

Behavioral Clustering Analysis

To determine where discrete behaviors may be occurring for turtles along their tracks, a k-means clustering analysis was used to cluster turtle's daily data points

by their mean surface current velocities and a variety of movement metrics. K-means clustering algorithms use unsupervised machine learning to aggregate data into *k* number of clusters, where *k* is specified by the user and each data point is assigned to a cluster with the nearest mean or centroid (Hartigan and Wong 1979).

Movement metrics used to define clusters were derived from both observed and current-corrected trajectories. A metric termed "deviation" was calculated by taking the pairwise geographic distances ("fields" R package, Douglas et al. 2021) between daily locations along observed vs current-corrected trajectories, with large values representing locations where turtles' actual movements deviated strongly from their observed movements that have not been corrected for current influence.

Another metric, termed "delta displacement", was derived by taking the absolute difference in daily displacement values for current-corrected vs observed trajectories. Large values for this may indicate areas where observed trajectories for turtles are largely dictated by current drift (to result in their observed daily displacements to be larger than their current-corrected or actual displacements) or where turtles may be actively swimming to maintain their headings with current drift (to result in their current-corrected or actual daily displacements being larger than their observed displacements) (Gaspar et al. 2006). Finally, to capture both the mean daily (actual) swimming speed and turning angle of turtles along their tracks, another metric termed "persistence velocity" was found for each turtle location. This variable represents the tendency and magnitude for an individual to persist in a given direction (Gurarie et al. 2009) and can be derived by multiplying the cosine of the turning angle for a given location by the corresponding velocity, here the current-corrected

swimming velocities. As persistence velocity can have both positive and negative values but we were only interested in the magnitude (not direction) of the persistence velocity, the absolute value of each daily mean persistence velocity was found.

K-means clustering was performed on the current velocity and movement metrics values for all datapoints and dispersive individuals, using the "cluster" and "factoextra" R packages. All input variables were scaled to prevent different units from affecting the clustering algorithm. The optimal number of clusters, *k*, was determined using a combination of methods, including ecological intuition of the number of behavioral clusters expected, visual assessments, and the mean vote from three cluster evaluation methods: within cluster sums of squares ("elbow" method), average silhouette, and gap statistic (Pham et al 2005).

Multinomial Logistic Regression with Environmental Variables

To determine if behavioral clusters identified with the k-means clustering analysis had different probabilities of occurrence with key environmental and ontogenetic variables, a multinomial logistic regression was used.

Environmental variables included mean daily sea surface temperature and daily presence/absence of *Sargassum*; mean daily current velocity was also included to control for any confounding effects with predictor and response variables. To determine if behavioral clusters had ontogenetic differences, body weight was included as a covariate. Tracking period (January, July) was additionally included to determine differences in behavior with release location and timing.

All models were fit using the "nnet" R package (Venables and Ripley, 2002). Model selection was performed by starting with a full model and then iteratively

dropping variables until only a null model remained. Akaike information criterion values (AIC) were used to compare models, with the final model being chosen based on a minimized AIC value with respect to other models. Predicted probabilities for each observation and outcome (cluster) level were obtained to aid in model interpretation. Model validation and accuracy was assessed by splitting the data into training (80% of data) and test (20% of data) sets and creating a classification table.

Results

Tag Summaries

Of the N=30 turtles released in January, N=2 (Table 4.1) reported only one location, each of which were outside the boundaries of Grand Cayman island- these turtles were dropped from further analysis. Of the remaining turtles released in January with viable positions (N=28), upon release, all moved in a primarily southerly direction and returned to Grand Cayman Island, matching the direction of the surface drifter (Fig 4.1.a).

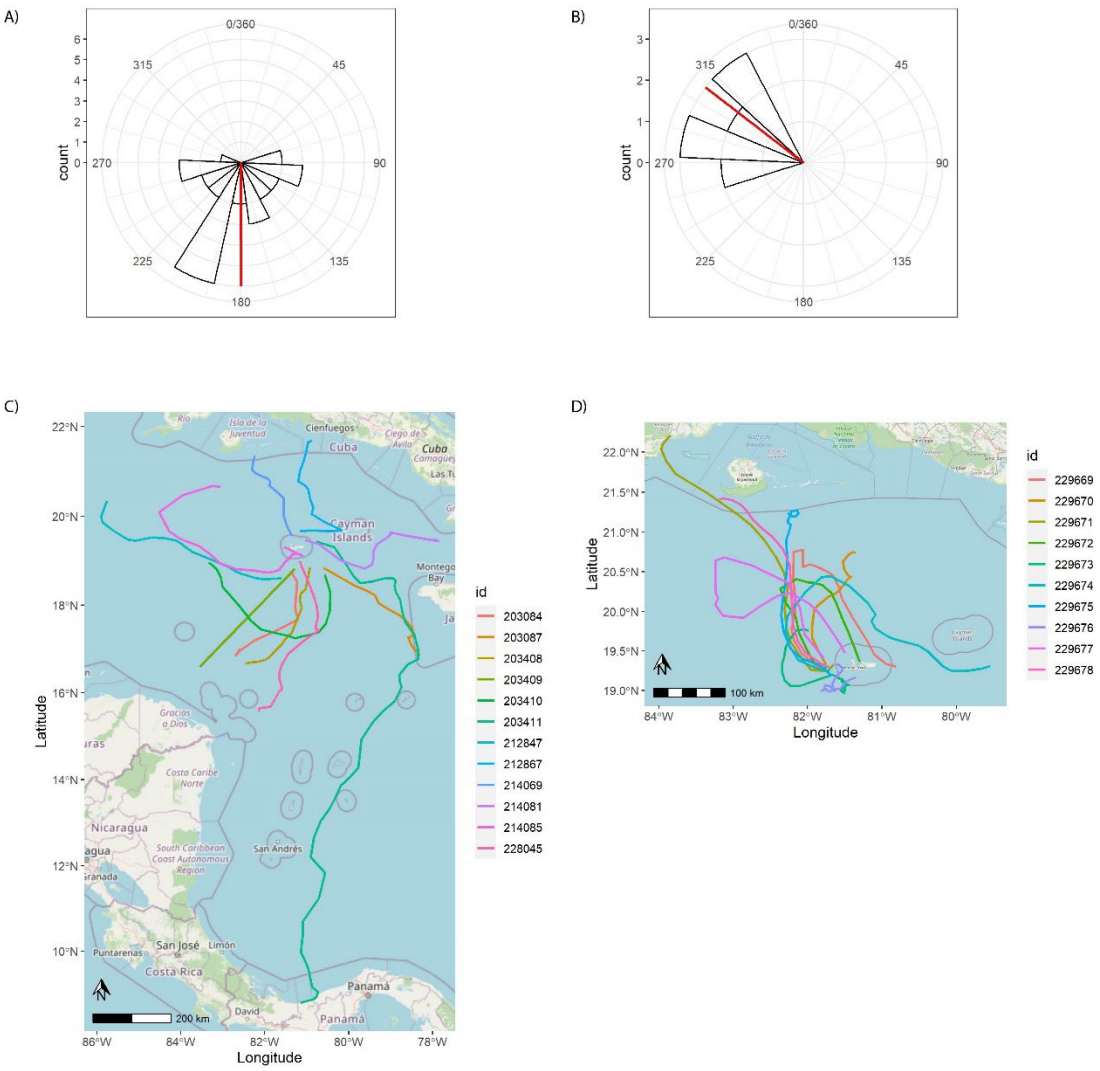

Fig 4.1. *Circular histogram of the initial bearing (first two reported locations) of a) turtles released in January (N=28) and b) turtles released in July (N=10), with the initial bearing of the surface drifter shown (red). Maps of c) tracks for dispersive turtles released in January (N=12) and d) tracks for dispersive turtles released in July (N=10), colored by individual.*

N=12 turtles then dispersed from the island in a radial fashion (Fig 4.1.c), whereas N=16 turtles remained within a 10 km buffer of the island for the duration of

their tags. The surface drifter washed up on Grand Cayman and was re-released on January 26, 2022.

Of the N=10 turtles released in July, all dispersed away from the island and had viable positions, with initial movements reflecting the direction of the surface drifter (Table 4.1, Fig 4.1.b, d).

Of the 22 dispersive turtles, there was an uneven distribution in the number of individuals represented from each age class (N=15 1-2 year olds, N=4 2-3 year olds, and N=3 3-4 olds) (Table 4.2).

Table 4.2. *Descriptive statistics for the daily locations of dispersive individuals (N=22), with columns for: tracking period (January, July), age class (1-2, 2-3, and 3-4 yrs), track duration (days, after positions near island were removed), mean 24-hour displacement (km), mean bearing (0-360 degrees from True North), days with Sargassum presence, mean sea surface temperature (deg C), mean surface current velocity (km/day) mean swimming speed (km/day), mean deviation (km, geographic difference between observed vs current-corrected trajectories), and straightness indices (SI) for observed and current-corrected trajectories.*

ID	Tracking Period	Age Class	Track Duration *days*	Mean 24-Hr Displacement *km*	Mean Bearing *0-360 deg*	Days with Sargassum	Mean Sea Surface Temp *deg C*	Mean Current Velocity *km/day*	Mean Swimming Speed *km/day*	Mean Deviation *km*	Observed SI	Current-Corrected SI
203084	Jan	1-2 Yrs	6	52 (± 39)	178	1	27 (± 0.20)	29 (± 10)	53 (± 22)	46 (± 44)	0.87	0.81
203408	Jan	1-2 Yrs	9	35 (± 9)	216	3	27 (± 0.16)	27 (± 9)	38 (± 17)	90 (± 81)	0.92	0.91
203410	Jan	1-2 Yrs	9	58 (± 22)	275	0	27 (± 0.17)	38 (± 12)	54 (± 38)	195 (± 114)	0.67	0.23
214069	Jan	1-2 Yrs	6	41 (± 13)	278	2	27 (± 0.36)	10 (± 5)	42 (± 10)	17 (± 10)	0.95	0.90
214085	Jan	1-2 Yrs	9	44 (± 33)	226	1	27 (± 0.36)	22 (± 9)	57 (± 29)	144 (± 94)	0.38	0.37
203087	Jan	2-3 Yrs	8	44 (± 26)	145	4	27 (± 0.23)	13 (± 5)	48 (± 42)	94 (± 43)	0.90	0.93
212847	Jan	2-3 Yrs	11	49 (± 10)	264	5	27 (± 0.33)	28 (± 10)	27 (± 12)	131 (± 84)	0.96	0.85
212867	Jan	2-3 Yrs	21	16 (± 22)	80	1	26 (± 0.37)	16 (± 7)	28 (± 23)	112 (± 59)	0.63	0.53
214081	Jan	2-3 Yrs	11	38 (± 28)	146	2	27 (± 0.38)	27 (± 13)	46 (± 32)	77 (± 49)	0.79	0.52
203409	Jan	3-4 Yrs	8	43 (± 34)	223	2	27 (± 0.19)	33 (± 10)	58 (± 23)	56 (± 30)	0.98	0.74
203411	Jan	3-4 Yrs	22	65 (± 27)	172	9	27 (± 0.24)	27 (± 12)	60 (± 22)	166 (± 111)	0.84	0.85
228045	Jan	3-4 Yrs	16	29 (± 30)	211	4	27 (± 0.13)	23 (± 14)	38 (± 33)	153 (± 94)	0.87	0.88
229669	Jul	1-2 Yrs	10	37 (± 12)	170	6	29 (± 0.13)	18 (± 9)	18 (± 15)	65 (± 34)	0.25	0.45
229670	Jul	1-2 Yrs	10	18 (± 14)	97	4	29 (± 0.10)	10 (± 5)	29 (± 11)	40 (± 22)	0.85	0.69
229671	Jul	1-2 Yrs	10	41 (± 12)	295	6	29 (± 0.41)	26 (± 7)	35 (± 16)	111 (± 71)	0.91	0.83
229672	Jul	1-2 Yrs	9	31 (± 14)	183	4	29 (± 0.13)	17 (± 7)	23 (± 14)	63 (± 37)	0.17	0.50
229673	Jul	1-2 Yrs	9	22 (± 13)	193	1	29 (± 0.19)	20 (± 4)	42 (± 10)	84 (± 52)	0.43	0.41
229674	Jul	1-2 Yrs	10	43 (± 12)	141	7	29 (± 0.17)	16 (± 5)	22 (± 15)	35 (± 16)	0.52	0.65
229675	Jul	1-2 Yrs	10	27 (± 18)	206	9	29 (± 0.11)	15 (± 4)	25 (± 13)	65 (± 41)	0.81	0.52
229676	Jul	1-2 Yrs	10	11 (± 5)	143	6	29 (± 0.15)	19 (± 8)	25 (± 11)	97 (± 53)	0.29	0.86
229677	Jul	1-2 Yrs	10	47 (± 23)	191	3	29 (± 0.23)	22 (± 9)	44 (± 23)	50 (± 23)	0.07	0.24
229678	Jul	1-2 Yrs	7	38 (± 13)	319	5	29 (± 0.20)	21 (± 6)	24 (± 13)	65 (± 43)	0.93	0.92

Dispersive turtles reported an average of 12.6 positions per day (range across individuals: 2.6 – 17.4 mean positions per day), whereas turtles remaining near the island ("residential") reported an average of 4.2 positions per day (range across individuals: 1.0 - 9.1 mean positions per day) (Table 4.1).

Of the tag types tested for turtles released in January, the solar tags had a longer mean tracking duration of 15.2 days (±8.0 SD) and 10.6 days (±0.9 SD), versus 8.4 days (± 2.7 SD) for the battery-powered tags (Fig A4.5). Of those with battery-powered tags (all released in January), 5 individuals dispersed from the vicinity of the island (mean tracking duration: 9.2 days ± 1.7 SD) and 9 individuals remained residential around the island for the duration of their tags (mean tracking duration: 7.4 days ± 3.4 SD). Of those with solar tags released in January, 7 individuals were dispersive (mean tracking duration: 15.1 days ± 7.5) and 7 residential (mean tracking duration: 15.3 days ± 9.1). Turtles released in July with solar tags were all dispersive (N=10, mean tracking duration: 10.6 days ± 0.9).

Solar tags also reported a higher average number (40.1 ± 17.1 SD for January release, 130.0 ± 30.4 SD for July release) of positions per day compared to battery-powered tags (12.2 ± 6.0 SD) (Fig A4.5). For adhesives tested with the tags (on an equal number of 1-2 years olds released in January), turtles having tags with Fast Cure adhesives had a longer mean tracking duration of 14.4 days (± 1.8 SD) compared to 8.7 days (± 1.8 SD) for those with epoxy adhesive (Fig A4.5). Of the 1-2 year olds with fast cure attachments released in January (N=5), 3 turtles were dispersive (mean tracking duration: 9.3 days ± 1.3) and 2 were residential (mean tracking duration: 19.9 days ± 7.4). Of the 1-2 year olds with epoxy tags, 2 turtles were dispersive (mean tracking duration: 9.3 days ± 1.3 SD) and 3 were residential (mean tracking duration: 6.1 days ± 1.2 SD). Fast cure attachment types for 1-2 year olds released in January also had a slightly higher average number of positions

reported per day (19.2 ± 10.5 SD) compared to epoxy tags (14.4 ± 7.1 SD) (Fig A4.5).

Comparison of Current-Corrected, Observed, and Simulated Passive Drift Trajectories

Circular histograms showed differences between tracking periods (January, July) in the distribution and circular means of daily bearings (from true north) for observed and current-correct trajectories (Fig 4.2.a-b).

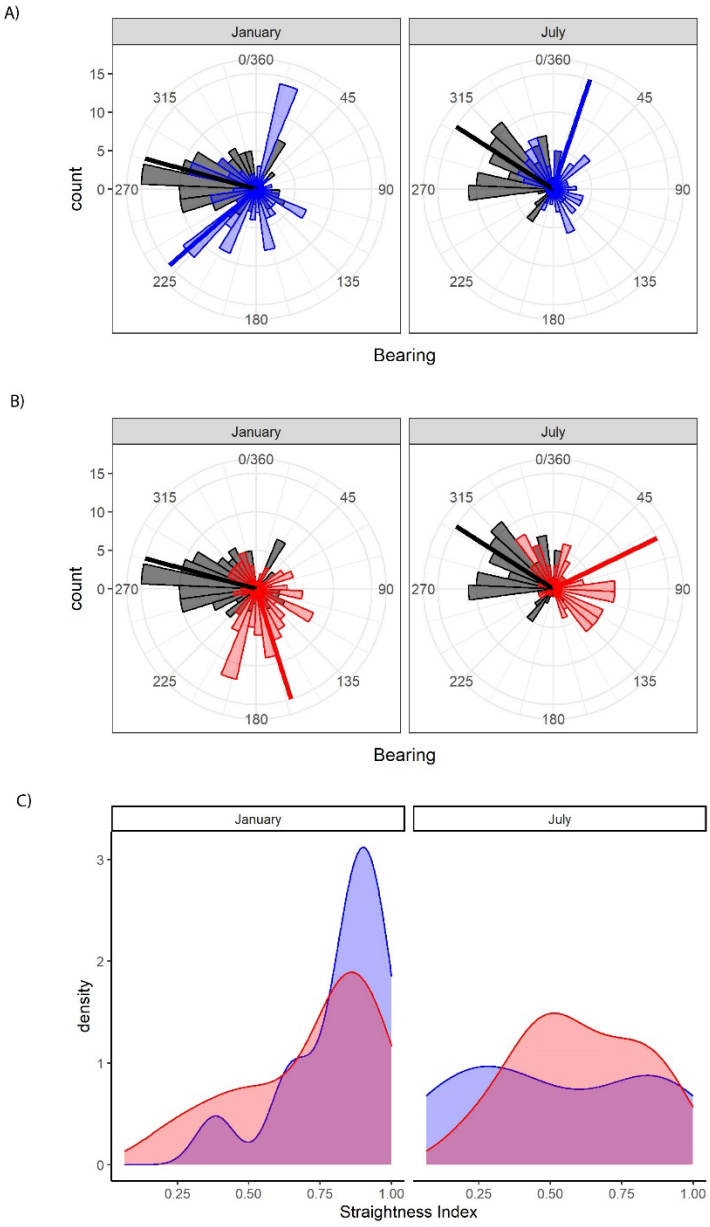

Fig 4.2. *Circular histograms of overall mean daily surface current bearings (black) versus a) overall observed track (blue) bearings and b) current-corrected track (red) bearings, in 0-360 deg from True North and split by tracking period (January, July). Thick, colored lines show circular means for each group. c) Density histograms show distributions of straightness indices for observed (blue) vs current-corrected (red) tracks for January and July tracking periods.*

In January, observed tracks had a more similar circular mean bearing to current-corrected tracks (observed: 229 deg ± 103 SD, current-corrected: 163 deg ± 98 SD) (Fig 4.2.a). In July, observed tracks had a lower mean bearing compared to current-corrected tracks (observed: 19 deg ± 99 SD, current-corrected: 64 deg ± 85 SD) (Fig 4.2.b). In both January and July, larger differences in circular mean bearings were seen for current-corrected tracks vs surface currents than for observed tracks vs surface currents (Fig 4.2.b).

Results showed that tracking periods (January, July) also had differences in SI indices (Fig 4.2.c). In January, both observed and current-corrected trajectories had high SI's across individuals, with observed trajectories having a higher mean SI than current-corrected trajectories (observed: 0.81 ± 0.18, current-corrected: 0.71 ± 0.24) (Fig 4.2.c). July turtles had markedly lower SI's compared to January turtles, with observed trajectories (in contrast to January) having a lower mean SI across individuals compared to current-corrected trajectories (observed: 0.52 ± 0.33, current-corrected: 0.60 ± 0.22) (Fig 4.2.c). Variability was also seen on an individual level, with some individuals having similar SI's between their observed and current-corrected trajectories and some either noticeably larger or smaller SI's for their observed vs current-corrected trajectories (Table 4.2).

Maps of observed, current-corrected, and passive-drift trajectories for each individual further reflected these differences (Fig 4.3).

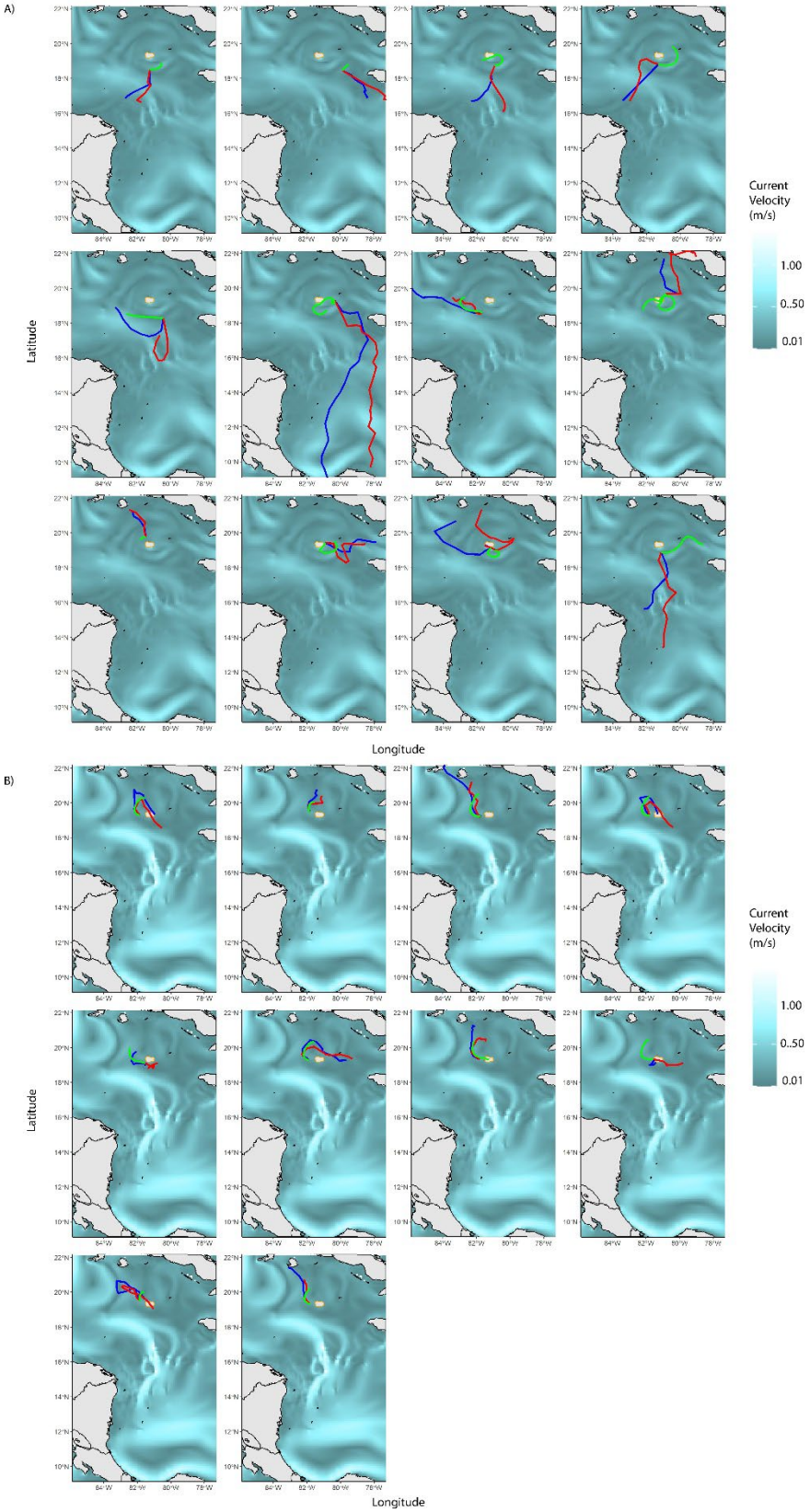
A)
Latitude
Longitude
Current Velocity (m/s)
1.00
0..50
0.01
B)
Latitude
Longitude
Current Velocity (m/s)
1.00
0..50
0.01

Fig 4.3. *Maps of mean surface current fields and observed (blue), current-corrected (red), and passive drift (green) trajectories for turtles tracking in a) January (N=12) and b) July (N=10). Simulated trajectories were created by single particles for each individual forced by surface currents from the PSY4V3 product provided by the Operational Mercator global ocean analysis and forecast system (DOI: https://doi.org/10.48670/moi-00016). Daily mean surface current fields were also derived from the PSY4V3 product and averaged over the maximum duration of the tracks from each tracking period (January: 28 days, July: 10 days). Passive drift simulations and surface current velocity fields were provided by the Copernicus Marine Service (https://marine.copernicus.eu/).*

Simulated trajectories following a completely passive drift scenario for each individual for the most part had large deviations from observed and current-corrected trajectories. However, one individual in January (Id 212847, Fig 4.3.a) and multiple individuals in July (Ids 229669, 229670, 229671, 229672, 229674, 229675, 229678, Fig 4.3.b) had current-corrected and observed trajectories that reflected simulated passive-drift paths, especially in early steps of the tracks. Between observed and current-corrected tracks, marked deviations were observed for some individuals, especially in January and for move steps further along the tracks.

Behavioral Clustering Analysis

Four distinct behavioral clusters were identified with the k-means clustering analysis, based on the three movement metrics (deviation, delta displacement, persistence velocity) and current velocity for all daily data points from dispersive individuals (N=22) (Fig 4.4).

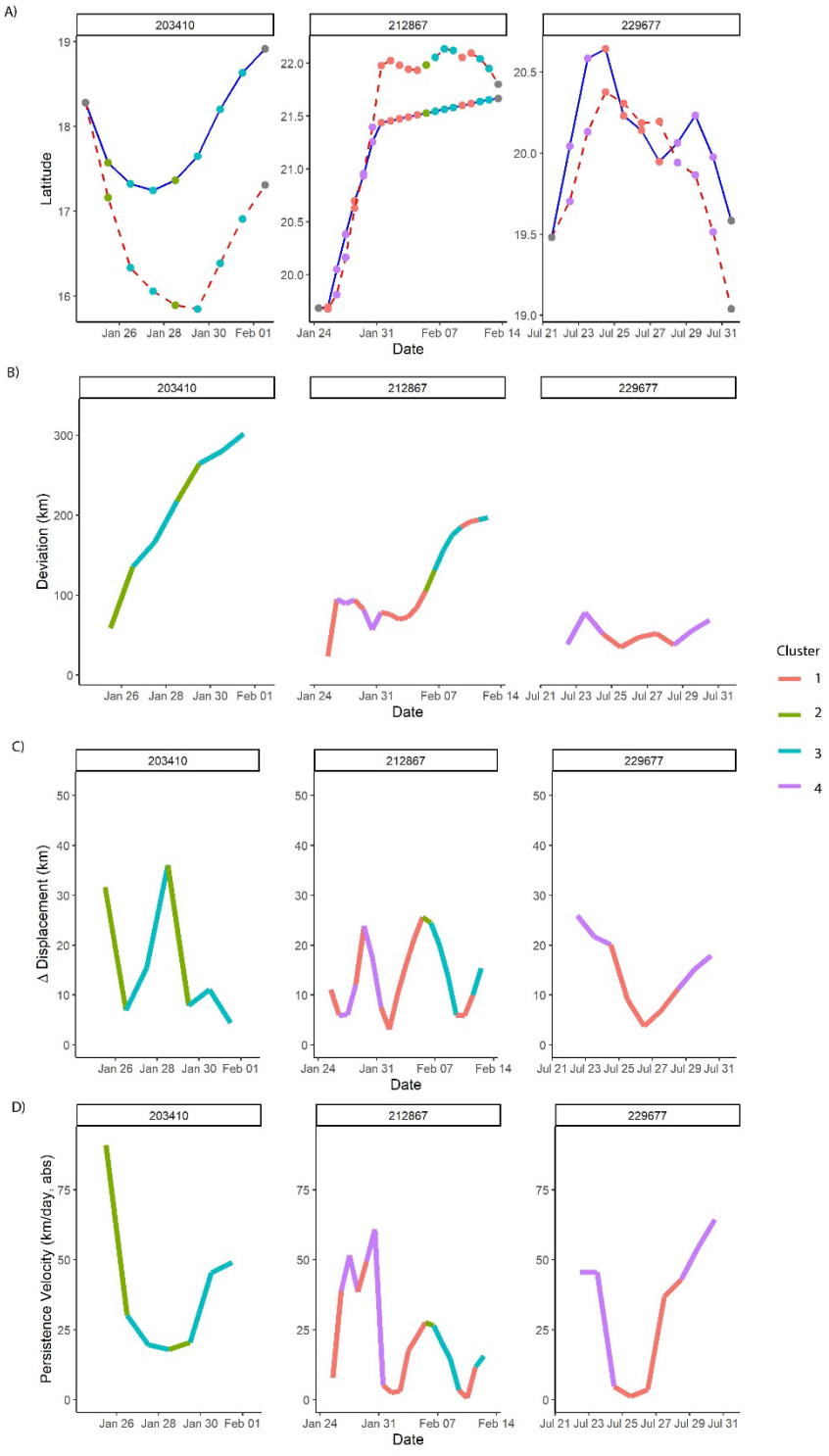

Fig 4.4. *Plots showing individual examples of the results of a k-means clustering analysis with k=4 clusters. a) Observed latitudes over time, with points colored by cluster. b) Deviation (km, geographic pairwise distance between observed*

and current-corrected trajectories), c) delta displacement (km, absolute difference in daily displacement for observed vs. current corrected trajectories), and d) persistence velocity (km/day, tendency to persist in a given direction) movement metrics over time with segments colored by cluster membership.

Overall, the majority of points (52%) were classified as cluster 1, followed by relatively similar proportions of clusters 3 (18%), and 4 (19%). Cluster 2 had the lowest number of points assigned to it (10%). Between the tracking periods, January had closer proportions of all four clusters, with clusters 1 and 3 having the highest proportions (cluster 1: 33%, cluster 2: 15%, cluster 3: 29%, cluster 4: 22%), whereas July was dominated by cluster 1 followed by cluster 4 (cluster 1: 79%, cluster 2: 4%, cluster 3: 2%, cluster 4: 15%).

Descriptive statistics and boxplots of clusters showed good separation amongst the clusters for variables (Table 4.3, Fig 4.5.a-d).

Table 4.3. *Counts (N) and descriptive statistics (mean and standard deviation) for behavioral clusters (N=4) identified with the k-means clustering analysis, applied to data for dispersive individuals (202 observations, N=22 individuals). Variables used to identify clusters included daily measurements of: surface current velocity (km/day), persistence velocity (km/day, tendency to persist in a given direction), deviation (geographic pairwise distances between observed and current corrected trajectories), and delta displacement (absolute difference in daily displacement for observed vs current-corrected trajectories).*

Cluster	N	Current Velocity *km/day*	Persistence Velocity *km/day*	Deviation *km*	Delta Displacement *km*
1	106	16 (± 7)	18 (± 12)	71 (± 38)	9 (± 6)
2	21	41 (± 8)	40 (± 26)	118 (± 84)	36 (± 7)
3	36	25 (± 11)	29 (± 15)	220 (± 57)	14 (± 7)
4	39	25 (± 10)	53 (± 15)	72 (± 37)	11 (± 7)

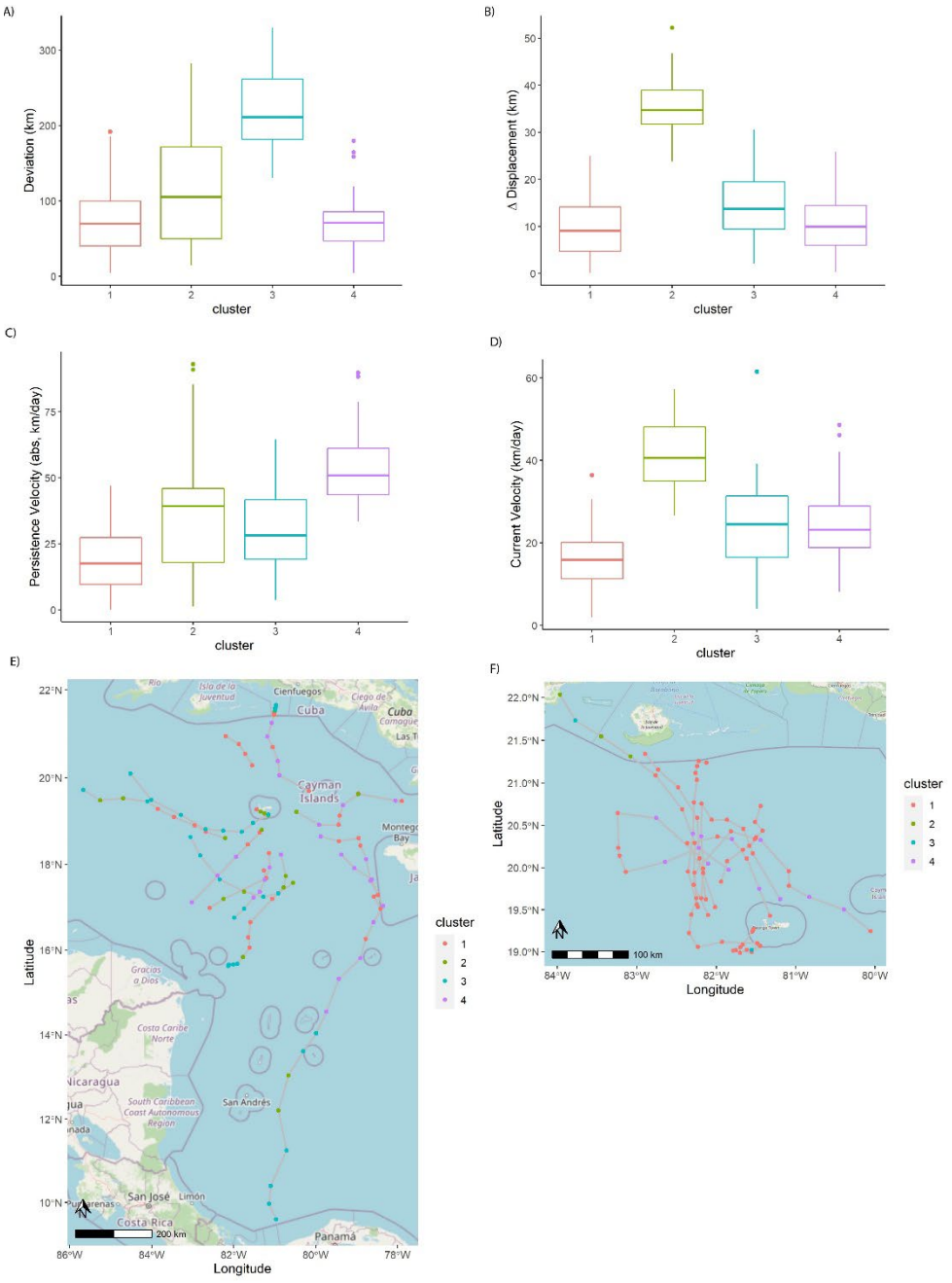

Fig 4.5. *Results of a k-means clustering analysis with k=4 clusters. Boxplots illustrate differences between clusters in a) deviation (km, geographic pairwise distance between observed and current-corrected trajectories) b) delta displacement (km, absolute difference in daily displacement for observed vs. current corrected trajectories) c) persistence velocity (km/day, tendency to persist in a given direction) and d) current velocity (km/day). Maps of daily observed locations for turtles colored by cluster membership for e) July (N=12 individuals) and f) January (N=10 individuals).*

Cluster 1 was defined by low mean current (16 ± 7 km/day) and persistence velocities (18 ± 12 km/day), low mean deviations (71 ± 38 km), and low mean delta displacements (9 ± 6 km). Cluster 2, in contrast, had high mean current velocities (41 ± 8 km/day), high mean persistence velocities (40 ± 26 km/day), high deviations (118 ± 84 km), and high delta displacements (36 ± 7 km). Clusters 3 and 4 had similar mean (intermediate) current velocities (cluster 3: 25 ± 11 km/day, cluster 4: 25 ± 10 km/day) and delta displacements (cluster 3: 14 ± 7 km, cluster 4: 11 ± 7 km), but cluster 4 was defined by very high persistence velocities (cluster 3: 29 ± 15 km/day, cluster 4: 53 ± 15 km/day), while cluster 3 had very high deviations (cluster 3: 220 ± 57 km, cluster 4: 72 ± 37 km).

Maps of turtle observed daily positions colored by cluster membership additionally showed good spatial separation and differences between the tracking periods (Fig 4.5.e-f). Overall, clusters 2 and 4 tended to occur towards the end of tracks and closer to land (Central America, Cuba), whereas clusters 1 and 3 occurred more in early/median portions of tracks and closer to the Cayman Islands. Between

the tracking periods, January had a good mixture of cluster types (Fig 4.5.e), whereas July was almost entirely clusters 1 and 4 (Fig 4.5.f).

Multinomial Logistic Regression with Environmental Variables

Model selection resulted in a final chosen model predicting the probability of a cluster being one of the four behavioral clusters identified with the k-means clustering analysis as a function of *Sargassum* (presence/absence), surface current velocity, and tracking period (January, July).

A likelihood ratio chi-square test showed that the model fit significantly better than the null model ($X^2 = 152$, df = 9, p-value = < 0.001). Chi-Squared tests were used to derive X^2-test and two-tailed p-values; all variables had small p-values (< 0.05) except *Sargassum*, which was only significant in comparing cluster 3 to cluster 1 (Table 4.4).

Table 4.4. *Model results for a multinomial logistic regression predicting the probability of clusters belonging to four different behavioral clusters (1, 2, 3, 4, with 1 being the reference level) found with a k-means clustering analysis and as a function of Sargassum (presence/absence), surface current velocity (km/day), and tracking period (January, July). A likelihood ratio chi-square test showed that the model fit significantly better than the null model (X^2=152 , df=9, p-value=<0.001). Chi-Squared tests were used to derive X^2-test and two-tailed p-values. A classification table found the model to have an overall classification efficiency of 75%.*

Explanatory Variable/ Parameter	Estimate	Std Error	X^2-value	Odds Ratio	df	p-value
cluster 2 (ref: cluster 1)						
Intercept	-9.31	1.63	-5.70	9.05e-05	1	1.19e-08
Sargassum, presence (ref: absence)	-0.54	0.81	-0.66	0.58	1	0.51
Surface current velocity (km/day)	0.31	0.05	6.50	1.36	1	8.26e-11
Tracking period, July (ref: January)	-0.64	0.88	-0.72	0.53	1	4.71e-01
cluster 3 (ref: cluster 1)						
Intercept	-2.32	0.64	-3.59	9.86e-02	1	3.25e-04
Sargassum, presence (ref: absence)	-1.23	0.59	-2.08	0.29	1	0.04
Surface current velocity (km/day)	0.12	0.03	4.23	1.13	1	2.29e-05
Tracking period, July (ref: January)	-0.92	0.45	-3.90	0.05	1	9.53e-05
cluster 4 (ref: cluster 1)						
Intercept	-3.12	0.67	-4.63	4.42e-02	1	3.62e-06
Sargassum, presence (ref: absence)	-0.59	0.59	-1.28	0.56	1	0.20
Surface current velocity (km/day)	0.14	0.03	4.86	1.15	1	1.16e-06
Tracking period, July (ref: January)	-0.92	0.45	-2.05	0.40	1	4.02e-02

A classification table found the model to have decent efficiency, with about 75% of the clusters from the test set being correctly categorized by the trained model.

Predicted probabilities for observed data showed that cluster 3 had a high probability of occurring in July, with *Sargassum*, and with lower current velocities (Fig 4.6).

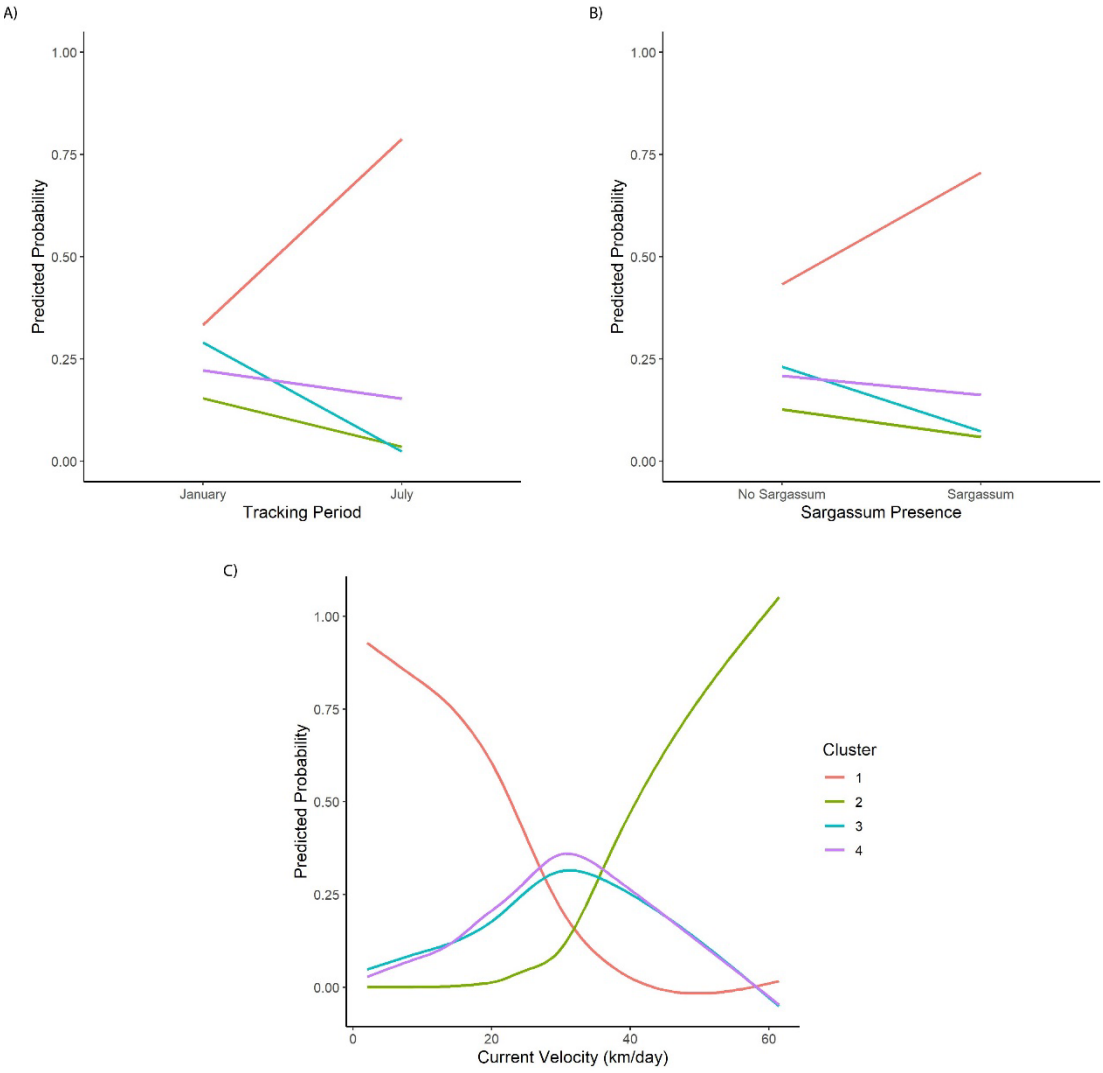

Fig 4.6. *Predicted probabilities from a fitted multinomial regression model for the probability of clusters belonging to one of four clusters identified with a k-means*

clustering analysis and as a function of predictor variables for: a) tracking period (January, July), b) Sargassum (presence, absence), and c) current velocity (km/day).

Clusters 3 and 4 were likely to occur with intermediate current velocities, but cluster 4 had a higher probability of occurring in July and with *Sargassum* compared to cluster 3 (Fig 4.6). Cluster 2 had high probabilities of occurring with high current velocities and low probabilities of occurring in July or with *Sargassum* (Fig 4.6).

Discussion

This work represents the first large sample size satellite tagging effort of juvenile green turtles in the Caribbean. Our results highlight the significance of surface currents for dispersal and specifically, release site and timing for captive bred turtles. Despite tagging multiple age classes of juvenile turtles, our statistical model did not detect significant ontogenetic differences in dispersal behavior. Rather, behavioral differences amongst turtles seemed largely to be a result of environmental variables (surface currents, *Sargassum* algae presence), where and when the turtles were released, and potentially individual drives to recruit to nearshore developmental habitats. Our results have important implications for head starting initiatives for this and other turtle species reared in captivity, as release site and timing in our study not only resulted in different behavioral patterns and dispersal trajectories but may also affect long-term survival of turtles if they recruit to habitats where serious threats (e.g., bycatch by fisheries) are more acute. Finally, our results provide an approach to understanding juvenile movement ecology of a cryptic species that could be modified for a variety of other taxa with migratory juvenile life stages, as these life stages are often understudied in movement ecology.

Marked differences were seen in the dispersal trajectories of turtles released at different sites and times of year. The majority of turtles (N=30) were released in January north of the Cayman Islands, whereas a smaller subset of turtles (N=10) were released in July west and somewhat south of the Islands. Simultaneous releases of surface drifters showed that turtles in both time periods initially followed the direction of surface currents (Fig 4.2.a-b). As currents during the release in January were moving in a southerly direction back towards Grand Cayman, all January turtles returned to the vicinity of the island, with a portion (N=12) eventually leaving the island after a time period of ~ 4.5 – 19.5 days. In contrast, surface currents in July near the release site were going in a north-west direction, resulting in all turtles heading towards waters north and north-west of the island. Turtles that eventually dispersed away from the island in January all seemed to leave from different and random locations around the island and overall, had very straight paths radiating out from the island (Fig 4.2.c-d, Table 4.2). Turtles released in July, however, seemed largely to converge on the direction of the currents, resulting in similar paths that were less straight than those in January and led into waters north of the island (Fig 4.4.b, Table 4.2). Although some (N=4) of these turtles had trajectories that would eventually take them to the southern coastal shelf waters off of Cuba, an equal number of turtles (N=4) had trajectories returning to waters adjacent to the Cayman Islands (Fig 4.4.b). The differences between January and July releases are evident of the role of favorable conditions (here, surface currents) near the release site to aid in dispersal of turtles away from the release point (Shillinger et al 2012b).

The eventual return of some of the July turtles to the vicinity of the Islands in contrast with the directed movements of all of the dispersive January turtles away from the Islands towards surrounding land masses (e.g., Cuba, Central America) may also be evidence of the effect of "soft" vs. "hard" releases for turtles. Soft vs. hard release strategies for releases of captive animals are common methods in terrestrial studies, where "soft" releases allow animals to acclimate to their surroundings and can be more successful in contrast to "hard" releases, which have no acclimatization period (Resende et al 2021). The effects of hard vs soft releases for captive-raised aquatic and marine animals are not as well studied (Resende et al 2021), but are probably best known for marine mammals (Wells et al 1998, Mazzoil et al 2008, Adimey et al 2016), where "sea pens" or enclosed areas in their natural habitat can be used to acclimate the animals to the ocean environment before a full release, potentially minimizing any harmful effects of sudden release (e.g., startling, confusion, and an inability find food, Resende et al 2021). For our study, January turtles appeared to have somewhat of a "soft" release, where ocean currents led them back to the island and they spent time familiarizing themselves with their environment and possibly foraging before leaving at their leisure to migrate to more favorable habitats in surrounding geographic areas; the downside of this, of course, was that only 12 of the original 28 turtles with active tags were recorded to leave the island. All of the turtles may have eventually left the island and recording this may not have been possible due to the rest of the turtles prematurely knocking off their tags on hard surfaces around the island (Hays et al 2007) or the tags themselves not lasting long enough to record eventual dispersal (the longest duration was 32.5 days,

Table 4.1). The potential benefits of a "soft" release for turtles (e.g., releasing turtles in current conditions that will return them to the home of the release and allow them to acclimate at their pace) may be outweighed by this high tag loss rate. However, for turtles released in July with more of a "hard" release, into currents that initially advected them away from the island into unfamiliar areas, a good proportion seemed to be caught up in an area characterized by a clockwise circulation called the "Cuban Vortex", an expansion of the Loop Current (Androulidakis et al 2021) that may have influenced them to have less directed movements towards nearby, productive offshore and coastal recruitment areas of the Cuban shelf. Given that turtles in both tracking periods initially responded strongly to the direction of the currents, conservation programs aiming to optimize tracking durations of released, post-captive individuals could potentially use long-term passive particle simulations set at different times of year to determine the best site and time of year for release (Shillinger et al 2012b, Gaspar et al 2012).

Turtles tracked in either January or July additionally had significant differences in their movement behaviors and relationships with environmental and physical variables that were not explained by differences in ontogeny. Three age classes of juvenile turtles were released in January (1-2, 2-3, and 3-4 years, CCL range: 35-65 cm) and one age class (1-2 years, CCL range: 36-40 cm) in July. Although the pelagic developmental stage for green turtles is thought to last on average 3 years (but with a range of 1-7 years, Reich et al 2007, Goshe et al. 2010), it is common for animals raised in captivity to have larger body sizes than their wild counterparts (Haskell et al 1996, Vander Haegan et al 2009, Bona et al 2012) and the

turtles in our study were all within the size range known for young juvenile green turtles that are recruiting to nearshore, benthic developmental habitats (Moncada et al 2006, Reich et al 2007, Meylan et al 2011). Indeed, the majority of dispersive turtles in our study (N=15, CCL range: 35-65 cm, Fig 4.5) seemed to have trajectories towards coastal habitats around the Caribbean. Results from previous mark-recapture of juveniles and adults combined with small satellite tagging studies of adults have shown that turtles will migrate to areas off of Cuba, Nicaragua, and Honduras, likely for high quality foraging and developmental habitat (Bell et al 2005, Moncada et al 2006, Blumenthal et al 2006). However, turtles in our study were also in size ranges close to where a transition between pelagic and nearshore developmental habitats is predicted to occur (Reich et al 2007) and the high proportion of positions classified as having behaviors associated with foraging like movements (e.g., low persistence velocities, cluster 1, Fig 4.5, Table 4.3) and a high probability of *Sargassum* presence (Fig 4.6.b, Table 4.4) may indicate that turtles are also foraging along the dispersal path, as floating patches of *Sargassum* algae are considered a key foraging resource for small juvenile green turtles in the pelagic stage (Witherington et al 2012). The similarity in sizes but significantly higher occurrence of these foraging-like behaviors for July versus January turtles in our study seems to rule out ontogeny as the driver of these differences; instead, turtles in July may have dispersed into higher quality areas for *Sargassum* based on current advection near the release location and the time of year (Fig A4.4). They also may have been more reliant on encountering *Sargassum* patches to restore their energy supplies, as January turtles first returned to the island to likely forage around its vicinity before dispersing on directed paths into pelagic

waters. Indeed, it took a minimum of 7 days for the individual with the more directed path in July (ID 229678, Fig 4.4.b, Table 4.2) to reach productive shelf areas of Cuba (Moncada et al 2006), a time period which if fasted completely, would likely result in drastically lowered metabolic rates that would hinder dispersal (Price et al 2013).

Although turtle movements were certainly impacted by current velocities, turtles in both tracking periods (January, July) demonstrated a directed drive to their movements independent of current influence. Trajectories for most turtles that had been corrected for current drift influences, reflecting their "true" movements (Gaspar et al 2006), tended to deviate from observed paths over time (e.g., behavioral cluster 3, Figures 1, 5, Table 4.3). These deviations might indicate an increased navigational sense as turtles near land masses and coastal foraging areas where a combination of possible cues (e.g., olfactory, auditory, chemical, visual, waves) may help direct them nearshore and in opposition to current drift (Hays et al 2003, Lohmann et al 2008). For the July turtles that returned "home" (Ids 229669, 229672, 229676, Fig 4.4.b), this brings up the possibility of homing or natal imprinting for captive-raised and/or juvenile turtles. For two of these individuals (Ids 229669, 229672), their observed and current-corrected trajectories had low deviations and differences in displacements (behavior clusters 1 and 4, Fig 4.5), potentially indicating that turtles were simply swimming with the currents that eventually brought them within the vicinity of the island. However, for one of these turtles (Id 229676), both its observed and current-corrected trajectory differed largely from its simulated, passive track; additionally, its current-corrected track was noticeably straight (directed east), with large deviations from the observed path (Fig 4.4.b, Table 4.2). This turtle, despite current influences,

seems to be the only turtle tracked in July that almost immediately diverged from the direction of the currents and turned around to stay near "home". This could be a "confusion" affect from the July hard release and/or the turtle may have found food (e.g., near *Sargassum*, Fig A4.4) and needed to swim in a directed manner to remain in the resource patch in the face of current drift (Gaspar et al 2006, Kobayashi et al 2014, Mansfield et al 2021). We were not able to test for relationships of turtle movements and behaviors with the magnetic field but we cannot rule out this possibility either, as previous laboratory studies have found evidence that turtles may use locational markers of the geomagnetic field (inclination and intensity) to imprint on and return to natal and foraging sites (Girard et al 2006, Luschi et al 2007, Lohmann and Lohmann 2019).

The variability in turtle movement behaviors was further seen with individuals that had large differences in daily displacement values for their observed vs. current-corrected trajectories. Behaviors associated with these large differences in displacement (e.g., behavioral cluster 2, Figures 4.1, 4.5, Table 4.3) had significantly higher probabilities of occurrence with high current velocities (Fig 4.6.c, Table 4.4). These behaviors may demonstrate turtles using current drift to "boost" their dispersal and potentially save energy reserves as they perform positive rheotaxis (swimming into currents) and have slower swim speeds as they allow themselves to be largely advected with the currents (Gaspar et al 2006, Kobayashi et al 2014). This is likely the case for individuals in our study where their observed displacements far outweighed their current-corrected displacements (Ids 212847, 229671, 229678, Fig 4.4). In contrast, individuals with larger current-corrected displacements compared to

observed (Ids 212867, 228045, Figures 4.1, 4.4), as well as large deviation and persistence velocity values, may be using oriented and elevated swimming speeds to overcome or correct for drift in the face of high current velocities and maintain their desired heading (Gaspar et al 2006, Kobayashi et al 2014, Putman and Mansfield 2015).

The results of our study demonstrate not only the importance of release site location and timing for tracking studies of captive-raised turtles, but also support that post-captive ("headstarted") individuals have the ability to use directed movements and a variety of behaviors to navigate through an unknown environment to potential foraging and developmental recruitment areas. This finding is important for this species and population of green sea turtle, which has a wild nesting population that is slowly recovering in the Cayman Islands from decades of overhunting (Blumenthal et al 2021) and is also a demonstration of how similar headstarting studies could be useful for other, more critically endangered species, such as the Eastern Pacific leatherback turtle (Abrego et al 2020). Headstarting initiatives, where animals are born or hatched in captivity and raised to an age where their larger body sizes make natural mortality less likely, have often been deemed unsuccessful ways of increasing sea turtle survivorship (Frazer 1992, Heppell et al 1996). However, these criticisms may partly be due to a lack of monitoring and/or tracking efforts for most headstarting projects that can support that there is long-term success (Burke 2015). Our study addresses one of the key concerns about headstarting programs, that individuals will not be able to effectively navigate, forage, and recruit to important habitats due to being raised in a synthetic environment (Protchard 1981). Indeed,

individuals in our study demonstrated the ability to disperse independently towards key habitat areas using a diversity of dispersal paths and behaviors. For January turtles especially, this resulted in individual spatial separation in foraging and developmental habitats that may provide resilience to the population in the face of high anthropogenic mortalities or inter/intra-specific competition for resources in these areas. Longer term monitoring, perhaps with the use of passive tags or mark-recapture efforts, is needed however to determine if individuals released in our study meet the criteria established for "successful" headstarting programs (Protchard 1981). These include the ability to fully recruit to nearshore, developmental habitats and mix with conspecifics; survive long term; and eventually return to nest at their natal site, although recent research of past releases of post-captive neonate, juvenile, and adult Caymanian green turtles support that they certainly have the capacity and potential to do so (Bell et al 2005, Moncada et al 2006, Blumenthal et al 2006, 2021).

Longer tracking studies with even larger sample sizes and more age classes (e.g., neonates, adults) are also needed to quantify spatial overlap and potentially mitigate harmful interactions between fisheries and turtles, both at sea and in nearshore foraging and internesting habitats. Although the small and novel satellite tags we used in this study unfortunately did not last long enough to determine spatial use of nearshore areas by our turtles, their duration was long enough to predict the final destination of the dispersive turtles, which included nearshore and shelf areas of Cuba, Grand Cayman, and Central America (likely, the Caribbean side of Honduras, Costa Rica, and Panama). All of these regions host intense fishing efforts where not only are turtles likely to be caught incidentally as bycatch but also intentionally

hunted for human consumption (Moncada et al 2006, Bell et al 2006, Blumenthal et al 2021). Although repopulation and mass headstarting efforts of decimated local turtle populations (such as by the Cayman Turtle Centre on Grand Cayman) have been successful in starting to restore local and wild nesting populations (Bell et al 2005, Blumenthal et al 2021), predictive management tools that combine near real-time movement and habitat use data with threat data (termed "dynamic management", Lewison et al 2015, Welch et al 2018) could be effective ways of managing bycatch and illegal hunting both at sea and in nearshore, shelf areas.

The methods we used in this study to determine ecologically significant, movement-based behaviors could be useful for future movement ecology studies of this and other species. We used the combination of a k-means clustering analysis with a binomial statistical regression to determine key behaviors and their probability of occurrence with environmental and biological variables, an approach that may be applicable to other studies that are also limited by shorter duration biotelemetry tracks and a coarser resolution to observations or environmental data. Future and longer tracking studies of this population could benefit from more rigorous and complex behavior parsing methods, such as discrete (Jonsen et al 2005, 2007, 2013) or continuous (Jonsen et al 2019, 2020) time state space movement models that can simultaneously account for hierarchical structures to the data, temporal autocorrelation, locational errors, and relationships with environmental variables. Studies of other migratory species that move through a fluid environment (e.g., other aquatic or aerial species) could also take advantage of our methods comparing simulated passive drift trajectories with observed and drift-corrected trajectories to

infer “true” movements and the effects of the fluid medium on their dispersal. These methods could be taken further by using Individual Based Models (IBMs) to model long-term dispersal and survival probabilities using both environmental variables (e.g., ocean currents, sea surface temperature) and habitat-directed movements. Models could both be parameterized by and compared to observations from empirical tracking studies (Briscoe et al 2016, Hays et al 2020). Examples of IBM’s such as this already exist for sea turtles (termed STAMM or “Sea Turtle Active Movement Model”) and although they have been successfully applied to other species (e.g., leatherbacks, Gaspar and Lalire 2017, Lalire and Gaspar 2019), their application to Caribbean green turtles could be useful in lieu of expensive tracking studies and limited availability of multiple age classes of turtles for releases. This approach would have the added benefit of gaining understanding of hatchling dispersal and habitat use in the pelagic developmental stage that we were unable to address with our study.

Overall, this work represents, to our knowledge, the first large-sample size biotelemetry tracking effort of green sea turtles across multiple juvenile age classes. Our use of behavioral classification methods and statistical models allowed us to determine ecologically important behaviors that will inform ongoing conservation efforts and future tracking studies for this population. Additionally, our methodology and findings have application to biotelemetry studies for post-captive (headstarted) and/or juvenile movements of other species, as these studies are still underrepresented in the field of movement ecology.

References

Ábrego, M.E. et al. (2020) 'Enhanced, coordinated conservation efforts required to avoid extinction of critically endangered Eastern Pacific leatherback turtles', Scientific Reports, 10(1), p. 4772. Available at: https://doi.org/10.1038/s41598-020-60581-7.

Adimey, N. et al. (2016) 'Twenty-Six Years of Post-Release Monitoring of Florida Manatees (Trichechus manatus latirostris): Evaluation of a Cooperative Rehabilitation Program', Aquatic Mammals, 42, pp. 376–391. Available at: https://doi.org/10.1578/AM.42.3.2016.376.

Androulidakis, Y. et al. (2021) 'Impact of Caribbean Anticyclones on Loop Current variability', Ocean Dynamics, 71(9), pp. 935–956. Available at: https://doi.org/10.1007/s10236-021-01474-9.

Barbour, N. et al. (2020) 'Environmental and Biological Factors Influencing Dispersal of Neonate Leatherback Turtles (Dermochelys coriacea) From an Endangered Costa Rican Nesting Population', Frontiers in Marine Science, 7. Available at: https://www.frontiersin.org/articles/10.3389/fmars.2020.582933 (Accessed: 23 September 2022).

Bell, C.D. et al. (2006) ‘Traditional Caymanian fishery may impede local marine turtle population recovery’, Endangered Species Research, 2, pp. 63–69. Available at: https://doi.org/10.3354/esr002063.

Bell, C.D. et al. (2007) ‘Monitoring and conservation of critically reduced marine turtle nesting populations: lessons from the Cayman Islands’, Animal Conservation, 10(1), pp. 39–47. Available at: https://doi.org/10.1111/j.1469-1795.2006.00068.x.

Bell, C.D.L. et al. (2005) ‘Some of them came home: the Cayman Turtle Farm headstarting project for the green turtle Chelonia mydas’, Oryx, 39(2), pp. 137–148. Available at: https://doi.org/10.1017/S0030605305000372.

Benhamou, S. (2004) ‘How to reliably estimate the tortuosity of an animal’s path:: straightness, sinuosity, or fractal dimension?’, Journal of Theoretical Biology, 229(2), pp. 209–220. Available at: https://doi.org/10.1016/j.jtbi.2004.03.016.

Blumenthal, J.M. et al. (2006) ‘Satellite tracking highlights the need for international cooperation in marine turtle management’, Endangered Species Research, 2, pp. 51–61. Available at: https://doi.org/10.3354/esr002051.

Blumenthal, J.M. et al. (2021) ‘Cayman Islands Sea Turtle Nesting Population Increases Over 22 Years of Monitoring’, Frontiers in Marine Science, 8. Available at: https://www.frontiersin.org/articles/10.3389/fmars.2021.663856 (Accessed: 23 September 2022).

Bolten, A.B. et al. (2003) ‘Variation in sea turtle life history patterns: neritic vs. oceanic developmental stages’, The biology of sea turtles, 2, pp. 243–257.

Bona, M. et al. (2012) ‘Headstarting in a small population of European pond turtles (Emys orbicularis) in Central European conditions: first results’, Herpetology Notes, 5, pp. 547–550.

Bonar, M. et al. (2018) ‘Implementing a novel movement-based approach to inferring parturition and neonate caribou calf survival’, PLOS ONE, 13(2), p. e0192204. Available at: https://doi.org/10.1371/journal.pone.0192204.

Breed, G.A. et al. (2018) ‘Seasonal sea ice dynamics drive movement and migration of juvenile bearded seals (Erignathus barbatus)’, Marine Ecology Progress Series, 600. Available at: https://doi.org/10.3354/meps12659.

Briscoe, D.K. et al. (2016) ‘Active dispersal in loggerhead sea turtles (Caretta caretta) during the “lost years”’, Proceedings of the Royal Society B: Biological Sciences, 283(1832), p. 20160690. Available at: https://doi.org/10.1098/rspb.2016.0690.

Burke, R.L. (2015) ‘Head-starting turtles: learning from experience’, Herpetological Conservation and Biology. HERPETOLOGICAL CONSERVATION & BIOLOGY C/OR BRUCE BURY, USGS FOREST ….

Carr, A. (1987) ‘New Perspectives on the Pelagic Stage of Sea Turtle Development’, Conservation Biology, 1(2), pp. 103–121. Available at: https://doi.org/10.1111/j.1523-1739.1987.tb00020.x.

Chambault, P. et al. (2020) ‘Contrasted habitats and individual plasticity drive the fine scale movements of juvenile green turtles in coastal ecosystems’, Movement Ecology, 8(1), p. 1. Available at: https://doi.org/10.1186/s40462-019-0184-2.

Cheng, Y. et al. (2019) '"Closer-to-home" strategy benefits juvenile survival in a long-distance migratory bird', Ecology and Evolution, 9(16), pp. 8945–8952. Available at: https://doi.org/10.1002/ece3.5395.

Douglas N, et al. (2021). "fields: Tools for spatial data." R package version 14.0. <https://github.com/dnychka/fieldsRPackage>.

Flack, A. et al. (2018) 'From local collective behavior to global migratory patterns in white storks', Science, 360(6391), pp. 911–914. Available at: https://doi.org/10.1126/science.aap7781.

Frazer, N.B. (1992) 'Sea Turtle Conservation and Halfway Technology*', Conservation Biology, 6(2), pp. 179–184. Available at: https://doi.org/10.1046/j.1523-1739.1992.620179.x.

Fuxjager, M.J., Eastwood, B.S. and Lohmann, K.J. (2011) 'Orientation of hatchling loggerhead sea turtles to regional magnetic fields along a transoceanic migratory pathway', Journal of Experimental Biology, 214(15), pp. 2504–2508. Available at: https://doi.org/10.1242/jeb.055921.

Gaspar, P. et al. (2006) 'Marine animal behaviour: neglecting ocean currents can lead us up the wrong track', Proceedings of the Royal Society B: Biological Sciences, 273(1602), pp. 2697–2702. Available at: https://doi.org/10.1098/rspb.2006.3623.

Gaspar, P. et al. (2012) 'Oceanic dispersal of juvenile leatherback turtles: going beyond passive drift modeling', Marine Ecology Progress Series, 457, pp. 265–284. Available at: https://doi.org/10.3354/meps09689.

Gaspar, P. and Lalire, M. (2017) 'A model for simulating the active dispersal of juvenile sea turtles with a case study on western Pacific leatherback turtles', PLOS

ONE, 12(7), p. e0181595. Available at: https://doi.org/10.1371/journal.pone.0181595.

Girard, C. et al. (2006) 'Homing in green turtles Chelonia mydas: oceanic currents act as a constraint rather than as an information source', Marine Ecology Progress Series, 322, pp. 281–289. Available at: https://doi.org/10.3354/meps322281.

Godley, B.J. et al. (2008) 'Satellite tracking of sea turtles: Where have we been and where do we go next?', Endangered Species Research, 4(1–2), pp. 3–22. Available at: https://doi.org/10.3354/esr00060.

Goshe, L.R. et al. (2010) 'Estimation of age at maturation and growth of Atlantic green turtles (Chelonia mydas) using skeletochronology', Marine Biology, 157(8), pp. 1725–1740. Available at: https://doi.org/10.1007/s00227-010-1446-0.

Groombridge, B. and Wright, L. (1982) 'The IUCN amphibia-reptilia red data book, Part 1', IUCN, Gland, Switzerland [Preprint].

Gurarie, E., Andrews, R.D. and Laidre, K.L. (2009) 'A novel method for identifying behavioural changes in animal movement data', Ecology Letters, 12(5), pp. 395–408. Available at: https://doi.org/10.1111/j.1461-0248.2009.01293.x.

Haegen, W.M.V. et al. (2009) 'Survival and Causes of Mortality of Head-Started Western Pond Turtles on Pierce National Wildlife Refuge, Washington', The Journal of Wildlife Management, 73(8), pp. 1402–1406. Available at: https://doi.org/10.2193/2008-484.

Hartigan, J.A. and Wong, M.A. (1979) 'Algorithm AS 136: A K-Means Clustering Algorithm', Journal of the Royal Statistical Society. Series C (Applied Statistics), 28(1), pp. 100–108. Available at: https://doi.org/10.2307/2346830.

Haskell, A. et al. (1996) ‘Size Related Survival of Headstarted Redbelly Turtles (Pseudemys rubriventris) in Massachusetts’, Journal of Herpetology, 30(4), pp. 524–527. Available at: https://doi.org/10.2307/1565695.

Hays, G.C. et al. (2003) ‘Island-finding ability of marine turtles’, Proceedings of the Royal Society of London. Series B: Biological Sciences, 270(suppl_1), pp. S5–S7.

Hays, G.C. et al. (2007) ‘Why do Argos satellite tags deployed on marine animals stop transmitting?’, Journal of Experimental Marine Biology and Ecology, 349(1), pp. 52–60. Available at: https://doi.org/10.1016/j.jembe.2007.04.016.

Hays, G.C. et al. (2020) ‘Open Ocean Reorientation and Challenges of Island Finding by Sea Turtles during Long-Distance Migration’, Current Biology, 30(16), pp. 3236-3242.e3. Available at: https://doi.org/10.1016/j.cub.2020.05.086.

Hazen, E.L. et al. (2012) ‘Ontogeny in marine tagging and tracking science: technologies and data gaps’, Marine Ecology Progress Series, 457, pp. 221–240. Available at: https://doi.org/10.3354/meps09857.

Heppell, S., Crowder, L. and Crouse, D. (1996) ‘Models to Evaluate Headstarting as a Management Tool for Long-Lived Turtles’, Ecological Applications, 6, p. 556. Available at: https://doi.org/10.2307/2269391.

Hoover, A.L. et al. (2020) ‘Nearshore neonate dispersal of Atlantic leatherback turtles (Dermochelys coriacea) from a non-recovering subpopulation’, Scientific Reports, 10(1), p. 18748. Available at: https://doi.org/10.1038/s41598-020-75769-0.

Hutchinson, M. et al. (2019) ‘Movements and habitat use of juvenile silky sharks in the Pacific Ocean inform conservation strategies’, Fisheries Research, 210, pp. 131–142. Available at: https://doi.org/10.1016/j.fishres.2018.10.016.

Jonsen, I.D. et al. (2013) ‘State-space models for bio-loggers: A methodological road map’, Deep Sea Research Part II: Topical Studies in Oceanography, 88–89, pp. 34–46. Available at: https://doi.org/10.1016/j.dsr2.2012.07.008.

Jonsen, I.D. et al. (2019a) ‘Movement responses to environment: fast inference of variation among southern elephant seals with a mixed effects model’, Ecology, 100(1), p. e02566. Available at: https://doi.org/10.1002/ecy.2566.

Jonsen, I.D. et al. (2019b) ‘Movement responses to environment: fast inference of variation among southern elephant seals with a mixed effects model’, Ecology, 100(1), p. e02566. Available at: https://doi.org/10.1002/ecy.2566.

Jonsen, I.D. et al. (2020) ‘A continuous-time state-space model for rapid quality control of argos locations from animal-borne tags’, Movement Ecology, 8(1), p. 31. Available at: https://doi.org/10.1186/s40462-020-00217-7.

Jonsen, I.D., Flemming, J.M. and Myers, R.A. (2005) ‘Robust State–Space Modeling of Animal Movement Data’, Ecology, 86(11), pp. 2874–2880. Available at: https://doi.org/10.1890/04-1852.

Jonsen, I.D., Myers, R.A. and James, M.C. (2007) ‘Identifying leatherback turtle foraging behaviour from satellite telemetry using a switching state-space model’, Marine Ecology Progress Series, 337, pp. 255–264. Available at: https://doi.org/10.3354/meps337255.

Kobayashi, D.R. et al. (2014) ‘“Going with the Flow” or Not: Evidence of Positive Rheotaxis in Oceanic Juvenile Loggerhead Turtles (Caretta caretta) in the South Pacific Ocean Using Satellite Tags and Ocean Circulation Data’, PLOS ONE, 9(8), p. e103701. Available at: https://doi.org/10.1371/journal.pone.0103701.

Lalire, M. and Gaspar, P. (2019) 'Modeling the active dispersal of juvenile leatherback turtles in the North Atlantic Ocean', Movement Ecology, 7(1), p. 7. Available at: https://doi.org/10.1186/s40462-019-0149-5.

Lewison, R. et al. (2015) 'Dynamic Ocean Management: Identifying the Critical Ingredients of Dynamic Approaches to Ocean Resource Management', BioScience, 65(5), pp. 486–498. Available at: https://doi.org/10.1093/biosci/biv018.

Lohmann, K.J. and Lohmann, C.M.F. (2019) 'There and back again: natal homing by magnetic navigation in sea turtles and salmon', Journal of Experimental Biology. Edited by B. el Jundi, A. Kelber, and B. Webb, 222(Suppl_1), p. jeb184077. Available at: https://doi.org/10.1242/jeb.184077.

Lohmann, K.J., Luschi, P. and Hays, G.C. (2008) 'Goal navigation and island-finding in sea turtles', Journal of Experimental Marine Biology and Ecology, 356(1), pp. 83–95. Available at: https://doi.org/10.1016/j.jembe.2007.12.017.

Luschi, P. et al. (2007) 'Marine Turtles Use Geomagnetic Cues during Open-Sea Homing', Current Biology, 17(2), pp. 126–133. Available at: https://doi.org/10.1016/j.cub.2006.11.062.

Mansfield, K.L. et al. (2017) 'First satellite tracks of South Atlantic sea turtle "lost years": seasonal variation in trans-equatorial movement', Proceedings of the Royal Society B: Biological Sciences, 284(1868), p. 20171730. Available at: https://doi.org/10.1098/rspb.2017.1730.

Mansfield, K.L., Wyneken, J. and Luo, J. (2021) 'First Atlantic satellite tracks of "lost years" green turtles support the importance of the Sargasso Sea as a sea turtle

nursery', Proceedings of the Royal Society B: Biological Sciences, 288(1950), p. 20210057. Available at: https://doi.org/10.1098/rspb.2021.0057.

Mazzoil, M. et al. (2008) 'Radio-Tracking and Survivorship of Two Rehabilitated Bottlenose Dolphins (Tursiops truncatus) in the Indian River Lagoon, Florida', Aquatic Mammals, 34, pp. 54–64. Available at: https://doi.org/10.1578/AM.34.1.2008.54.

McLean, D. J., and Skowron Volponi, M. A. (2018). trajr: An R package for characterisation of animal trajectories. Ethology, 124(6), 440-448. https://doi.org/10.1111/eth.12739

Meylan, P.A., Meylan, A.B. and Gray, J.A. (2011) 'The Ecology and Migrations of Sea Turtles 8. Tests of the Developmental Habitat Hypothesis', Bulletin of the American Museum of Natural History, 2011(357), pp. 1–70. Available at: https://doi.org/10.1206/357.1.

Moncada, F. et al. (2006) 'Movement Patterns of Green Turtles (Chelonia mydas) in Cuba and Adjacent Caribbean Waters Inferred from Flipper Tag Recaptures', Journal of Herpetology, 40(1), pp. 22–34. Available at: https://doi.org/10.1670/39-05A.1.

Nathan, R. et al. (2008) 'A movement ecology paradigm for unifying organismal movement research', Proceedings of the National Academy of Sciences, 105(49), pp. 19052–19059. Available at: https://doi.org/10.1073/pnas.0800375105.

Orgeret, F. et al. (2019) 'Exploration during early life: distribution, habitat and orientation preferences in juvenile king penguins', Movement Ecology, 7(1), p. 29. Available at: https://doi.org/10.1186/s40462-019-0175-3.

Péron, C. and Grémillet, D. (2013) 'Tracking through Life Stages: Adult, Immature and Juvenile Autumn Migration in a Long-Lived Seabird', PLOS ONE, 8(8), p. e72713. Available at: https://doi.org/10.1371/journal.pone.0072713.

Pham, D.T., Dimov, S.S. and Nguyen, C.D. (2005) 'Selection of K in K-means clustering', Proceedings of the Institution of Mechanical Engineers, Part C: Journal of Mechanical Engineering Science, 219(1), pp. 103–119. Available at: https://doi.org/10.1243/095440605X8298.

Price, E.R. et al. (2013) 'Serum triglycerides and ß-hydroxybutyrate predict feeding status in green turtles (Chelonia mydas): Evaluating a single blood sample method for assessing feeding/fasting in reptiles', Journal of Experimental Marine Biology and Ecology, 439, pp. 176–180. Available at: https://doi.org/10.1016/j.jembe.2012.11.005.

Pritchard, P.C.H. (1981) 'Criteria for scientific evaluation of head-starting', Marine turtle newsletter, 19, p. 3â.

Putman, N.F. et al. (2015) 'Magnetic navigation behavior and the oceanic ecology of young loggerhead sea turtles', Journal of Experimental Biology, 218(7), pp. 1044–1050. Available at: https://doi.org/10.1242/jeb.109975.

Putman, N.F. and Mansfield, K.L. (2015) 'Direct Evidence of Swimming Demonstrates Active Dispersal in the Sea Turtle "Lost Years"', Current Biology, 25(9), pp. 1221–1227. Available at: https://doi.org/10.1016/j.cub.2015.03.014.

Reich, K.J., Bjorndal, K.A. and Bolten, A.B. (2007) 'The "lost years" of green turtles: using stable isotopes to study cryptic lifestages', Biology Letters, 3(6), pp. 712–714. Available at: https://doi.org/10.1098/rsbl.2007.0394.

Resende, P.S. et al. (2021) ‘What is better for animal conservation translocation programmes: Soft- or hard-release? A phylogenetic meta-analytical approach’, Journal of Applied Ecology, 58(6), pp. 1122–1132. Available at: https://doi.org/10.1111/1365-2664.13873.

Shillinger, G.L., Di Lorenzo, E., et al. (2012) ‘On the dispersal of leatherback turtle hatchlings from Mesoamerican nesting beaches’, Proceedings of the Royal Society B: Biological Sciences, 279(1737), pp. 2391–2395. Available at: https://doi.org/10.1098/rspb.2011.2348.

Shillinger, G.L., Bailey, H., et al. (2012) ‘Tagging through the stages: technical and ecological challenges in observing life histories through biologging’, Marine Ecology Progress Series, 457, pp. 165–170. Available at: https://doi.org/10.3354/meps09816.

Vega, M.L. et al. (2016) ‘First-Time Migration in Juvenile Common Cuckoos Documented by Satellite Tracking’, PLOS ONE, 11(12), p. e0168940. Available at: https://doi.org/10.1371/journal.pone.0168940.

Venables, W. N. & Ripley, B. D. (2002). Modern Applied Statistics with S. Fourth Edition. Springer, New York. ISBN 0-387-95457-0

Wang, M. and Hu, C. (2016) ‘Mapping and quantifying Sargassum distribution and coverage in the Central West Atlantic using MODIS observations’, Remote Sensing of Environment, 183, pp. 350–367. Available at: https://doi.org/10.1016/j.rse.2016.04.019.

Welch, H. et al. (2019) ‘Practical considerations for operationalizing dynamic management tools’, Journal of Applied Ecology, 56(2), pp. 459–469. Available at: https://doi.org/10.1111/1365-2664.13281.

Wells, R.S., Bassos-Hull, K. and Norris, K.S. (1998) 'Experimental Return to the Wild of Two Bottlenose Dolphins', Marine Mammal Science, 14(1), pp. 51–71. Available at: https://doi.org/10.1111/j.1748-7692.1998.tb00690.x.

Witherington, B., Hirama, S. and Hardy, R. (2012) 'Young sea turtles of the pelagic Sargassum-dominated drift community: habitat use, population density, and threats', Marine Ecology Progress Series, 463, pp. 1–22. Available at: https://doi.org/10.3354/meps09970.

Appendices

Appendix 1

Table A1.1. Summary statistics of body morphometric variables for neonates in 2016 and 2018, separated by treatment (incubator, hatchery) and including overall statistics for each year.

Variable		**2016**			**2018**		
		Incubator	Hatchery	Overall	Incubator	Hatchery	Overall
Mass (g)							
	Mean	42.7	42.4	42.5	45.9	49.9	48.3
	Std.Dev	3.8	3.3	3.5	2.5	3.8	3.9
	Range	33.0-48.0	37.0-50.0	33.0-50.0	43.2-52.7	42.3-56.0	42.3-56.0
Standard Carapace Length (mm)							
	Mean	60.3	60.5	60.4	61.8	62.4	62.1
	Std.Dev	3.3	2.2	2.6	1.9	3.5	2.9
	Range	51.5-64.8	55.1-64.6	51.5-64.8	58.0-64.0	53.0-69.0	53.0-69.0
Standard Carapace Width (mm)							
	Mean	41.6	42.0	41.8	40.8	41.0	40.9
	Std.Dev	1.6	1.6	1.6	1.2	2.9	2.3
	Range	36.8-43.9	38.6-45.1	36.8-45.1	38.0-43.0	37.0-52.0	37.0-52.0
Head Width (mm)							
	Mean	17.5	17.9	17.8	15.6	16.3	16.0
	Std.Dev	0.6	0.5	0.6	1.2	0.9	1.1
	Range	15.8-18.3	17.0-18.9	15.8-18.9	14.0-18.0	15.0-18.0	14.0-18.0
Flipper Length (mm)							
	Mean	*NA*	*NA*	*NA*	55.2	57.6	56.6
	Std.Dev	*NA*	*NA*	*NA*	3.1	3.3	3.4
	Range	*NA*	*NA*	*NA*	52.0-64.0	51.0-65.0	51.0-65.0

Table A1.2. Results of a linear mixed effects model predicting the variance in neonate swimming speed (residuals from final neonate GAMM model, see Table 3 in text) as a function of time along the track (move number). Individual neonates were included as random effects.

Fixed Effect	Estimate	Estimate Error	p-value
Intercept	0.001	0.011	0.924
Time Along Track (*Move Number*)	-0.000	0.001	0.619
Current Speed	0.008	0.014	0.569

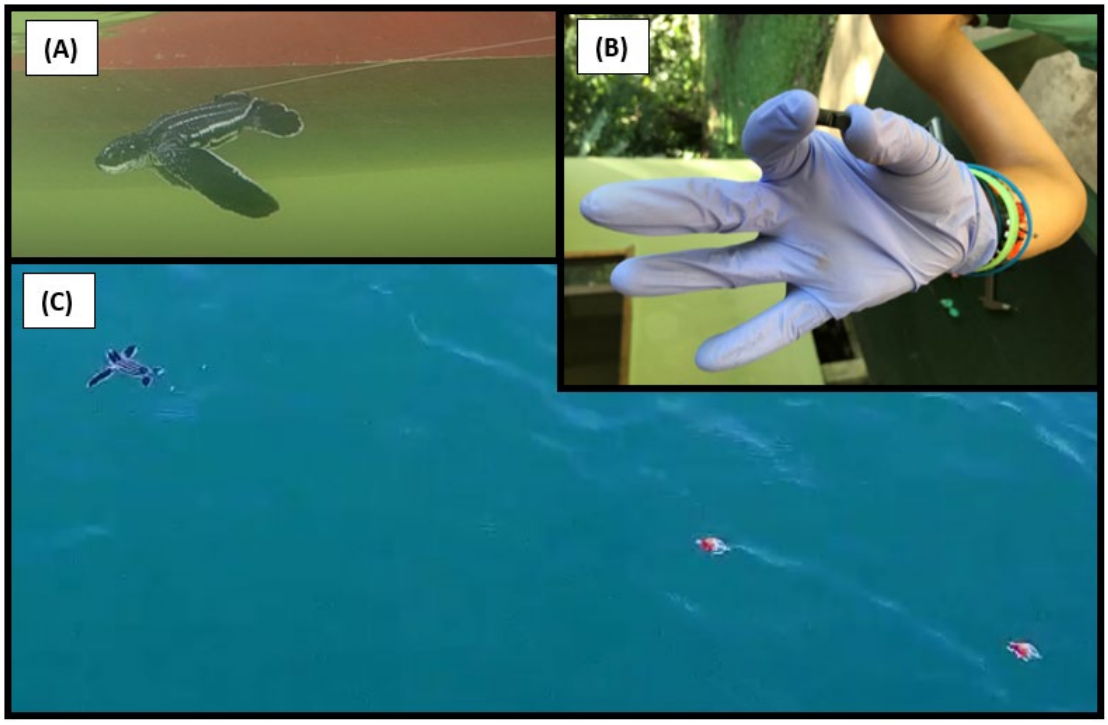

Figure A1.1. a) Illustration of the Velcro attachment to neonate carapace dorsal-ventrally. b) Picture of Vemco V5 acoustic tag. Tag design from Hoover et al. (2017). c) Tag design attached to neonate, with 2 m of monofilament line with orange floats and acoustic tag.

Figure A1.2. Surface drifter design, with orange floats, GPS-enabled phone in a waterproof phone case, orange flag, and metal drogue, tethered together with orange Paracord®. Drifter design from Hoover et al. 2020.

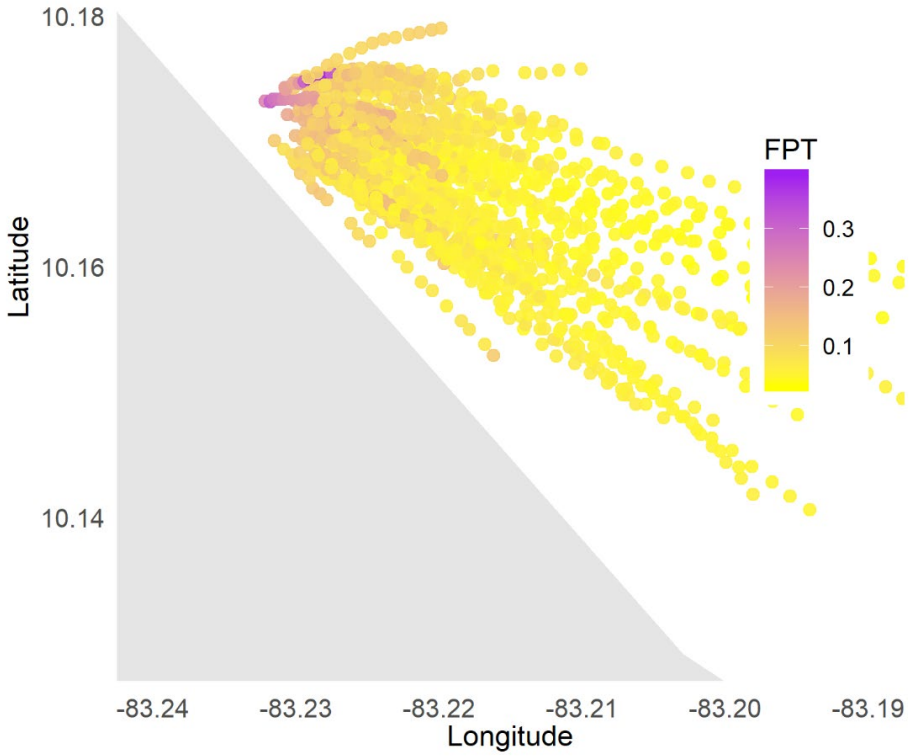

Figure A1.3. Map of first passage time values (hours) for all neonate tracks (n=94) within the study region in Pacuare, Costa Rica, with each point representing an observation. Warmer colors correspond with higher first passage time values.

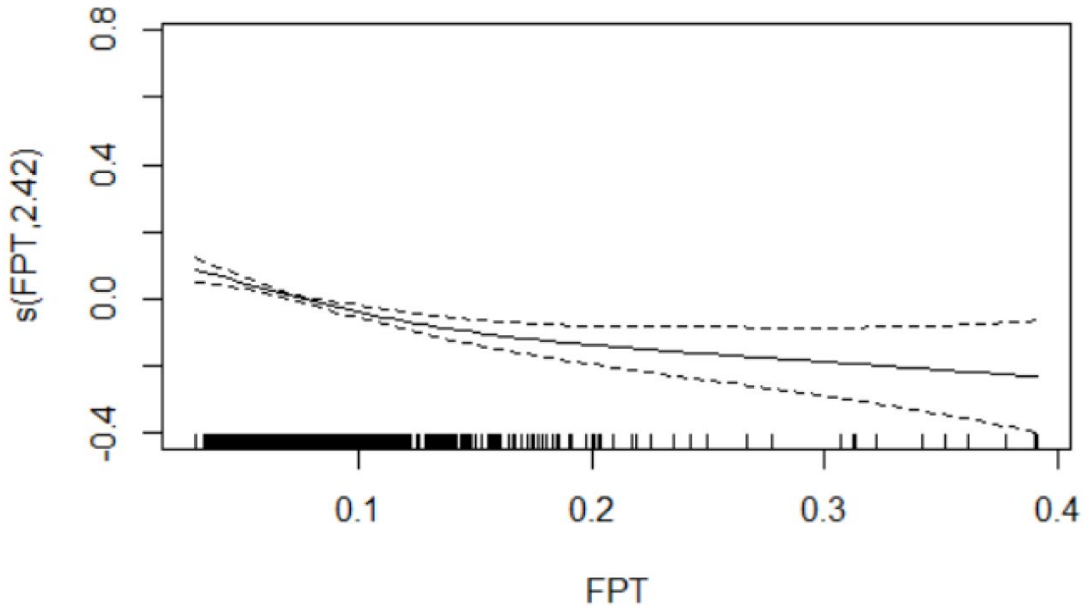

Figure A1.4. Generalized additive mixed model (GAMM) smoothing curve for neonate in-water speeds (in-water movements, m s-1) as a function of first passage time (FPT, hours) for 2016 and 2018. A higher first passage time value indicates that neonates spent more time in a given spatial radius of 59 m.

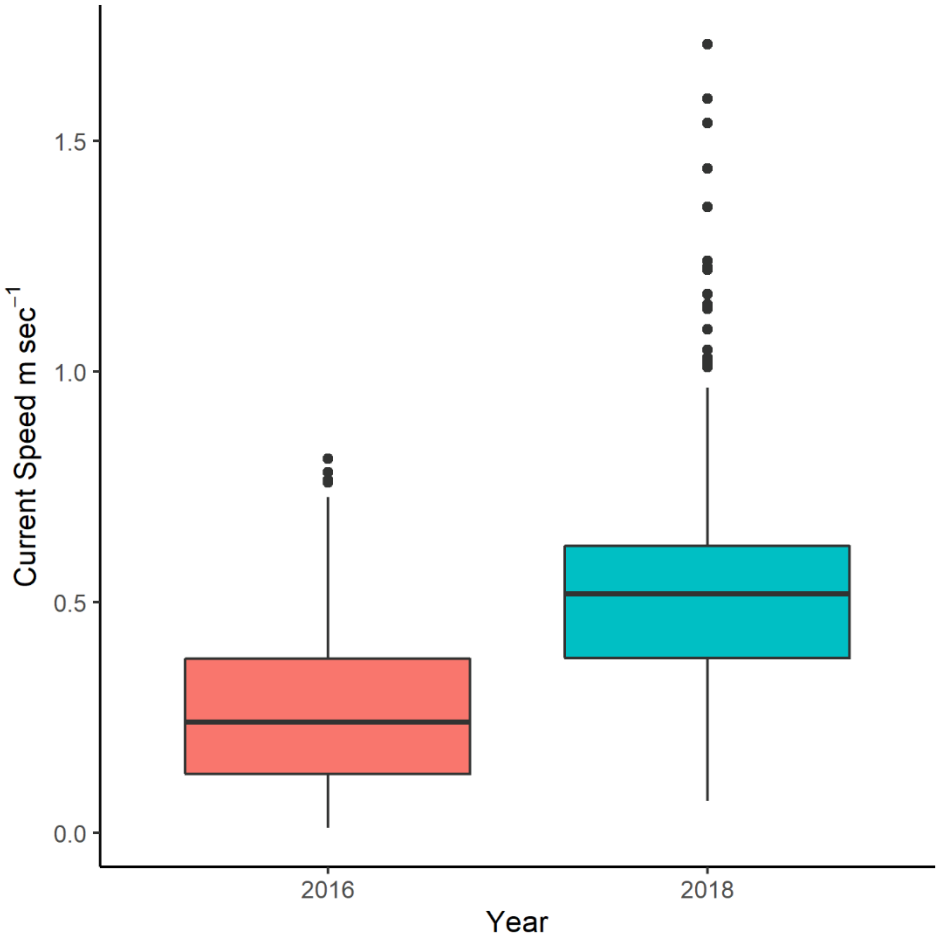

Figure A1.5. Boxplots of the current speeds (m s-1) for 2016 (red) versus 2018 (blue).

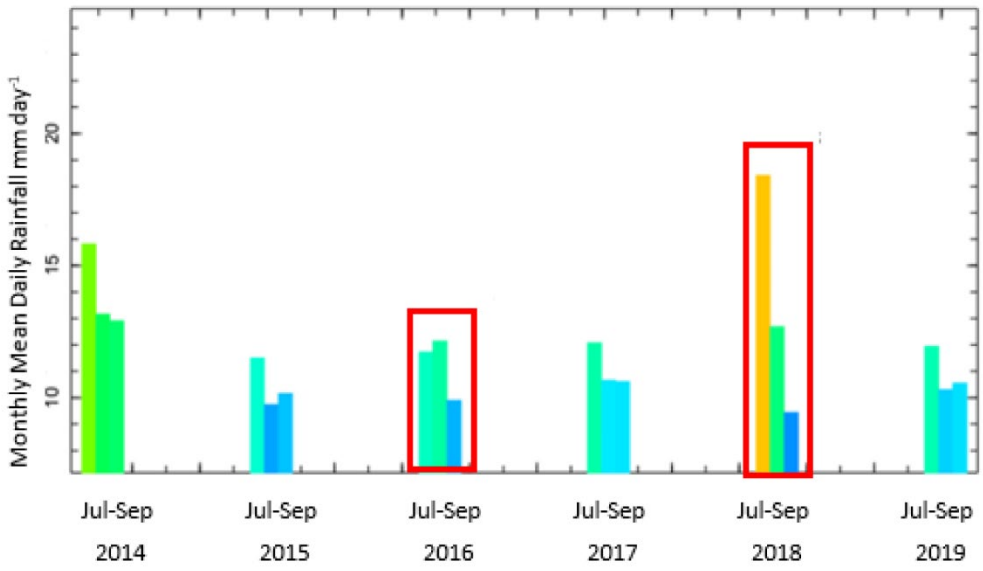

Figure A1.6. Monthly mean time series for daily rainfall data (resolution 0.5° x 0.5°) for July-September 2014 to 2019, in the region of 83-84°W and 9-11°N. The monthly mean daily rainfall (mm day-1) for July-September for the study period (2016, 2018) are highlighted with red boxes (11.96 mm day-1 for 2016 and 15.57 mm day-1 for 2018). The time series average for July to September for 1948-2019 was 12.53 mm day-1. Plots were created using the data visualization tool from the online IRI/LDEO Climate Data Library for the NOAA National Centers for Environmental Prediction (NCEP) Climate Prediction Center (CPC) dataset for daily rainfall.

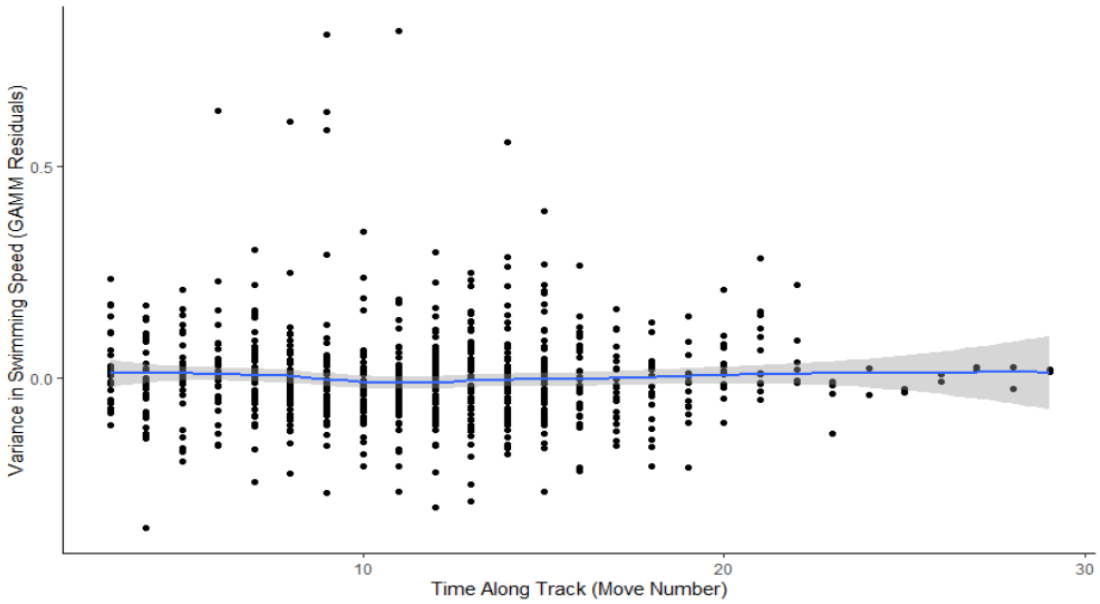

Figure A1.7. Scatter plot of the variance in swimming speed (extracted residuals from final neonate GAMM model, see Table 3 in text) as a function of the time along the track (move number). A loess smoother was applied to show any relationship present.

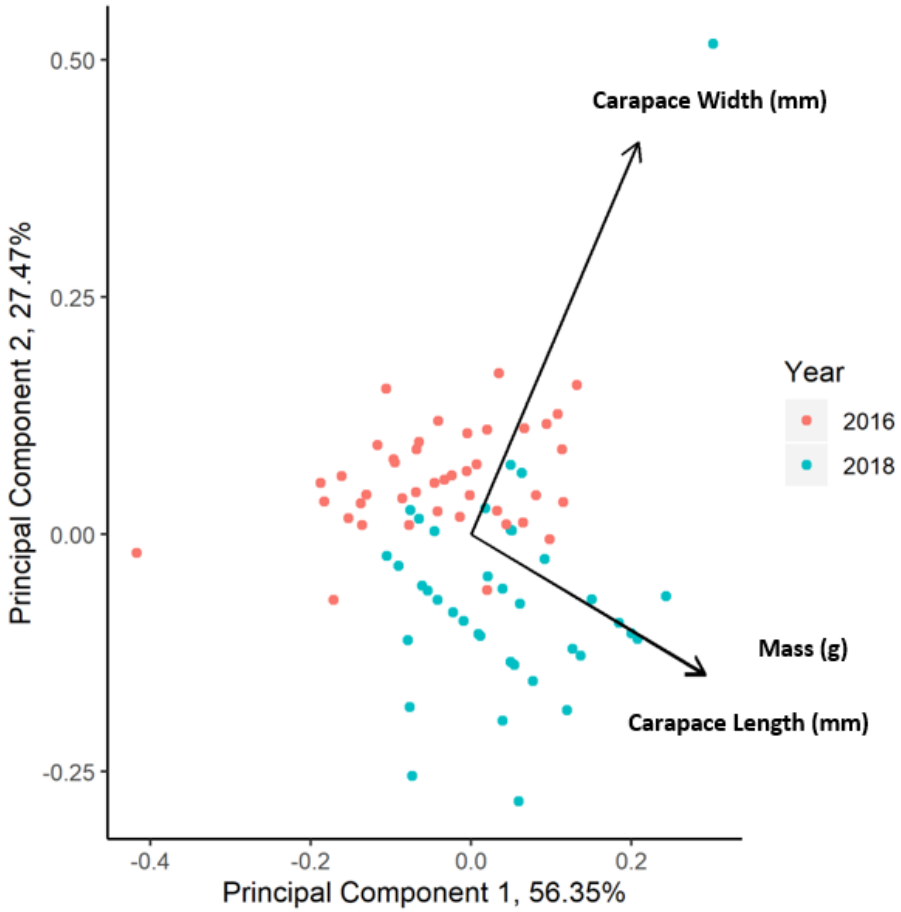

Figure A1.8. Biplot of the results of the principal component analysis, using body morphometric variables carapace length (mm), carapace width (mm), and body mass (g) and with observations colored by year (2016, 2018). The first component explained 56% of the total variance, with mass and carapace length having the largest correlations with the first principal component.

Appendix 2

Table A2.1. List of product sources for remote sensing environmental variables used in the generalized additive mixed model (GAMM) for the proportion of dive clusters. All variables were obtained from the National Oceanic and Atmospheric Administration CoastWatch ERDDAP server, accessible through the "rerddap" R package (Chamberlain 2021). Variables with 30-day lags included as candidate variables are indicated.

Variable	**Lagged Variable**	**Product name (ERDDAP)**	**Units**	**Spatial resolution**	**Temporal range**	**Composite**
Ekman upwelling	no	erdQSstress8day	$m*s^{-1}$	0.125˚	1999-2009	8 day
Sea surface height anomaly	no	erdTAsshmday_LonPM180	m	0.25˚	1992-2010	monthly
Chlorophyll-*a*	yes	erdMH1chla8day	$mg*m^{-3}$	4 km	2003-2021	8 day
Sea surface temperature	no	erdPH2sstd8day	˚C	0.042˚	1981-2012	8 day
Bathymetry	no	usgsCeSrtm30v1	m	30 arc sec	*na*	*na*

Table A2.2. Results of a generalized additive mixed model (GAMM) for the proportion of cluster 1 dives (quasibinomial family, logit link function) in relation to variables for the 30-day lag for log chlorophyll-a (log chla), sea surface temperature (sst), sea surface height anomaly (ssha), and bathymetry (bathy), with each individual track included as a random effect. Because the response variable of dives identified with the cluster analysis was a proportion with only 2 levels (cluster 1 and 2, e.g. proportion of cluster 2 dives = 1 – proportion of cluster 1 dives), only the GAMM results for cluster 1 dives are reported, as the GAMM for the proportion of cluster 2 dives had mirrored coefficients and opposite relationships to the GAMM for proportion of cluster 1 dives.

Fixed effect	**Estimate**	**Estimate error**	***p*-value**
Intercept	-0.929	0.111	< 2e-16
Smoother term	**edf**	**F**	***p*-value**
sst	3.523	7.128	4.26e-5
log chla (30-day lag)	2.971	9.901	4.84e-6
ssha	2.903	36.089	< 2e-16
bathy	4.390	5.541	7.55e-5

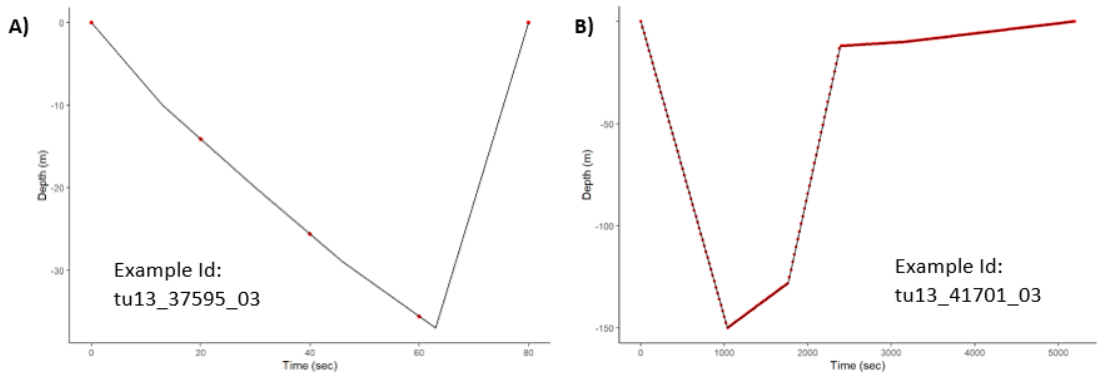

Figure A2.1. Plots showing the ability of the chosen interpolation interval (20 sec) to capture the shape of both short and long duration dives, with interpolated points (red) over the original dive profile for both a a) short duration dive (80 sec) and b) long duration dive (5,190 sec), using example dives from the dataset.

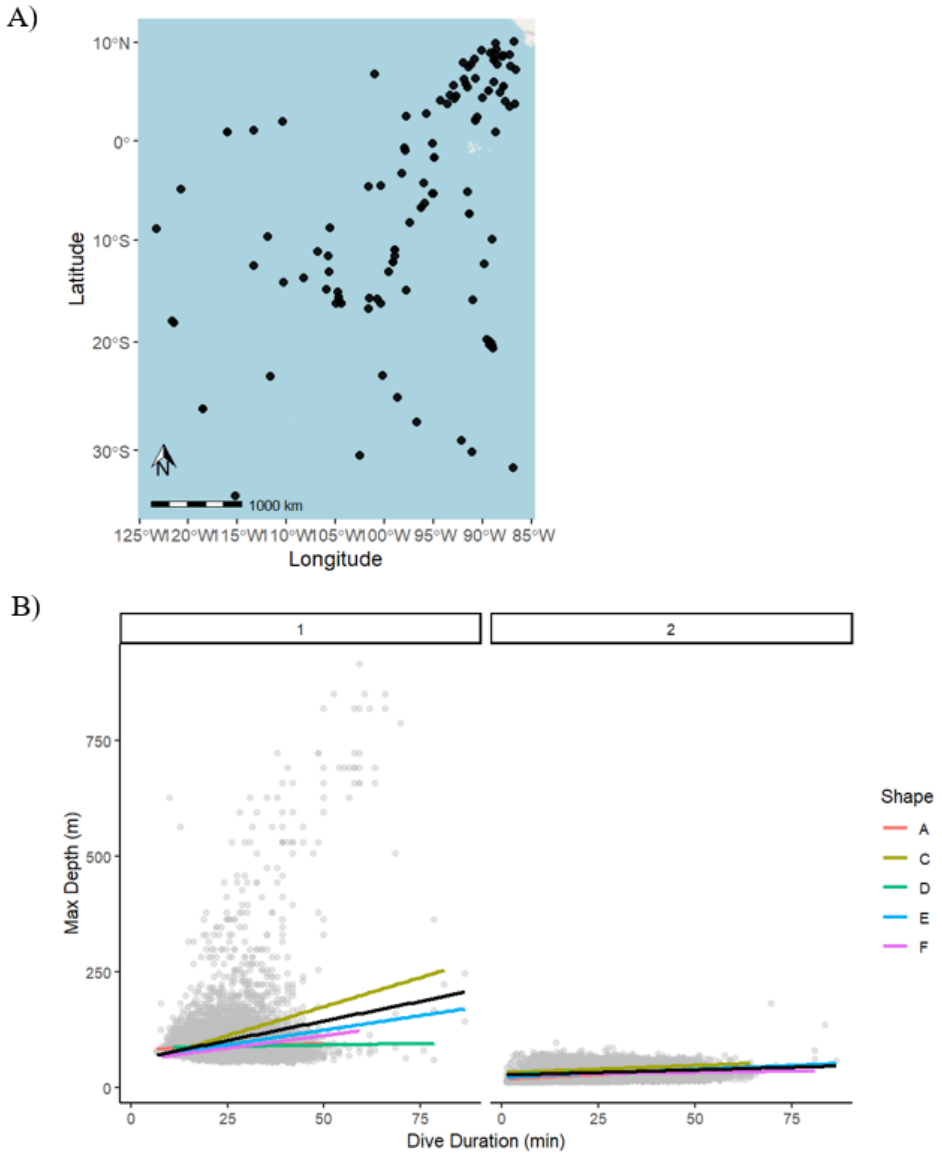

Figure A2.2. A) Map of spatial locations for deep dives (> 300 m) for cluster 1 dives (deeper) identified with a Dynamic Time Warp (DTW) analysis B) Scatter plots of the maximum depth (m) versus duration (min) for dives in each DTW cluster (1, 2), with linear smoothers shown for all dives in each cluster group (black) and for different profile shapes within each cluster (colored).

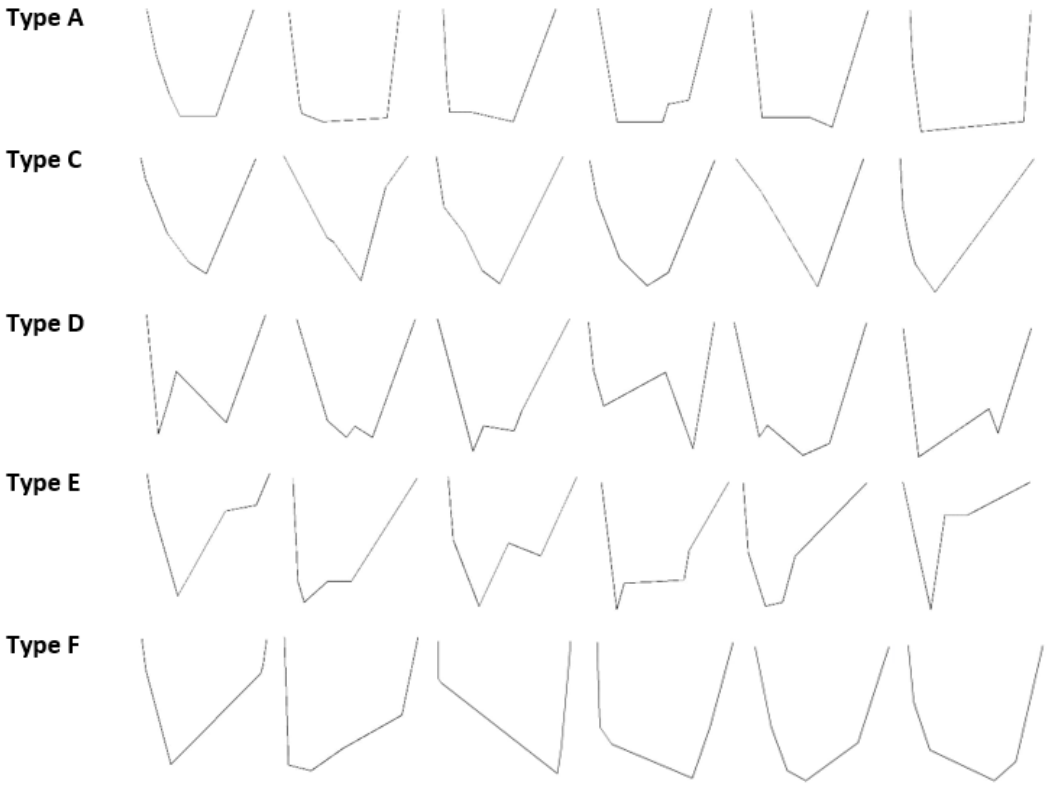

Figure A2.3. Images showing the variety in shapes possible for each dive profile shape (A, C, D, E, F). Each shape is a real dive profile from the dataset of N=139 random dives that were manually labeled by their shape and used as part of a training dataset for the Convolutional Neural Network Model (CNN). The general shape for each category used to manually label images originate from five published, standardized shapes known for sea turtles performing pelagic diving behaviors (Hochscheid 2014).

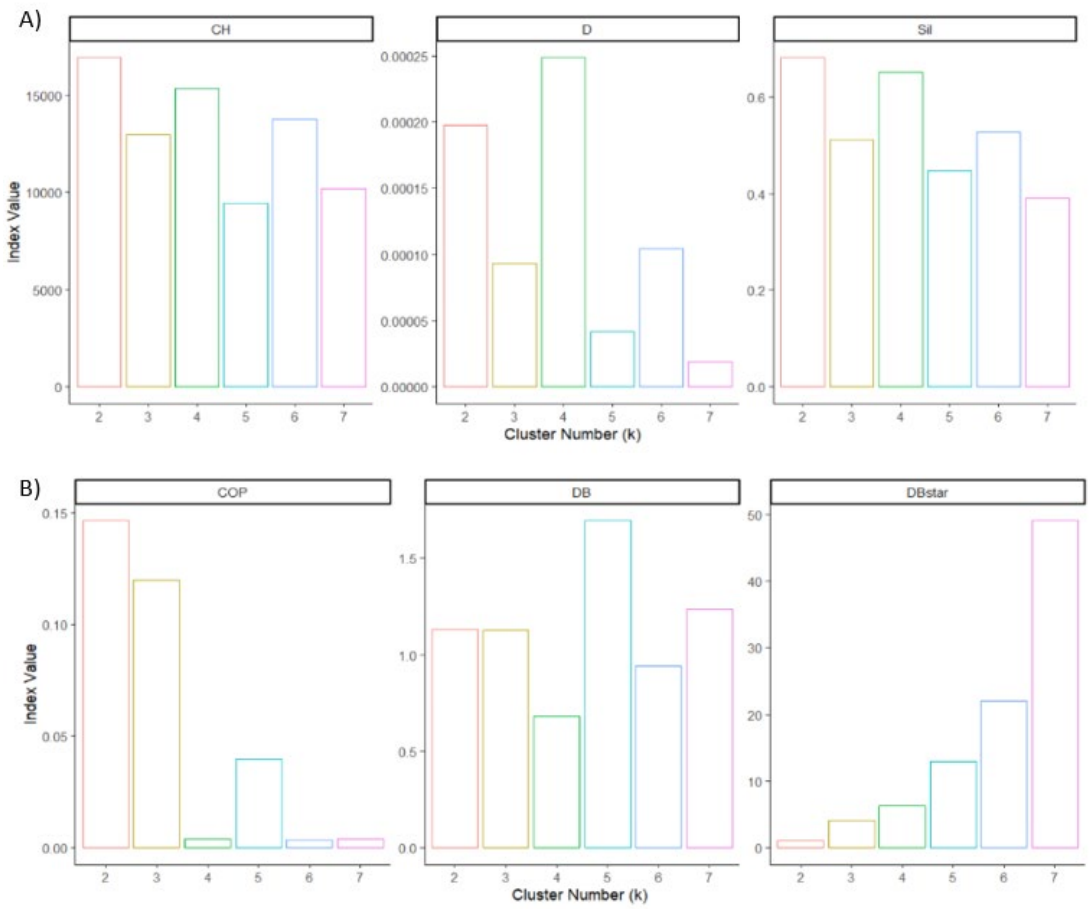

Figure A2.4. Results of a quantitative and visual assessment for the appropriate number of clusters (k) to be used in the Dynamic Time Warp analysis. A range of values for k (2-7) were tested and six internal cluster validity indices were used to assess these values, using a majority vote amongst the indices (Sarda-Espinosa 2019). A) Three indices (Silhouette- Sil, Dunn- D, Calinski-Harabasz- CH) look for maximum values and B) three indices (COP, Davies-Bouldin- DB, Modified Davies-Bouldin- DBstar) look for minimized values (Sarda-Espinosa 2019). The results of the majority vote for these indices showed a tie between a k of 2 and 4. To further assess the ecological logic of these values for k, the clusters were examined for spatial and temporal overlap. Results showed that for a k of 4, there was an obvious

bimodal distribution to spatial and temporal distribution of the clusters, specifically between clusters (1, 4) and (2 ,3). These results indicated that a k of 2 was most appropriate for further analysis.

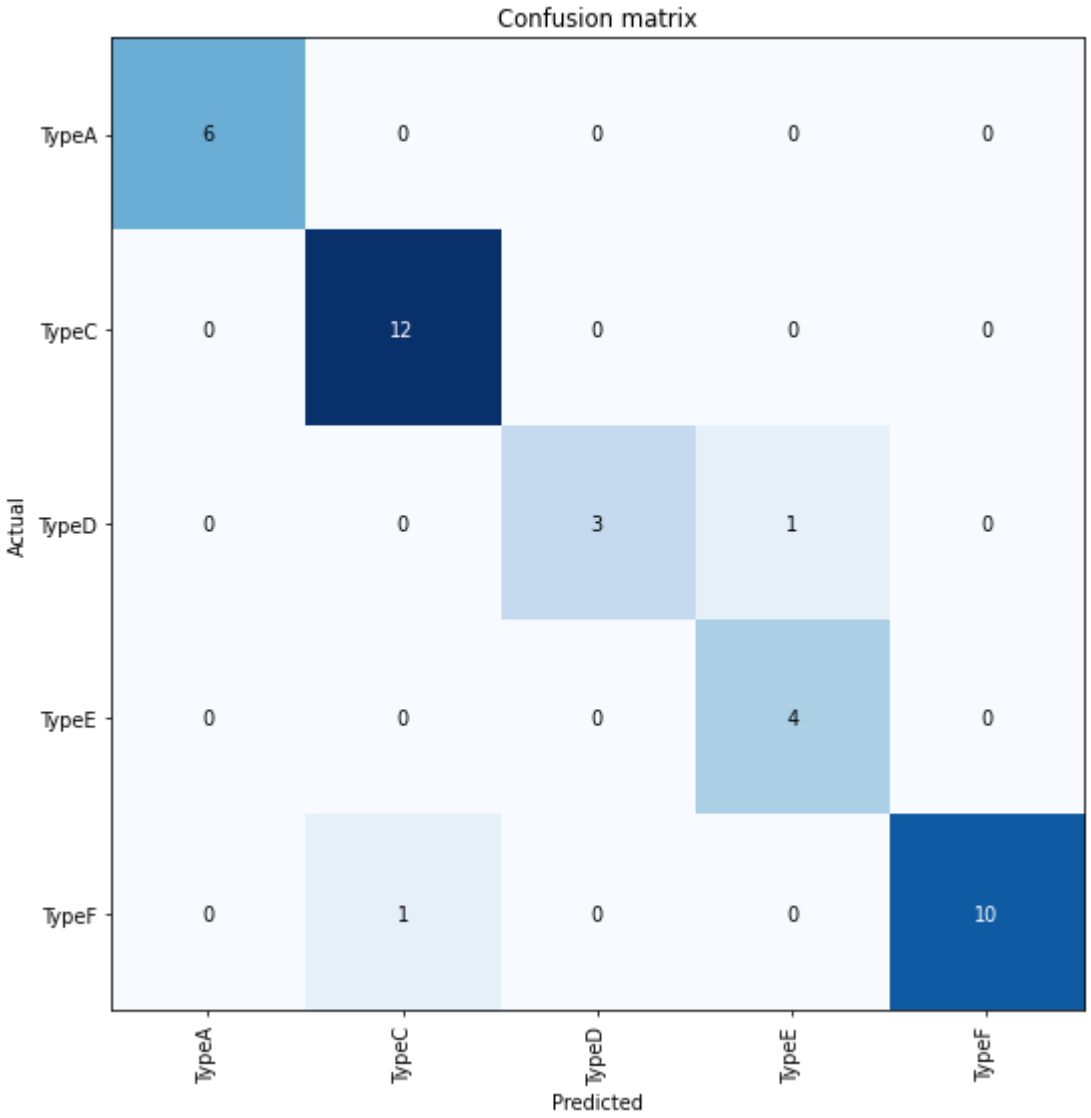

Figure A2.5. Confusion matrix for the results of the final epoch of the image classifier convolutional neural network model (CNN), trained with a combination of images of N=139 random, manually-labelled dive profiles and N=50 synthetic images of 5 standardized dive shape from the literature (Hochscheid 2014). The matrix shows the actual shape versus the predicted shape for each dive profile in the validation set (N=37). The CNN achieved 95% accuracy with the final training iteration.

Appendix 3

Data Processing Details

Tracks were regularized to estimate daily positions (at 00:00:00 each day) using the R package "foieGras", which fits a continuous-time state-space model to predict locations at regular time intervals and account for location error (Jonsen et al. 2019, Jonsen & Patterson 2020). Each daily position from these regularized tracks was then used to estimate daily mean velocities on the ground. Corresponding, daily mean ocean surface current velocities along the regularized trajectories were also estimated using GLORYS12, the latest global ocean reanalysis at a 1/12th degree resolution (Lellouche et al., 2021). This reanalysis is provided by the Copernicus Marine Service (https://marine.copernicus.eu/). Daily mean swimming speeds were then simply obtained by subtracting each daily surface current velocity value from the corresponding daily velocity value on the ground (Gaspar et al., 2006).

In addition to the daily mean swimming speed estimates obtained using the methods above, the turning angle (angle between two successive swimming speed vectors) was derived for each daily position using the "bcpa" R package (Gurarie 2014). The persistence velocity, or the tendency and magnitude of a given movement to persist in a given direction, was then determined by multiplying the magnitude of each daily displacement by the cosine of the corresponding turning angle (Gurarie et al. 2009).

Vertical movement variables were derived using the results of a prior study (Barbour et al., in review), where dives for each individual in this dataset were grouped into ecologically significant clusters using a Dynamic Time Warp (DTW) clustering analysis. This analysis determined two dive groups (D1 and D2) that differed in their

maximum dive depth, relationship with environmental covariates, and composition of dive profile types (see Barbour et al., in review). To match the 24-hour temporal resolution of biotelemetry locations, each individual's daily proportion of dives belonging to either D1 or D2 dive clusters was calculated. Additional vertical movement variables of the median maximum dive depth and time-at-depth (TAD) were also derived for each daily position.

Hidden Markov Model Details

Hidden Markov Model (HMM) state dependent distributions are specified below, with parameters for the distributions including μ and σ for move persistence speed (V, Cauchy distribution) (1) λ, the mean number of dives per day, and *P* the probability of a given dive being D1 rather than D2. Thus, the number of N_1 and N_2 dives is modeled as a Poisson process with respective means (Eqs. 2 and 3):

State Index: $k \in \{1,2,3\}$

$$V_k \sim \text{Cauchy}\ (\mu_k, \sigma_k) \quad (1)$$

$$N_{1,k} \sim \text{Poisson}\ (P_k * \lambda_k) \quad (2)$$

$$N_{2,k} \sim \text{Poisson}\ ((1-P_k) * \lambda_k) \quad (3)$$

The transition probability matrix (4), which determines the switch probability between states or the state transition probabilities, was specified with **Φ**. It can be read as the probability of moving from the previous behavioral state *i* at time *t-1* to behavioral state *j* at time *t*. This assumption of the HMMs, that transitions between states were described by a transition probability matrix, allowed a given turtle to remain in a given state for longer than would be expected with uncorrelated transitions.

$$\mathbf{\Phi}_{i,j} = \Pr\ (S_t = j \mid S_{t-1} = i) \quad (4)$$

In total, we estimated 18 unique parameters: μ, σ, P, and λ for each of the three states and 6 unique elements of the transition matrix $\mathbf{\Phi}_{i \neq j}$. These parameters were estimated using a Markov Chain Monte Carlo (MCMC) algorithm implemented in STAN, a programming language designed for Bayesian interface, via the rstan interface in R (Stan Development Team 2019). Posterior distributions provided point estimates and credible intervals for each of the 18 parameters detailed above, and the most likely sequence of states was obtained using the Viterbi algorithm. The Bayesian approach allowed us to provide vague or informative priors for our parameters as needed. Informative priors specifically being placed on the μ parameter, such that $\mu_1 > \mu_3 > \mu_2$. A similar ordering was placed on the P parameter (Leos-Barajas & Michelot 2018), such that $P_1 < P_2 < P_3$.

We fitted the model to each individual movement track separately. Each individual HMM was fit using four chains and 2,000 Markov Chain iterations, with a warm-up of 1,000 iterations. Model diagnostics were conducted using plots of state-dependent parameter means and standard deviations, state-parameter specific traceplots of chains, and model fit summaries (Auger Méthé et al. 2020), with checks for chain convergence, distinct state-dependent parameter means and distributions, and any other pathological model issues. Our HMM model structure (three states, with variables for dive type and move persistence) was determined both by disregarding models with convergence issues and using a model selection process with approximate Leave-One-Out Cross Validation (LOO) and Pareto smoothed importance sampling (PSIS) using the "loo" R package (Vehtari et al. 2017, Yao et al. 2017).

Example code and data for how to implement these HMMs, diagnostics, and model selection can be found on my GitHub repository (see "Code and Tool Availability" section).

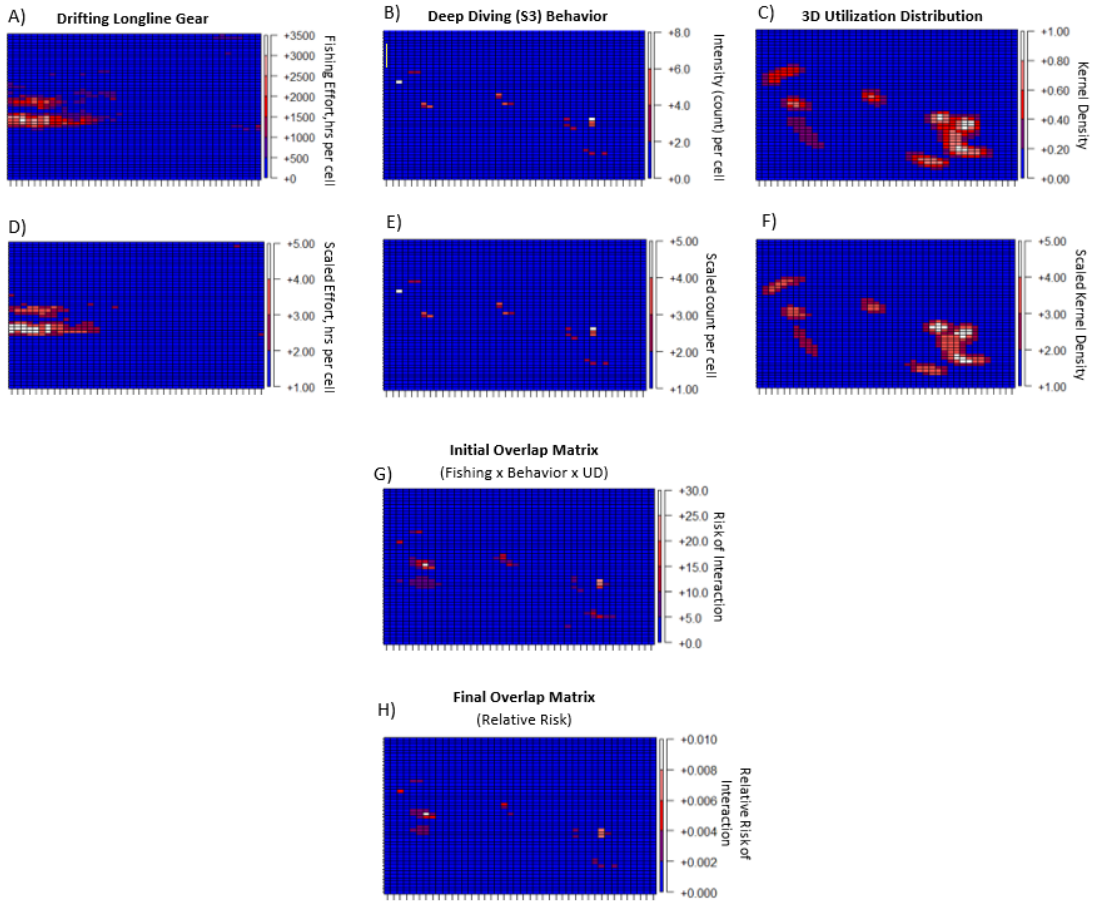

Figure A3.1. Example of original matrices for: a) gear-specific fishing effort (drifting longline); b) intensity of a particular behavioral state (state S3 or deep diving behavior); and, c) normalized 3D utilization distributions. Matrices are shown for one example month (November). d-f) Each matrix was scaled to obtain values ranging from 1-5 on a 1˚ resolution grid of the study area (48 x 42 cells). g) Matrices were then combined using elementwise multiplication to create an initial matrix of overlap. h) A final matrix, representing the relative risk of interaction for turtles in a particular behavioral state with a particular fishing gear for a particular month, was found by dividing the values of the initial overlap matrix (g) by the sum of its values.

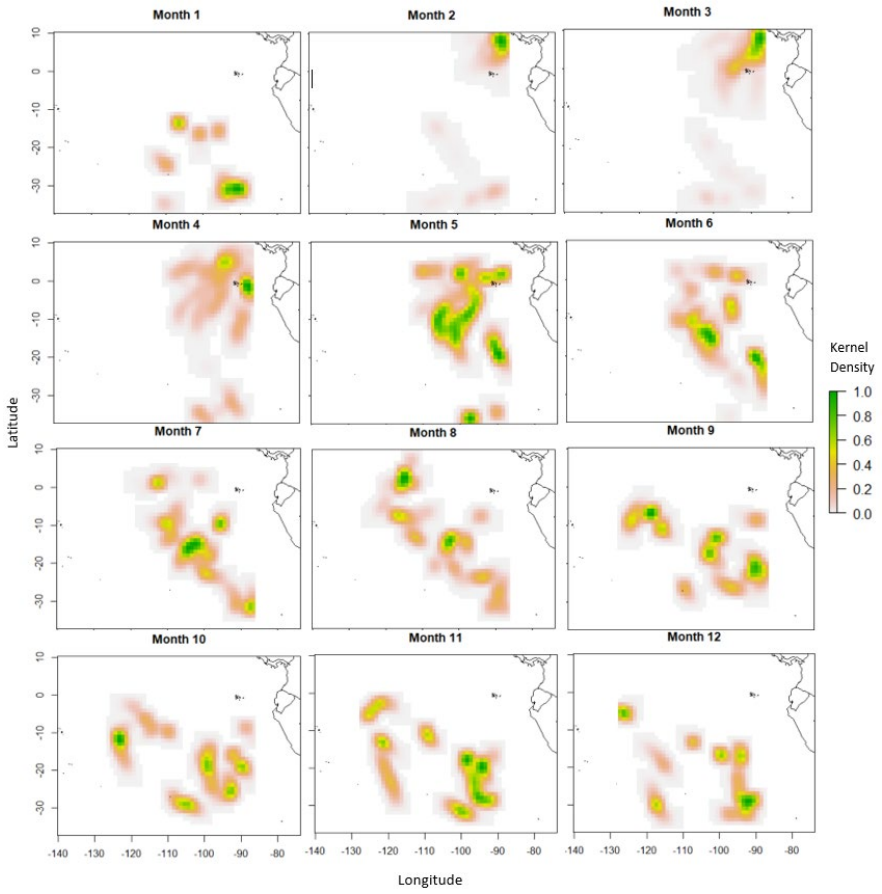

Figure A3.2. Results of estimating the 3D utilization distribution (UD) at the population level for N=28 tracks of leatherback turtles in the Eastern Pacific. The 3D UD is found by applying the product kernel estimator algorithm to each track position in three dimensions (time and space, XY coordinates), then finding the sum of the kernel functions ('adehabitatHR' and 'kernelkcbase', Calenge 2006). The time dimension was supplied as a vector of months (1-12), and the UD estimate for each individual track was plotted onto a 1˚resolution grid. The final population level UD estimate was found by finding the monthly mean UD estimate across individuals. To reduce biases from initial high movement densities due to turtles departing their nesting beach, each monthly UD surface was normalized to have values ranging from 0-1.

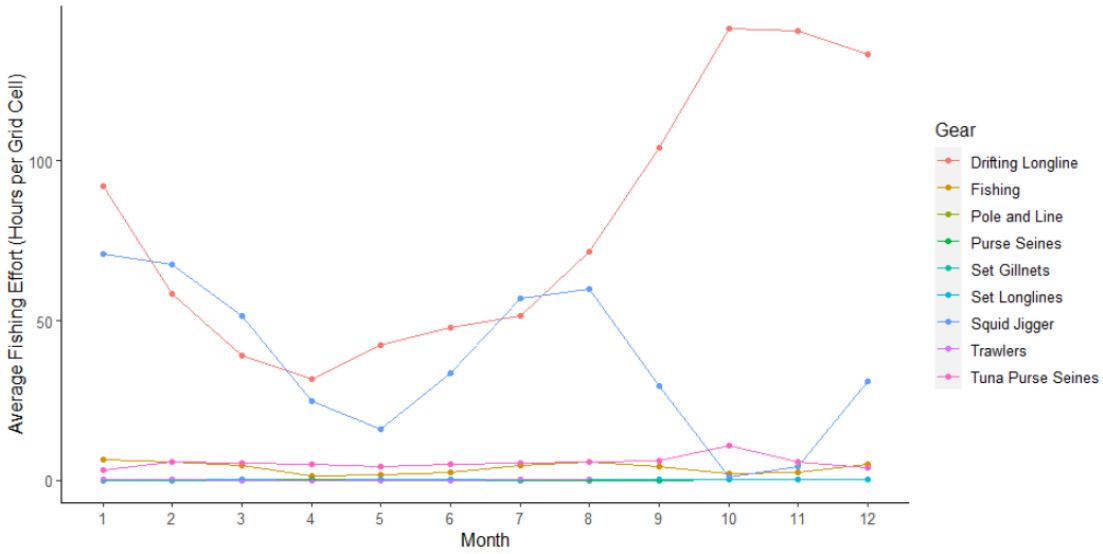

Figure A3.3. Average fishing effort (hours per 1˚resolution grid cell) for nine different fishing gears as a function of month of year.

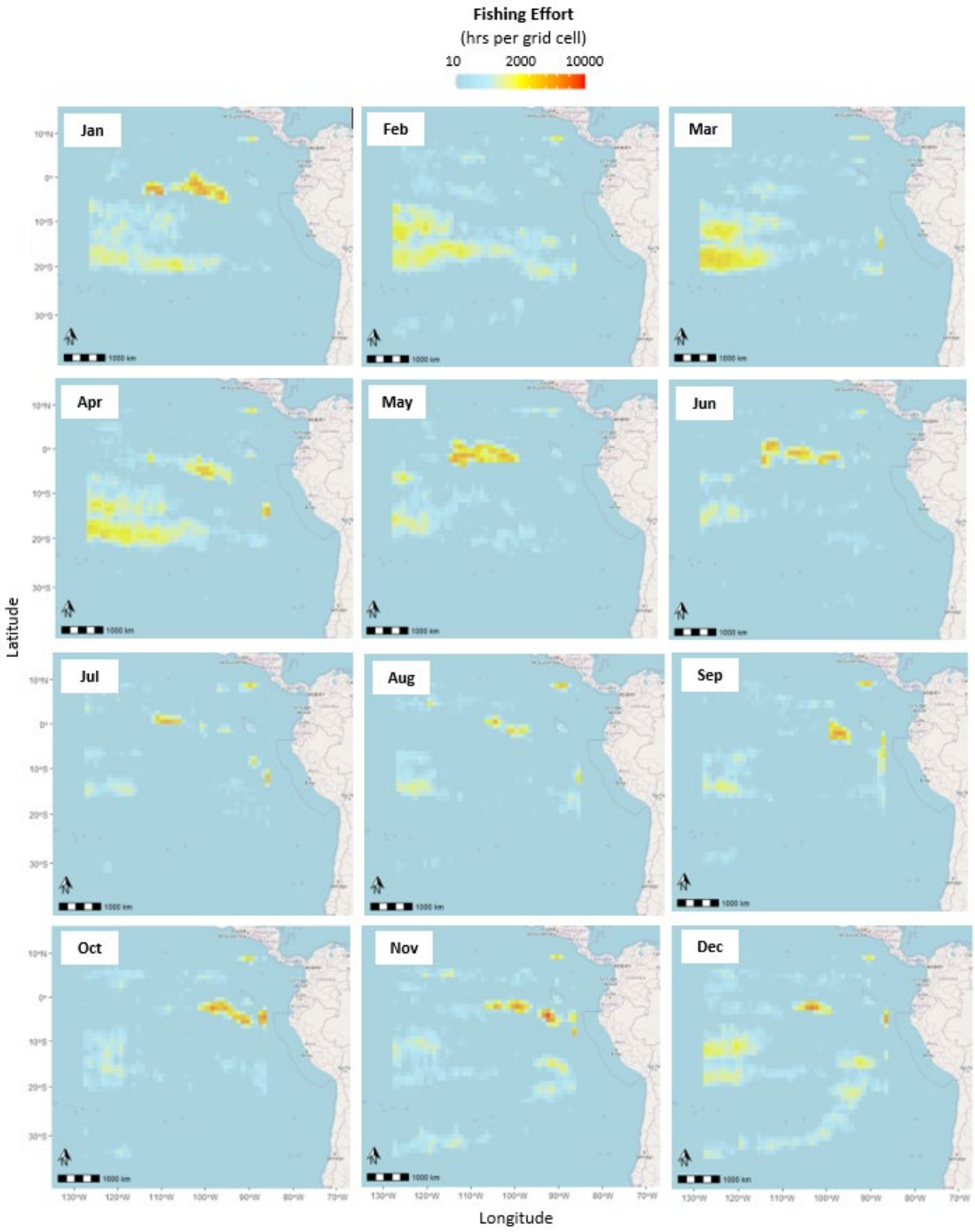

Figure A3.4. Maps of 1˚resolution monthly fishing effort (hrs per grid cell), with orange areas indicating high effort and blue areas low effort. Fishing effort was aggregated over 8 different gear types to represent overall monthly fishing effort.

Appendix 4

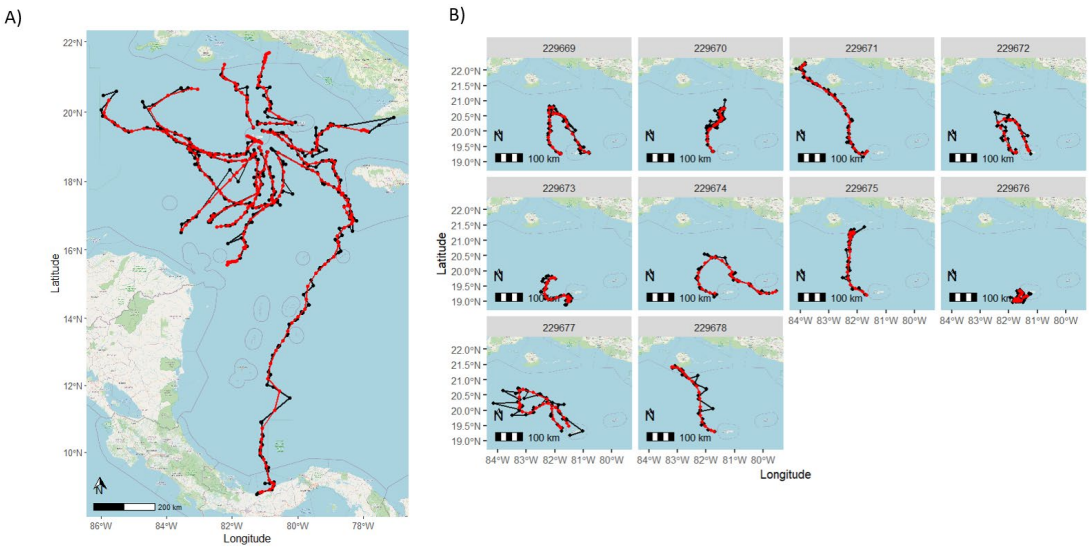

Figure A4.1. Maps of raw tracks and positions (black) overlaid with interpolated trajectories (red) for dispersive individuals in a) the January tracking period (N=12) and b) the July tracking period (N=10). To match the resolution of environmental data products and filter out error positions, locations within a 1 km buffer of the island were removed prior to interpolation. All remaining raw locations were filtered and regularized through the "foieGras" R package (Jonsen et al. 2019), resulting in daily positions for each individual.

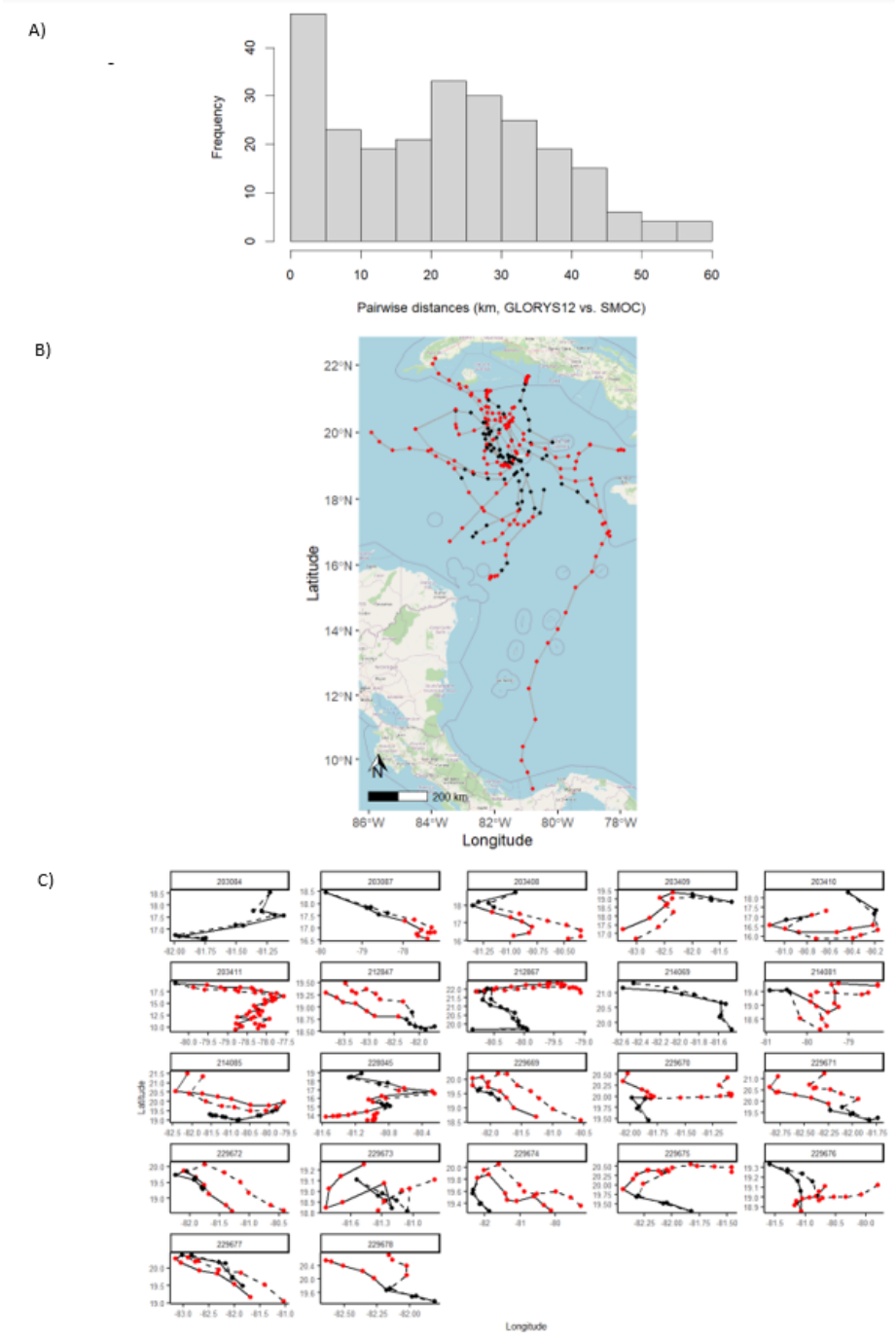

Figure A4.2. a) Histogram of pairwise geographic distances (km) between current-corrected trajectories from the PSY4V3 versus the SMOC ocean products; b) Map of empirical (observed) trajectories (black), with locations where geographic distances are greater 1 standard deviation apart between the PSY4V3 and SMOC products

shown (red); c) Current-corrected trajectories for each individual turtle (N=22), using the PSY4V3 (black) and SMOC (dashed) products, with red locations showing where geographic distances between these were greater than 1 standard deviation apart. Pairwise distances (geographic) were extracted using the "fields" R package (Douglas et al. 2021) and results showed that 65% of locations (159/246) had marked, large distances (> 1 SD or 14.9 km) between the PSY4V3 versus the SMOC current-corrected trajectories.

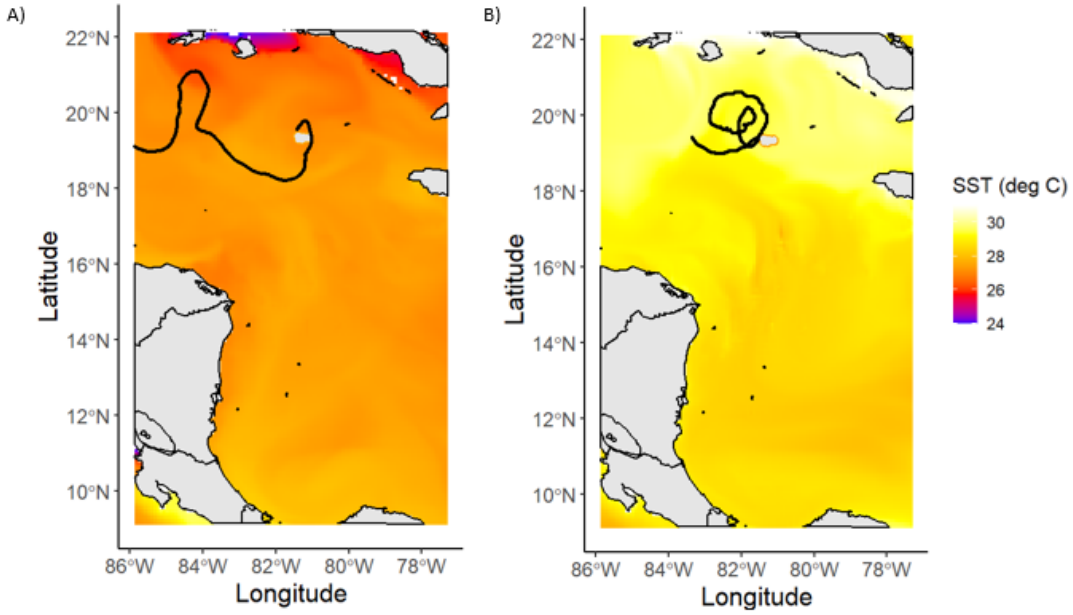

Figure A4.3. Maps of mean sea surface temperature (SST, deg C) fields for the study region during a) the January tracking period (1/23-1/24) and b) the July tracking period (7/21-7/31). Black lines show the paths of the two surface drifters released during each tracking period. A tan polygon illustrates the 1 km buffer around the island. SST fields were derived from the PSY4V3 product, provided by the Operational Mercator global ocean analysis and forecast system (DOI: https://doi.org/10.48670/moi-00016).

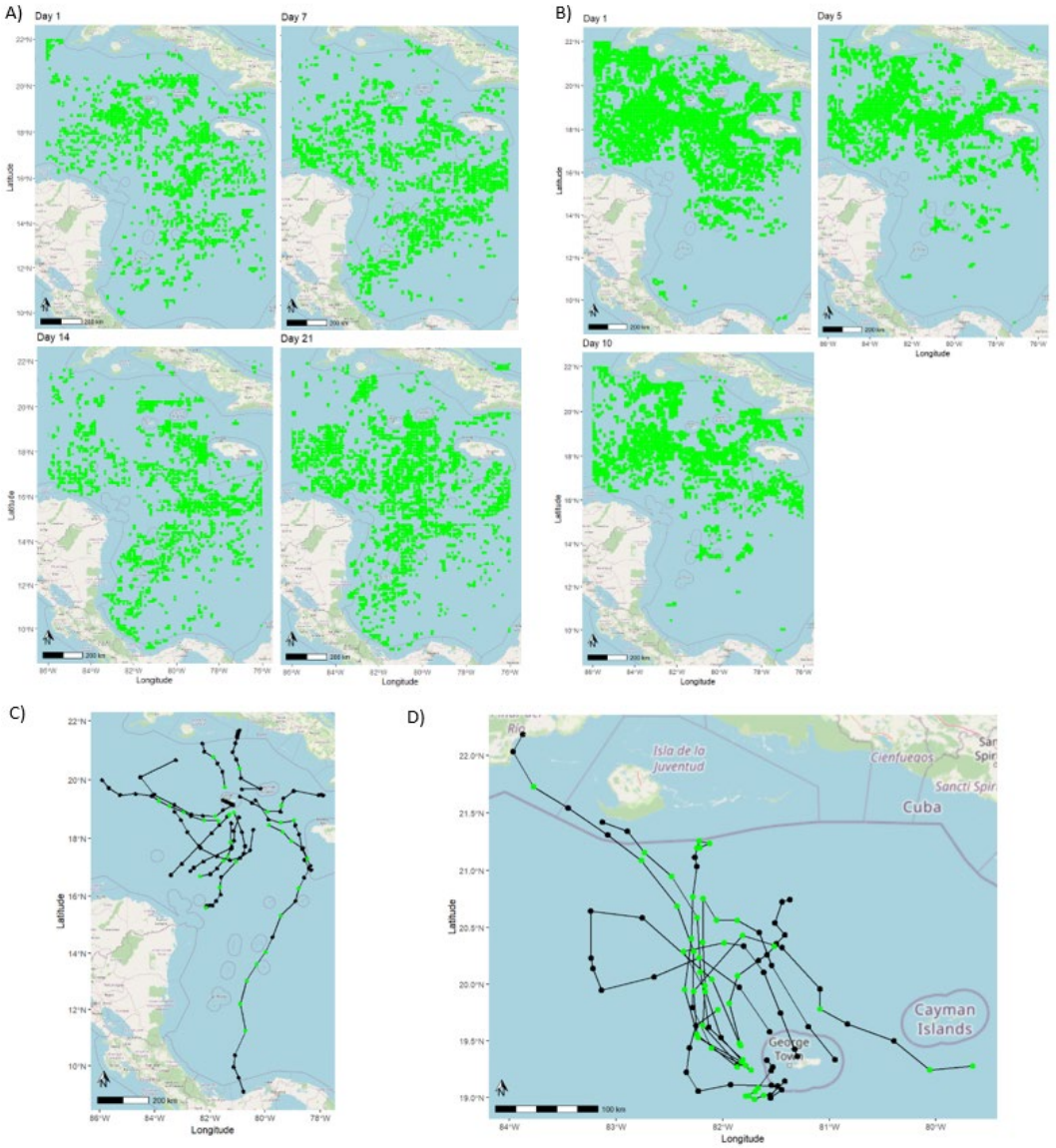

Figure A4.4. Daily estimates of *Sargassum* presence (0.01 degree resolution) in the study region, with a) days 1, 7, 14, and 21 shown during the January tracking period and b) days 1, 5, and 10 shown during the July tracking period, as example. Estimates were derived from the University of South Florida's *Sargassum* weekly density product (Wang and Hu, 2016). Tracks of dispersive turtles in c) January (N=12) and d) July (N=10), showing locations with *Sargassum* present within a 1 km buffer (green).

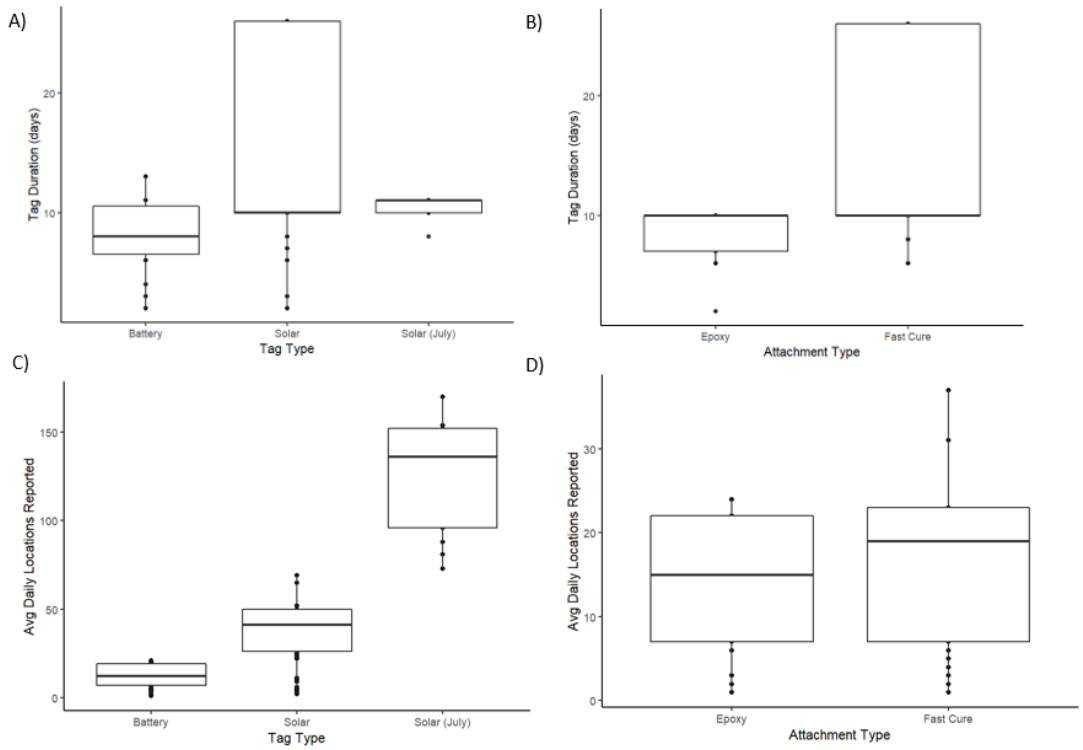

Figure A4.5. Boxplots of the tag duration by a) tag type (battery-powered vs. solar satellite tags) for all N=40 turtles and b) attachment type (fast-cure vs. epoxy) for N=10 turtles in the 1-2 year age class released in January. Note that turtles released in July are shown in a separate group due to being released at a different time period and location. Boxplots are also shown for the average daily number of locations reported for c) tag type (N=40) and d) attachment type (N=10 turtles in the 1-2 years age class released in January).